

Cover Page



Universiteit Leiden



The handle <http://hdl.handle.net/1887/21624> holds various files of this Leiden University dissertation.

Author: Lin, Jingwen

Title: Generation of genetically attenuated blood-stage malaria parasites : characterizing growth and virulence in a rodent model of malaria

Issue Date: 2013-09-03

**Generation of genetically attenuated
blood-stage malaria parasites;
characterizing growth and virulence
in a rodent model of malaria**

Jingwen Lin

林静雯

ISBN: 978-94-6182-322-9

Cover design: Jingwen Lin

Lay-out: Jingwen Lin

Printing: Off Page (www.offpage.nl)

© 2013 Jingwen Lin

Generation of genetically attenuated blood-stage malaria parasites; characterizing growth and virulence in a rodent model of malaria

Proefschrift

ter verkrijging van
de graad Doctor aan de Universiteit Leiden,
op gezag van de Rector Magnificus Prof.mr.dr. C.J.J.M. Stolker,
volgens besluit van het College voor Promoties
te verdedigen op dinsdag 3 September 2013
klokke 15.00 uur

door

Jingwen Lin

Geboren te Xiamen, China
in 1982

Promotiecommissie

Promotor: Prof.Dr. A.M. Deelder

CopromotorsJune: Dr. S.M. Khan

Overige Leden: Prof.Dr. M. Yazdanbakhsh
Prof.Dr. T.H.M. Ottenhoff
Prof.Dr. H.J. Tanke
Prof.Dr. R. Sauerwein
(Radboud University Nijmegen Medical Centre,
The Netherlands)
Prof.Dr. P. Van den Steen
(Rega Institute for Medical Research, Belgium)
Dr. J. Langhorne
(MRC National Institute for Medical Research,
United Kingdom)

The research presented in this thesis was performed at the Leiden Malaria Research Group, Department of Parasitology at the Leiden University Medical Center.

Table of content

Chapter 1	Introduction	1
	1. Malaria and malaria vaccines	2
	2. Aim of this study	7
	3. Whole parasite based vaccine approaches against <i>Plasmodium</i>	9
	4. Genetic modification of malaria parasites	12
	5. Outline and structure of this thesis	14
Chapter 2	A novel 'gene insertion/marker out' (GIMO) genetic modification method for transgene expression and complementation in rodent malaria parasites	21
Chapter 3	Screening inhibitors of <i>P. berghei</i> blood stages using bioluminescent reporter parasites	53
Chapter 4	Loss-of-function analyses defines vital and redundant functions of the <i>Plasmodium</i> rhomboid protease family	71
Chapter 5	Malaria parasites lacking critical proteases involved in hemoglobin degradation are viable and are less sensitive to chloroquine	115
Chapter 6	Generation of growth and virulence attenuated blood-stage malaria parasites	161
Chapter 7	Conclusions and discussion	195
	1. Progress in genetic modification technology for <i>Plasmodium</i> rodent malaria parasites	196
	2. Generation of growth- and virulence-attenuated attenuated blood stage parasites (GAP _{BS}) by targeted gene deletion	197
	3. Future research on growth- and virulence-attenuated <i>P. berghei</i> mutants	200

Summary	207
Samenvatting	211
List of publication	217
Acknowledgements	219
Curriculum Vitae	221

CHAPTER 1

Introduction

1. Malaria and malaria vaccines

Humans develop malaria after being inoculated, via the bite of an infected female mosquito, with the unicellular protozoan parasite, *Plasmodium*. There were an estimated 219 million cases of malaria and 660 000 deaths in 2010 and it is one of the world's most important global health challenges ([1]; http://www.who.int/malaria/publications/world_malaria_report_2012/en/). Indeed, a recent systematic analysis on global malaria mortality showed that malaria was the underlying cause of death for 1.24 million individuals in 2010 and that malaria mortality therefore is likely to be larger than previously estimated [2]. Many prevention and elimination initiatives, such as distribution of insecticide-treated nets, indoor residual spraying with insecticides or implementation of drug treatment programmes, are underway to limit both the incidence and spread of the infection, as well as to limit the severity of the disease (http://www.who.int/malaria/publications/world_malaria_report_2012/en/). While these measures have contributed to the global decline in malaria, they are all under threat to the acquisition of drug resistance, either by *Plasmodium* parasites to antimalarial drugs or mosquitoes to insecticides [3-5]. Among the human malaria parasites, *P. falciparum* is the species responsible for most severe disease and accounts for the largest numbers of deaths, and therefore has been the target of most antimalarial drugs and vaccine development efforts.

Problems with the costs and logistics involved in mass drug administration campaigns targeting *Plasmodium* infected and at risk populations in resource and infrastructure poor settings, as well as the above mentioned acquisition of drug resistance, mean that vaccination remains the most (cost) effective method of malaria disease control, and ultimately eradication [6-8]. To date, disease elimination or eradication in humans has only been effectively achieved through the mass administration of vaccines [9]. However, a vaccine against malaria has not been licensed and indeed, only 1 vaccine candidate RTS,S has advanced to Phase III clinical testing (http://www.who.int/vaccine_research/links/Rainbow/en/index.html). Several features of a *Plasmodium* infection would appear to hamper the development of a vaccine against malaria. Specifically, for most of its development, the malaria parasite is intracellular, developing either inside hepatocytes or erythrocytes and thereby limiting its recognition and removal by the immune system. Moreover it exists as many morphologically and antigenically different forms, and parasite molecules most readily detected by the host immune response exhibit high levels of antigenic diversity (highly diverse allelic polymorphisms) and several of these critical parasite proteins are immunologically variant (where the genome encodes multiple copies of antigenically diverse but functionally related proteins). As the parasite

is itself eukaryotic, a number of parasite antigens may provoke relatively weak immune responses that do not contribute to protection against infection [6-8].

While *P. falciparum* blood stages can be effectively propagated *in vitro*, understanding the complexity of the host response to a malaria infection is best performed *in vivo*. And while very powerful, the expense and safety concerns of performing experimental studies in humans and non-human primates have limited their use. Consequently, rodent malaria parasites are recognized as valuable models to investigate the developmental biology of malaria parasites, parasite-host interactions, vaccine development and drug testing (<http://www.lumc.nl/con/1040/81028091348221/810281121192556/811070740182556/811070744452556/>).

1.1. The malaria parasite life cycle

Plasmodium parasites infect a wide variety of hosts, including birds, reptiles and mammals via an insect vector, usually a mosquito. There are five species associated with infecting humans, *P. falciparum*, *P. vivax*, *P. ovale*, *P. malariae* and *P. knowlesi* [10]. Most of the severe pathologies and deaths due to malaria are associated with *P. falciparum* and it is consequently the most studied human malaria parasite (http://www.who.int/malaria/publications/world_malaria_report_2012/en/).

1.1.1. The *P. falciparum* life cycle

One of the main difficulties in developing an effective vaccine against *P. falciparum* is the complex lifecycle of the parasite with its many different developmental stages (Figure 1). *P. falciparum* can only undergo sexual reproduction in *Anopheles* mosquitoes, its definitive host. The human being the intermediate host where parasites only reproduce asexually, both in the liver and the blood. When an infected female mosquito takes a blood meal, it injects parasites, sporozoites, into the skin and these then enter the bloodstream and migrate to the liver where they invade hepatocytes. Within the hepatocyte, the sporozoite grows and multiplies forming a hepatic schizont that contains several thousands of daughter parasites, the so-called exo-erythrocytic merozoites. These merozoites are released into the blood stream where they invade red blood cells (RBC). The development of the *P. falciparum* schizonts in the liver take 7–10 days, but the infection of the liver is not associated with any clinical symptoms. After merozoite invasion of a RBC, the parasite grows and multiplies, forming a blood-stage schizont containing 16–32 daughter parasites (merozoites) in a 44–48 hour period. When schizonts rupture, they release merozoites that can invade new RBC initiating a proliferative stage of development with new waves of parasites being released into the blood approximately every 48 hours. In other *Plasmodium* species that infect humans, replication inside RBC

can vary from 24–72 hours. The rapid increase in parasite numbers, destruction of RBC and the ability of infected RBC (iRBC) to attach to uninfected red blood cells and host tissue (sequestration) contribute to the clinical symptoms associated with *P. falciparum* infections [11]. *P. falciparum* infections lead to severe symptoms and death if untreated; the most common clinical features of severe malaria are high fever, respiratory distress, vascular obstructions, metabolic acidosis, multi-organ derangement, severe anaemia and neurological syndrome known as cerebral malaria (CM) [11]. CM is believed to be associated with iRBC sequestration in brain microvasculature and is thought to be enhanced by the proinflammatory status of the host and virulence characteristics of the infecting parasites [12].

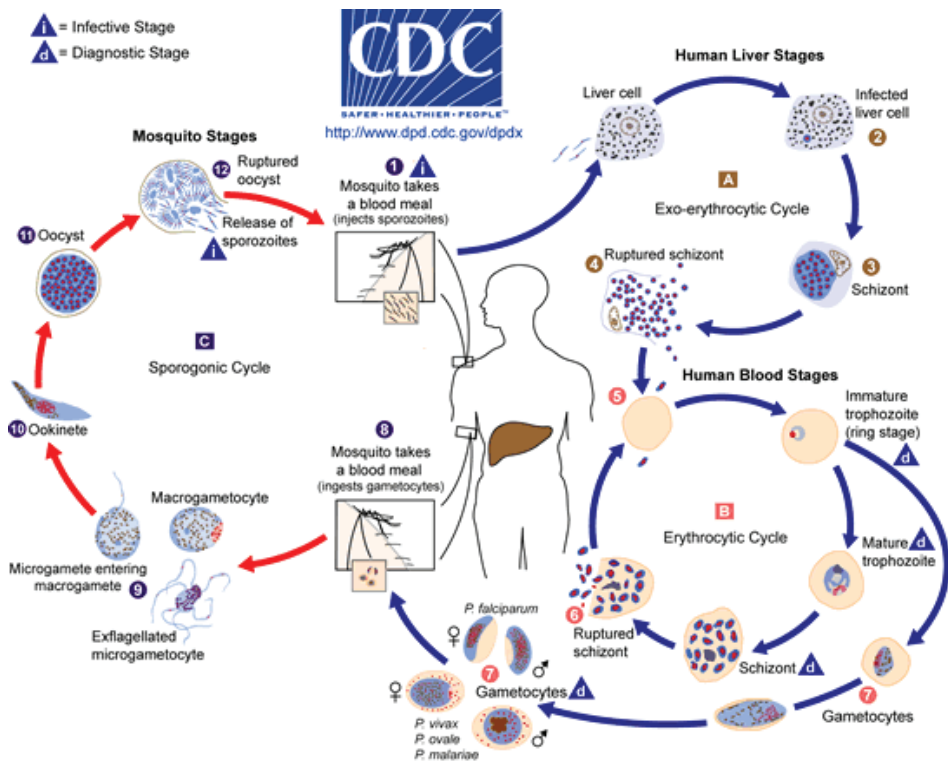


Figure 1. The life cycle of *Plasmodium falciparum*.

P. falciparum replication and maturation in humans (blue arrows) and mosquitoes (red arrows). This image was taken from Center for Disease Control and Prevention website (<http://www.cdc.gov/malaria>).

Some merozoites that invade RBC do not proceed with asexual multiplication but differentiate into male or female gametocytes, the sexual precursor cells of gametes. These gametocytes are responsible for transmission between host and mosquito and

once taken up by mosquitoes rapidly develop into male and female gametes in the mosquito midgut where fertilisation takes place. The resulting zygote matures into a motile ookinete, which can traverse the mosquito's midgut wall and attach onto the hemocoel side of the midgut where it differentiates into an oocyst. Through sporogony the oocyst forms thousands of daughter parasites, sporozoites. When these are released from the oocyst, they invade the mosquito salivary glands where they further mature and become infectious to humans.

1.1.2. The life cycle of *P. berghei*, the rodent malaria parasite used as a model in this study

In this study we have used the rodent malaria model, *Plasmodium berghei*. This parasite is the most genetically tractable of the four murine *Plasmodium* species (*P. berghei*, *P. vinckei*, *P. chabaudi* and *P. yoelii*). Several different *P. berghei* strains have been isolated, either from its natural host *Grammomys surdaster* (thicket rat) or from the natural vector *Anopheles durenii*. These parasites are infectious to laboratory rodents such as mice and rats, and can infect *A. stephensi* in the laboratory (<http://www.lumc.nl/con/1040/81028091348221/810281121192556/811070740182556/811070746282556>). Rodent parasites are recognized as valuable model organisms to investigate human malaria, because they are similar in most essential aspects of morphology, physiology and lifecycle and the manipulation of the complete lifecycle of these parasites, including mosquito infections, is simple and safe [13].

Like the four human malaria parasites, *P. berghei* is transmitted by *Anopheles* mosquitoes and it infects the liver after being injected into the bloodstream by a bite of an infected female mosquito. After a short period (a few days) of development and multiplication, these parasites leave the liver and invade RBCs. The multiplication of the parasite in the blood causes the pathology such as anemia and damage of essential organs of the host such as lungs, liver and spleen. *P. berghei* infections may also affect the brain and can be the cause of cerebral complications in laboratory mice. These symptoms are to a certain degree comparable to symptoms of cerebral malaria in patients infected with the human malaria parasite [14]. The complete genome of *P. berghei* has been sequenced and it shows a high level of similarity with the genome of the human malaria parasite *P. falciparum* [15]. Despite the similarities between the life cycle stages of *P. berghei* and *P. falciparum*, some important differences exist. The *P. berghei* asexual blood cycle takes 22–24 hours to complete, unlike the 44–48 hours required by *P. falciparum*. *P. berghei* parasites have, like the human parasite *P. vivax*, a strong preference for invading and growing in immature RBCs (reticulocytes), whereas *P. falciparum* can invade both mature and immature RBCs. The *P. berghei* development in the liver does not, like *P. falciparum*,

1

take 7–10 days but only 48–52 hours. When studying host-parasite interactions, pathology and immune responses induced by *Plasmodium* infections in rodents, not only do the differences between the parasites but also clearly the differences between the rodent and human host have to be taken into consideration, since differences in host physiologies and immune responses will strongly influence how a host will cope with an infection and manifest malarial disease. In a recent review, the relevance of rodent *Plasmodium* infections in mice and rats as models of severe disease induced by *P. falciparum* infections in humans, have been discussed in depth [11]. For example, cerebral malaria is one of the most severe of all malaria pathologies observed in humans infected with *P. falciparum*, and C57BL/6 mice infected with *P. berghei* ANKA strain can also develop cerebral pathologies resulting in death, termed experimental cerebral malaria (ECM). Currently, the *P. berghei* ANKA-C57BL/6 system is the only available experimental model for the study of cerebral malaria *in vivo* [14], however, the similarities between the inflammatory context and the induced immuno-pathology between humans and rodent infections is under considerable debate [11,16].

1.2. Malaria vaccine intervention strategies

Most initiatives to develop a malaria vaccine target one or more of the following 3 stages of parasite development: 1) pre-erythrocytic vaccines that target the sporozoites and/or liver stages; 2) erythrocytic vaccines targeting merozoites or iRBC; and 3) transmission blocking vaccines that targets sexual and ookinete stages within the mosquito midgut [8]. Specifically:

Pre-erythrocytic vaccines aim to generate antibody responses against sporozoites and thereby preventing hepatocyte invasion and/or T-cell (cellular) immune responses against intra-hepatic parasites that can kill intracellular liver stages. These vaccines prevent an infection from progressing beyond the asymptomatic liver stage and into a malaria infection in the blood [8]. However, to be successful such vaccine it has to be 100% effective in preventing blood stage infection, as any liver stage parasite that escape immune detection could generate an unregulated and potentially fatal blood stage infection.

Erythrocytic vaccines aim to generate antibody responses that target either merozoite antigens or parasite antigens expressed on the iRBC surface, therefore blocking parasite entry into a RBC or opsonising parasite/iRBC for phagocytic destruction. There is a strong rationale for the development of vaccines based on antigens of blood-stage parasites as most naturally acquired (albeit partial) protective immunity in humans is believed to target *Plasmodium* antigens expressed at the blood stage of development. Ideally, these

vaccines should reduce parasite densities to levels that do not cause disease [17]. Due to parasite antigenic variation, polymorphism and mutation, sterile immunity is likely to be very difficult for single antigen subunit blood-stage vaccines, but vaccination with such vaccines may allow the host to mount a better and more effective immune response thereby reducing the risk of the individual developing severe clinical disease [8,18].

Transmission-blocking vaccines target the stages of the parasite that establish an infection in a mosquito, specifically the sexual stages and/or the ookinetes, or even target mosquito midgut proteins. Vaccines targeting the parasite mainly rely on inducing a neutralizing antibody and/or antibody-complement based responses to eliminate parasites in the mosquito midgut, i.e. gametes and zygotes/ookinetes. These vaccines aim to reduce transmission and thereby limiting new infections within the community, and such vaccines do not provide protection against a malaria infection for the immunized individual. Consequently, they are likely to be deployed as part of multi-stage vaccine strategies, for example with vaccines that limit disease in the host and transmission to the population as a whole. Further, the importance of transmission blocking vaccines is that they may contribute to the eventual removal of reservoir populations of parasites in semi-immune individuals who carry the parasite but do not exhibit malaria symptoms [8].

The recent interest is not only in malaria control but in eradication, these different vaccination strategies may either be effectively brought together or different immunization methods used to best protect the populations at risk from malaria, such as young children, pregnant women, travellers, semi-immune adults etc [18,19].

2. Aim of this study

Despite major efforts over the past 50 years to develop one, there is currently no licensed malaria vaccine available. The most advanced vaccine is the sub-unit vaccine RTS,S that is based on the immunodominant sporozoite surface antigen, circumsporozoite protein (CSP). It targets the sporozoite/liver stage of *P. falciparum* and has advanced to Phase III clinical trials. The preliminary results from the trial have shown a 55.8% reduction in the acquisition of clinical malaria, a 34.8% efficacy against severe malaria in young children aged between 5 to 17 month [20], and a 26% efficacy against severe malaria in infants 6–12 weeks of age [21]. The limited success achieved in inducing sterile and long-lasting protective immunity against malaria using subunit vaccines has led to renewed interest in whole-organism vaccination strategies [22,23]. Indeed, most licensed vaccines against other infectious diseases are based on killed or live attenuated whole organisms (<http://>

www.cdc.gov/vaccines/). It has been shown in studies with rodent and primate models of malaria and in experimental clinical studies with humans, that sterile immunity could be achieved by immunization with live radiation-attenuated sporozoites (RAS) [24-26], which has constituted the gold standard for the malaria vaccine research field. In rodent models of malaria (both *P. berghei* and *P. yoelii*), similar or even better levels of protective immunity have been achieved by immunization using genetically-attenuated sporozoites [27]. These genetically attenuated parasites (GAP) in which critical genes in liver stages are deleted (GAP_{LS}), after the invasion in hepatocytes, abort liver stage development at different time points, inducing CD8+ T-cell immunity that are capable of killing liver stage parasites, which is comparable to RAS [28], (see Section 3.1). In addition to immunization with attenuated sporozoites, it has been demonstrated that both in rodent and primate models, partial to full protective immunity can be achieved through immunization with either killed or radiation attenuated blood stages or with low doses of viable blood stage parasites followed by drug cure (reviewed in detail [23,29]). Moreover, it has been shown in humans that experimental blood stage immunity can be induced by repeated administration of ultra-low doses of infected RBC under drug cover, which induces CD4+ T-cell based protective immunity [30].

The renewed interest in whole parasite malaria vaccine strategies, due to the lack of significant progress on subunit vaccines, not only exists in developing a vaccine consisting of attenuated sporozoites, but also in exploring possibilities for inducing protective and long-lived immunity by immunization with whole blood stages (see Section 3.2). It has recently been shown in rodent malaria models that immunity against malaria can be achieved by immunization using genetically attenuated blood stage parasites (GAP_{BS}), which are growth and/or virulence attenuated through genetic modification [31-34]. Infection of mice with these GAP_{BS} resulted in self-resolving infections, and after a single infection with these parasites, all convalescent mice were protected against subsequent parasite challenge for prolonged periods. These results show that infection of mice with growth and virulence attenuated malaria parasites can induce long-lasting protective immunity [31-34], (see also Section 3.2). The major advantages of immunization with GAPs over immunization with radiation attenuated parasites are that they constitute a homogeneous population of parasites with defined genetic identity and attenuation phenotype [35]; moreover, gene insertion techniques also permit the introduction of transgenes into GAP genome that may enhance attenuation phenotype and/or improve the potency of the vaccine [35].

The aim of this study is to identify additional rodent GAPs that demonstrate growth- and virulence-attenuation of their blood stages, specifically GAP_{BS} that shows only short,

low-parasitemia blood infection and that can induce protective immune responses (see Section 3.2 and 5). In order to screen for a larger array of GAPs, we first aimed at improving methods for both the generation of genetically attenuated parasites and for analysing blood stage growth attenuation of GAP_{BS} (see Section 5).

3. Whole parasite based vaccine approaches against *Plasmodium*

Most of the licensed human vaccines available today belong to one of three categories—live attenuated microbes (e.g. measles, mumps), killed/inactivated microbes (e.g. Polio, rabies) or protein subunit/conjugate (e.g. Hepatitis B, HPV) (<http://www.cdc.gov/vaccines/>). A large number of subunit-vaccine candidates against *Plasmodium* malaria parasites have been tested in animal models and humans, mainly as a protein (antigen) formulation or expressed by a (DNA or viral) vector system in order to generate protective immunity [36]. Most malaria antigens that have been selected as subunit-vaccine candidates have been characterized as targets of natural immunity, most often associated with strong humoral responses [37]. However, the most advanced leading subunit pre-erythrocytic vaccine candidate RTS,S showed only limited efficacy as in Phase III testing with clinical malaria episodes in children being reduced by only 30–50% [20,21]. Progress on clinical trials of blood stage subunit-vaccines has been slow: the testing of more than 10 candidate subunit vaccines targeting *Plasmodium* blood stages have not progressed to or further than Phase 2 trials, with only 3 candidates having reached Phase 2b trials [38]. The limited success with subunit-vaccine development has renewed interest in developing vaccines consisting of whole, killed or attenuated, parasites [23,35]. While sustained and sterile immunity has been achieved using live liver stage parasites attenuated by radiation or genetic modification or administered under curative doses of chemoprophylaxis [35,39,40], full protective immunity with either killed sporozoites or blood stage parasites have so far been unsuccessful [29,39].

3.1. Immunization with attenuated sporozoites

In 1967, a study using *P. berghei* in rodents demonstrated that complete immune protection can be achieved by delivering live but attenuated sporozoites damaged by a specific dose of irradiation [24]. In contrast to killed sporozoites, which induce strong humoral responses, mostly to the major sporozoite surface protein—CSP, radiation attenuated sporozoites infect hepatocytes but fail to replicate and elicit antibody and cellular responses against sporozoites and infected hepatocyte [41]. Long lasting sterile

1

protective immunity induced by irradiated sporozoites was not only demonstrated in animal models of malaria, but also importantly in humans where malaria naïve volunteers were immunized by bites of infected mosquitoes delivering irradiated *P. falciparum* sporozoites [26,42,43]. These findings provided the paradigm for a whole organism malaria vaccination, demonstrating that complete protective immunity against a malaria infection was achievable.

In rodent models of malaria, similar or even higher levels of protective immunity has been achieved by immunization using genetically attenuated sporozoites [27,35]. These liver-stage genetically attenuated parasites (GAP_{LS}) were created by targeted deletions of genes that result in developmental arrest in liver stage after invasion of attenuated sporozoites and have been shown to induce high level of sterile protective immunity in mice [35,44-46]. Techniques to create multiple gene deletion could ensure the safety of GAP_{LS}, specifically to ensure that any parasites that are able to survive without the presence of one gene are be unable to develop without the presence of another. Moreover, genes have been identified that when removed create GAP_{LS} that arrest at late into liver development and induce protective immunity that is better than that induced by irradiated sporozoites [27]. Equivalents of some of the liver stage GAP_{LS} candidates have been also generated in the human parasite *P. falciparum*, and importantly, showed similar phenotypes. For example, a *P. berghei* GAP_{LS} lacking P36p expression arrests in liver stage and can confer long lasting protective immunity in mice [44], and a *P. falciparum* GAP lacking expression of the same gene (termed P52 in *P. falciparum*) also arrests during liver stage development [47].

Up until now, it has only been possible to establish *P. falciparum* infections in humans via the bite of infected mosquitoes. To overcome this limitation for vaccine delivery, the company Sanaria Inc. has produced aseptic sporozoites that can be administered to humans by needle inoculation. These sporozoites are reared in sterile mosquitoes and have been purified and cryopreserved, and formulated for use in humans in compliance with all regulatory requirements [48].

3.2. Immunization with attenuated or killed blood stage parasites

Whole *Plasmodium* blood-stage formulations used for immunization have generally consisted of iRBC. These formulations have included killed parasites in adjuvant, radiation-attenuated iRBCs or infection with wild-type iRBC administered under curative doses of chemotherapy, and they have been used to immunize both rodents and primates [23,29,49,50]. The results of these immunizations, while varied in their protective efficacies for the different combinations, have demonstrated protective immunity

including complete protection against a challenge with wild-type parasites. Furthermore, in an immunization study in humans, evidence was found for the generation of complete protective immunity against *P. falciparum* that was achieved via repeated inoculations of ultra low numbers of iRBC (~30), resulting in sub-patent infections that were controlled by curative dose of chemotherapy [30]. These studies were remarkable in that not only they showed that immunization with whole blood stages can induce complete protection in humans, but also that protective immunity could be achieved using only limited amounts of parasite material and in the absence of a major antibody response [23].

Currently practical limitations exist for immunization strategies that require humans be infected with parasites inside RBCs, either killed or attenuated. For example it is unclear if regulatory authorities would approve, as part of a mass vaccination program, the intravenous administration of infected red blood cells to humans [23,37]. Nonetheless, such studies can provide important insights into how protective immune responses can be induced and maintained against *Plasmodium* blood stages [51,52]. Similar to immunization studies using genetically attenuated parasites that arrest in the liver (GAP_{LS}) [35], studies into blood-stage vaccination would clearly benefit from creating genetically attenuated blood stage parasites (GAP_{BS}) in animal models that induce limited, self-resolving infections that are virulence-attenuated and that can provoke strong and long-lasting immunity without the induction of malarial symptoms or additional pathologies. Such parasites can be instructive tools to uncover important correlates of protection and disease, and to better understand how iRBC are detected and eliminated by host immune response.

A number of gene-deletion mutants generated in both rodent and human parasites have been reported that exhibit moderate to severe reduction in their blood-stage multiplication rates. However, the first growth- and virulence-attenuated GAP_{BS} was only recently reported for the rodent model malaria parasite *P. yoelii* YM (a lethal strain); this GAP_{BS}, which lacks the gene encoding purine nucleoside phosphorylase (PNP), is virulence-attenuated and produces a self-resolving infection in mice [31]. Importantly, after a single infection with this parasite, all convalescent mice were protected against subsequent wild-type parasite challenge for prolonged periods (>5 months). Since then, other rodent malaria GAP_{BS} have also been reported which show growth- and virulence-attenuation and that induce self-resolving infections after which mice are protected against wild type challenge. These include a GAP_{BS} in *P. yoelii* XNL (a non-lethal strain) that lacks the gene encoding nucleotide transporter 1 (NT1), which is strongly attenuated and generates a self-resolving infection in mice [33]. Other GAP_{BS} characterized in the rodent model *P. berghei* include GAP_{BS} lacking expression of rhomboid 1 [53], plasmepsin-4

(PM4) [32], and a GAP_{BS} that lacks both PM4 and MSP7 (a merozoite-specific protein) [34]. These GAP_{BS} that have been created in *P. berghei* ANKA do not cause experimental cerebral malaria (ECM) in ECM-susceptible mice [34]. These studies show that not only is it possible to generate growth- and virulence-attenuated blood stage parasites by targeting specific genes in the parasite genome, but also that strong and long-lasting protective immune responses can be induced in mice that have resolved their infections. However, despite growth- and virulence-attenuation, most of the reported GAP_{BS} still produce infections with relatively high parasitemias (parasite loads). An ideal GAP_{BS} should result in infections with low parasitemias that spontaneously resolve shortly after parasites are introduced into the blood. An infection with low (sub-patent) parasitemias was only achieved with low dose inoculation of $\Delta nt1$ mutant generated in non-lethal *P. yoelii* XNL in mice [33]. This sub-patent, self-resolving infections generated strong cellular and humoral immune responses that provided complete protective immunity in BALB/c, C57BL/6 and SWISS mice [33]. However, this mutant was not created in a virulent rodent parasite line (i.e. *P. yoelii* YM or *P. berghei* ANKA), where the kinetics and virulence phenomena of a gene-deletion mutant might be substantially different.

As the research in rodent malaria model can serve as a template to create *P. falciparum* GAPs to be used as live-vaccines in humans, the research on generation of GAP_{BS} is better focused on identification of GAP_{BS} in normally virulent rodent *Plasmodium* parasite strains. The double gene-deletion mutant $\Delta pm4/\Delta msp7$ showed greater growth- and virulence attenuation than either of the single gene-deletion mutants, $\Delta pm4$ and $\Delta msp7$ [34]. The $\Delta pm4/\Delta msp7$ infections could be resolved in BALB/c, C57BL/6 and CD1 mice, whereas only BALB/c mice could survive $\Delta pm4$ infections. However, creating an equivalent *pm4* and *msp7* deficient *P. falciparum* parasites is complicated, as it is not clear what the functional *msp7* ortholog in *P. falciparum* is, being a member of a multigene family [34]. Therefore, up to now, there is no ideal GAP_{BS} that could be translated to *P. falciparum*.

4. Genetic modification of malaria parasites

Reverse genetic technologies have been widely applied to gain an understanding of *Plasmodium* gene function and to provide an insight into the biology of malaria parasites and their interactions with the host [54-56]. Targeted gene disruption and loss-of-function analyses have provided insight into *Plasmodium* gene function and biology, and protein-tagging methodologies have helped reveal the pattern of expression, localization and transportation of *Plasmodium* proteins. Furthermore, reverse genetics is increasingly being used to generate parasites that express transgenes encoding heterologous proteins, for example fluorescent and/or luminescent reporter proteins. Such reporter parasites

have been instrumental to visualize and analyse parasite-host interactions, in real-time, *in vitro* and *in vivo* [57-59]. Transgenic parasites expressing luciferase have also been used to develop sensitive and simple assays to measure blood and liver stage parasite drug sensitivity both *in vitro* and *in vivo* [60-62]. Genetic modification technologies have been developed for different *Plasmodium* species (*P. falciparum*, *P. knowlesi*, *P. cynomolgi* and three rodent parasites *P. berghei*, *P. yoelii* and *P. chabaudi*) [54,63]. The availability of efficient reverse-genetic technologies for the rodent parasites *P. berghei* and *P. yoelii* and the fact that these parasites can be followed throughout their complete life cycle in laboratory conditions, both *in vitro* and *in vivo*, have made them the most frequently used animal malaria models for so called functional genomics, helping ascribe functions to *Plasmodium* genes, and also for analysing host-parasite interactions through the use of transgenic parasites expressing heterologous proteins such as GFP or luciferase [54].

4.1. Generation of attenuated rodent malaria parasites by genetic modification

Genetic modification of the malaria parasite has not only been used to understand the of *Plasmodium* biology and to analyse parasite-host interactions, but also to generate GAPs (as mentioned above). These mutants permit us to explore the possibilities of whole organism vaccines against malaria. Specifically, by deleting genes from the *Plasmodium* genome critical for liver stage development, GAP_{LS} have been produced that arrest during development in the liver and induce strong protective immunity (see Section 3.1). Similarly, by deleting genes that play an important role during blood-stage growth and/or multiplication, GAP_{BS} have been generated that are both growth- or virulence-attenuated (See Section 3.2). For these purposes, the rodent models *P. berghei* and *P. yoelii*, are frequently employed to generate and analyse GAPs, both for liver and blood stages.

4.2. Generation of transgenic *Plasmodium* parasites expressing heterologous proteins

The creation of parasites that express heterologous proteins, most commonly fluorescent or luminescent reporter proteins (e.g. GFP, luciferase etc) either by themselves or fused to *Plasmodium* proteins, are now being routinely used to investigate parasite protein localization and interactions (<http://www.pberghei.eu>). Reference reporter parasites, which express reporter proteins either constitutively at high levels or in a stage-specific manner, are now invaluable tools in *Plasmodium* research. For example, GFP-expressing parasites have been used in conjunction with flow cytometry to provide quantitative information on the parasites development in both red blood cells [32] and hepatic cells [64]. Transgenic parasites expressing luciferase have been used to unravel and monitor

1

the pattern of sequestration in live mice [65,66], to visualize and quantify the *in vivo* liver stage development [62] and to screen and evaluate antimalarial activity of drugs both *in vitro* and *in vivo* [60-62]. Other transgenes have also been introduced into *Plasmodium* genome to dissect the host-pathogen interaction. Model antigen OVA (Ovalbumin) is used to examine immune responses of antigen-specific CD8+ T cells during malaria infection [67,68]. Creation of GAPs in these reference lines could allow better examination and evaluation of their efficacy and potency, and this requires multiple genetic manipulation of the parasite genome. Therefore, it has become increasingly important to develop a robust and versatile transfection system to both introduce genes and re-cycle selectable markers that permit subsequent transfections.

The application of reverse genetics in *P. berghei* and *P. yoelii* for generation of gene-deletion mutants or transgenic parasites is however restricted by the limited number (only 2) of drug resistance genes (permitting the selection of transformed parasites) that are currently available. This low number of selection markers hampers multiple genetic modifications in the genome of the same parasite line. In order to circumvent this problem, GFP has been utilized as a selection marker, permitting the selection of transformed parasites by flow cytometry [69,70]. In addition, a method has been developed for removing drug-selection markers from transformed *P. berghei* parasites by utilizing the yeast *fcu* (*yfcu*) selection marker and negative selection with the drug 5-fluorocytosine (5-FC) [71]. Both the selection of GFP-expressing mutants by flow cytometry and selection of marker-free mutants by negative selection have their limitations. They are laborious and time consuming, and also require the use of many extra animals as additional cloning steps in mice are required [72]. In Chapter 2, we present a novel transfection method in two rodent malaria parasites, *P. berghei* and *P. yoelii*, which generate transgenic mutants ready for subsequent genetic modification easily and quickly.

5. Outline and structure of this thesis

The main purpose of the studies described in this thesis was to generate and characterize genetically modified *P. berghei* ANKA parasites that are growth- and virulence-attenuated during blood stage development in mice. The availability of such GAP_{BS} parasites permits us to explore the possibilities for the use of these GAP_{BS} for inducing protective immune responses *in vivo* in mice. In addition, studies of infections with growth- and virulence-attenuated parasites may also provide insights into the development of protective immunity, the correlates of protection and disease, as well as increase our knowledge of parasite factors that underlie malarial pathology. This knowledge may help to frame studies that explore the use of whole blood stages of the human parasite *P. falciparum*

to induce strong and long-lasting protective immunity. Several GAP_{BS} have already been reported in both *P. yoelii* and *P. berghei* virulent strains, however the disadvantage of these GAP_{BS} is that they still result in infections with relatively high parasitemias (see Section 3.2). We therefore decided to perform a large screening study to identify additional GAP_{BS} with a more severe growth- and virulence-attenuated phenotype (see below for a rationale for the choice of the different genes we have targeted for gene deletion in order to generate GAP_{BS}).

In order to improve and speed up the generation of gene-insertion or gene-deletion mutants necessary for large screening assays, we sought to improve the existing transfection methods. In **Chapter 2**, we report on the development of a novel 'gene insertion/marker out' (GIMO) method in two rodent malaria parasites, *P. yoelii* and *P. berghei*, which uses negative selection to rapidly generate transgenic mutants ready for subsequent modifications. This method greatly simplifies and speeds up the generation of mutants expressing heterologous proteins, free of drug-resistance genes, and requires far fewer laboratory animals. It can be used to rapidly and more easily generate reporter parasites useful for phenotype characterization, and it also facilitates the generation of reporter parasites expressing multiple transgenes and GAP_{BS} in which multiple genes have been deleted. In addition to improving methods for generation of GAP_{BS}, we improved the assays for analysing *in vitro* and *in vivo* growth kinetics of GAP_{BS}. The improved protocols of these assays, which were based on published methods to analyse growth and drug-sensitivity of blood stage and liver stage parasites [62,73], are described in **Chapter 3**. These optimised assays for analysing drug-sensitivity of *Plasmodium* blood stages to newly-developed drugs are deployed by other groups and their use has also been published [74,75].

In **Chapter 4**, we present systematic gene deletion analyses of all eight *Plasmodium* rhomboid-like proteins as a means to screen for mutants with a growth- and virulence-attenuated phenotype. Rhomboid proteases cleave membrane-anchored proteins within their transmembrane domains, and in apicomplexan parasites, these substrates include molecules involved in parasite motility and host cell invasion [76-79]. Understanding the biological functions of apicomplexan rhomboids is an active area of research and the critical roles have been identified for several of these proteases in host cell invasion and pathogenesis [76-78]. Rhomboid 1 and 4 of *Plasmodium* have been reported to play critical roles in host-cell invasion [53,80,81], through cleavage of various parasite adhesins [79]. Both *P. berghei* and *P. yoelii* mutants lacking rhomboid 1 were reported to have reduced growth rate in asexual blood stages and are virulence attenuated [82,83]. To confirm this phenotype of *rhomboid 1* mutant and to identify additional growth-attenuated mutants,

we targeted all 8 rhomboid genes for deletion and characterized the phenotypes of the gene deletion mutants throughout the whole parasite life cycle.

In **Chapter 5** we present systematic gene deletion analyses for 12 enzymes with a possible role in hemoglobin digestion and hemozoin formation, including all 8 predicted hemoglobinasases in *P. berghei*. All clinical symptoms of a malaria infection are associated with growth of *Plasmodium* parasites inside RBCs, where the parasite ingests and catabolises more than half of the host hemoglobin (Hb) [84,85]. Because *Plasmodium* has a limited capacity to synthesize amino acids *de novo*, Hb digestion is believed to be essential in supplying the parasite with amino acids [86]. During Hb degradation, free heme is released, which is cytotoxic and is rapidly detoxified by the parasite through polymerization into inert crystals known as hemozoin (Hz). Hz is released into the circulation during schizont rupture and is rapidly removed by phagocytosis by cells in the liver and spleen. Upon host-cell phagocytosis, Hz cannot be further degraded and persists for some time in host tissues, and it has long been considered as a virulence factor. Indeed, the number of pigment containing leukocytes in the peripheral blood correlates with disease severity in *P. falciparum*-infected patients [87,88], and several inflammatory and immunomodulatory effects of Hz have been reported (reviewed in [89,90]). Interestingly, evidence has been presented that both *P. falciparum* and *P. berghei* mutants lacking *plasmepsin 4* have reduced Hz production and are reduced in their growth rates [32,91]. Furthermore, *P. berghei* mutants lacking *pm4* in mice are also virulence attenuated [32]. In the studies described in chapter 5 and 6, we generated additional gene deletion mutants lacking different hemoglobinasases (some in combination) to screen for mutants with a more severe reduction in growth and reduction of Hz production.

In **Chapter 6** we present experiments where we targeted a total of 41 *P. berghei* genes in this study, in order to generate genetically attenuated blood stage parasites that are growth- and virulence- attenuated (i.e. GAP_{BS}), and that may serve as immunogens and as tools to study protective immunity. Using GAP_{BS} generated in this study and studies described in Chapter 4 and 5, we examined their infection and virulence characteristics by assessing experimental cerebral malaria (ECM) in C57BL/6 mice and the development of hyper-parasitemia in BALB/c mice.

In **Chapter 7** the studies of the Chapters 2–6 are summarized and discussed, including a critical evaluation of the use of rodent malaria models for generation of GAP_{BS} and analysing their growth- and virulence-attenuated phenotypes.

Reference

1. Greenwood BM, Fidock DA, Kyle DE, Kappe SH, *et al* (2008) Malaria: progress, perils, and prospects for eradication. *J Clin Invest* 118: 1266-1276.
2. Murray CJ, Rosenfeld LC, Lim SS, Andrews KG, Foreman KJ, *et al* (2012) Global malaria mortality between 1980 and 2010: a systematic analysis. *Lancet* 379: 413-431.
3. Trape JF, Tall A, Diagne N, Ndiath O, Ly AB, *et al* (2011) Malaria morbidity and pyrethroid resistance after the introduction of insecticide-treated bednets and artemisinin-based combination therapies: a longitudinal study. *Lancet Infect Dis* 11: 925-932.
4. Alonso PL, Brown G, Arevalo-Herrera M, Binka F, Chitnis C, *et al* (2011) A research agenda to underpin malaria eradication. *PLoS Med* 8: e1000406.
5. Enayati A, Hemingway J (2010) Malaria management: past, present, and future. *Annu Rev Entomol* 55: 569-591.
6. Thera MA, Plowe CV (2012) Vaccines for malaria: how close are we? *Annu Rev Med* 63: 345-357.
7. Greenwood BM, Targett GA (2011) Malaria vaccines and the new malaria agenda. *Clin Microbiol Infect* 17: 1600-1607.
8. The malERA Consultative Group on Vaccines (2011) A research agenda for malaria eradication: vaccines. *PLoS Med* 8: e1000398.
9. Andre FE, Booy R, Bock HL, Clemens J, Datta SK, *et al* (2008) Vaccination greatly reduces disease, disability, death and inequity worldwide. *Bull World Health Organ* 86: 140-146.
10. Cox-Singh J, Davis TM, Lee KS, Shamsul SS, Matusop A, *et al* (2008) *Plasmodium knowlesi* malaria in humans is widely distributed and potentially life threatening. *Clin Infect Dis* 46: 165-171.
11. Craig AG, Grau GE, Janse C, Kazura JW, Milner D, *et al* (2012) The role of animal models for research on severe malaria. *PLoS Pathog* 8: e1002401.
12. Grau GE, Craig AG (2012) Cerebral malaria pathogenesis: revisiting parasite and host contributions. *Future Microbiol* 7: 291-302.
13. Killick-Kendrick, R and Peters, W (1978) *Rodent Malaria*. London: Academic Press Inc.
14. Engwerda C, Belnoue E, Gruner AC, Renia L (2005) Experimental models of cerebral malaria. *Curr Top Microbiol Immunol* 297: 103-143.
15. Hall N, Karras M, Raine JD, Carlton JM, Kooij TW, *et al* (2005) A comprehensive survey of the *Plasmodium* life cycle by genomic, transcriptomic, and proteomic analyses. *Science* 307: 82-86.
16. Langhorne J, Buffet P, Galinski M, Good M, Harty J, *et al* (2011) The relevance of non-human primate and rodent malaria models for humans. *Malar J* 10: 23.
17. Riley EM, Stewart VA (2013) Immune mechanisms in malaria: new insights in vaccine development. *Nat Med* 19: 168-178.
18. Ellis RD, Sagara I, Doumbo O, Wu Y (2010) Blood stage vaccines for *Plasmodium falciparum*: current status and the way forward. *Hum Vaccin* 6: 627-634.
19. Goodman AL, Draper SJ (2010) Blood-stage malaria vaccines - recent progress and future challenges. *Ann Trop Med Parasitol* 104: 189-211.
20. Agnandji ST, Lell B, Soulanoudjingar SS, Fernandes JF, Abossolo BP, *et al* (2011) First results of phase 3 trial of RTS,S/AS01 malaria vaccine in African children. *N Engl J Med* 365: 1863-1875.
21. Agnandji ST, Lell B, Fernandes JF, Abossolo BP, Methogo BG, *et al* (2012) A phase 3 trial of RTS,S/AS01 malaria vaccine in African infants. *N Engl J Med* 367: 2284-2295.
22. Hoffman SL, Billingsley PF, James E, Richman A, Loyevsky M, *et al* (2010) Development of a metabolically active, non-replicating sporozoite vaccine to prevent *Plasmodium falciparum* malaria. *Hum Vaccin* 6: 97-106.
23. Good MF (2011) A whole parasite vaccine to control the blood stages of *Plasmodium*: the case for lateral thinking. *Trends Parasitol* 27: 335-340.
24. Nussenzweig RS, Vanderberg J, Most H, Orton C (1967) Protective immunity produced by the injection of x-irradiated sporozoites of *Plasmodium berghei*. *Nature* 216: 160-162.
25. Gwadz RW, Cochrane AH, Nussenzweig V, Nussenzweig RS (1979) Preliminary studies on vaccination of rhesus monkeys with irradiated sporozoites of *Plasmodium knowlesi* and characterization of surface antigens of these parasites. *Bull World Health Organ* 57 Suppl 1: 165-173.

26. Hoffman SL, Goh LM, Luke TC, Schneider I, Le TP, *et al* (2002) Protection of humans against malaria by immunization with radiation-attenuated *Plasmodium falciparum* sporozoites. *J Infect Dis* 185: 1155-1164.
27. Butler NS, Schmidt NW, Vaughan AM, Aly AS, Kappe SH, *et al* (2011) Superior antimalarial immunity after vaccination with late liver stage-arresting genetically attenuated parasites. *Cell Host Microbe* 9: 451-462.
28. Vaughan AM, Kappe SH (2012) Malaria vaccine development: persistent challenges. *Curr Opin Immunol* 24: 324-331.
29. McCarthy JS, Good MF (2010) Whole parasite blood stage malaria vaccines: a convergence of evidence. *Hum Vaccin* 6: 114-123.
30. Pombo DJ, Lawrence G, Hirunpetcharat C, Rzepczyk C, Bryden M, *et al* (2002) Immunity to malaria after administration of ultra-low doses of red cells infected with *Plasmodium falciparum*. *Lancet* 360: 610-617.
31. Ting LM, Gissot M, Coppi A, Sinnis P, Kim K (2008) Attenuated *Plasmodium yoelii* lacking purine nucleoside phosphorylase confer protective immunity. *Nat Med* 14: 954-958.
32. Spaccapelo R, Janse CJ, Caterbi S, Franke-Fayard B, Bonilla JA, *et al* (2010) Plasmepsin 4-deficient *Plasmodium berghei* are virulence attenuated and induce protective immunity against experimental malaria. *Am J Pathol* 176: 205-217.
33. Aly AS, Downie MJ, Mamoun CB, Kappe SH (2010) Subpatent infection with nucleoside transporter 1-deficient *Plasmodium* blood stage parasites confers sterile protection against lethal malaria in mice. *Cell Microbiol* 12: 930-938.
34. Spaccapelo R, Aime E, Caterbi S, Arcidiacono P, Capuccini B, *et al* (2011) Disruption of plasmepsin-4 and merozoites surface protein-7 genes in *Plasmodium berghei* induces combined virulence-attenuated phenotype. *Sci Rep* 1: 39.
35. Khan SM, Janse CJ, Kappe SH, Mikolajczak SA (2012) Genetic engineering of attenuated malaria parasites for vaccination. *Curr Opin Biotechnol* 23(6):908-916.
36. Anders RF, Adda CG, Foley M, Norton RS (2010) Recombinant protein vaccines against the asexual blood stages of *Plasmodium falciparum*. *Hum Vaccin* 6: 39-53.
37. Anders RF (2011) The case for a subunit vaccine against malaria. *Trends Parasitol* 27: 330-334.
38. Schwartz L, Brown GV, Genton B, Moorthy VS (2012) A review of malaria vaccine clinical projects based on the WHO rainbow table. *Malar J* 11: 11.
39. Nussenzweig R, Vanderberg J, Most H (1969) Protective immunity produced by the injection of x-irradiated sporozoites of *Plasmodium berghei*. IV. Dose response, specificity and humoral immunity. *Mil Med* 134: 1176-1182.
40. Roestenberg M, Teirlinck AC, McCall MB, Teelen K, Makamdop KN, *et al* (2011) Long-term protection against malaria after experimental sporozoite inoculation: an open-label follow-up study. *Lancet* 377: 1770-1776.
41. Doolan DL, Martinez-Alier N (2006) Immune response to pre-erythrocytic stages of malaria parasites. *Curr Mol Med* 6: 169-185.
42. Clyde DF, Most H, McCarthy VC, Vanderberg JP (1973) Immunization of man against sporozoite-induced *falciparum* malaria. *Am J Med Sci* 266: 169-177.
43. Rieckmann KH, Carson PE, Beaudoin RL, Cassells JS, Sell KW (1974) Letter: Sporozoite induced immunity in man against an Ethiopian strain of *Plasmodium falciparum*. *Trans R Soc Trop Med Hyg* 68: 258-259.
44. van Dijk MR, Douradinha B, Franke-Fayard B, Heussler V, van Dooren MW, *et al* (2005) Genetically attenuated, P36p-deficient malarial sporozoites induce protective immunity and apoptosis of infected liver cells. *Proc Natl Acad Sci U S A* 102: 12194-12199.
45. Mueller AK, Labaied M, Kappe SH, Matuschewski K (2005) Genetically modified *Plasmodium* parasites as a protective experimental malaria vaccine. *Nature* 433: 164-167.
46. Mueller AK, Deckert M, Heiss K, Goetz K, Matuschewski K, *et al* (2007) Genetically attenuated *Plasmodium berghei* liver stages persist and elicit sterile protection primarily via CD8 T cells. *Am J Pathol* 171: 107-115.
47. van Schaijk BC, van Dijk MR, van de Vegte-Bolmer M, van Gemert GJ, van Dooren MW, *et al* (2006) Pfs47, paralog of the male fertility factor Pfs48/45, is a female specific surface protein in *Plasmodium falciparum*. *Mol Biochem Parasitol* 149: 216-222.

48. Epstein JE, Tewari K, Lyke KE, Sim BK, Billingsley PF, *et al* (2011) Live attenuated malaria vaccine designed to protect through hepatic CD8(+) T cell immunity. *Science* 334: 475-480.
49. Renia L, Gruner AC, Mauduit M, Snounou G (2006) Vaccination against malaria with live parasites. *Expert Rev Vaccines* 5: 473-481.
50. Amante FH, Engwerda CR, Good MF (2011) Experimental asexual blood stage malaria immunity. *Curr Protoc Immunol Chapter 19: Unit. 19.4*.
51. Engwerda CR, Minigo G, Amante FH, McCarthy JS (2012) Experimentally induced blood stage malaria infection as a tool for clinical research. *Trends Parasitol* 28: 515-521.
52. Woodberry T, Minigo G, Piera KA, Amante FH, Pinzon-Charry A, *et al* (2012) Low-level *Plasmodium falciparum* blood-stage infection causes dendritic cell apoptosis and dysfunction in healthy volunteers. *J Infect Dis* 206: 333-340.
53. Srinivasan P, Coppens I, Jacobs-Lorena M (2009) Distinct roles of *Plasmodium* rhomboid 1 in parasite development and malaria pathogenesis. *PLoS Pathog* 5: e1000262.
54. Carvalho TG, Menard R (2005) Manipulating the *Plasmodium* genome. *Curr Issues Mol Biol* 7: 39-55.
55. Janse CJ, Kroeze H, van WA, Mededovic S, Fonager J, *et al* (2011) A genotype and phenotype database of genetically modified malaria-parasites. *Trends Parasitol* 27: 31-39.
56. Balu B, Adams JH (2007) Advancements in transfection technologies for *Plasmodium*. *Int J Parasitol* 37: 1-10.
57. Heussler V, Doerig C (2006) In vivo imaging enters parasitology. *Trends Parasitol* 22: 192-195.
58. Amino R, Menard R, Frischknecht F (2005) In vivo imaging of malaria parasites--recent advances and future directions. *Curr Opin Microbiol* 8: 407-414.
59. Silvie O, Mota MM, Matuschewski K, Prudencio M (2008) Interactions of the malaria parasite and its mammalian host. *Curr Opin Microbiol* 11: 352-359.
60. Sanchez BA, Mota MM, Sultan AA, Carvalho LH (2004) *Plasmodium berghei* parasite transformed with green fluorescent protein for screening blood schizontocidal agents. *Int J Parasitol* 34: 485-490.
61. Franke-Fayard B, Trueman H, Ramesar J, Mendoza J, van der KM, *et al* (2004) A *Plasmodium berghei* reference line that constitutively expresses GFP at a high level throughout the complete life cycle. *Mol Biochem Parasitol* 137: 23-33.
62. Ploemen IH, Prudencio M, Douradinha BG, Ramesar J, Fonager J, *et al* (2009) Visualisation and quantitative analysis of the rodent malaria liver stage by real time imaging. *PLoS One* 4: e7881.
63. Spence PJ, Cunningham D, Jarra W, Lawton J, Langhorne J, *et al* (2011) Transformation of the rodent malaria parasite *Plasmodium chabaudi*. *Nat Protoc* 6: 553-561.
64. Prudencio M, Rodrigues CD, Ataide R, Mota MM (2008) Dissecting in vitro host cell infection by *Plasmodium* sporozoites using flow cytometry. *Cell Microbiol* 10: 218-224.
65. Franke-Fayard B, Janse CJ, Cunha-Rodrigues M, Ramesar J, Buscher P, *et al* (2005) Murine malaria parasite sequestration: CD36 is the major receptor, but cerebral pathology is unlinked to sequestration. *Proc Natl Acad Sci U S A* 102: 11468-11473.
66. Fonager J, Pasini EM, Braks JA, Klop O, Ramesar J, *et al* (2012) Reduced CD36-dependent tissue sequestration of *Plasmodium*-infected erythrocytes is detrimental to malaria parasite growth in vivo. *J Exp Med* 209: 93-107.
67. Miyakoda M, Kimura D, Yuda M, Chinzei Y, Shibata Y, *et al* (2008) Malaria-specific and nonspecific activation of CD8+ T cells during blood stage of *Plasmodium berghei* infection. *J Immunol* 181: 1420-1428.
68. Lundie RJ, de Koning-Ward TF, Davey GM, Nie CQ, Hansen DS, *et al* (2008) Blood-stage *Plasmodium* infection induces CD8+ T lymphocytes to parasite-expressed antigens, largely regulated by CD8alpha+ dendritic cells. *Proc Natl Acad Sci U S A* 105: 14509-14514.
69. Janse CJ, Franke-Fayard B, Mair GR, Ramesar J, Thiel C, *et al* (2006) High efficiency transfection of *Plasmodium berghei* facilitates novel selection procedures. *Mol Biochem Parasitol* 145: 60-70.
70. Janse CJ, Franke-Fayard B, Waters AP (2006) Selection by flow-sorting of genetically transformed, GFP-expressing blood stages of the rodent malaria parasite, *Plasmodium berghei*. *Nat Protoc* 1: 614-623.
71. Braks JA, Franke-Fayard B, Kroeze H, Janse CJ, Waters AP (2006) Development and application of a positive-negative selectable marker system for use in reverse genetics in *Plasmodium*. *Nucleic Acids Res* 34: e39.

72. Goldberg DE, Janse CJ, Cowman AF, Waters AP (2011) Has the time come for us to complement our malaria parasites? *Trends Parasitol* 27: 1-2.
73. Franke-Fayard B, Djokovic D, Dooren MW, Ramesar J, Waters AP, *et al* (2008) Simple and sensitive antimalarial drug screening in vitro and in vivo using transgenic luciferase expressing *Plasmodium berghei* parasites. *Int J Parasitol* 38: 1651-1662.
74. Booker ML, Bastos CM, Kramer ML, Barker RH, Jr., Skerlj R, *et al* (2010) Novel inhibitors of *Plasmodium falciparum* dihydroorotate dehydrogenase with anti-malarial activity in the mouse model. *J Biol Chem* 285: 33054-33064.
75. Barker RH, Jr., Uргаonkar S, Mazitschek R, Celatka C, Skerlj R, *et al* (2011) Aminoindoles, a novel scaffold with potent activity against *Plasmodium falciparum*. *Antimicrob Agents Chemother* 55: 2612-2622.
76. Freeman M (2009) Rhomboids: 7 years of a new protease family. *Semin Cell Dev Biol* 20: 231-239.
77. Buguliskis JS, Brossier F, Shuman J, Sibley LD (2010) Rhomboid 4 (ROM4) affects the processing of surface adhesins and facilitates host cell invasion by *Toxoplasma gondii*. *PLoS Pathog* 6: e1000858.
78. Santos M, Graindorge A, Soldati-Favre D (2011) New insights into parasite rhomboid proteases. *Mol Biochem Parasitol* 182(1-2):27-36.
79. Baker RP, Wijetilaka R, Urban S (2006) Two *Plasmodium* rhomboid proteases preferentially cleave different adhesins implicated in all invasive stages of malaria. *PLoS Pathog* 2: e113.
80. O'Donnell RA, Hackett F, Howell SA, Treeck M, Struck N, *et al* (2006) Intramembrane proteolysis mediates shedding of a key adhesin during erythrocyte invasion by the malaria parasite. *J Cell Biol* 174: 1023-1033.
81. Ejigiri I, Ragheb DRT, Pino P, Coppi A, Bennett BL, *et al* (2012) Shedding of TRAP by a Rhomboid Protease from the Malaria Sporozoite Surface Is Essential for Gliding Motility and Sporozoite Infectivity. *PLoS Pathog* 8: e1002725.
82. Srinivasan P, Coppens I, Jacobs-Lorena M (2009) Distinct roles of *Plasmodium* rhomboid 1 in parasite development and malaria pathogenesis. *PLoS Pathog* 5: e1000262.
83. Vera IM, Beatty WL, Sinnis P, Kim K (2011) *Plasmodium* protease ROM1 is important for proper formation of the parasitophorous vacuole. *PLoS Pathog* 7: e1002197.
84. BALL EG, McKEE RW, *et al* (1948) Studies on malarial parasites; chemical and metabolic changes during growth and multiplication in vivo and in vitro. *J Biol Chem* 175: 547-571.
85. Loria P, Miller S, Foley M, Tilley L (1999) Inhibition of the peroxidative degradation of haem as the basis of action of chloroquine and other quinoline antimalarials. *Biochem J* 339 (Pt 2): 363-370.
86. Divo AA, Geary TG, Davis NL, Jensen JB (1985) Nutritional requirements of *Plasmodium falciparum* in culture. I. Exogenously supplied dialyzable components necessary for continuous growth. *J Protozool* 32: 59-64.
87. Nguyen PH, Day N, Pram TD, Ferguson DJ, White NJ (1995) Intraerythrocytic malaria pigment and prognosis in severe malaria. *Trans R Soc Trop Med Hyg* 89: 200-204.
88. Amodu OK, Adeyemo AA, Olumese PE, Gbadegesin RA (1998) Intraerythrocytic malaria pigment and clinical severity of malaria in children. *Trans R Soc Trop Med Hyg* 92: 54-56.
89. Hanscheid T, Egan TJ, Grobusch MP (2007) Haemozoin: from melatonin pigment to drug target, diagnostic tool, and immune modulator. *Lancet Infect Dis* 7: 675-685.
90. Shio MT, Kassa FA, Bellemare MJ, Olivier M (2010) Innate inflammatory response to the malarial pigment hemozoin. *Microbes Infect* 12: 889-899.
91. Bonilla JA, Moura PA, Bonilla TD, Yowell CA, Fidock DA, *et al* (2007) Effects on growth, hemoglobin metabolism and paralogous gene expression resulting from disruption of genes encoding the digestive vacuole plasmepsins of *Plasmodium falciparum*. *Int J Parasitol* 37: 317-327.

CHAPTER 2

A Novel ‘Gene Insertion/Marker Out’ (GIMO) Genetic Modification Method For Transgene Expression and Complementation In Rodent Malaria Parasites

Jing-wen Lin[#], Takeshi Annoura[#], Mohammed Sajid, Séverine Chevalley-Maurel,
Jai Ramesar, Onny Klop, Blandine M.D. Franke-Fayard,
Chris J. Janse, Shahid M. Khan

[#]These authors contributed equally to this work

Leiden Malaria Research Group, Department of Parasitology, Leiden University Medical Center,
2333 ZA Leiden, The Netherlands

PLoS ONE. 2011, 6(12): e29289.

Abstract

Research on the biology of malaria parasites has greatly benefited from the application of reverse genetic technologies, in particular through the analysis of gene deletion mutants and studies on transgenic parasites that express heterologous or mutated proteins. However, transfection in *Plasmodium* is limited by the paucity of drug-selectable markers that hampers subsequent genetic modification of the same mutant. We report the development of a novel 'gene insertion/marker out' (GIMO) method for two rodent malaria parasites, which uses negative selection to rapidly generate transgenic mutants ready for subsequent modifications. We have created reference mother lines for both *P. berghei* ANKA and *P. yoelii* 17XNL that serve as recipient parasites for GIMO-transfection. Compared to existing protocols GIMO-transfection greatly simplifies and speeds up the generation of mutants expressing heterologous proteins, free of drug-resistance genes, and requires far fewer laboratory animals. In addition we demonstrate that GIMO-transfection is also a simple and fast method for genetic complementation of mutants with a gene deletion or mutation. The implementation of GIMO-transfection procedures should greatly enhance *Plasmodium* reverse-genetic research.

Introduction

Reverse genetic technologies have been widely applied to gain an understanding of the function of genes in *Plasmodium* and to provide insight into the biology of malaria parasites and interactions with their hosts (for reviews see [1–3]). The availability of efficient genetic modification technologies for the rodent malaria parasites *P. berghei* and *P. yoelii* and the possibilities for analysis of these parasites throughout the complete life cycle have made *P. berghei* and *P. yoelii* the most frequently used models for analysis of gene function [2]. Targeted disruption or mutation of genes coupled with protein tagging has provided insight into *Plasmodium* gene function and parasite protein expression, localization and transport. Reverse genetics is not only applied to understand *Plasmodium* gene function by gene deletion but is also increasingly being used to generate parasites that express heterologous proteins, for example parasites having transgenes introduced into their genome to encode fluorescent or luminescent reporter proteins. Such reporter parasites have been instrumental in the visualization and analysis of parasite-host interactions in real-time *in vitro* and *in vivo* [4–6]. The use of mutant parasites to investigate host-parasite interactions as well as parasite gene function requires genetic modification systems that are flexible and easy to perform. The application of reverse genetics in *P. berghei* and *P. yoelii* is however restricted by the limited number of drug resistance genes (permitting the selection of transformed parasites) that are currently available. This low number of selection markers hampers and slows down successive modifications in the genome of the same parasite line. Currently only two resistance gene/drug combinations exist for use in rodent malaria parasites that can be used in successive transfections, specifically *dhfr-ts*/pyrimethamine and *dhfr*/WR99210 [7]. Since both drug-selection markers confer resistance against pyrimethamine, the introduction of consecutive genetic modifications in the same parasite can only be performed by first selecting with pyrimethamine followed by WR99210 selection [7]. In order to circumvent the problem of limited drug-selection markers, GFP has been utilized as a selection marker and permits the selection of transformed *P. berghei* parasites by flow cytometry [8,9]. In addition, a method has been developed for removing drug-selection markers from transformed *P. berghei* parasites by utilizing the yeast *fcu* (*yfcu*) selection marker and negative selection with the drug 5-fluorocytosine (5-FC) [10], which kills all parasites expressing *yfcu*. In this method transformed parasites expressing the fusion gene *dhfr::yfcu* are first selected by positive selection with pyrimethamine. Subsequently, negative selection with 5-FC is applied to select for marker-free parasites that have ‘spontaneously’ lost the *dhfr::yfcu* marker from their genome, achieved by a homologous recombination/excision event around the selection cassette [10]. Both the selection of GFP-expressing mutants by flow cytometry

and selection of 'spontaneous' marker-free mutants by negative selection have their limitations. They are laborious and time consuming, and also require the use of many extra animals as additional cloning steps in mice are required; therefore these methods are not commonly used for successive genetic modifications or for complementation studies [11].

Here we report the development and application of a novel 'gene insertion/marker out' (GIMO) system for transfection of two rodent malaria parasites, *P. berghei* and *P. yoelii*. For both species we have created reference mother lines that contain the *hdhfr::yfcu* selection marker stably integrated into the silent *230p* genomic locus. We show that transfection of these mother lines with DNA-constructs that target the modified *230p* locus, followed by negative selection of transformed parasites with 5-FC is a simple and fast method to generate mutants that stably express heterologous proteins and are free of drug-selectable markers. These mother lines are therefore useful tools to generate a wide range of mutants expressing reporter and/or other heterologous proteins (under the control of different promoters) without restricting subsequent modification of the genome of these parasites. In addition, we demonstrate that GIMO-transfection is a simple and fast method to genetically complement, restoring the wild-type genotype of parasite mutants with a gene deletion or gene mutation. Importantly, GIMO transfection can be easily partnered for use with a recently developed 'recombineering' system for high-throughput, genome wide and highly efficient generation of gene targeting constructs [12].

Results

Generation of the *P. berghei* and *P. yoelii* 'gene insertion/marker out' (GIMO) mother lines

For both *P. berghei* ANKA and *P. yoelii* 17XNL transgenic parasites were generated that express a fusion of a drug resistance gene and a drug sensitivity gene, the so called positive-negative selectable marker (SM), constitutively expressed by the *P. berghei* *eef1α* promoter (Figure 1A). Specifically, these parasites contain a fusion gene of *hdhfr* (human *dihydrofolate reductase*; positive SM) and *yfcu* (yeast *cytosine deaminase* and *uridyl phosphoribosyl transferase*; negative SM) stably integrated into the *230p* locus (PBANKA_030600 in *P. berghei* and PY03857 in *P. yoelii*) through double cross-over recombination. These lines are named GIMO mother lines (gene insertion/marker out); for *P. berghei* GIMO_{PBANKA} (line 1596cl1) and for *P. yoelii* GIMO_{PY17X} (line 1923cl1). Both GIMO mother lines were cloned after transfection by positive selection with pyrimethamine.

Correct integration of the *hdhfr::yfcu* selectable marker cassette in the *230p* locus was demonstrated by PCR and Southern analyses of chromosomes separated by pulse-field gel electrophoresis (Figure 1B and C). The multiplication rate of asexual blood stages per 24 h as determined in mice infected with a single parasite [13], gametocyte production and production of oocysts and sporozoites were identical to those of the parent *P. berghei* and *P. yoelii* lines (data not shown). These GIMO mother lines are used for introduction of transgenes into the modified *230p* locus through transfection with constructs that target the *230p* locus. These constructs insert into the *230p* locus ('gene insertion'), thereby removing the *hdhfr::yfcu* selectable marker ('marker out') from the genome of the mother lines. Transgenic parasites that are marker-free are subsequently selected by applying negative drug selection using 5-FC (see below).

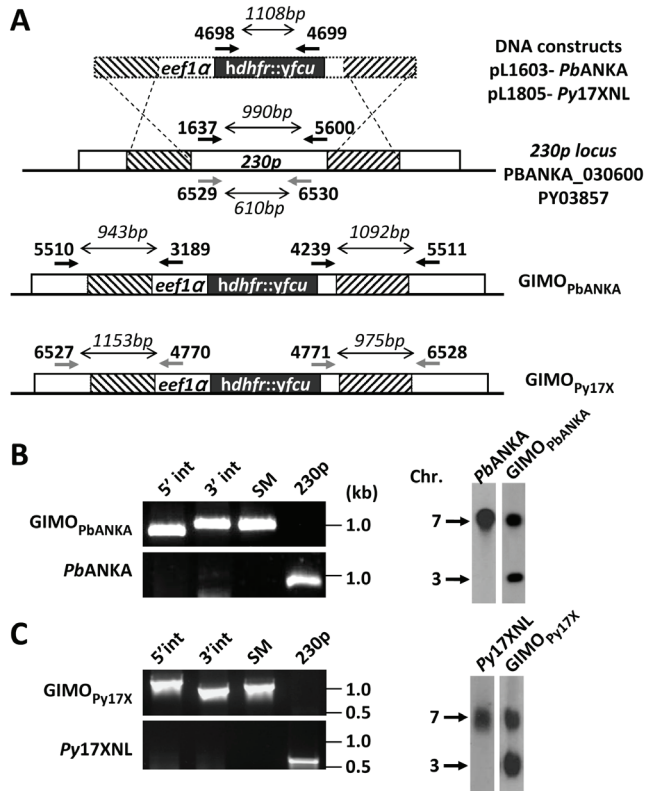


Figure 1. Generation and genotype analyses of *P. berghei* and *P. yoelii* GIMO mother lines.

A. Schematic representation of the constructs used to introduce the positive-negative selectable marker cassette in the *P. berghei* (*PbANKA*) or *P. yoelii* (*Py17XNL*) *230p* locus. DNA constructs pL1603 (targeting *P. berghei* *230p*, PBANKA_030600) and pL1805 (targeting *P. yoelii* *230p*, PY03857) containing a fusion of the positive drug selectable marker *hdhfr* (human *dihydrofolate reductase*) and negative marker *yfcu* (yeast *cytosine deaminase*)

and *uridyl phosphoribosyl transferase*) under the control of the *eef1α* promoter target the *230p* locus at the target regions (hatched boxes) by double cross-over homologous recombination. Location of primers used for PCR analysis and sizes of PCR products are shown (see Table S2 for all primer sequences).

B. Diagnostic PCR and Southern analysis of PFG-separated chromosomes confirming correct integration of the construct in the *P. berghei* mother line GIMO_{PbANKA}: 5' integration PCR (5' int; primers 5510/3189), 3' integration PCR (3' int; primers 4239/5511), amplification of *hdhfr::yfcu* marker (SM; primers 4698/4699) and the original *P. berghei 230p* (230p; primers 1637/5600). Primer location (black arrows) and product sizes are shown in **A**. For Southern analysis, PFG-separated chromosome were hybridized using a 3'UTR *pbdhfr* probe that recognizes the construct integrated into *P. berghei 230p* locus on chromosome 3 and the endogenous locus of *dhfr/ts* on chromosome 7.

C. Diagnostic PCR and Southern analysis of PFG-separated chromosomes confirming correct integration of the construct in the *P. yoelii* mother line GIMO_{Pv17x}: 5' integration PCR (primers 6527/4770), 3' integration PCR (primers 4771/6528), amplification of *hdhfr::yfcu* marker (primers 4698/4699) and the *P. yoelii 230p* original locus (primers 6529/6530). Primer location (grey arrows) and product sizes are shown in **A**. For Southern analysis, chromosomal hybridization using a 3'UTR *pbdhfr* probe recognizes the construct integrated into *P. yoelii 230p* locus on chromosome 3 and the endogenous locus of *dhfr/ts* on chromosome 7.

Assessing the efficiency of GIMO-transfection to select transgene expressing, drug-selectable marker-free *P. berghei* parasites

We generated a test DNA-construct containing a transgene expression-cassette to test the efficiency of selection of transgenic mutants through the application of negative selection using 5-FC after transfection into the GIMO_{PbANKA} mother line. This construct contains the *mCherry* gene under the control of the constitutive *eef1α* promoter and *230p* targeting sequences (Figure 2A) and lacks a drug selectable marker cassette. This DNA-construct, pL1628, targets the same regions in the *230p* locus in which *hdhfr::yfcu* selection cassette was introduced in the GIMO_{PbANKA} mother line (Figure 2A). Transfection of GIMO_{PbANKA} (exp. 1645) was performed using standard procedures [14] except that after transfection negative drug selection was applied instead of positive drug selection. This negative selection was performed by treating mice that were infected with transfected parasites with the drug 5-FC for 4 consecutive days (one dose per day of 10 mg), starting 24 hours after transfection.

Transfected parasites of line 1645 were collected at day 7 and 8 after transfection (at a parasitemia of 0.5–3%) for phenotype and genotype analyses. Diagnostic PCR and Southern analysis of separated chromosomes confirmed the correct integration of the test construct and simultaneous removal of the *hdhfr::yfcu* selection cassette (Figure 2B). Analysis of mCherry expression by fluorescence microscopy in blood stage parasites of line 1645 showed that >90% of the parasites expressed mCherry (Figure 2C). Quantification of the percentage of mCherry-expressing parasites was performed by FACS analysis of mature schizonts collected from overnight blood stage cultures. Expression of transgenes, such as *mCherry*, under the control of the *eef1α* promoter increases with the maturation

of parasites inside blood cells and therefore FACS quantification is improved by analysing mature schizont stages (these stages are selected based on Hoechst-fluorescence) [15]. FACS analysis confirmed that > 90% (93%±1.1 Figure 2D) of the schizonts were mCherry positive. Since episomal constructs cannot be maintained during selection in GIMO-transfected parasites (see Discussion), these analyses demonstrate that GIMO-transfection permits the selection parasites that express transgenes and are marker-free.

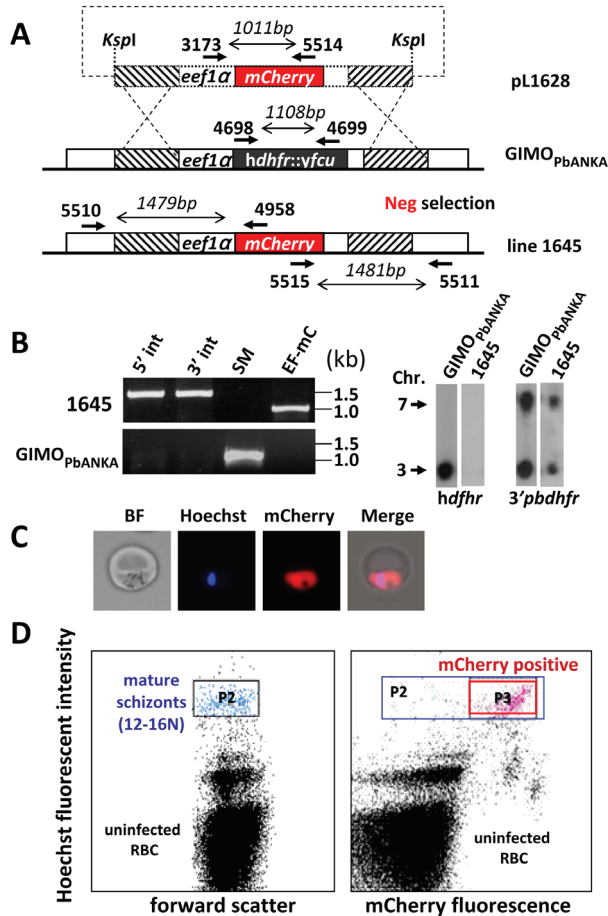


Figure 2. Generation of a marker-free mCherry-expressing parasite using GIMO-transfection

A. Schematic representation of the introduction of a mCherry-expression cassette into the GIMO_{PbANKA} mother line. Construct pL1628 containing the *eef1α*-mCherry-3'*pbdhfr* cassette (mCherry; red box) is integrated into the modified *P. berghei* 230p locus containing the *hdhfr::yfcu* selectable marker cassette (black box) by double cross-over homologous recombination at the target regions (hatched boxes). Negative (Neg) selection with 5-FC selects for parasites (line 1645) that have mCherry reporter introduced into the genome and the *hdhfr::yfcu* marker removed. Location of primers used for PCR analysis and sizes of PCR products are shown (see

Supplementary Table S2 for primer sequences).

B. Diagnostic PCRs and Southern analysis of PFG-separated chromosomes confirms the correct integration of construct pL1628 in line 1645 parasites shown by the absence of the *hdhfr::yfcu* marker and the presence of the *mCherry* gene: 5' integration PCR (5' int; primers 5510/4958), 3' integration PCR (3' int; primers 5515/5511), amplification of *hdhfr::yfcu* (SM; primers 4698/4699) and the *eef1 α -mCherry* (EF-mC; primers 3173/5514). Primer locations and product sizes are shown in **A**. (primer sequences in Supplementary Table S2). Hybridization of separated chromosomes of GIMO_{PbANKA} and line 1645 using a *hdhfr* probe recognizes the *hdhfr::yfcu* marker in the *230p* locus on chromosome 3 in GIMO_{PbANKA} but is absent in line 1645. Hybridization with 3'UTR *dhfr* probe recognizes both modified the *230p* locus on chromosome 3 (both marker and *mCherry* expression cassettes contain the 3'*pbdhfr* sequence) and the endogenous *dhfr/ts* gene on chromosome 7 as loading control.

C. Fluorescence microscopy of a live mCherry-expressing trophozoite of line 1645; bright field (BF), DNA staining (Hoechst; Blue) and mCherry expression (red).

D. FACS analysis of mCherry-expressing blood stages of line 1645. The percentage of mCherry-expressing parasites was performed by FACS analysis on cultured blood stage. Mature schizonts (12–16N) were selected based on their Hoechst fluorescent intensity (gate P2) and mCherry-expressing schizonts were selected in gate P3 (right panel).

To further investigate the efficiency of the GIMO system, we performed a set of independent transfections with the DNA-construct pL1628 (exp. 1794–1799) in the GIMO_{PbANKA} mother line. In these experiments transfected parasites were selected using negative selection as described above and mCherry expression analysed by FACS (Figure 3A). In 5 out of 6 transfection experiments, the percentage of mCherry-expressing parasites was higher than 75%, whereas in one experiment (exp. 1798) 32% of schizonts were mCherry positive (Figure 3A). The presence of mCherry negative parasites in the drug-selected population indicates that non-transformed parasites survived the drug-selection but presumably still carry the *hdhfr::yfcu* cassette. We therefore analysed the genotype of the selected populations of all experiments by quantitative real-time PCR (qPCR) and Southern analysis of separated chromosomes to determine the ratio between parasites with and without *hdhfr::yfcu*. For qPCR, C_t values of amplification of mCherry, *hdhfr::yfcu* and the control *hsp70* gene were determined and the percentage of mCherry positive parasites was calculated as the relative ratio between *mCherry* and *hdhfr::yfcu* using the $2^{-\Delta\Delta C_t}$ method [16]. The percentage of mCherry positive parasites based on qPCR correlated well with the percentage determined by FACS analysis (Figure 3A). Southern analysis also showed that in the selected populations a low percentage of parasites still contain the *hdhfr::yfcu* gene (Figure 3B). These observations indicate that the application of negative selection after transfection of GIMO_{PbANKA}, while it highly enriches for transformed parasites, it does not generate a pure population of marker-free parasites. Therefore, parasite cloning after negative selection is an essential step in GIMO-transfection in order to obtain correctly transformed parasites that express the transgene and are drug-selectable marker free.

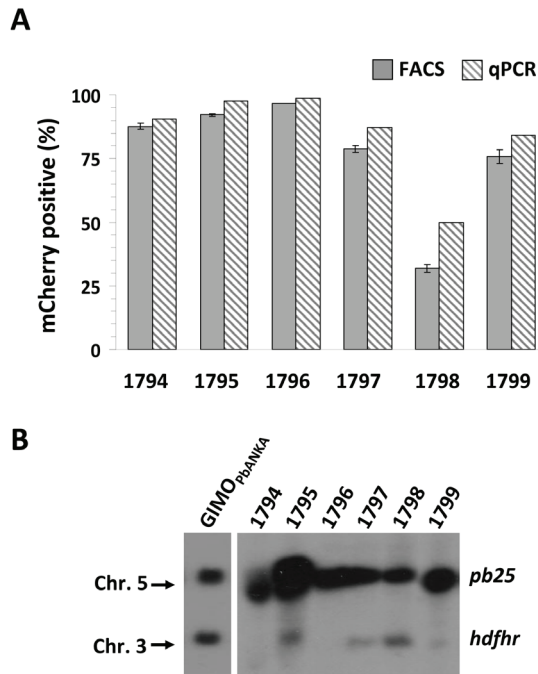


Figure 3. The efficiency of GIMO-transfection to select marker-free parasites that express mCherry.

A. Percentage of mCherry-positive parasites in GIMO-transfection of GIMO_{PBANKA} (shown in Figure 2) after negative selection. The percentage of mCherry-positive parasites in six independent transfections (1794–1799) was determined by FACS analysis (see Figure 2D) and quantitative PCR (qPCR). By qPCR the ratio of mCherry and *hdhfr::yfcu* marker positive parasites was determined relative to the presence of a control gene *hsp70*, using the $2^{-\Delta\Delta CT}$ method (primers used in qPCR are described in Table S2).

B. Efficiency of selection of *hdhfr::yfcu* marker-free determined by Southern analysis of PFG-separated chromosomes. Hybridization performed using a mixture of two probes, one specific for *pb25* (chromosome 5) and one for *hdhfr* (chromosome 3) showing the efficiency of selecting *hdhfr::yfcu* marker-free parasites in the different experiments.

Generation of a *P. yoelii* reporter line, *PyGFP-luc_{con}*, which is marker-free and expresses a GFP-luciferase fusion protein, by GIMO-transfection

The application of negative selection to genetic modification of *P. yoelii* has not been reported. To test the possibility to select *P. yoelii* parasites lacking *hdhfr::yfcu* from a population of *hdhfr::yfcu*-containing parasites by negative selection, we generated a construct (pL1847) that targets the modified *py230p* locus of the GIMO_{Py17X} mother line by double cross-over homologous recombination. Plasmid pL1847 contains a fusion gene of *gfp* and *luciferase* under the control of the *P. berghei eef1 α* promoter (Figure 4A). Integration of this construct will result in the introduction of the *gfp-luc* expression cassette and a simultaneous removal of the *hdhfr::yfcu* gene from GIMO_{Py17X}

(Figure 4A). Transfection of GIMO_{Py17X} parasites and negative selection was performed as described above for GIMO_{PbANKA}. Comparable to results obtained with the transfection of GIMO_{PbANKA}, two mice (exp. 1970 & 1971) that were infected with GIMO_{Py17X} transfected parasites became positive at day 6 (parasitemia 1–2%) after selection with the drug 5-FC. Analysis by fluorescence microscopy showed that ~30% and ~70% of the parasites of line 1970 and 1971, respectively, were GFP positive (Figure 4B). Southern analysis of PFG-separated chromosomes confirmed that most drug-selected parasites of line 1971 had removed the *hdhfr::yfcu* selectable marker (Figure 4C). We obtained three clones of line 1971 and all three expressed luciferase as shown by *in vivo* imaging of mice infected with 1971cl1–3 blood stages parasites (Figure 4D). PCR analysis confirmed the correct integration of the fusion gene *gfp-luciferase* and removal of *hdhfr::yfcu* (Figure 4E). The results demonstrate that GIMO-transfection and the negative selection procedure can

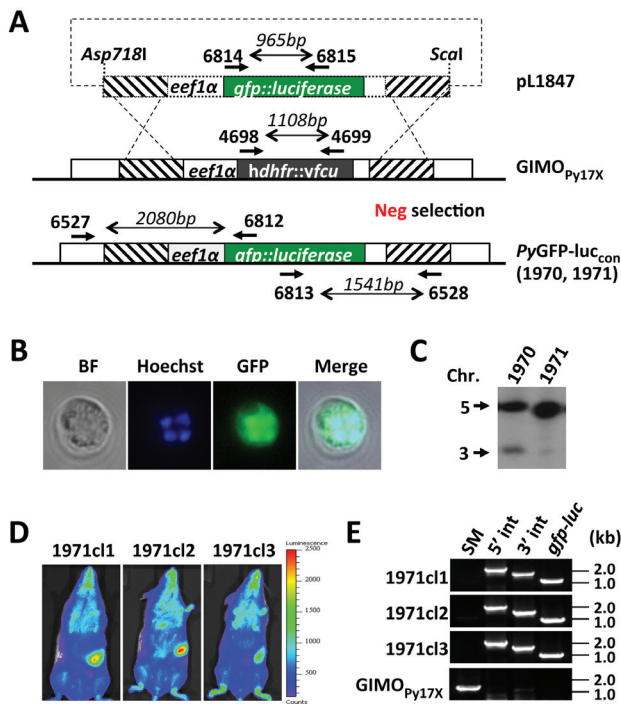


Figure 4. Generation of a *P. yoelii* reporter line, PyGFP-luc_{con} that is marker-free and expresses a fusion protein of GFP and luciferase.

A. Schematic representation of the introduction of a *gfp-luciferase* expression cassette into the GIMO_{Py17X} mother line. Construct pL1847 containing the *eef1α-gfp::luciferase-3'pbdhfr* cassette is integrated into the modified *P. yoelii* 230p locus containing the *hdhfr::yfcu* selectable marker cassette (black box) by double cross-over homologous recombination at the target regions (hatched boxes). Negative selection with 5-FC results in selection of parasites that have the *gfp-luciferase* reporter introduced into the genome and the *hdhfr::yfcu*

marker removed. Location of primers used for PCR analysis and sizes of PCR products are shown (see Table S2 for primer sequences).

B. Fluorescence microscopy of a live schizont of *PyGFP-luc_{con}*; bright field (BF), DNA staining (Hoechst; Blue) and GFP expression (green).

C. PFG-separated chromosomal Southern analysis of two independent GIMO transfection parasite lines (exp. 1970 and 1971). Hybridization performed with a mixture of two probes, one specific for *pb25* (chromosome 5) and the other for *hdhfr::yfcu* (chromosome 3), demonstrating the efficiency of selection of *hdhfr::yfcu* 'marker-free' parasites in the different experiments.

D. Analysis of luciferase-expression of blood stages of 3 clones of *PyGFP-luc_{con}* (exp. 1971). Luciferase-activity was measured by real time *in vivo* imaging of live mice with a parasitemia of 1–3%.

E. Diagnostic PCR analysis confirming correct integration of the *gfp-luciferase* gene in *PyGFP-luc_{con}* clones (exp. 1971): amplification of *hdhfr::yfcu* marker (SM, primers 4698/4699), 5' integration PCR (5' int, primers 6527/6812), 3' integration PCR (3' int, primers 6813/6528) and *gfp-luc* (primers 6814/6815). Primer location, product sizes are shown in **A.** and primer sequences in Table S2.

be applied to *P. yoelii* in order to generate parasites that express transgenes and are free of drug-selectable markers. In addition, these marker-free *P. yoelii* 1971 cloned lines (*PyGFP-luc_{con}*), are excellent tools to quantitatively analyse *P. yoelii* development in blood and liver stages using both *in vivo* and *in vitro* luminescent assays as has been achieved with *P. berghei* reporter parasites [17,18].

GIMO-transfection is a rapid and simple method for gene complementation

Gene complementation is used to prove that the phenotype of a gene deletion/modified parasite is the direct result of the gene mutation and not a consequence of an unintended alteration of the parasites genome [11]. Complementation is performed by reintroduction of a wild-type copy of the gene into the genome of a mutant in order to restore the wild-type phenotype, thereby establishing the association of the phenotype to the deletion genotype. We analysed whether GIMO-transfection can be used for gene complementation using a published gene deletion mutant of *P. berghei* with a defined phenotype. Complementation of a mutant using GIMO-transfection requires that the mutant contain the negative selectable marker *yfcu* in its genome. We therefore choose to complement a *P. berghei* mutant (Δ *gr*) which lacks expression of glutathione reductase [19]. In this mutant, the *glutathione reductase* (*gr*) has been deleted using a construct containing the *hdhfr::yfcu* marker and the mutant becomes arrested in the mosquito during oocyst development with a complete absence of sporozoite production [19]. For complementation of the Δ *gr* mutant we generated a restoration DNA-construct by simply amplifying the *gr* gene from wild-type *P. berghei* genomic DNA and therefore avoided any cloning steps. Using the same primers that amplified the 5' and 3' targeting

regions for the DNA construct used to generate the Δgr gene deletion mutant [19] (See Supplementary Table S1), specifically the forward primer of 5' targeting region and reverse primer of 3' targeting region, a 2.8kb PCR product that contained the complete *gr* gene and both targeting regions was amplified by a high fidelity proof reading polymerase (see Figure 5A). This PCR product was used to transfect Δgr parasites, with the aim to introduce the complete *gr* gene ('gene insertion') and thereby replacing the deleted *gr* locus, containing the *hdhfr::yfcu* ('marker out') as shown in Figure 5A. Selection of transfected parasites, using negative selection was as described above for other GIMO-transfections, and resulted in the selection of parasites (exp. 1761; $\Delta gr(+gr)$) in which the deleted *gr* had been replaced by the wild-type *gr* gene as confirmed by both diagnostic PCR and Southern analysis of digested genomic DNA (Figure 5B). We next analysed the phenotype of the complemented $\Delta gr(+gr)$ parasites by comparing oocyst and sporozoite development of $\Delta gr(+gr)$ and Δgr parasites in *Anopheles stephensi* mosquitoes. As previously reported [19], Δgr produced oocysts that abort development resulting in small degenerated oocysts without any signs of sporoblast or sporozoite formation (Figure 5C) at day 12 post infection (p.i.). The Δgr infected mosquitoes are not able to infect naive mice at day 21 p.i. In contrast, the complemented $\Delta gr(+gr)$ have normal development in mosquitoes producing normal sized mature oocysts, which contain sporozoites at day 12 p.i. and salivary glands contained sporozoites at day 21 p.i. (Figure 5D). The $\Delta gr(+gr)$ sporozoites are infectious as shown by injection of 10^4 salivary gland sporozoites in two naïve Swiss mice. Both mice developed a blood stage infection with a prepatency period of 5 days which is comparable to the prepatency of mice infected with 10^4 wild type sporozoites. Genotype analysis of $\Delta gr(+gr)$ blood stage parasites after mosquito passage and sporozoite infection, by diagnostic PCR and Southern analysis of digested genomic DNA, confirmed that *gr* was indeed restored (i.e. complemented) in the $\Delta gr(+gr)$ parasites and no deletion mutants were present (Figure 5B). The restoration of the phenotype of Δgr parasites using a PCR-amplified construct in combination with negative selection demonstrates that GIMO transfection is a fast method for gene complementation (see also the Discussion section). In addition it is a relatively simple method, requiring only PCR-amplified DNA-constructs that can be used as the constructs do not require a drug-selectable marker cassette.

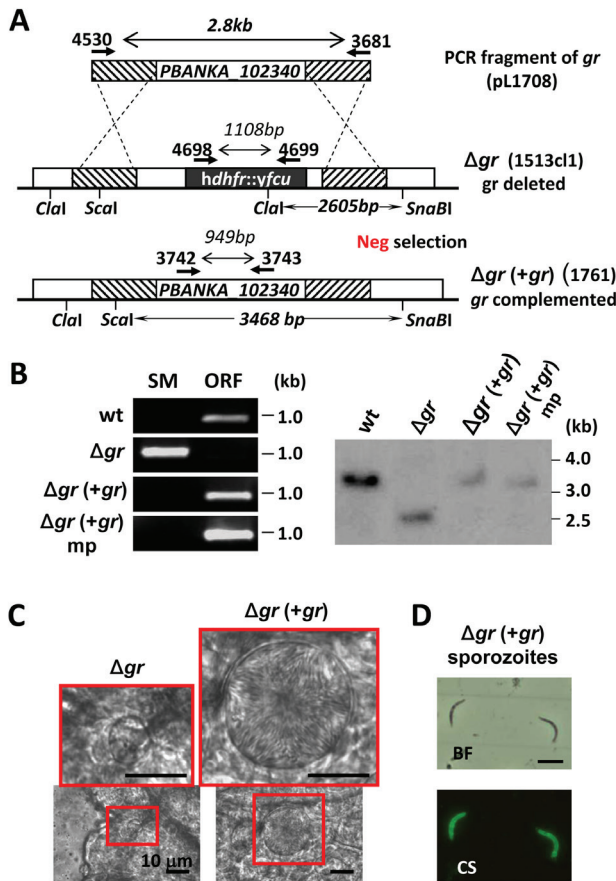


Figure 5. Gene complementation using GIMO-transfection.

A. Schematic representation of the re-introduction of the glutathione reductase (*gr*) gene into the *gr* gene deletion mutant (Δgr , 1513c1); 1513c1 expresses the *hdhfr::yfcu* selectable marker (black box). Transfection with a 2.8kb PCR-fragment amplified from wild type genomic DNA (primers 4530/3681) containing the *gr* gene, as well as the 5'- and 3'-targeting sequences, was used to re-introduce *gr* gene into the Δgr mutant. Negative selection with 5-FC selects for parasites that have the *gr* gene re-introduced into the genome replacing the *hdhfr::yfcu* marker (line 1761; Δgr (+*gr*)). Location of primers used for PCR analysis, sizes of PCR products, restriction enzyme sites and sizes of the expected fragments in Southern analysis are indicated (see Table S1 and S2 for primer sequences).

B. Diagnostic PCR analysis and Southern analysis of restricted genomic DNA confirm correct integration of the PCR fragment and complementation in Δgr (+*gr*) parasites: amplification of *hdhfr::yfcu* marker (SM; primers 4698/4699) and *gr* (ORF; primers 3742/3743). Primer location, product sizes are shown in **A.** and primer sequences in Table S2. Southern blot was hybridized with 3'UTR *gr* probe (i.e. 3' targeting region). The localization of the restriction enzymes used and the expected size of the fragments are shown in **A.**: wt (wild type); Δgr (*gr* deletion mutants); Δgr (+*gr*) (complemented Δgr); mp (blood stages after mosquito passage).

C. Oocyst development of Δgr and Δgr (+*gr*) parasites. Only small, aberrant oocysts with no signs of sporozoite formation are present in Δgr infected mosquitoes at days 10–21 after feeding. In Δgr (+*gr*) infected mosquitoes sporozoite-containing oocysts with wild-type morphology are visible at day 12.

D. Salivary gland sporozoites of $\Delta gr(+gr)$ examined by immuno-fluorescence microscopy: bright field (BF) and anti-CS antibody staining (CS, green).

Discussion

Genetic modification of malaria parasites is limited by the paucity of drug-selection markers that permit selection of transformed mutants, which in turn hampers the generation of multiple genetic modifications in the same mutant. The novel GIMO-transfection method reported in this study permits the generation of mutants stably expressing heterologous proteins free of drug-selectable markers, facilitating further genetic modification of the transgenic parasites. In addition, it provides a fast and simple way for gene complementation of gene deletion/mutation mutants. We have generated reference mother lines and standard 'knock-in' constructs for both *P. berghei* ANKA and *P. yoelii* 17XNL, which we will make available for the research community. In GIMO-transfection of these mother lines, transgenes are introduced in the *230p* locus of both *P. berghei* and *P. yoelii*. For *P. berghei* ANKA it has been shown that *230p* is a 'silent' locus [20] and different reporter lines with transgenes introduced in this locus has been generated that show wild-type progression through the complete life-cycle [8,21]. Whether *230p* is also a 'silent' locus in *P. yoelii* has not been reported before. Our observations of normal development of asexual stages, mosquito development and sporozoite infectivity of the *P. yoelii* mother line and *PyGFP-luc_{con}* indicates that *p230* is also a suitable locus to introduce transgenes in *P. yoelii*.

Several *P. berghei* reference lines exist that express reporter proteins, such as GFP and luciferase, and do not contain drug-selection markers. Most of these parasites have been obtained by FACS-sorting where GFP expression is used as the selectable marker [8,9]. However, selection of transgenic fluorescent-expressing parasites by FACS-sorting has been only reported for selecting GFP-expressing parasites and not with parasites that express other fluorescent proteins. In our hands, FACS-sorting of GFP-expressing parasites is not a highly efficient selection method as often the selected population consists of both mutant and wild type parasites. Moreover, introducing a GFP-selection cassette increases the size of the transfection construct. This limits the size of the heterologous DNA that can be cloned into these vectors as it is difficult to maintain *Plasmodium* transfection vectors with a size larger than 14kb in *E. coli*. Therefore, in comparison with FACS-sorting, the GIMO-transfection system is a more flexible and simpler system to introduce a wide range of heterologous genes into the parasite genome with the additional advantage that GIMO transfection constructs are far smaller since a selection-marker cassette is not required.

In addition to the use of FACS-sorting for the generation of marker-free *P. berghei* mutants a 'marker-recycling' method has also been employed in *P. berghei* [10]. Specifically, transformed parasites expressing the fusion gene *dhfr::yfcu* are first selected by positive selection with pyrimethamine; subsequently negative selection with 5-FC is applied to select parasites that have lost the resistance genes. The efficiency of selection of marker-free parasites is dependent on the frequency of the loss of the *dhfr::yfcu* marker from the genome by homologous recombination and excision [10]. This method has been successfully used to generate marker-free reporter lines [22], to introduce two independent genetic modifications in the same parasite lines [22–24] and for complementation [10]. However, this marker-recycling method is relatively laborious and time consuming since it involves both positive and negative selection procedures and two parasite-cloning steps, a procedure requiring at least 9 weeks to complete. Further, marker-recycling method requires at least 24 mice in order to obtain a marker-free mutant (Figure 6A), in part a consequence of essential cloning procedures [19,22]. In contrast, the generation of marker-free mutants with GIMO-transfection can be achieved in only 4 weeks and requires only 11 mice (Figure 6A). The marker-recycling transfection constructs consist of the *dhfr::yfcu* drug-selectable marker cassette, a transgene expression and two targeting sequences for integration into the genome (See Supplementary Figure S2A). In addition, they have two identical regions of DNA sequence that can recombine (in the parasite genome) and excise the selectable marker cassette. In contrast the GIMO-constructs contain only the two genome targeting sequences and the transgene expression cassette (see Supplementary Figure S2 for a comparison of the marker-recycling and GIMO constructs). The simple structure of GIMO constructs permits the cloning of larger transgenes (the GIMO constructs are smaller as the selectable marker cassette is absent) and improves the retention of plasmids in bacteria as internally repetitive regions of AT-rich *Plasmodium* DNA are absent. Further, after transfection with the GIMO construct, the selection of integration mutants is improved as no episomal construct DNA is maintained in the parasites and negative selection kills parasites expressing *yfcu*.

GIMO-transfection is dependent on the transgene-expression construct replacing the *dhfr::yfcu* selection cassette present in the mother line genome and the efficiency of the drug 5-FC to kill all parasites where this integration has not occurred and that are still expressing *yFCU*. Interestingly, in both *P. berghei* and *P. yoelii* GIMO-transfection experiments we always observed that populations of 5-FC selected parasites contain (low numbers of) parasites that still have the *dhfr::yfcu* selection cassette in their genome. Further research is required to determine whether these parasites express *yFCU* but are able to survive 5-FC drug treatment or if these parasites have lost expression of *yFCU*

through the mutation of *hdhfr::yfcu* selectable marker cassette. Experiments in our laboratory are now focused on improving the application of negative selection to mutant parasites in mice by providing 5-FC in the drinking water, which may permit treatment with higher concentrations of 5-FC and for longer periods. Notwithstanding the presence

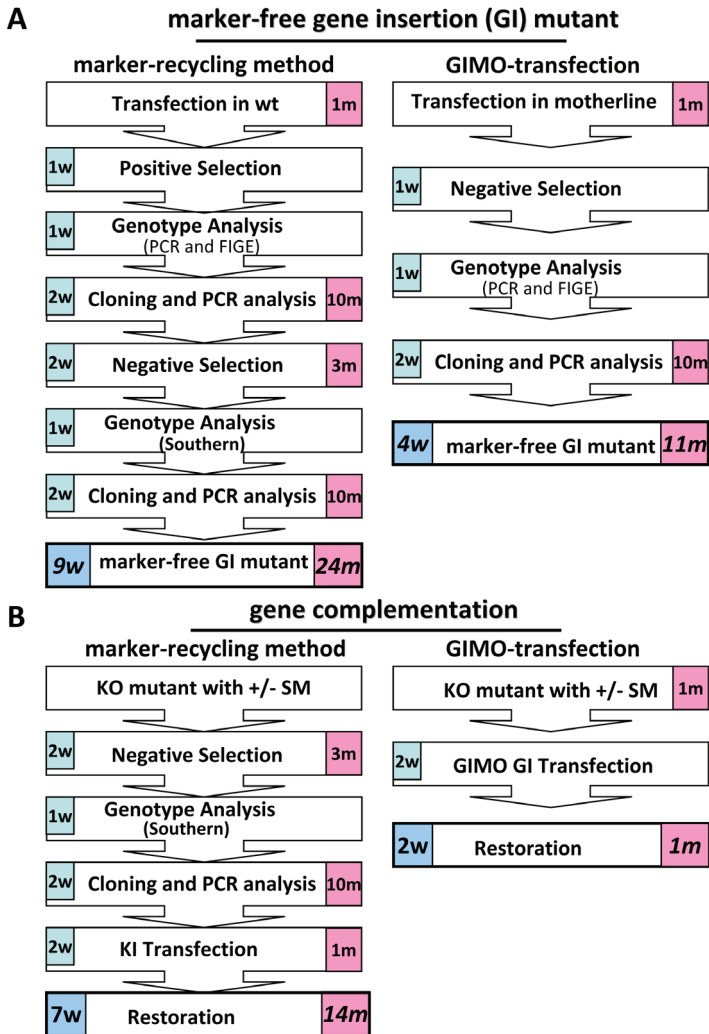


Figure 6. Compared to the marker-recycling method GIMO-transfection is faster and requires fewer animals to both generate marker-free gene insertion (GI) mutants and to complement gene deletion mutants.

A. Number of weeks (w) and number of mice (m) needed to generate ‘marker-free’ gene insertion mutants expressing transgenes using GIMO-transfection (right) and using the marker-recycling method (left).

B. Number of weeks (w) and number of mice (m) needed for complementation of a gene deletion mutant using GIMO-transfection (right) and using the marker-recycling method (left).

of non-transformed parasites after selection of GIMO-transfected parasites, the high percentages of transformed parasites in the populations permit the collection of the desired mutants by cloning. Using GIMO- transfection we have already been able to successfully generate multiple marker-free lines that express a variety of heterologous proteins (unpublished data JWL and SK).

GIMO-transfection was used to generate a *P. yoelii* GFP-luciferase reporter parasite and is the first report describing the use of negative selection with 5-FC in combination with the yFCU marker for genetic modification of this parasite species. Moreover, the PyGFP-luc_{con} line is the first *P. yoelii* reporter line that is marker-free and can be easily further genetically modified. Similar *P. berghei* reporter lines have been used to visualize and quantify host parasite interactions *in vivo* [13,21,25,26], analysis of drug-susceptibility [17,27,28] and *in vivo* quantification of liver stage development [18,29].

In this study we demonstrate that GIMO-transfection can not only be used to introduce heterologous genes but also is a fast and simple method for gene complementation. Restoration of the wild type phenotype by gene complementation is the most optimal strategy to show that a mutant phenotype is the result of the intended deletion (or mutation) and is not due to unrelated alterations in the parasite genome [2,11]. Genetic complementation has not been widely applied in *Plasmodium* due to difficulties in making successive genetic modifications in the same parasite, and to problems inherent in cloning full-length AT-rich *Plasmodium* genes into bacterial plasmid vectors [11]. Till now two methods have been used to complement gene deletion mutants in *P. berghei*. The first method re-introduces the wild-type gene using a construct containing *hdhfr* as a positive selectable marker [30,31]. The encoded protein confers resistance to WR99210, and can be used to transfect gene deletion mutants that already contain the pyrimethamine resistance markers *dhfr/ts* from *P. berghei* or the *dhfr* from *Toxoplasma gondii* (*tgdhfr*) [7]. However, selection with WR99210 is not straightforward because of problems with dissolving this drug and because there is a reduced sensitivity to WR99210 of parasites that already contain the *dhfr/ts* or *tgdhfr* marker [7,10] (unpublished observations CJJ). The second complementation method is based on the marker-recycling, as described above. Gene deletion mutants (containing *hdhfr::yfcu*) are first subjected to negative selection to select for marker-free parasites, cloned and then transfection is performed with constructs containing the gene for complementation and a drug selection cassette [10] (see Supplementary Figure S3A). This method requires generally 7 weeks and 14 mice to perform (Figure 6B). In contrast, complementation with GIMO-transfection takes only 2 weeks and 1 mouse (Figure 6B). Not only is the GIMO method much faster, requiring far fewer mice, but also a big advantage is that a simple PCR amplicon containing the

wild-type gene can be used for complementation as no drug selectable needs to be used in the construct (see Supplementary Figure S3 for schematics of the marker-recycling and GIMO methods).

In summary, we have developed a novel method that simplifies and speeds up both the generation of marker-free parasites expressing heterologous proteins and for the genetic complementation of gene deletion/mutation mutants. Moreover the application of this method greatly reduces the numbers of animals required to generate and complement mutants. We have also generated the first marker-free *P. yoelii* reporter line and established the successful use of negative selection in transfection of *P. yoelii* parasites. The GIMO-transfection is a simple, fast and efficient approach to generate mutants permissive to subsequent genetic modification. Therefore we recommend that, where possible, transfection of *P. berghei* and *P. yoelii* parasites be performed with constructs that contain the positive-negative selectable marker cassette, *hdhfr::yfcu*. The presence of this marker in mutants permits subsequent GIMO transfection that not only simplifies the creation of additional deletions or modifications but also gene complementation experiments. A recent study has reported high-throughput, genome wide and highly efficient 'recombineering' system, for high-throughput, genome wide and highly efficient generation of gene targeting constructs [12]. This exciting development can be partnered with GIMO transfection by ensuring all these targeting constructs have a positive-negative (*hdhfr::yfcu*) selectable marker cassette. Consequently all resulting mutants would be receptive to GIMO transfection thereby permitting further modification (e.g. reporter protein expression) and complementation.

Materials and Methods

Experimental animals and parasites

Female Swiss OF1 mice (6–8 weeks old; Charles River/Janvier) were used. All animal experiments of this study were approved by the Animal Experiments Committee of the Leiden University Medical Center (DEC 07171; DEC 10099). The Dutch Experiments on Animal Act is established under European guidelines (EU directive no. 86/609/EEC regarding the Protection of Animals used for Experimental and Other Scientific Purposes). Two reference rodent malaria parasite lines were used: *P. berghei* ANKA line cl15cy1 [14] and *P. yoelii* 17XNL (clone 1.1) parasite line [32].

Generation of GIMO mother lines in *P. berghei* ANKA and *P. yoelii* 17XNL

To generate the GIMO mother line in *P. berghei*, a DNA-construct pL1603 was generated

for integration into the *230p* gene (PBANKA_030600) by cloning the 5' and 3' regions of *230p* as previously described [8]. The targeting sequences were amplified from genomic DNA using primer sets 5585/5586 and 5587/5588 (See Table S1 for the sequence of all primers) and cloned into the restriction sites of HindIII/KspI and Asp718I/EcoRI of the standard cloning vector pL0034 (MRA-849, www.mr4.org), which contains the *hdhfr::yfcu* selectable marker under the control of the *eef1 α* promoter [10]. The *hdhfr::yfcu* marker is a fusion gene of the positive selection marker human *dihydrofolate reductase* and the negative selection marker which is a fusion gene of yeast *cytosine deaminase* and *uridyl phosphoribosyl transferase* [10]. Prior to transfection the DNA-construct pL1603 was linearized with HindIII and EcoRI.

To generate the GIMO mother line in *P. yoelii*, a modified two step PCR method [33] was used to generate DNA-construct pL1805 for integration into the *230p* gene (PY03857) of *P. yoelii* (Figure S1A). In the first PCR reaction two fragments (5'- and 3'- targeting sequences, both ~1kb) of *230p* were amplified from *P. yoelii* 17XNL genomic DNA with the primer sets 6523/6524 and 6525/6526 (Table S1). Primers 6524 and 6525 have 5'- extensions homologous to the *hdhfr::yfcu* selectable marker cassette (CATCTACAAGCATCGTCGACCTC in 6524 and CCTTCAATTCGGATCCACTAG in 6525). This selectable marker cassette was excised by digestion with XhoI and NotI from a plasmid (pL0048) that contains the *P. berghei eef1 α -hdhfr::yfcu-3' dhfr/ts* (i.e. promoter-drug selectable marker-3' terminator sequence) selection cassette. Primers 6523 and 6526 have 5'-terminal extensions with an anchor-tag suitable for the second PCR reaction. In the second PCR reaction, the amplified 5'- and 3'- targeting sequences were annealed to either side of the selectable marker cassette, and the joint fragment was amplified by the external anchor-tag primers 4661/4662, resulting in the PCR-based targeting construct with an expected size of 4.7 kb (2.7 kb of the selectable marker cassette plus two targeting sequences of 1kb). Before transfection, the PCR-based construct was digested with Asp718I and Scal (in primers 6523 and 6526, respectively) to remove the 'anchor-tag' and with DpnI that digests any residual pL0048 plasmid.

Transfection in *P. berghei* ANKA and *P. yoelii* 17XNL, selection and cloning of the mother lines were performed by standard procedures described for transfection of *P. berghei* [14]. DNA-construct pL1603 was introduced into *P. berghei* generating mother line, GIMO_{PBANKA} (1596cl1), and DNA construct pL1805 was introduced into *P. yoelii* generating mother line, GIMO_{PY17X} (1923cl1). Correct integration of the constructs was verified by diagnostic PCR analysis (see Table S2 for primers used) and Southern blot analysis of pulse-field gel (PFG) electrophoresis-separated chromosomes probed with the 3' untranslated region (UTR) of the *dhfr/ts* gene of *P. berghei*.

Generation of basic constructs without selection marker and that target the *230p* locus of the GIMO_{PbANKA} and GIMO_{PY17X} mother lines

To generate a basic *P. berghei* *230p*-targeting construct (pL0043), the *230p* targeting regions as well as the ampicillin resistance gene were amplified from plasmid pL1063 (MRA-852, www.mr4.org) using primers 5116/5117 (Table S1). A multiple cloning site (MCS) was amplified from pCRII-Blunt-TOPO vector (Zero Blunt TOPO PCR Cloning Kit, Invitrogen, Groningen, The Netherlands) using M13 forward and reverse primers. The two PCR products were digested with Asp718I and NotI restriction enzymes and ligated together creating the targeting construct pL0043.

A basic *P. yoelii* *230p*-targeting construct (pL1849) was generated using a modified 2-step PCR method (Figure S1B). In the first PCR reaction, 5'- and 3'- targeting sequences (both ~1kb) of *230p* were amplified from *P. yoelii* 17XNL genomic DNA with the primer set 6523/6534 and 6525/6526 (Table S1). As described above these primers contain 5'-extensions homologues to the *hdhfr::yfcu* selectable marker cassette and 5'-terminal extensions with an anchor-tag suitable for the second PCR reaction. A 55nt oligo (oligo 6598; GAGGTCGACGATGCTTGTAGATGCCCCGGCCTCAATTCGGATCCACTAG) containing a XmaI restriction site flanked by 2 sequences homologues to the *hdhfr::yfcu* selectable marker cassette was used to join the two *230p* targeting regions (Figure S1B). In the second PCR reaction an fragment containing both *230p* targeting sequences interrupted by the XmaI site was amplified, using the external anchor-tag primers 4661/4662, resulting in the PCR product of ~2 kb. The PCR product was cloned into TOPO TA vector (TOPO TA Cloning® Kit, Invitrogen, Groningen, The Netherlands) resulting in construct pL1849.

Generation of a mCherry reporter test construct and GIMO-transfection in the *P. berghei* mother line, GIMO_{PbANKA}

A test construct (pL1628) for GIMO-transfection in the GIMO_{PbANKA} mother line was generated by transferring the mCherry-expression cassette (5'*pbeef1α-mCherry*-3'*pbdhfr*) from plasmid pL0017-mCherry [34] into the basic *230p* targeting construct pL0043 (see above) using restriction sites EcoRV/Asp718I. This plasmid was linearized with KspI before transfection. Transfection was performed as described [14]. Transformed parasites were selected by negative selection by the administration the drug 5-FC (Sigma) to mice infected with transfected parasites. Specifically; 0.4g/kg bodyweight of 5-FC (stock: 20mg/mL in 1×PBS) administered by intra-peritoneal injection; one dose per day; for a period of 4 days, starting at 24 hours after transfection. Transformed parasites were collected at day

6/7 (infected tail blood) for phenotype analysis by fluorescence microscopy and FACS (see below) and at day 7/8 (infected heart blood) for genotype analysis using standard methods of diagnostic PCR and Southern analysis of PFG-separated chromosomes [14].

Generation of a constitutively GFP-luciferase expressing *P. yoelii* (PyGFP-luc_{con}) reporter line using GIMO-transfection

A construct (pL1847) for GIMO-transfection in the GIMO_{Py17X} mother line was generated by cloning an PCR-amplified GFP-luciferase expression cassette into the XmaI site of the basic *P. yoelii* 230p targeting construct pL1849 (see above). The GFP-luciferase expression cassette (5' *eef1α-gfp::luciferase-3'pbdhfr*) was amplified from pL1603 (MRA-852, www.mr4.org) using primers 6599 and 6600.

Transfection of GIMO_{Py17X} parasites and negative selection of transformed parasites was performed as described above for transfection of GIMO_{PbANKA}. Transformed parasites were collected for genotype analyses using standard methods of diagnostic PCR and Southern analysis of PFG-separated chromosomes [14]. Cloned parasites were analysed for luciferase expression using the *in vivo* imaging technology described below.

Gene complementation using GIMO transfection

Gene complementation was performed using the published *glutathione reductase* deletion mutant (Δgr) of *P. berghei* [19]. In this mutant ($\Delta gr4$; 1531cl1) the *glutathione reductase* (*gr*) gene has been deleted by a replacement construct (pL1538) that contains the positive-negative *hdhfr::yfcu* selectable marker cassette [19]. The pL1538 construct contains 5' and 3' targeting regions of *gr*. We used two of the primers that have been used to generate the replacement construct pL1538 to amplify *gr* gene from *P. berghei* genomic DNA using a proof reading polymerase (Phusion®, Finnzymes, Espoo, Finland). These primers (4049; forward primer for 5' targeting region and 3681; reverse primer for 3' targeting region) amplify the complete *gr* gene including the 5' and 3' targeting regions (see Table S1 for primer sequences). PCR resulted in amplification of a 2.8 kb fragment which was used to transfect Δgr parasites using standard transfection procedures [14]. Transformed parasites were selected by negative selection as describe above. Transformed parasites were collected for genotype analyses using standard methods of diagnostic PCR and Southern analysis of digested genomic DNA. Analysis of the phenotype of the complemented parasites, $\Delta gr(+gr)$, was analysed by mosquito transmission experiments (see below).

Fluorescence microscopy and FACS analysis

For analysis of GFP- or mCherry- expression in blood stages of transgenic parasites, infected tail blood was collected in PBS and examined by microscopy using a Leica DMR fluorescent microscope with standard GFP and Texas Red filters. Parasites nuclei were labeled by staining with Hoechst-33258 (2 $\mu\text{mol/L}$, Sigma, NL). Images were recorded with the digital camera CoolSNAP HQ² (Photometrics, NL) and processed with the ColourProc software [35]. The percentage of blood stages parasites that express mCherry was determined by FACS analysis of cultured blood stages. In brief, infected tail blood (10 μL) with a parasitemia between 0.5 and 1% was cultured overnight in 1mL complete RPMI1640 culture medium at 37°C under standard conditions for the culture of *P. berghei* blood stages [36]. Cultured blood samples were then collected and stained with Hoechst-33258 (2 $\mu\text{mol/L}$, Sigma, NL) for 1 hr at 37°C in the dark and analysed using a FACScan (BD LSR II, Becton Dickinson, CA, USA) with filter 440/40 for Hoechst signals and filter 610/20 for mCherry fluorescence. For FACS analysis the population of mature schizonts were selected based on the their Hoechst-fluorescence intensity [37]; see gate P2 in the left panel of Figure 2D. The percentage of mCherry-expressing parasites was calculated by dividing the number of mCherry-positive schizonts (gate P3 in right panel of Figure 2D) by the total number of schizonts (gate P2).

Quantitative real-time PCR (qPCR) analysis of transformed parasites

Genomic DNA extracted from blood stage parasites was used for qPCR analysis. To determine the ratio of transformed/non-transformed parasites in the selected parasite populations, PCR amplifications of the *mCherry* gene (only present in transformed parasites) and the *hdhfr::yfcu* selectable marker (only present in non-transformed) were carried out using the QuantiTect SYBR Green PCR Kit (Qiagen, Hilden, Germany) on a CFX96 thermal cycler (Bio-Rad Laboratories, The Netherlands). The housekeeping gene, *P. berghei hsp70*, was used as reference (see Table S2 for primers used). Real-time PCR cycle thresholds (C_T) were calculated as the average of triplicate analyses (per genomic DNA from transgenic parasite). The ratio between *mCherry* and *hdhfr::yfcu* was calculated by the $2^{-\Delta\Delta C_T}$ method relative to *hsp70* [16]. The amplification efficiencies of *mCherry* and *hsp70* did not violate assumptions of the $\Delta\Delta C_T$ method (data not shown).

Real time *in vivo* imaging of the *PyGFP-luc_{con}* reporter parasites in whole bodies of live mice

Expression of luciferase and imaging of distribution of luciferase-expressing *PyGFP-luc_{con}* parasites in whole bodies of live mice was determined by measuring bioluminescent

activity using the IVIS100 *in vivo* imaging system (Caliper Life Sciences, USA) as described previously [21,38]. Bioluminescence of blood stage parasites was imaged in Swiss mice with asynchronous infections of *PyGFP-luc_{con}* parasites at a parasitemia of 0.5–2%.

Analysis of the phenotype of Δgr and complemented $\Delta gr(+gr)$ parasites during mosquito transmission

Infection of *Anopheles stephensi* mosquitoes with Δgr and $\Delta gr(+gr)$ parasites as well as determination of production of oocysts and salivary gland sporozoites was performed as previously described [39]. Infectivity of sporozoites was tested by intravenous injection of Swiss OF1 mice with 10^4 hand dissected salivary gland sporozoites. The prepatent period was determined by light microscopy analysis of Giemsa-stained thin smears of tail blood. Prepatency (measured in days after sporozoite inoculation) is defined as the day when parasitemia reaches 0.5–2%.

Indirect Immunofluorescence assay

10^4 $\Delta gr(+gr)$ salivary gland sporozoites in 10 μL were allowed to adhere to polylysine coating slides, fixed for 15 minutes with 4% PFA, and washed 3 \times 5 minutes with PBS. Sporozoites were then permeabilized with 0.5% Triton-X100 for 15 minutes followed by a 3 \times 5 minutes wash with PBS. Slides were blocked 30 minutes at room temperature in 10% FCS and incubated over night with polyclonal rabbit anti-CS antiserum [40] (dilution 1:1000, kindly provided by Dr M. Yuda) at 4°C. Slides were washed 3 \times 5 minutes in PBS and incubated with donkey anti-rabbit, Alexa 488-conjugated secondary antibody (dilution 1:500), 1 hr in room temperature. Slides were washed 3 \times 5 minutes in PBS, and then incubated 15 minutes with Hoechst 33342 in room temperature. Prior to mounting, slides were washed for 5 minutes and analysed with were analyzed using a Leica DMR fluorescence microscope at 1000 \times magnification.

Funding

This work was supported by a Gates Foundation Grand Challenges Explorations Grant (to SMK; KHAN OPP1008310). JWJ is supported by the China Scholarship Council-Leiden University Joint Program, and CJJ by a grant of the European Community's Seventh Framework Programme (FP7/2007–2013) under grant agreement no. 242095. The funders had no role in study design, data collection and analysis, decision to publish, or preparation of the manuscript.

Acknowledgements

We would like to thank Dr. Stephen Hoffman for kindly providing us with *P. yoelii* 17XNL parasites and Dr. Masao Yuda for providing us with anti-CS antibodies.

References

1. Carvalho TG, Menard R (2005) Manipulating the *Plasmodium* genome. *Curr Issues Mol Biol* 7: 39-55.
2. Janse CJ, Kroeze H, van WA, Mededovic S, Fonager J, *et al.* (2011) A genotype and phenotype database of genetically modified malaria-parasites. *Trends Parasitol* 27: 31-39.
3. Balu B, Adams JH (2007) Advancements in transfection technologies for *Plasmodium*. *Int J Parasitol* 37: 1-10.
4. Heussler V, Doerig C (2006) In vivo imaging enters parasitology. *Trends Parasitol* 22: 192-195.
5. Amino R, Menard R, Frischknecht F (2005) In vivo imaging of malaria parasites—recent advances and future directions. *Curr Opin Microbiol* 8: 407-414.
6. Silvie O, Mota MM, Matuschewski K, Prudencio M (2008) Interactions of the malaria parasite and its mammalian host. *Curr Opin Microbiol* 11: 352-359.
7. de Koning-Ward TF, Fidock DA, Thathy V, Menard R, van Spaendonk RM, *et al.* (2000) The selectable marker human dihydrofolate reductase enables sequential genetic manipulation of the *Plasmodium berghei* genome. *Mol Biochem Parasitol* 106: 199-212.
8. Janse CJ, Franke-Fayard B, Mair GR, Ramesar J, Thiel C, *et al.* (2006) High efficiency transfection of *Plasmodium berghei* facilitates novel selection procedures. *Mol Biochem Parasitol* 145: 60-70.
9. Janse CJ, Franke-Fayard B, Waters AP (2006) Selection by flow-sorting of genetically transformed, GFP-expressing blood stages of the rodent malaria parasite, *Plasmodium berghei*. *Nat Protoc* 1: 614-623.
10. Braks JA, Franke-Fayard B, Kroeze H, Janse CJ, Waters AP (2006) Development and application of a positive-negative selectable marker system for use in reverse genetics in *Plasmodium*. *Nucleic Acids Res* 34: e39.
11. Goldberg DE, Janse CJ, Cowman AF, Waters AP (2011) Has the time come for us to complement our malaria parasites? *Trends Parasitol* 27: 1-2.
12. Pfander C, Anar B, Schwach F, Otto TD, Brochet M, *et al.* (2011) A scalable pipeline for highly effective genetic modification of a malaria parasite. *Nat Methods* . nmeth.1742 [pii];10.1038/nmeth.1742 [doi].
13. Spaccapelo R, Janse CJ, Caterbi S, Franke-Fayard B, Bonilla JA, *et al.* (2010) Plasmeprin 4-deficient *Plasmodium berghei* are virulence attenuated and induce protective immunity against experimental malaria. *Am J Pathol* 176: 205-217.

14. Janse CJ, Ramesar J, Waters AP (2006) High-efficiency transfection and drug selection of genetically transformed blood stages of the rodent malaria parasite *Plasmodium berghei*. *Nat Protoc* 1: 346-356.
15. Franke-Fayard B, Trueman H, Ramesar J, Mendoza J, van der KM, *et al.* (2004) A *Plasmodium berghei* reference line that constitutively expresses GFP at a high level throughout the complete life cycle. *Mol Biochem Parasitol* 137: 23-33.
16. Livak KJ, Schmittgen TD (2001) Analysis of relative gene expression data using real-time quantitative PCR and the 2⁻(Delta Delta C(T)) Method. *Methods* 25: 402-408.
17. Franke-Fayard B, Djokovic D, Dooren MW, Ramesar J, Waters AP, *et al.* (2008) Simple and sensitive antimalarial drug screening *in vitro* and *in vivo* using transgenic luciferase expressing *Plasmodium berghei* parasites. *Int J Parasitol* 38: 1651-1662.
18. Ploemen IH, Prudencio M, Douradinha BG, Ramesar J, Fonager J, *et al.* (2009) Visualisation and quantitative analysis of the rodent malaria liver stage by real time imaging. *PLoS One* 4: e7881.
19. Pastrana-Mena R, Dinglasan RR, Franke-Fayard B, Vega-Rodriguez J, Fuentes-Caraballo M, *et al.* (2010) Glutathione reductase-null malaria parasites have normal blood stage growth but arrest during development in the mosquito. *J Biol Chem* 285: 27045-27056.
20. van Dijk MR, van Schaijk BC, Khan SM, van Dooren MW, Ramesar J, *et al.* (2010) Three members of the 6-cys protein family of *Plasmodium* play a role in gamete fertility. *PLoS Pathog* 6: e1000853.
21. Franke-Fayard B, Janse CJ, Cunha-Rodrigues M, Ramesar J, Buscher P, *et al.* (2005) Murine malaria parasite sequestration: CD36 is the major receptor, but cerebral pathology is unlinked to sequestration. *Proc Natl Acad Sci U S A* 102: 11468-11473.
22. Ponzi M, Siden-Kiamos I, Bertuccini L, Curra C, Kroeze H, *et al.* (2009) Egress of *Plasmodium berghei* gametes from their host erythrocyte is mediated by the MDV-1/PEG3 protein. *Cell Microbiol* 11: 1272-1288.
23. Mair GR, Lasonder E, Garver LS, Franke-Fayard BM, Carret CK, *et al.* (2010) Universal features of post-transcriptional gene regulation are critical for *Plasmodium* zygote development. *PLoS Pathog* 6: e1000767.
24. Boisson B, Lacroix C, Bischoff E, Gueirard P, Bargieri DY, *et al.* (2011) The novel putative transporter NPT1 plays a critical role in early stages of *Plasmodium berghei* sexual development. *Mol Microbiol* 81: 1343-1357.
25. Engwerda C, Belhoue E, Gruner AC, Renia L (2005) Experimental models of cerebral malaria. *Curr Top Microbiol Immunol* 297: 103-143.
26. Engwerda CR, Beattie L, Amante FH (2005) The importance of the spleen in malaria. *Trends Parasitol* 21: 75-80.
27. Booker ML, Bastos CM, Kramer ML, Barker RH, Jr., Skerlj R, *et al.* (2010) Novel inhibitors of *Plasmodium falciparum* dihydroorotate dehydrogenase with anti-malarial activity in the mouse model. *J Biol Chem* 285: 33054-33064.
28. Barker RH, Jr., Urgaonkar S, Mazitschek R, Celatka C, Skerlj R, *et al.* (2011) Aminoindoles, a Novel Scaffold with Potent Activity against *Plasmodium falciparum*. *Antimicrob Agents Chemother* 55: 2612-2622.
29. Portugal S, Carret C, Recker M, Armitage AE, Goncalves LA, *et al.* (2011) Host-mediated regulation of superinfection in malaria. *Nat Med* 17: 732-737.
30. Billker O, Dechamps S, Tewari R, Wenig G, Franke-Fayard B, *et al.* (2004) Calcium and a calcium-dependent protein kinase regulate gamete formation and mosquito transmission in a malaria parasite. *Cell* 117: 503-514.
31. Sultan AA, Thathy V, de Koning-Ward TF, Nussenzweig V (2001) Complementation of *Plasmodium berghei* TRAP knockout parasites using human dihydrofolate reductase gene as a selectable marker. *Mol Biochem Parasitol* 113: 151-156.
32. Weiss WR, Good MF, Hollingdale MR, Miller LH, Berzofsky JA (1989) Genetic control of immunity to *Plasmodium yoelii* sporozoites. *J Immunol* 143: 4263-4266.
33. Ecker A, Moon R, Sinden RE, Billker O (2006) Generation of gene targeting constructs for *Plasmodium berghei* by a PCR-based method amenable to high throughput applications. *Mol Biochem Parasitol* 145: 265-268.
34. Graewe S, Retzlaff S, Struck N, Janse CJ, Heussler VT (2009) Going live: a comparative analysis of the suitability of the RFP derivatives RedStar, mCherry and tdTomato for intravital and *in vitro* live imaging of *Plasmodium* parasites. *Biotechnol J* 4: 895-902.

35. Tanke HJ, Wiegant J, van Gijlswijk RP, Bezrookove V, Pattenier H, *et al.* (1999) New strategy for multi-colour fluorescence in situ hybridisation: COBRA: COmbined Binary RAtio labelling. *Eur J Hum Genet* 7: 2-11.
36. Janse CJ, Waters AP (1995) *Plasmodium berghei*: the application of cultivation and purification techniques to molecular studies of malaria parasites. *Parasitol Today* 11: 138-143.
37. Janse CJ, Haghparast A, Speranca MA, Ramesar J, Kroeze H, *et al.* (2003) Malaria parasites lacking *eef1a* have a normal S/M phase yet grow more slowly due to a longer G1 phase. *Mol Microbiol* 50: 1539-1551.
38. Franke-Fayard B, Waters AP, Janse CJ (2006) Real-time *in vivo* imaging of transgenic bioluminescent blood stages of rodent malaria parasites in mice. *Nat Protoc* 1: 476-485.
39. Sinden R.E. (1997) Infection of mosquitoes with rodent malaria. In: Crampton J.M., Beard C.B., Louis C., editors. *Molecular biology of insect disease vectors: a method manual*. London, United Kingdom: Chapman and Hall. pp. 67-91.
40. Ishino T, Chinzei Y, Yuda M (2005) Two proteins with 6-cys motifs are required for malarial parasites to commit to infection of the hepatocyte. *Mol Microbiol* 58: 1264-1275.

Supplementary Material

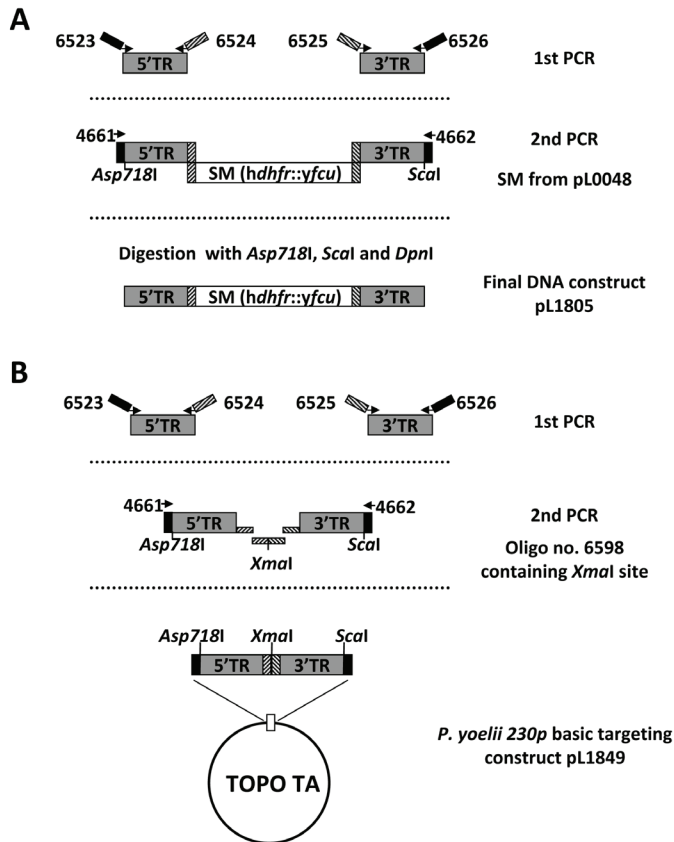


Figure S1. Generation of *P. yoelii* 230p targeting constructs using a PCR method

A. The DNA construct (pL1805) used to generate the *P. yoelii* GIMO mother line was created using a modified two-step PCR method. In the first PCR reaction, 5'- and 3'- targeting sequences of *230p* were amplified from *P. yoelii* 17XNL genomic DNA with the primer sets 6523/6524 and 6525/6526 (Table S1). Primers 6524 and 6525 have 5'- extensions homologous to the *hdhfr::yfcu* selectable marker cassette (hatched boxes). This selectable marker cassette was excised from plasmid pL0048 digested with *Xho*I and *Not*I. Primers 6523 and 6526 have 5'-terminal extensions (black boxes) for the second PCR reaction. In the second PCR reaction, the 5'- and 3'-targeting sequences annealed to either side of the selectable marker cassette, and the joint fragment was amplified by the external anchor-tag primers 4661/4662. Before transfection, the PCR construct was digested with *Asp*718I and *Scal* to remove the anchor-tag and with *Dpn*I to digest any residual pL0048 plasmid.

B. The basic *P. yoelii* 230p targeting construct (pL1849) was generated by a modified PCR method. In the first PCR reaction, 5'-and 3'- targeting sequences with homologous sequences (hatched boxes) and anchor-tag sequences (black boxes) were amplified as shown in **A**. Oligo no. 6598 that contains the joint homologous sequences interrupted by an *Xma*I site (hatched boxes) was used as template for the second PCR reaction. Using the external anchor-tag primers 4661/4662, a PCR product containing both targeting sequences now with the *Xma*I site in the middle was amplified and subsequently cloned into TOPO TA vector resulting in construct pL1849.

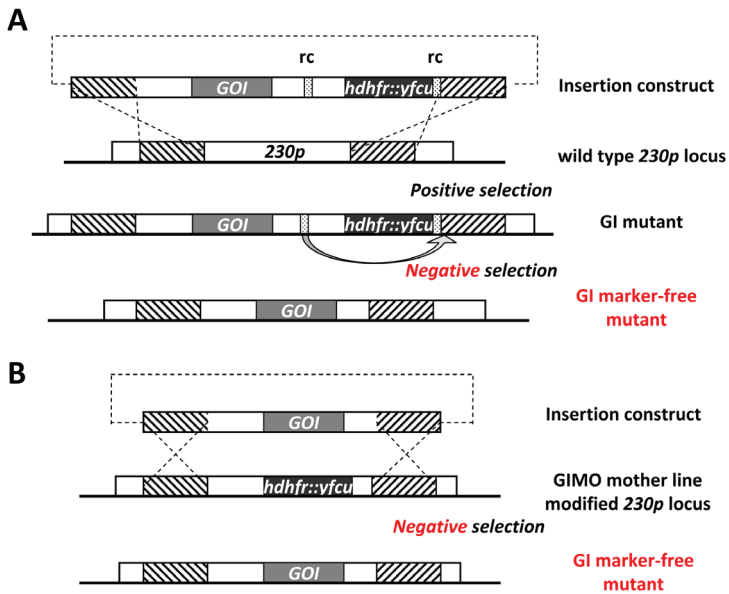


Figure S2. Schematic representation of the generation of marker-free gene insertion (GI) mutants using GIMO-transfection method or using the marker-recycling method.

A. Generation of marker-free gene insertion mutants expressing a gene of interest (GOI; grey box) using the standard marker-recycling method. The construct containing the *dhfr::yfcu* selectable marker (black box) flanked by the recombination sequences (rc, shaded boxes) targets the *230p* locus by double cross-over homologous recombination at specific target regions (hatched boxes). GI mutants are obtained after transfection, using positive selection with pyrimethamine and then cloning. Subsequently, marker-free GI mutants are selected by negative selection using 5-FC. Only those mutants that have 'spontaneously' lost the *dhfr::yfcu* marker from their genome, achieved by a homologous recombination/excision (see arrow), survive negative selection.

B. Generation of marker-free gene mutants that express a GOI (grey box) using GIMO-transfection. The construct that contains no selectable marker cassette and targets the modified GIMO mother line *230p* locus that contains the *dhfr::yfcu* (black box) marker, by double cross-over homologous recombination at the target regions (hatched boxes). Marker-free GI mutants, that have GOI expression cassette introduced into the *230p* locus replacing the *dhfr::yfcu* marker, are obtained by negative selection with 5-FC.

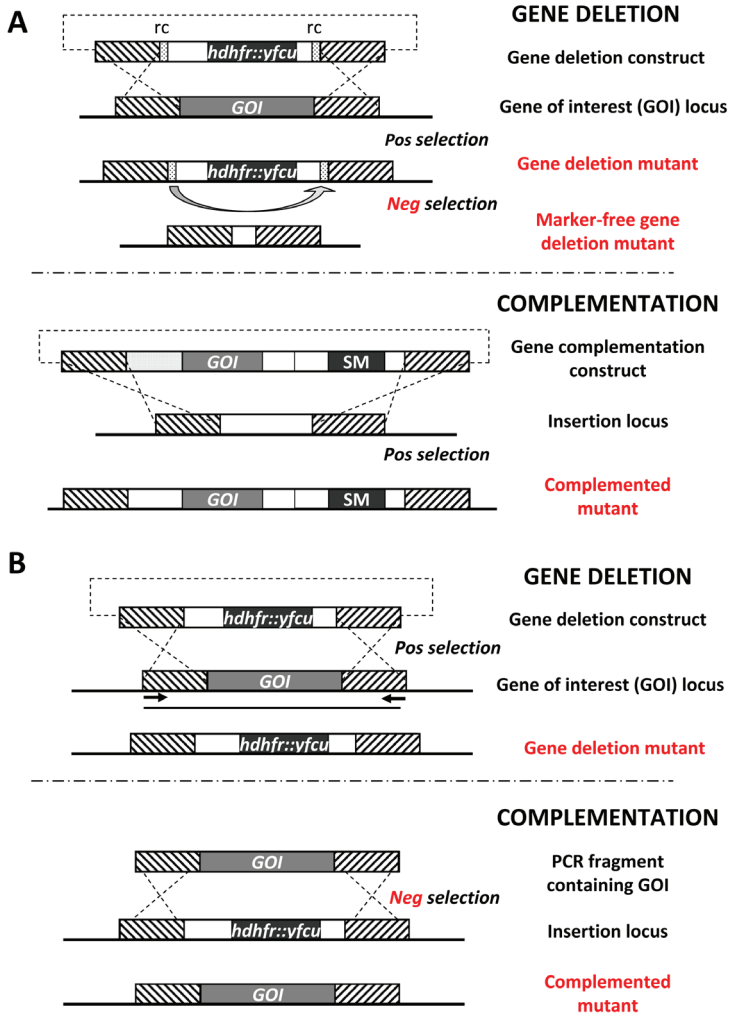


Figure S3. Schematic representation of gene complementation using GIMO-transfection and the marker-recycling method

A. Gene deletion and complementation using the marker-recycling method. The gene deletion construct, containing the *hdhfr::yfcu* selectable maker (black box) flanked by the recombination sequences (*rc*; shaded boxes), targets the gene of interest (GOI) by double cross-over homologous recombination at the target regions (hatched boxes). Gene deletion mutants are obtained after transfection and positive selection with pyrimethamine, and cloning. Subsequently, marker-free gene deletion mutants are selected by negative selection using 5-FC. Only those mutants that have 'spontaneously' lost the *hdhfr::yfcu* marker from their genome, achieved by a homologous recombination/excision event (see arrow), survive negative selection. Complementation of the (cloned) marker-free gene deletion mutant is performed using constructs that contain a GOI expression cassette and a positive selectable marker cassette. These constructs can target either the original deleted locus or a locus that is redundant or functionally silent. Complemented parasites are selected by positive selection.

B. Gene deletion and complementation using the GIMO-transfection method. The gene deletion construct

containing the *dhfr::yfcu* selectable marker fusion (black box) targets the GOI by double cross-over homologous recombination at specific target regions (hatched boxes). Gene deletion mutants are obtained after transfection using positive selection with pyrimethamine and then cloning. These constructs do not include recombination (*rc*) sequences (see A). Complementation of the gene deletion mutant is performed using a PCR fragment amplified from genomic DNA using the same outer primers used to generate the gene deletion construct (i.e. the forward primer of the 5'UTR and the reverse primer of 3'UTR, indicated by arrows). Integration of the PCR fragment by homologous recombination restores the deleted gene locus replacing the *dhfr::yfcu* maker. Complemented parasites are selected by negative selection.

Table S1. Primers used for DNA construct generation

DNA Construct	No.	Primer sequences	Restriction sites	Description
pL1603	5585	CTTTGGTACGAAAGCTTGTATATGGTAAAGAACCTACTAACAC	<i>Hind</i> III	<i>pb230p</i> 5'-targeting sequence, F
	5586	CTTTGGTACGCGCGGAGGATGTTTTATTTGGATGTG	<i>Ksp</i> I	<i>pb230p</i> 5'-targeting sequence, R
	5587	CCGGGGTACCAATTCTCTTGAGCCCGTTAATG	<i>Asp</i> 718I	<i>pb230p</i> 3'-targeting sequence, F
	5588	CCGGGAATTGGTATGGAACTACATCATATAGG	<i>Eco</i> RI	<i>pb230p</i> 3'-targeting sequence, R
pL1805	6523	GAACTCGTACTCTTGGTGACGGGTACCGTGAATGGCAACATCTG	<i>Asp</i> 718I	<i>py230p</i> 5'-targeting sequence, F
	6524	CATCTACAAGCATCGTCGACCTGGTTGGACAATGTAATGCTAC		<i>py230p</i> 5'-targeting sequence, R
	6525	CCTTCAATTTCCGATCCACTAG AGTAAAGGGGTAAGACAGC		<i>py230p</i> 3'-targeting sequence, F
	6526	AGGTTGGTCAITTGACACTCAGCAGTACTAAGAGATCTGGAAACCACTGG	<i>Sca</i> I	<i>py230p</i> 3'-targeting sequence, R
4661	GAACTCGTACTCTTGGTGACG		anchor-tag primer, F	
4662	AGGTTGGTCAITTGACACTCAGC		anchor-tag primer, R	
pL0043	5116	GGGGTACCGAGCTCGAATTCCTTTGAGC	<i>Asp</i> 718I	<i>pb230p</i> targeting sequences and <i>Amp</i> marker of pL1063, F
	5117	ATAGTTTAGCGCGCCCTCGAGGCATGCAAGCTTG	<i>Not</i> I	<i>pb230p</i> targeting sequences and <i>Amp</i> marker of pL1063, R
pL1847	6598	GAGTGCAGATGCTGTAGATGCCCGGCCCTTCAATTTGGGATCCTAG	<i>Xma</i> I	anchor-tag cloning sequence
	6599	TCCCCCGGGCCCACTTAATTCITTCGAGCTC	<i>Xma</i> I	5' <i>pbef1α</i> , F
pL1538	6600	TCCCCCGGGTTGAAGGAAAGAAAAACATCATTGTG	<i>Xma</i> I	3' <i>pbdfhr/ls</i> , R
	4049*	TCCCGGGGGGATTAATCATAAACCATATTTG	<i>Ksp</i> I	<i>gr</i> 5'targeting sequence, F
	4050**	GCCAAGCTTCAATTAACCAAAATAAAAATCG	<i>Hind</i> III	<i>gr</i> 5'targeting sequence, R
	3680**	CGGGGTACCGTTGCTATAAATCGGGGGGATTTAGCTG	<i>Asp</i> 718I	<i>gr</i> 3'targeting sequence, F
3681*	CCGGATATCCCTCTTTGATCATATCCCTTATTTGTC	<i>Eco</i> RV	<i>gr</i> 3'targeting sequence, R	

pb = *P. berghei*, *py* = *P. yoelii*

* Primers used in this study to amplify the complete *gr* gene

** Primers that have been used to amplify the 5' and 3' UTR target regions of *gr* (Pastrana-Mena et al, 2010, J. Biol Chem, 285: 27045-27056)

Table S2. Primers used for genotype analysis

No.	Primer sequences	Restriction sites	Description
Primers for PCR analysis			
5510	GCAAAGTGAAGTTCAAATATGTG		5'- intgr <i>pb230p</i> , F
5511	AGTGACTTTCAGTGAAATCGC		3'- intgr <i>pb230p</i> , R
3189	CTGGTGCTTTGAGGGGTG		5' <i>pbef1a</i> , R
4239	GATTTTTAAATGTTTATAATGATTAGC		3' <i>pbdhfr</i> , F
4698	GTTTCGCTAAACTGCATCGTC		<i>hdhfr</i> , F
4699	GTTTGAGGTAGCAAGTAGACG		<i>yfcu</i> , R
1637	AATATGTAGCATTACATTGTCC		<i>pb230p</i> , F
5600	ATTCATATCCAATAAAAAATCTG		<i>pb230p</i> , R
6527	GAAGGATATGAATTAGATCCACC		5'- intgr <i>py230p</i> , F
6528	AGACATTGGCATATGAGCAAG		3'- intgr <i>py230p</i> , R
4770	CATCTACAAGCATCGTCGACCTC		pL0048, R
4771	CCTTCAATTCGAGTCCACTAG		pL0048, F
6529	GAGGCCATAGAAAATGATGTAG		<i>py230p</i> , R
6530	TTGTTCCGAAGTGGGTTCCAGG		<i>py230p</i> , F
4958	GCATGAACCTCTTGATGATG		<i>mCherry</i> , R
5515	GCATGGACGAGCTGTACAAG		<i>mCherry</i> , F
3173	TGCCCTTTATTAAGTATCG		5' <i>pbef1a</i> , F
5514	CTTGACAGCTCGTCCATGC		<i>mCherry</i> , R
6812	CTCGAAAGCATTGAACACC		<i>gfp</i> R
6813	CTTACCGGAAAACCTGCACGC		<i>luciferase</i> , F
6814	TGACGGAACTACAAGACAC		<i>gfp</i> , F
6815	ACGAACGTGTACATCGACTG		<i>luciferase</i> , R
3742	GGGAGCTTCGCTAGTTTATATACACGTGG	<i>HindIII</i>	<i>gr</i> ORF, F
3743	TCCC CGCGGCATGAACCTTTTCTATTCTCTAC	<i>KspI</i>	<i>gr</i> ORF, R
Primers for PCR probes			
692	CTTATATATTATACCAATTG		3' <i>pbdhfr/ts</i> , F
693	GTTTTTTTTAATTTTTCAAC		3' <i>pbdhfr/ts</i> , R
886	GGAAGATCTATGGTGTGGTCGCTAAACTGCATCG		<i>hdhfr</i> , F
887	GGAAGATCTTAAATCATTCTTCTCATATACTTC		<i>hdhfr</i> , R
1462	CATGCCATGGATGAATACTTATTACAGTG		<i>pb25</i> , F
1463	CCGGAATCTTAAATGATATTTGAAAATATTAG		<i>pb25</i> , R
3680	CGGGGTACCGTTGCTATAAATGCGGGGCGATTATTAGCTG	<i>Asp718I</i>	3' UTR <i>gr</i> , F
3681	CCGGATATCCCTCTTTGATCATATCCCTTATTTTGTC	<i>EcoRV</i>	3' UTR <i>gr</i> , R
Primers for qPCR analysis			
5530	TTCAGCCTCTGCTTGATCTC		<i>mCherry</i> , F
6248	GCGCGTGATGAACCTCGAG		<i>mCherry</i> , R
6246	CCAGAATACCCAGGTGTTCTC		<i>hdhfr</i> , F
6247	ACATCCGCCAATAGGAACAC		<i>yfcu</i> , R
6249	CAATTGCAGGGTTAAATGTTATGAG		<i>pbhsp70</i> , F
6250	TTCACCACCTAAATGGGTATCAC		<i>pbhsp70</i> , R

pb = *P. berghei*, *py* = *P. yoelii*; h = human, γ =yeast

CHAPTER 3

Screening Inhibitors of *P. berghei* Blood Stages Using Bioluminescent Reporter Parasites

Jing-wen Lin, Mohammed Sajid, Jai Ramesar, Shahid M. Khan,
Chris J. Janse, Blandine Franke-Fayard

Leiden Malaria Research Group, Department of Parasitology, Leiden University Medical Center,
2333 ZA Leiden, The Netherlands

Methods Mol Biol. 2013; 923: 507–522.

Abstract

We describe two improved assays for *in vitro* and *in vivo* screening of inhibitors and chemicals for anti-malarial activity against blood stages of the rodent malaria parasite, *Plasmodium berghei*. These assays are based on the determination of bioluminescence in small blood samples that is produced by reporter parasites expressing luciferase. Luciferase production increases as the parasite develops in a red blood cell and as the numbers of parasites increase during an infection. In the first assay, *in vitro* drug luminescence (ITDL) assay, the *in vitro* development of ring-stage parasites into mature schizonts in the presence and absence of candidate inhibitor(s) is quantified by measuring luciferase activity after the parasites have been allowed to mature into schizonts in culture. In the second assay, the *in vivo* drug luminescence (IVDL) assay, *in vivo* parasite growth (using a standard 4-day suppressive drug test) is quantified by measuring the luciferase activity of circulating parasites in samples of tail blood of drug-treated mice.

1. Introduction

Antimalarial drug screening and validation is relatively time-consuming and complicated. The first phase of drug screening usually comprises the following two steps. Initially it involves the use of whole cell (infected red blood cell) assays that are used to determine the efficacy of drugs on *in vitro* growth of the human parasite *Plasmodium falciparum* in erythrocytes. The second step involves the testing of the *in vivo* efficacy of the most promising drug candidates in small animal models of malaria, principally using the rodent parasite *P. berghei* in laboratory mice. Compared to progress in the development for automated drug screening assays using the human parasite *P. falciparum* [1–7], the development of simple and sensitive assays for drug-screening in small animal models has been slow in part because the new technologies developed for *P. falciparum* cannot be directly applied in drug screening using rodent malaria parasites [8]. Usually *in vivo* drug screening is performed using the standard ‘4-day suppressive drug test’ [9], in which inhibition of parasite growth (*P. berghei*) in drug-treated mice is determined by manual counting the parasitemia in Giemsa-stained smears from small blood samples. Analysis of *in vitro* drug susceptibility has only been reported for one of the four rodent parasites, i.e. *P. berghei*. Since *P. berghei* blood stages can be cultured for only one developmental cycle, drug potency can only be determined during the development of ring forms into mature schizonts, which is established by determination of schizont maturation in Giemsa stained smears or by FACS analysis [10,11]. The availability of a *P. berghei* *in vitro* drug susceptibility assay is important since it permits to determine whether a discrepancy between *in vitro* *P. falciparum* drug-sensitivity and *in vivo* *P. berghei* drug-sensitivity is the result of intrinsic differences between the two parasites or is caused by pharmacokinetic and/or pharmacodynamic characteristics of the drug in a live animal. Because of the limitations of manual counting of rodent parasites in Giemsa stained slides and automated counting of rodent parasites stained with fluorescent, DNA/RNA-specific dyes, possibilities have been explored of using transgenic rodent parasites expressing reporter proteins, such as GFP or luciferase, for drug screening [12,13]. Herein we describe simple and sensitive *in vitro* and *in vivo* screening assays to test inhibitors and chemicals for antimalarial activity against blood stages of a reporter *P. berghei* parasite [8]. These assays are based on the determination of luciferase activity (luminescence) in small blood samples containing transgenic blood stage parasites that express luciferase under the control of a promoter that is either schizont-specific (*ama-1*) or constitutive (*eef1a*). The reading of luminescence assays is rapid, requires a minimal number of handling steps and no experience with parasite morphology or handling fluorescence-activated cell sorters, produces no radioactive waste and test-plates can be stored for

prolonged periods before processing. Both tests are suitable for use in larger-scale *in vitro* and *in vivo* screening of drugs.

2. Materials

2.1. Reporter parasites

For the *in vitro* drug luminescence (ITDL) assay, reporter parasite line *PbGFP-Luc_{ama1}* (1037m1f1m1cl1; see **Note 1**) is used, which expresses a fusion protein of GFP (mutant3) and firefly luciferase (LUC-IAV) under the control of the schizont-specific *ama-1* promoter [14]. For details of *PbGFP-Luc_{ama1}*, see RMgm-32 (<http://www.pberghei.eu/index.php?rmgm=32>).

For the *in vivo* drug luminescence (IVDL) assay, reporter parasite line *PbGFP-Luc_{con}* (676m1cl1; see **Note 1**) is used. This line expresses a fusion protein of GFP (mutant3) and firefly luciferase (LUC-IAV) under the control of the constitutive *eef1a* promoter [13]. For details of *PbGFP-Luc_{con}*, see RMgm-29 (<http://www.pberghei.eu/index.php?rmgm=29>).

2.2. Laboratory animals

In our laboratory, we use Swiss mice (OF1 ico, Construct 242; age, 6 weeks (25–26 g); Charles River). However, other mouse strains such as C57BL/6 and BALB/c can also be used (see Note 2).

2.3. Reagents

1. Fetal bovine serum, heat inactivated (FBS; Invitrogen, cat. no. 10108-165); store at -20°C.
2. Sörensen staining buffer: 2.541 g KH_2PO_4 and 8.55 g $\text{Na}_2\text{HPO}_4 \cdot 2\text{H}_2\text{O}$ in 5 L distilled water, pH adjusted to 7.2 with NaOH). Store at room temperature.
3. Giemsa solution working solution: 10% Giemsa solution (Merck, cat. no. 1666 789) in Sörensen staining buffer.
4. Phosphate-buffered saline (PBS): PBS stock solution (10×), 0.01 M KH_2PO_4 , 0.1 M Na_2HPO_4 , 1.37 M NaCl, 0.027 M KCl, pH 7.4; for a working solution, dilute the stock solution with nine volumes of distilled water, adjust the pH to 7.2 with 1.0 M HCl and sterilize by autoclaving for 20 min at 120 °C.
5. Heparin: Grade I-A, cell culture tested, 140 mUSP units/mg (Sigma, cat. no. H3149); dissolve the heparin powder in distilled water to a concentration

of 25,000 units/mL; filter sterilized (0.2 μm) and store at 4 °C. For a working solution, add 0.2 mL of the stock solution to 25 mL RPMI1640 culture medium without FBS to create a final solution of 200 units/mL. Store at 4°C.

6. Neomycin: (Gibco, cat. no. 21810-031): stock solution of 10.000 I.U./mL.
7. Insulin syringes: MicroFine +, 0.5 mL; 0.30 mm (30G) \times 8 mm (Becton Dickinson, cat. no. 324870).
8. RPMI1640 culture medium (Invitrogen; cat. no. 13018-015): add the RPMI1640 powder (with L-glutamine and 25 mM HEPES) to 1 L distilled water. In addition, add 0.85 g NaHCO_3 and 5 mL neomycin-sulfate stock solution (10.000 I.U./mL). Filter sterilize (0.2 μm) and store in 100 mL aliquots at -20 °C.
9. Complete RPMI1640 culture medium: RPMI1640 culture medium supplemented with FBS to a final concentration of about 20% (v/v) (see **Note 3**).
10. Gas mixture: 5% CO_2 , 5% O_2 , 90% N_2 (in a gas bottle or cylinder).
11. Dimethylsulfoxide (DMSO, Merck, cat. no. 1.16743.1000): store in room temperature in dark.
12. Inhibitors/antimalarial drugs: dissolve the powder in DMSO, sterile Milli-Q water or culture medium in high concentration as stock solution (see **Note 4**); store at 4 °C or -20 °C. For serial dilutions, dilute the working stock solution with DMSO or culture medium (see **Note 5**; **Subheading 3.1.2, step 7**).
13. Chloroquine diphosphate salt (CQ; Sigma, cat. no. C6628): dissolve the powder in Milli-Q water to 10 mM as stock solution.
14. Cell culture lysis reagent (CCLR): Luciferase Assay System Kit® (Promega, cat. no. E1500). For working solution, dilute the 'Cell Culture Lysis 5 \times Reagent' provided in the kit with Milli-Q water.
15. Luciferase assay substrate solution: Luciferase Assay System Kit® (Promega, cat. no. E1500). For working solution, mix 1 vial of Luciferase Assay Substrate and 1 vial of 10 mL Luciferase Assay Buffer together. The mixed solution can be stored at -20 °C and can be subsequently freeze/thawed multiple times without a significant loss of activity, however, the solution must be kept in the dark at all times.

2.4. Equipment

1. Vortex mixer (IKA Labortechnik).

2. Table-top centrifuge (Beckman Coulter Allegra); most table-top centrifuges with a swing-out rotor are suitable.
3. Eppendorf microcentrifuge (13,000 rpm or 16,000 × *g*); most microcentrifuges are suitable.
4. Eppendorf Centrifuge 5810 (equipped with 96-well plate holders).
5. Light microscope, Carl Zeiss Standard 25 (Zeiss); all light microscopes with an oil-immersed × 100 objective are suitable.
6. Incubator or water bath (37 °C).
7. Sonicator bath.
8. Fluovac isofluorane-halothane scavenger (Stoelting Co., see **Note 6**).
9. 24-well and 96-well cell culture plates, sterile, with lids.
10. Biohazard Class II safety cabinet (see **Note 7**).
11. Glass desiccator (e.g., candle jar).
12. Heparinized capillary pipettes.
13. 96-well optical flat-bottomed and black-framed microplates (Nalge Nunc Intl.): all 96-well microplates with black frames and clear flat bottoms are suitable for luminescence measurement (see **Note 8**).
14. Luminescence microplate reader: Wallac Multilabel Counter 1420 (PerkinElmer, NL). Other microplate readers that can measure bioluminescence are suitable.

2.5. Software

1. Microsoft Excel is used to conduct preliminary data analyses.
2. GraphPad Prism software (Graph-Pad software, Inc., US) is used for statistical analyses (best-fit) effective concentration (EC_{50}) calculation.

3. Methods

3.1. The *in vitro* drug luminescence (ITDL) assay

In the ITDL assay, the *in vitro* development of ring-stage parasites into mature schizonts in the presence of drugs/inhibitors is quantified by measuring the luciferase activity in cultured mature schizonts; the luciferase activity has been shown to directly correlate with the number of schizonts [8]. The ITDL assay generates standard *in vitro* inhibition curves and EC_{50} of the inhibitors. The reporter parasite *PbGFP-Luc_{ama1}* (see **Note 1**) is used in ITDL assay (see **Fig. 1** for the workflow).

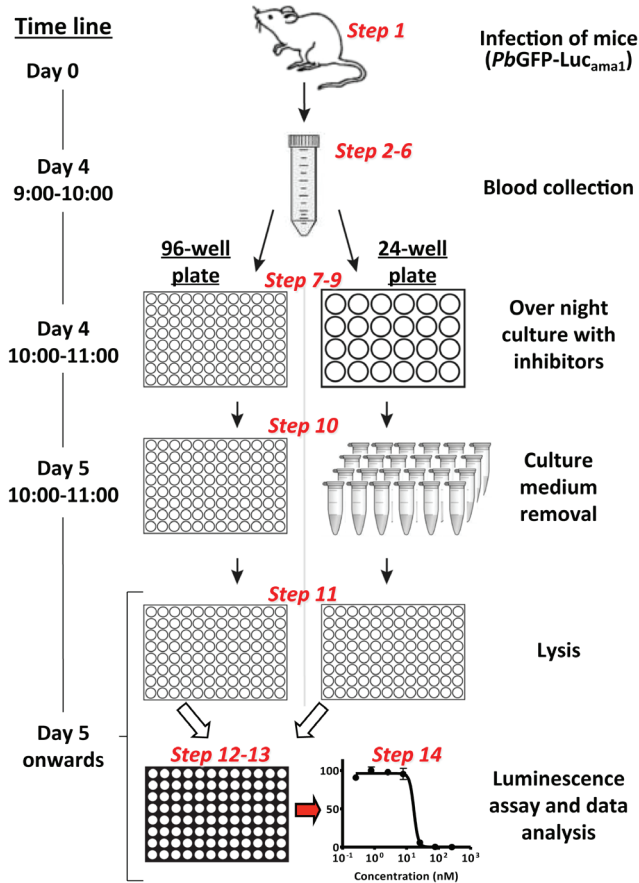


Figure 1. Workflow scheme of the ITDL assay

3.1.1. Collection of *P. berghei* ring forms for *in vitro* cultivation

1. On Day 0, infect 2 mice with 1×10^6 parasites of line *PbGFP-Luc_{ama1}* as follows:
 - 1) Collect one to four droplets (4–16 μ L) of tail blood in 0.4 mL PBS from a mouse infected with parasite line *PbGFP-Luc_{ama1}*. The parasitemia (i.e. the percentage of infected erythrocytes) in this mouse must be in the range of 5–15% (see **Note 9**).
 - 2) Immediately inject the suspension intraperitoneally into two mice, 0.2 mL per mouse.

After infection of the two mice, it will take several days before the parasitemia reaches the required level for the transfer to *in vitro* culture for the ITDL assays. Usually blood is collected from the infected mice on day 4

after infection when the parasitemia reaches 1–3%.

2. Between 8:00 am and 9:00 am (see **Note 10**) on day 4, make a thin blood smear from one droplet of tail blood from the two mice infected on day 0. If the parasitemia ranges between 1 and 3%, proceed to the next step. If the parasitemia is lower than 1%, it is best to wait one more day when the parasitemia has increased to 1–3% (see **Note 11**).
3. Prepare complete RPMI1640 culture medium by adding 25 mL freshly thawed FBS to 100 mL RPMI1640 culture medium.
4. Collect a total of 0.8–1.0 mL blood from the infected mice by cardiac puncture under anesthesia between 9:00 am and 10:00 am (see **Note 10**). Immediately add the blood to a 50-mL tube containing 5 mL complete culture medium supplemented with 0.3 mL heparin stock solution.
5. Harvest the (infected) red blood cells (RBC) by centrifugation (table-top centrifuge) for 8 min at $450 \times g$ and discard the supernatant.
6. Resuspend the (infected) RBC in complete culture medium into a final concentration of (infected) RBC of 0.5–1% (v/v) in complete culture medium. The total volume is dependent on how many serial dilutions are required for testing the inhibitors. For other details see the section below.

3.1.2. Overnight *In vitro* cultivation of ring forms in the presence of serial dilutions of inhibitors/antimalarial drugs

7. Preparation of dilution serials of inhibitors/antimalarial drugs:

The inhibitors in stock solution (see **Subheading 2.3, item 12**) can be diluted with DMSO or culture medium according to their properties (see **Note 5**). For additional information about preparation of serial dilutions of the inhibitors, see **Note 12**. We routinely use chloroquine (at a concentration of 100 nM) as a control for complete inhibition of blood-stage development (see **step 14**).

8. Add the suspension of infected RBC in complete culture medium to wells of 24- or 96-well culture plates and subsequently add the serial dilutions of inhibitor to the wells (in triplicates) resulting in a total volume of 1 mL (24-well plates) or 75 μ L (96-well plates) in each well.
9. Incubate the culture plates for a period of 24 h under standard *in vitro* culture conditions [15] (see **Note 13**), allowing the ring forms/young trophozoites to develop into mature schizonts.

- 1) Put culture plates into a small glass desiccator (e.g., candle jar) placed on a shaker in an incubator at 37 °C (see **Note 14**).
- 2) Flush the desiccator for 2 min at 1.5–2 bar pressure with the following gas mixture: 5% CO₂, 5% O₂, 90% N₂, and then either switch to lower gas flow and continuously gas overnight, or seal the desiccator once the air inside has been replaced with the gas mixture.
- 3) Switch on the shaker at a speed that is just fast enough to keep the cells in suspension and incubate the cultures (shaken) at 37 °C until the next day (day 5) for a period of 24 h.

3.1.3. Quantification of development of ring forms into mature schizonts in the presence of inhibitors/antimalarial drugs

10. Between 10:00 am and 11:00 am on day 5, the overnight cultures are collected and cells pelleted in the following ways:

24-well plate cultures: transfer 500 µL of cell suspension of each well to 1.5-mL Eppendorf tubes and pellet the cells by centrifugation (microcentrifuge) at full speed (13,000 × *g*) for 1 min. Remove the supernatant (culture medium). Samples can be stored at -80 °C until you are ready to perform the luciferase assay (see **step 12**).

96-well plate cultures: centrifuge the plates at 1000 × *g* for 5 min (Eppendorf Centrifuge 5810) and remove the supernatant (culture medium). These plates can be stored -80 °C until you are ready to perform the luciferase assay (see **step 12**).

11. Lyse RBC with 1 × cell culture lysis reagent (CCLR) as follows:

24-well plate cultures: add 100 µL of 1× CCLR into each Eppendorf tube, mix by pipetting until all the cells are lysed, and then transfer solution to wells of new 96-well plates (see **Note 15**).

96-well plate cultures: add 50 µL of 1× CCLR into each well and shake the plate for 5 min until the lysis is complete (see **Note 15**).

12. Luminescence assay:

24-well plate cultures: add 100 µL of luciferase assay substrate solution and 10 µL of lysed cell samples into wells of a black-framed 96-well plate (see **Note 8**).

96-well plate cultures: add 50 µL of luciferase assay substrate to the 96-well plate with lysed cells, mix them well and transfer the solution to a black-framed

96-well plate (see **Note 8**).

Wells containing PBS or lysed uninfected RBC are used as negative controls.

13. Luminescence spectra measurement:

Measure the light reaction of each well of the plates for 10 s using a microplate luminometer. The luciferase activities are expressed as relative luminescence units (RLU) for each sample. The RLU for each drug concentration is calculated from the same experiment performed in triplicate.

14. Data analysis:

- 1) The mean RLU value of 'complete inhibition control' (i.e. cultures with 100 nM chloroquine) is subtracted from the mean RLU values of all the other wells/concentrations.
- 2) The mean RLU value of wells without drug ('no inhibition control') is taken as the maximal RLU value and given to indicate normal parasite development. All RLU values of experimental wells (i.e. parasites in the presence of inhibitors) are divided by the mean value of the 'no inhibition control' in order to calculate the percentage of inhibition.
- 3) Growth inhibitory curves are plotted as a percentage of growth against concentration on a semi-log graph using the GraphPad Prism software. The non-linear regression function for sigmoidal dose-response (variable slope) is used to calculate the (best-fit) effective concentration (50% of the maximal inhibition; EC_{50} values) (see **Fig. 2** for examples).

3.2. The *in vivo* drug luminescence (IVDL) assay

In the IVDL assay, the *in vivo* parasite growth in mice is quantified by measuring the luciferase activity of circulating *PbGFP-Luc_{con}* parasites (see **Note 1**) in samples of tail blood. The IVDL assay generates growth-curves that are identical to those obtained by manual counting of parasites in Giemsa-stained smears [8]. The IVDL assay can be applied to the standard 4-day suppressive drug test [9] or other assays in which the course of parasitemia is monitored in groups of mice (see **Fig. 3** for the correlation between luciferase activity and number of parasites). This assay has been used to determine the growth/multiplication of asexual blood stages of (genetically modified mutant) parasites (see **Fig. 4** for examples), and in other assays where infected mice have been drug-treated.

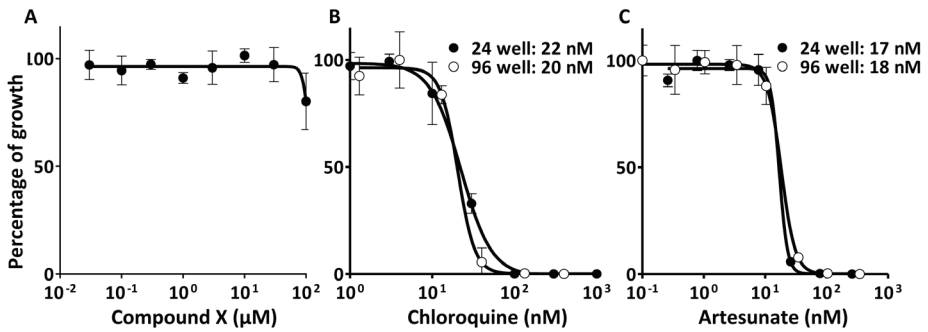


Figure 2. ITDL assay in 24- and 96-well plate cultures

Inhibition of the *in vitro* development of blood stages of *P. berghei* by compound X, chloroquine and artesunate. Inhibition of development was determined by measuring (the inhibition of) luciferase expression in parasites during development from ring forms into mature schizonts in over night culture (parasites of line *PbGFP-Luc_{ama1}*). (A) The ITDL assay of compound X in 24-well culture plate, no inhibition was observed (unpublished data JWL and SMK). The ITDL assay of well-known inhibitors chloroquine (B) and artesunate (C) performed in both 24-well and in 96-well culture plates with the EC_{50} values shown (adapted from Ref. [8]).

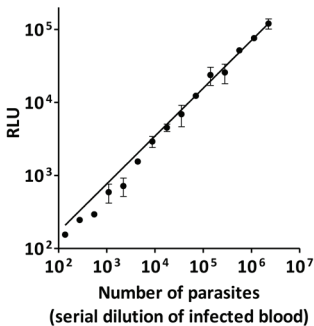


Figure 3. Correlation between luciferase activity (luminescence intensity) and the number of parasites or parasitemia.

Relationship between luminescence intensity (expressed as Relative Light Units, RLU) and numbers of parasites (*PbGFP-Luc_{con}*). The infected blood was serially diluted with PBS (adapted from Ref. [8]).

3.2.1. The IVDL assay in combination with the standard 4-day suppressive drug test (see Fig. 5 for the workflow).

1. On Day 0, infect 3 mice with 1×10^6 parasites of line *PbGFP-Luc_{con}* (see **Subheading 3.1.1, step 1**) for every inhibitor/drug concentration that is used.
2. Administer the first drug at 3 h after parasite inoculation and then subsequently every 24 h for 3 more days (day 1–3 post infection, p.i.), which is comparable to the standard 4-day suppressive drug test.
3. Every morning (10:00 – 11:00 am, from day 4 to 15 p.i.), using heparinized capillary pipettes, collect 10 μL of tail blood from each mouse and transfer the blood into separate 1.5-mL Eppendorf tubes.

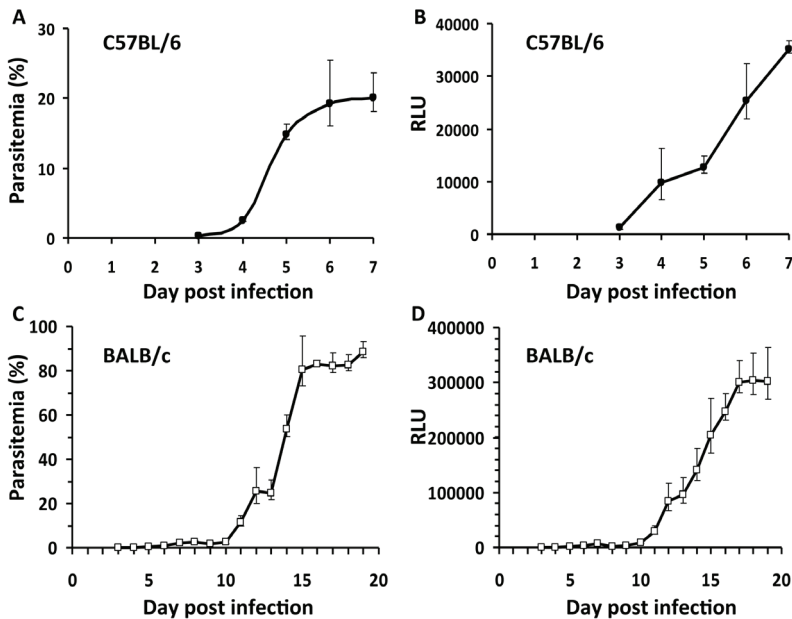


Figure 4. The course of blood stage infections in mice determined by counting parasites in Giemsa-stained blood films or measuring luminescence activity (RLU).

(A) (B) C57BL/6 mice infected with 10^6 *PbGFP-Luc_{con}* parasites. (C) (D) BALB/c mice infected with 10^6 blood stages of mutant $\Delta nt1$, made in the *PbGFP-Luc_{con}* background (unpublished data JWL, SMK).

4. Briefly spin down the droplet of blood to the bottom of the Eppendorf tubes and store them at -80°C , until all samples are collected for the luminescence assay.
5. On day 16 p.i., all stored blood samples are collected and ready for the luminescence assay:
 - 1) Lyse blood samples with 100 μL of $1\times$ cell culture lysis reagent (CCLR) and transfer the lysed cells to wells of 96-well plates (see **Note 15**).
 - 2) Add 100 μL of luciferase assay substrate solution and 10 μL of lysed cells samples into wells of a black-framed 96-well plate. Samples containing lysed uninfected red blood cells are used as negative controls.
 - 3) Measure the light reaction of each well for 10 s using a microplate luminometer. The luciferase activities are expressed as relative luminescence units (RLU) for each sample.
6. Data analysis: growth inhibitory curves are plotted as RLU against day p.i. using Microsoft Excel or GraphPad Prism.

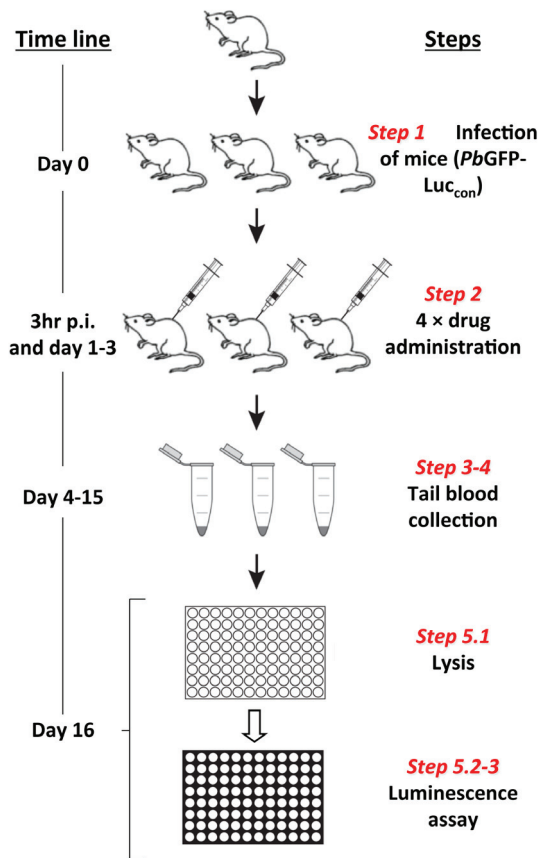


Fig. 5. Workflow scheme of the IVDL assay

3.2.2. The IVDL assay in combination with standard growth tests

1. On Day 0, infect mice with 10^4 – 10^5 parasites of line *PbGFP-Luc_{con}* as follows: collect 10 μ L of tail blood in 10 mL PBS from a mouse infected with line *PbGFP-Luc_{con}* and with a 5–15% parasitemia (see **Note 9**); immediately inject the suspension intraperitoneally into 3–6 mice, 0.2 mL per mouse.
2. Each day (from day 3 p.i. onwards), using heparinized capillary pipettes, collect 10 μ L of tail blood from each mouse and transfer the blood into separate 1.5-mL Eppendorf tubes. Spin the droplet of blood to the bottom of Eppendorf tubes and store them at -80°C for until all samples are collected (see **Note 16**) and proceed to step 3.
3. When all samples are collected, proceed to the luminescence assay and data analysis as described under **Subheading 3.2.1, steps 5–6**.

4. Notes

1. The two reporter parasite lines (*PbGFP-Luc_{ama1}* and *PbGFP-Luc_{con}*) are used that stably express a fusion protein of GFP and luciferase (GFP-luc) without the expression of a drug-selectable marker. In both lines the *gfp-luciferase* gene is integrated into the 'phenotypically neutral' *230p* genomic locus by double cross-over integration.

To quantify schizont development in the ITDL assay using luciferase as a reporter, a schizont-specific promoter is required. For this purpose we have used the *ama-1* promoter to generate the reporter line as this promoter drives expression of the reporter protein only in the late schizont stage [16]. In previous papers the use of GFP-Luc-expressing reporter lines 354cl4 and 875m2cl1 [8] has been described for the ITDL assay. However, now we recommend using the reporter line 1037m1f1m1cl1 (*PbGFP-Luc_{ama1}*) because of the absence of a drug-selectable marker and stable integration of the reporter gene into the *230p* locus. The *PbGFP-Luc_{ama1}* line is available from the Leiden Malaria Research Group (http://www.lumc.nl/con/1040/8102_8091348221/810281121192556/).

Line 676m1cl1 (*PbGFP-Luc_{con}*) has GFP-Luc under the control of *eef1α* promoter which permits the expression of the reporter in all blood stages [13]. This constitutive expression of luciferase is essential for a reporter parasite line used for the quantitative analysis of parasitemia or parasite densities in infected blood in the IVDL assay. The *PbGFP-Luc_{con}* line is available from MR4 (<http://www.mr4.org/>).

2. All experiments using mice must be performed according to the applicable national guide lines and regulations. Diets of laboratory rodents with low content of total protein, energy and/or *p*-aminobenzoic acid (PABA) can negatively influence *P. berghei* infections [17]. In our laboratory, we therefore provide diets with high protein content (20–25% of total and gross energy content; 18,000–20,000 kJ/kg).
3. For optimal *in vitro* parasites growth a relatively high percentage (~20%) of FBS is used.
4. It is important to dissolve inhibitors/antimalarial drugs completely; vortexing and/or sonication and/or 37 °C incubation can help to dissolve compounds.
5. It is better to make drug serial dilutions fresh, though they can also be stored at -20 °C or -80 °C.

6. Mice are anesthetized in the 'induction chamber,' which is prefilled with the anesthetic vapor (a mixture of isoflurane and air) via the vaporizer unit. The injection of parasites/ drugs or collecting blood by heart puncture is performed in mice that are kept under anesthesia by holding their muzzles to the small mask that is connected to the vaporizer unit.
7. Most manipulations with blood infected with genetically modified *P. berghei* parasites are performed in a Class II safety cabinet.
8. For luminescence measurements, we routinely use black-framed microplates as they best reduce light scattering between wells, which can artificially increase the signals detected in neighboring wells and thereby calculated EC₅₀ values.
9. The start of the procedure at day 0 requires a mouse infected with *P. berghei* reference line (*PbGFP-Luc_{ama1}* in ITDL or *PbGFP-Luc_{con}* in IVDL) which has a parasitemia of 5–15%, obtained either by mechanical passage or initiated from a cryopreserved parasite stock.
10. It is important to perform steps 2–4 early in the morning (8:00 – 10:00 am). *P. berghei* has a 22–24-h asexual blood-stage cycle which is partly 'synchronized' in mice with the normal day-night light regime. In these mice, the rupture of schizonts and invasion of RBC mainly occur between 02:00 and 04:00 am every day. This results in the presence of mainly young ring forms in blood of infected mice at 8:00 – 9:00 am. Most inhibitor tests are performed with these partly synchronous parasites. However, if pure populations of young ring forms are required for drug-susceptibility testing, these can be obtained by standard techniques of schizont culture and purification procedure and intravenously injecting purified schizonts into tail veins of mice to set up highly synchronized infections [15].
11. A parasitemia higher than 3% is suboptimal because many erythrocytes will become multiply infected or parasites will reside in the 'older' erythrocytes (normocytes) and not in reticulocytes. In both cases, the development of schizonts in culture is greatly impaired.
12. In case of inhibitors that are difficult to dissolve in water, dilutions need to be made in DMSO. We prepare stock solutions at a 100 times the final concentration required in the well so that when the drug is added to the well the concentration of DMSO in overnight culture is ≤1%, which is not harmful to the schizont development. No inhibition controls (i.e. culture without inhibitors) also contain ≤1% DMSO.

In our laboratory we usually prepare 10–12 different concentrations of the inhibitors (including no inhibition control). Two different 10-fold dilution serials are prepared, one is diluted into 1, 10, 100... serial and the other 0.3, 3, 30... serial. For example, for an inhibitor with observed $EC_{50} \sim 50$ nM in *P. falciparum*, we prepared a final dilution serial of 0, 0.3, 1, 3, 10, 30, 100, 300, 1000, 3000, 10,000 nM for the *P. berghei* ITDL assay.

13. In the overnight cultures, the ring forms and (young) trophozoites develop into schizonts that reach maturity in the morning of the next day. The mature schizonts do not rupture spontaneously and remain viable for several hours. For optimal development of the schizonts, the correct gas conditions (lowered oxygen concentration compared to air), the pH of the culture medium (7.2–7.4) and the temperature are crucial. The temperature is crucial because it influences the rate of development of the schizonts. Above 38.5 °C, parasites will degenerate. Lower than 37 °C, the parasites will develop into healthy parasites but the developmental time of one complete cycle will be longer than the standard 22–24 hrs. A temperature of between 36 and 37 °C is optimal to collect viable, mature schizonts between 09:00 and 11:00 am on day 5.
14. It is very important to transfer the cultures to the CO₂ gassed glass desiccator as soon as possible, as parasites easily degenerate in O₂-rich environment.
15. The lysed samples can also be stored at -20 °C or -80 °C until being used in luminescence assay. Transferring lysed samples from Eppendorf tubes to 96-well plates is not essential but helpful for using multi-channel pipettes in later steps.
16. The period of collecting infected tail blood is dependent on the experiment, the mouse strain used and the growth rate of the parasites. Parasites of reference lines of *P. berghei* ANKA induce cerebral complications (Experimental cerebral malaria; ECM) in ECM-sensitive mouse-strains such as C57BL/6, Swiss-OF1, CBA/J or Swiss-CD1. These mice usually die at day 6 to 9 after infection with 10⁴ to 10⁶ parasites at a parasitemia of 10–25%. ECM-resistant mice (e.g., BALB/c or NIH Swiss mice) usually die in week 3 after infection with a parasitemia of >60% and die from complications such as severe anaemia and multiple organ failure [18,19].

References

1. Smilkstein M, Sriwilaijaroen N, Kelly JX, Wilairat P, Riscoe M (2004) Simple and inexpensive fluorescence-based technique for high-throughput antimalarial drug screening. *Antimicrob Agents Chemother* 48: 1803-1806.
2. Baniecki ML, Wirth DF, Clardy J (2007) High-throughput *Plasmodium falciparum* growth assay for malaria drug discovery. *Antimicrob Agents Chemother* 51: 716-723.
3. Gamo FJ, Sanz LM, Vidal J, de CC, Alvarez E, Lavandera JL, Vanderwall DE, Green DV, Kumar V, Hasan S, Brown JR, Peishoff CE, Cardon LR, Garcia-Bustos JF (2010) Thousands of chemical starting points for antimalarial lead identification. *Nature* 465: 305-310.
4. Guiguemde WA, Shelat AA, Bouck D, Duffy S, Crowther GJ, Davis PH, Smithson DC, Connelly M, Clark J, Zhu F, Jimenez-Diaz MB, Martinez MS, Wilson EB, Tripathi AK, Gut J, Sharlow ER, Bathurst I, El MF, Fowble JW, Forquer I, McGinley PL, Castro S, ngulo-Barturen I, Ferrer S, Rosenthal PJ, DeRisi JL, Sullivan DJ, Lazo JS, Roos DS, Riscoe MK, Phillips MA, Rathod PK, Van Voorhis WC, Avery VM, Guy RK (2010) Chemical genetics of *Plasmodium falciparum*. *Nature* 465: 311-315.
5. Plouffe D, Brinker A, McNamara C, Henson K, Kato N, Kuhlen K, Nagle A, Adrian F, Matzen JT, Anderson P, Nam TG, Gray NS, Chatterjee A, Janes J, Yan SF, Trager R, Caldwell JS, Schultz PG, Zhou Y, Winzeler EA (2008) In silico activity profiling reveals the mechanism of action of antimalarials discovered in a high-throughput screen. *Proc Natl Acad Sci U S A* 105: 9059-9064.
6. rastu-Kapur S, Ponder EL, Fonovic UP, Yeoh S, Yuan F, Fonovic M, Grainger M, Phillips CI, Powers JC, Bogoy M (2008) Identification of proteases that regulate erythrocyte rupture by the malaria parasite *Plasmodium falciparum*. *Nat Chem Biol* 4: 203-213.
7. Rottmann M, McNamara C, Yeung BK, Lee MC, Zou B, Russell B, Seitz P, Plouffe DM, Dharia NV, Tan J, Cohen SB, Spencer KR, Gonzalez-Paez GE, Lakshminarayana SB, Goh A, Suwanarusk R, Jegla T, Schmitt EK, Beck HP, Brun R, Nosten F, Renia L, Dartois V, Keller TH, Fidock DA, Winzeler EA, Diagna TT (2010) Spiroindolones, a potent compound class for the treatment of malaria. *Science* 329: 1175-1180.
8. Franke-Fayard B, Djokovic D, Dooren MW, Ramesar J, Waters AP, Falade MO, Kranendonk M, Martinelli A, Cravo P, Janse CJ (2008) Simple and sensitive antimalarial drug screening *in vitro* and *in vivo* using transgenic luciferase expressing *Plasmodium berghei* parasites. *Int J Parasitol* 38: 1651-1662.
9. Peters, W (1987) *Chemotherapy and Drug Resistance in Malaria*. London: Academic Press. 273 p.
10. Janse CJ, Van Vianen PH (1994) Flow cytometry in malaria detection. *Methods Cell Biol* 42 Pt B: 295-318.
11. Janse CJ, Waters AP, Kos J, Lugt CB (1994) Comparison of *in vivo* and *in vitro* antimalarial activity of artemisinin, dihydroartemisinin and sodium artesunate in the *Plasmodium berghei*-rodent model. *Int J Parasitol* 24: 589-594.
12. Sanchez BA, Mota MM, Sultan AA, Carvalho LH (2004) *Plasmodium berghei* parasite transformed with green fluorescent protein for screening blood schizontocidal agents. *Int J Parasitol* 34: 485-490.
13. Franke-Fayard B, Trueman H, Ramesar J, Mendoza J, van der KM, van der LR, Sinden RE, Waters AP, Janse CJ (2004) A *Plasmodium berghei* reference line that constitutively expresses GFP at a high level throughout the complete life cycle. *Mol Biochem Parasitol* 137: 23-33.
14. Spaccapelo R, Janse CJ, Caterbi S, Franke-Fayard B, Bonilla JA, Syphard LM, Di CM, Dottorini T, Savarino A, Cassone A, Bistoni F, Waters AP, Dame JB, Crisanti A (2010) Plasmeprin 4-deficient *Plasmodium berghei* are virulence attenuated and induce protective immunity against experimental malaria. *Am J Pathol* 176: 205-217.
15. Janse CJ, Waters AP (1995) *Plasmodium berghei*: the application of cultivation and purification techniques to molecular studies of malaria parasites. *Parasitol Today* 11: 138-143.
16. Franke-Fayard B, Janse CJ, Cunha-Rodrigues M, Ramesar J, Buscher P, Que I, Lowic C, Voshol PJ, den Boer MA, van Duinen SG, Febbraio M, Mota MM, Waters AP (2005) Murine malaria parasite sequestration: CD36 is the major receptor, but cerebral pathology is unlinked to sequestration. *Proc Natl Acad Sci U S A* 102: 11468-11473.
17. Gilks CF, Jarra W, Harvey-Wood K, McLean SA, Schettters T (1989) Host diet in experimental rodent malaria: a variable which can compromise experimental design and interpretation. *Parasitology* 98 Pt 2: 175-177.
18. Chen L, Sendo F (2001) Cytokine and chemokine mRNA expression in neutrophils from CBA/NSlc mice infected with *Plasmodium berghei* ANKA that induces experimental cerebral malaria. *Parasitol Int* 50: 139-143.

19. de Souza JB, Riley EM (2002) Cerebral malaria: the contribution of studies in animal models to our understanding of immunopathogenesis. *Microbes Infect* 4: 291-300.

CHAPTER 4

Loss-of-Function Analyses Defines Vital and Redundant Functions of the *Plasmodium* Rhomboid Protease Family

Jing-wen Lin¹, Patrícia Meireles², Miguel Prudêncio², Sabine Engelmann³, Takeshi Annoura¹, Mohammed Sajid¹, Séverine Chevalley-Maurel¹, Jai Ramesar¹, Carolin Nahar⁴, Cristina M.C. Avramut⁵, Abraham J. Koster⁵, Kai Matuschewski^{3,4}, Andrew P. Waters⁶, Chris J. Janse¹, Gunnar R. Mair⁷, Shahid M. Khan¹

¹Leiden Malaria Research Group (Parasitology); ⁵Section Electron Microscopy (Molecular Cell Biology), Leiden University Medical Centre, Leiden, The Netherlands

²Malaria Unit, ⁷Molecular Parasitology Unit, Instituto de Medicina Molecular, Faculdade de Medicina, Universidade de Lisboa, Lisboa, Portugal

³Parasitology, Department of Infectious Diseases, University of Heidelberg Medical School, Heidelberg, Germany

⁴Max Planck Institute for Infection Biology, Parasitology Unit, Berlin, Germany

⁶Division of Infection and Immunity, Institute of Biomedical Life Sciences & Wellcome Centre for Molecular Parasitology, Glasgow Biomedical Research Centre, University of Glasgow, Glasgow, Scotland

Molecular Microbiology 2013, 88(2): 318–338.

Abstract

Rhomboid-like proteases cleave membrane-anchored proteins within their trans-membrane domains. In apicomplexan parasites substrates include molecules that function in parasite motility and host cell invasion. While two *Plasmodium* rhomboids, ROM1 and ROM4, have been examined, the roles of the remaining six rhomboids during the malaria parasite's life cycle are unknown. We present systematic gene deletion analyses of all eight *Plasmodium* rhomboid-like proteins as a means to discover stage-specific phenotypes and potential functions in the rodent malaria model, *P. berghei*. Four rhomboids (ROM4, 6, 7 and 8) are refractory to gene deletion, suggesting an essential role during asexual blood-stage development. In contrast ROM1, 3, 9 and 10 were dispensable for blood stage development and exhibited no, subtle or severe defects in mosquito or liver development. Parasites lacking ROM9 and ROM10 showed no major phenotypic defects. Parasites lacking ROM1 presented a delay in blood stage patency following liver infection, but in contrast to a previous study blood stage parasites had similar growth and virulence characteristics as wild type parasites. Parasites lacking ROM3 in mosquitoes readily established oocysts but failed to produce sporozoites. ROM3 is the first apicomplexan rhomboid identified to play a vital role in sporogony.

Introduction

Rhomboid-like proteins are intramembrane serine proteases that hydrolyse a substrate within its transmembrane (TM) spanning domain [1]. The first rhomboid protease described was *Drosophila melanogaster* Rhomboid-1 that initiates cell signaling by cleaving the membrane-resident Spitz, an epidermal growth factor (EGF)-like ligand precursor, releasing it as an activated molecule from the membrane and promoting subsequent EGF-receptor signaling [2]. With the exception of viruses, rhomboid-like proteins are found in all kingdoms of life and share a conserved core structure of six TM domains that contains the catalytic serine-histidine diad [3–7]. Interestingly, as a family of proteins, they share only around 5% sequence identity in the core region [8] and have highly variable amino termini. Some members have additional TM domains at either N- or C- termini of the core six, but their precise functions are unknown. Rhomboids function in cell-cell signaling in metazoans [9,10], quorum sensing between bacteria [11], facilitate mitochondrial membrane fusion in yeast [12] and regulate apoptosis [13].

Many eukaryotic organisms contain large rhomboid gene families. Multiple rhomboid-like enzymes are also found in the genomes of apicomplexan parasites such as *Toxoplasma gondii*, *Plasmodium* spp., *Eimeria tenella*, *Cryptosporidium* spp., *Theileria* spp. and *Babesia bovis*. Based on a phylogenetic clustering of rhomboid-like proteins, a nomenclature has been defined according to the initial assignment of *T. gondii* rhomboids [14], which expresses six rhomboid-like proteins TgROM1–6. Only four TgROMs (i.e. ROM1, 3, 4 and 6) have direct *Plasmodium* homologs [14]; there are no direct homologs of TgROM2 and TgROM5 in *Plasmodium* and ROM7–10 are only present in *Plasmodium* but not in *T. gondii*. Although *Plasmodium* species do not have a direct TgROM5 homolog, *P. falciparum* ROM1 and ROM4 share substrate specificities with TgROM5 [15]. Apicomplexan ROM6 is most likely an evolutionarily ancient mitochondrial PARL-like rhomboid, whereas all the others seem to be unique to apicomplexan parasites [14]. Interestingly, *Plasmodium* ROM9 also has a putative mitochondrial-targeting sequence and clusters with PARL-like rhomboids [16].

Although *in vitro* certain rhomboids of apicomplexan parasites can cleave adhesins that are known to mediate recognition of, and attachment to host cells, their *in vivo* substrate specificities are largely unknown [16,17]. Understanding the biological functions of apicomplexan rhomboids is an active area of research because of the critical roles identified for several of these molecules in host cell invasion and pathogenesis [16–18]. In *T. gondii*, TgROM4 has been shown to process surface adhesins including MIC 2, 3 (microneme proteins) and apical membrane antigen 1 (AMA1 [18]); this TgROM4-mediated AMA1 cleavage critically regulates the parasite's switch from an invasive to a

4

replicative mode [19]. TgROM1 is localized in micronemes [20] and although it is critical for parasite growth, TgROM1 is not essential for parasite invasion [21]. From the eight *Plasmodium* rhomboids, only ROM1 and ROM4 have been analyzed in more detail. *In vitro* substrates of the *P. falciparum* proteins include the merozoite-specific proteins AMA1 and proteins of the EBL (erythrocyte binding ligands) and RBL (reticulocyte binding ligands) families as well as several proteins of the invasive ookinete- and sporozoite-stages, such as TRAP (thrombospondin-related anonymous protein), CTRP (circumsporozoite- and TRAP-related protein) and MAEBL (merozoite adhesive erythrocytic binding protein) [15]. Structural analysis of the RBL protein EBA175 (Erythrocyte-binding antigen 175) and TRAP provided evidence for shedding of these proteins by a rhomboid-like protease [22] and indeed both proteins are cleaved *in vitro* by ROM4 [22,23]. In *P. falciparum* only a small fraction of AMA1 is shed by ROM1 and the intramembrane cleavage can be reduced to undetectable levels by mutagenesis without discernible phenotypic consequences [24]. The successful generation of *P. berghei* and *P. yoelii* mutants that lack expression of ROM1 also demonstrated that ROM1 is not essential for blood stage multiplication [25,26]. Blood stages of these mutants suffer only from a minor reduction in growth, again indicating that intramembrane cleavage of AMA1 by ROM1 is not essential for invasion of erythrocytes. ROM1 mutants in *P. yoelii* also showed a slight growth defect during liver stage development which has been attributed to reduced cleavage of the parasitophorous vacuole protein UIS4 (upregulated in sporozoites 4) by ROM1 [26]. Whether additional proteins are processed by *Plasmodium* ROM4 or ROM1 *in vivo* is still unknown. The non-essential nature of ROM1 during the complete lifecycle indicates that other rhomboids or proteases from other families can cleave substrates of ROM1. ROM4 on the other hand has been reported to be essential for blood stage growth as attempts to mutate the *rom4* gene of *P. falciparum* failed [22]. However, differences in cellular localization and *in vitro* substrate specificities of ROM1 and ROM4 [15,22] raise questions as to whether these rhomboids cleave the same substrates *in vivo*. In blood stage *P. falciparum* ROM1 is located in micronemes of merozoites and ROM4 is embedded into the merozoite plasma membrane [22].

Due to the absence of data defining *Plasmodium* rhomboid expression, cellular localization, or importance during the parasite's life cycle, it is largely unknown which, if any rhomboids are biologically essential, redundant or perhaps share overlapping functions. We therefore undertook a genetic screen of all 8 rhomboids by targeting each gene for deletion by homologous recombination using the genetically most tractable malaria parasite, *P. berghei*. Multiple attempts to disrupt genes encoding ROM4, ROM6, ROM7 and ROM8 failed, suggesting that these proteins have essential, non-redundant functions during blood stage development. We show that in addition to ROM1, three

other rhomboid-like proteases – ROM3, ROM9 and ROM10 – are redundant for asexual blood stage development in mice. Parasites lacking ROM9 and ROM10 showed no major phenotypic defects during the entire life cycle; however parasites lacking ROM1 were slightly compromised with respect to their ability to develop in the liver. Although already transcribed strongly in the female gametocyte, ROM3 is crucial during oocyst development inside the mosquito. Parasites lacking ROM3 produce normal numbers of ookinetes that readily establish oocysts in the mosquito. Although normal in size and number, oocysts fail to sporulate, suggesting that ROM3 plays a key role in the regulation of cytokinesis and production of individual sporozoites.

Results

The gene expression profiles of rhomboids across the parasite life cycle

The genome of the rodent malaria parasite *P. berghei* contains eight genes encoding rhomboid proteases [14] (Gene IDs are shown in Table 1) Each member shows a high level of sequence identity (70–85%) with its rhomboid ortholog from the human malaria parasite *P. falciparum* and shares a syntenic location in the genome (www.plasmodb.org) with an identical exon/intron gene structure.

We compared expression data of all rhomboid genes in *P. berghei* and *P. falciparum* in publicly available literature as well as transcriptome and proteome datasets across the life cycle (Table 1) (www.plasmodb.org and [27]). Immunofluorescence assays (IFA) on HA-tagged ROM1 and ROM4 show expression of these proteins in dividing schizonts and merozoites in *P. falciparum* [22]. A similar pattern of expression of *P. berghei* and *P. yoelii* ROM1 has been shown in schizonts and merozoites by IFA [25–26]. In both *P. berghei* and *P. falciparum* ROM1 is located in the micronemes. *P. berghei* ROM1 and ROM4 of *P. falciparum* and *P. berghei* have been detected in the sporozoite stage [25, 23] (Table 1). Our RT-PCR analyses (Fig. S1) demonstrate transcription of *P. berghei rom1* and *rom4* in blood stages and sporozoites. These different observations indicate that both ROM1 and ROM4 of human and rodent parasites have comparable patterns of expression and cellular location. For other rhomboids the information on stage-specific expression is much more limited. Proteome analyses indicate that ROM6, ROM9 and ROM10 are expressed in *P. falciparum* gametocytes (Table 1); however, proteome evidence for expression of these proteins in *P. berghei* gametocytes or other blood stages is absent. ROM7 and ROM8 are absent in all *P. falciparum* and *P. berghei* proteomes and ROM3 is only detected in *P. falciparum* blood stages. EST, RNAseq (Table 1) and RT-PCR analyses (Fig. S1), however, indicate that ROM3, ROM7 and ROM8 are expressed in blood stages and therefore the

absence in proteomes may suggest that rhomboids are relatively low abundant proteins, although we have to take into account the difficulties of proteomic sequencing multi-pass transmembrane proteins. *P. falciparum* RNAseq analyses indicate that transcription of *rom3* and *rom4* is upregulated in gametocytes compared to asexual stages (Table 1). RNAseq analyses of different *P. berghei* blood stages also showed strongly increased transcripts levels of *rom3* and *rom4* in gametocytes (W.A.M. Hoeijmakers, A. Religa, C.J. Janse, A.P. Waters, & H.G. Stunnenberg, unpublished data). We confirmed transcription of these rhomboids in *P. berghei* gametocytes by RT-PCR (Fig. S1).

The similarities between the eight rhomboid genes of *P. falciparum* and *P. berghei* and similarities in expression patterns and cellular locations of several rhomboids point towards a conserved function between rhomboid orthologs across the parasites' life-cycle in both species. Since most rhomboids appear to be expressed in multiple life cycle stages, the expression pattern is however not a good indicator for a putative role at a distinct life cycle stage.

Table 1. Expression profile of *Plasmodium rhomboids*

Protein	Gene ID	mRNA						Protein	
<i>P. berghei</i>									
		As ^{1,2}	Gct ^{1,2}	Ook ¹	Sp ^{1,2}	As ³	Gct ⁴	Ooc ³	Sp ³
ROM1	PBANKA_093350	+ (-)	+ (-)	++	+ (++)	- (+ ⁵)	±	-	- (+ ⁵)
ROM3	PBANKA_070270	- (++)	+ (-)	-	- (-)	-	-	-	-
ROM4	PBANKA_110650	+ (++)	+ (-)	++	+ (++)	- (+ ⁶)	-	-	- (+ ⁶)
ROM6	PBANKA_135810	+ (-)	+ (-)	-	- (+)	-	-	-	-
ROM7	PBANKA_113460	+ (-)	- (-)	-	- (+)	-	-	-	-
ROM8	PBANKA_103130	+ (-)	- (-)	-	- (-)	-	-	-	-
ROM9	PBANKA_111470	± (-)	± (-)	-	+ (-)	-	-	-	-
ROM10	PBANKA_111780	+ (++)	± (-)	+	- (-)	-	-	-	-
<i>P. falciparum</i>									
		As ⁷	Gct ⁷		Sp ⁸	As ³	Gct ³	Ooc ³	Sp ³
ROM1	PF3D7_1114100	+	±		+	+	-	-	-
ROM3	PF3D7_0828000	±	++		+	±	-	-	-
ROM4	PF3D7_0506900	+	++		+	++	-	-	+
ROM6	PF3D7_1345200	±	±		+	-	±	-	-
ROM7	PF3D7_1358300	±	-		-	-	-	-	-
ROM8	PF3D7_1411200	+	+		+	-	-	-	-
ROM9	PF3D7_0515100	±	±		+	-	±	-	-
ROM10	PF3D7_0618600	+	±		+	±	+	-	-

AS, asexual stages; Gct, gametocytes; Ook, ookinetes; Ooc, oocysts; Sp, sporozoites

¹ RT-PCR results in this study (see Figure S1)

² (PlasmoDB EST data in parentheses: - = no data; + = 1 EST; ++ = 2-7 ESTs)

³ PlasmoDB proteome data (- = no data; ±=1-2; +=3-10; +++>10)

⁴ PbANKA Male vs female gametocyte proteome (Khan *et al*, 2005)

⁵ IFA evidence using anti-PbROM1 serum (Srinivasan *et al*, 2009)

⁶ Western and IFA evidence using anti-PbROM4 serum (Ejigiri I *et al*, 2012)

⁷ PlasmoDB RNAseq data (- = no data; ± = 0-6; + = 6-10) RPKM (log2)

⁸ PlasmoDB oligo array (- = no data; ± = 1-100; + = 100-1000; ++ > 1000) RMA value

Evidence for an essential role of ROM4, 6, 7 and 8 in asexual blood stage parasites – ROM1, 3, 9 and 10 are dispensable.

As a first step towards understanding the roles of rhomboid proteases during the *Plasmodium* life cycle, we undertook a systematic, individual gene deletion approach for each of the eight *P. berghei* rhomboid genes and provide here a detailed analysis of the growth characteristics of gene deletion mutants for four rhomboids. Using well-established standard assays, the following phenotypes of the gene deletion mutants were characterized throughout the complete life cycle including blood, mosquito and liver stages: *in vivo* asexual blood stage multiplication rate, *in vivo* gametocyte production, *in vitro* ookinete formation, oocyst and sporozoite development in *A. stephensi* mosquitoes and the prepatent period in mice after injection of sporozoites. The prepatent period is defined as the time taken to achieve a 0.5–2% blood stage parasitemia in mice after intravenous inoculation of 10^4 sporozoites.

Standard genetic modification technologies used to replace entire *rhomboid* genes by double cross-over integration with a drug resistant marker resulted in gene deletion mutants for *rom1*, *3*, *9* and *10*, while multiple attempts to disrupt *rom4*, *6*, *7* and *8* were unsuccessful (see Table S1, S2 and S3 for details of these unsuccessful gene-deletion attempts including primers used to amplify the targeting sequences, generate the gene-deletion constructs and genotype). We demonstrated by RT-PCR that *rom4*, *6*, *7* and *8* are transcribed in blood stages (Fig. S1) and the multiple unsuccessful attempts to disrupt *rom4*, *6*, *7* and *8* may indicate that these genes have a critical function for asexual blood stage growth and multiplication. While a failure to disrupt a gene is not an unequivocal proof that the encoded protein is essential for blood stage growth/multiplication for *rom4* we show that the failure of disruption is not due to refractoriness of the genetic locus to genetic modification by creating a transgenic mutant (*rom4::mCherry*) that expresses a C-terminally mCherry-tagged ROM4 (Fig. S2). Genotype analysis of the *rom4::mCherry* parasites and analysis of ROM4::mCherry expression (Fig. S2) demonstrates that correct genetic modification of the *rom4* locus is possible. Immunofluorescence analysis of ROM4::mCherry revealed its expression in gametocytes (Fig. S2); however, the very weak fluorescence signals in asexual blood stages prevented confirmation of merozoite surface location observed in *P. falciparum* (Fig. S2). The normal asexual multiplication rate (Table 2) indicates that the mCherry-tagged ROM4 functions normally during blood stage development. All information on the failed attempts to disrupt *rom4*, *6*, *7* and *8*, including DNA constructs and primers have been submitted to the RMgMDB database of genetically modified rodent malaria parasites (www.pberghei.eu).

The correct integration of the constructs and successful disruption of the other

rhomboids, *rom1*, 3, 9 and 10, were confirmed by diagnostic PCR and Southern analysis of separated chromosomes (Figs. 1 and 2). Northern analyses showed transcription of all four genes in blood stages of wild type *P. berghei* ANKA parasites and confirmed the lack of transcription in the blood stages of the respective gene-deletion mutants (Figs. 1 and 2). The clonal lines of the gene-deletion mutants $\Delta rom1$, $\Delta rom3$, $\Delta rom9$ and $\Delta rom10$ showed no change in asexual growth rates *in vivo* (Table 2). Despite the evidence for transcription and protein expression of ROM1, 9 and 10 in asexual blood stages (Figs. 1, 2 and S1; Table 1), this indicates a non-essential, redundant function for these proteins during asexual blood stage multiplication.

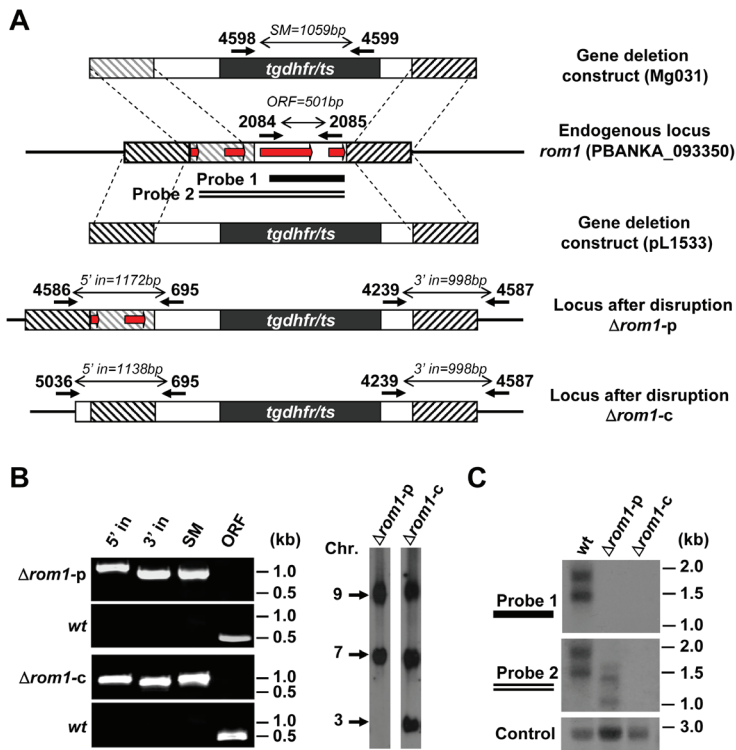


Figure 1. Generation of mutants lacking expression of *P. berghei* rhomboid 1.

A. Schematic representation of the constructs Mg031 and pL1533 targeting *rhomboid-1* for gene deletion by double cross-over homologous recombination at the target regions (hatched boxes), and the locus before and after disruption. Each construct contains the *tgdhfr/ts* selection cassette (black box). Mg031 replaces the 3rd and 4th exons (red arrows) of the open reading frame (ORF) but retains 1st and 2nd exons in mutant $\Delta rom1$ -p. pL1533 replaces the complete ORF in $\Delta rom1$ -c. Primer positions for diagnostic PCRs, amplicon sizes and the location of two PCR probes for the Northern blot analyses are shown (see Table S3 for primer sequences).

B. Diagnostic PCRs (left) and Southern analyses of separated chromosomes (right) confirm the correct

integration of the constructs in $\Delta rom1$ -p and $\Delta rom1$ -c. Primer pairs and amplicon sizes are shown in **A**: 5'/3' in, integration PCR; SM, amplification of the *tgdhfr/ts* selection cassette; ORF, deleted ORF. For Southern analyses, pulsed field gel-separated chromosomes were hybridized with a 3'UTR *pbdhfr* probe that recognizes the constructs integrated into *rom1* locus on chromosome 9 and the endogenous *dhfr/ts* locus on chromosome 7; in the $\Delta rom1$ -c line, the probe also hybridizes to the GFP-luciferase reporter cassette in the *230p* locus on chromosome 3.

C. Northern blot analyses of mRNA from mixed blood stage parasites confirm the loss of wild type *rom1* transcripts in $\Delta rom1$ -p and $\Delta rom1$ -c. Locations of the PCR probes used for hybridization were shown in **A** (PCR probes were generated by PCR-amplification from wild type *P. berghei* genomic DNA using primers 2084/2085 for Probe 1, and primers 2082/2085 for Probe 2; see Table S3 for primer sequences). In blood stages of $\Delta rom1$ -p, truncated transcripts were detected with Probe 2, recognizing exons 1 and 2 of *rom1*. In $\Delta rom1$ -c, no transcripts were detected. As a loading control, hybridization was performed with probe L644R that recognizes the large subunit ribosomal RNA. wt, wild-type *P. berghei* ANKA.

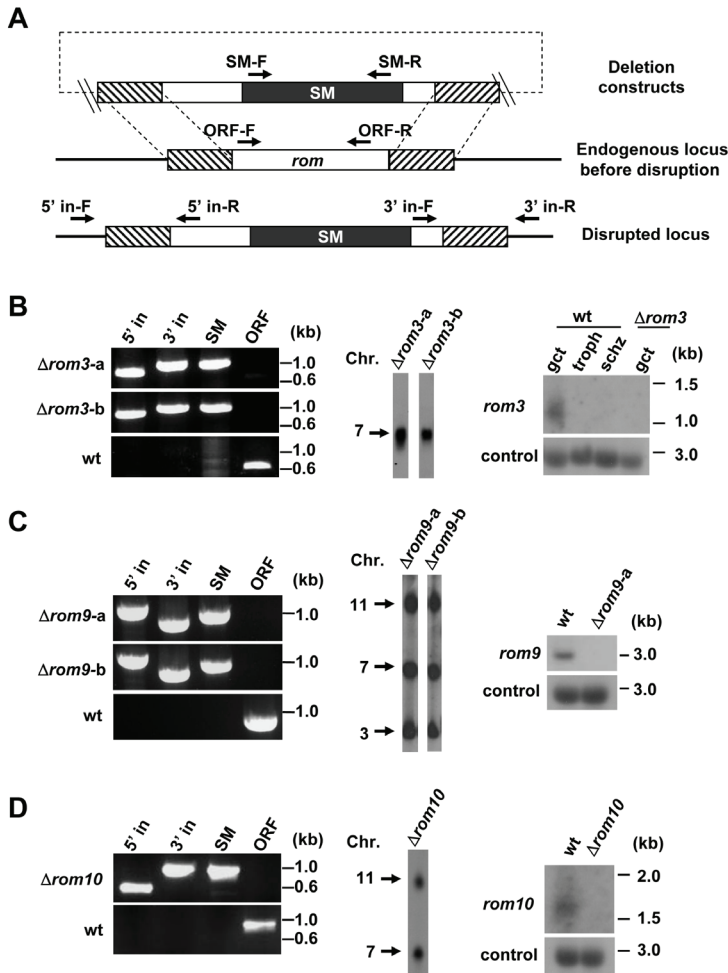


Figure 2. Generation of mutants lacking expression of *P. berghei* rhomboid 3, 9 and 10

A. Schematic representation of the DNA construct used for targeting rhomboid genes for deletion and the gene locus before and after disruption. The constructs which contain a drug-selectable marker cassette (SM; black box) disrupt the genes by double cross-over homologous recombination at the target regions (hatched boxes). The locations of primers for diagnostic PCRs are shown.

B. Diagnostic PCRs, Southern and Northern analyses confirm correct disruption of *rhomboid 3 (rom3)* in 2 independent mutants, $\Delta rom3$ -a and $\Delta rom3$ -b. For diagnostic PCRs (left), the following primers were used: 5' integration (5' in): 2389/695; 3' integration: (3' in) 4239/1886; amplification of the *tgdhfr/ts* selection cassette (SM): 4598/4599; deleted ORF (ORF): 1812/1813. For Southern analyses of separated chromosomes (middle), pulsed field gel-separated chromosome were hybridized using a *tgdhfr/ts* probe that recognizes the construct integrated into *rom3* locus on chromosome 7. Northern blot analysis (right) of mRNA of different blood stages shows transcripts only present in wild type gametocytes (gct). No transcripts are detected in trophozoites (troph) or schizonts (schz). The analysis also confirms the loss of *rom3* transcripts in gct of $\Delta rom3$. Hybridization was performed using a PCR probe recognizing *rom3* ORF (primers 1812/1813). As a loading control, hybridization was performed with probe L644R that recognizes the large subunit ribosomal RNA.

C. Analysis of two independent mutants, $\Delta rom9$ -a and $\Delta rom9$ -b, lacking expression of ROM9. For diagnostic PCRs (left), the following primers were used: 5' in: 7083/4906; 3' in: 4239/7084; SM (*hdhfr::yfcu*): 4698/4699; ORF: 7085/7086. For Southern analyses (middle), chromosomes were hybridized using a 3'UTR *pbdhfr* probe that recognizes the construct integrated into *rom9* on chromosome 11, the *dhfr/ts* on chromosome 7 and the GFP-luciferase reporter cassette in the *230p* locus on chromosome 3. Northern blot was hybridized with a PCR probe recognizing *rom9* ORF (primers 7085/7086) (right).

D. Analysis of $\Delta rom10$ lacking expression of ROM10. For diagnostic PCRs (left), the following primers were used: 5' in: 6939/4179; 3' in: 4239/2088; SM (*tgdhfr/ts*): 4598/4599; ORF: 6940/2066. Chromosomes were hybridized using a 3'UTR *pbdhfr* probe that recognizes the construct integrated into *rom10* on chromosome 11 and the *dhfr/ts* on chromosome 7 (middle). Northern blot was hybridized with a PCR probe recognizing *rom10* ORF (primers 6940/2066) (right). See Table S3 for all primer sequences and product sizes.

ROM9 and ROM10 are dispensable for the entire life cycle

Two independent gene-deletion mutants were generated for *rom9*: $\Delta rom9$ -a and $\Delta rom9$ -b (Fig. 2C). Asexual blood stage multiplication, gametocyte production and ookinete production of both $\Delta rom9$ mutants were similar to that of wild type *P. berghei* parasites.

We analyzed $\Delta rom9$ -a parasites during development in mosquitoes and in hepatocytes. The $\Delta rom9$ parasites produced wild type levels of oocysts (Table 2). Although we showed that *rom9* is transcribed in salivary gland sporozoites (Fig. S1), we found no significant differences between $\Delta rom9$ parasites and wild type parasites with respect to the production of sporozoites, their gliding motility (data not shown), traversal and invasion of hepatocytes and in the prepatent period in mice after injection of sporozoites (Table 2). Immunofluorescence analyses of liver stage parasites stained with antibodies against markers for parasite development (HSP70), parasitophorous vacuole membrane (UIS4 and EXP1) and merozoite formation (MSP1), also revealed no distinct differences in morphology between $\Delta rom9$ and wild type liver stage parasites at 24h or 48h after sporozoite invasion (Fig. 3 A). However, $\Delta rom9$ parasite loads between 53 and 57 hours after infection (measured by RT-PCR, FACS and luciferase assay) were consistently lower both *in vitro* and *in vivo* (Fig. 3 B&C) which may indicate that this enzyme plays a (minor)

Table 2. Phenotypes of *P. berghei* mutants lacking expression of rhomboids

Lines	Asexual multiplication rate ¹ (s.d.)	Gametocyte production ² % (s.d.)	Ookinete production ³ % (s.d.)	Oocyst production ⁴ (s.d.)	Sporozoite production ⁵ × 10 ³ (s.d.)	Sporozoite traversal ⁶ % (s.d.)	Sporozoite invasion rate ⁷ % (s.d.)	Prepatent period compare to wt ⁸
Mutants								
<i>Δrom1-p</i>	10 (0) n= 2	16.4 (0.5)	56.6 (1.8)	156.3 (151.8)	ND	ND	ND	ND
<i>Δrom1-c</i>	10 (0) n= 3	17.3 (1.0)	68.9 (9.5)	155.6 (118.9)	35.9 (3.3)	27.3 (7.6)	23.3 (8.5) *	+1 (n=3)
				220.0 (70.3)	49.0 (1.6)	ND	35.6 (10.6) **	+1 (n=3)
				ND	ND	ND	58.5 (6.8)	ND
<i>Δrom3-a</i>	10 (0) n= 3	17.9 (1.3)	61.3 (5.9)	148.4 (136.8)	NA	NA	NA	NA
<i>Δrom3-b</i>	10 (0) n= 2	18.9 (3.0)	71.0 (6.1)	259.7 (155.8)	NA	NA	NA	NA
<i>Δrom9-a</i>	10 (0) n= 4	18.9 (4.1)	74.3 (11.0)	145.8 (123.8)	43.2 (6.5)	21.1 (2.1)	51.7 (9.2)	+0 (n=5)
<i>Δrom9-b</i>	10 (0) n= 4	19.0 (2.7)	74.2 (4.6)	ND	ND	ND	ND	ND
<i>Δrom10</i>	10 (0) n= 4	18.1 (2.6)	63.8 (7.4)	191.8 (147.2)	44.7 (8.0)	ND	53.3 (4.5)	+0 (n=3)
Tagging mutants								
<i>rom3::gfp</i>	10 (0) n= 3	18.0 (2.7)	66.5 (4.7)	298.2 (110.7)	51.4 (8.9)	ND	ND	ND
<i>rom4::mCherry</i>	10 (0) n= 7	ND	ND	ND	ND	ND	ND	ND
<i>wt</i> ⁹	10 (0) n>10	15-25	50-90	120-290	35-80	19.3-25.7	53.0 -61.8	+0

¹ The multiplication rate per 24 hour of blood stage parasites in mice infected with a single parasite;

² The percentage of blood stage parasites developing into gametocytes *in vivo*;

³ The percentage of female gametes developing into mature ookinets *in vitro*;

⁴ The mean number of oocysts per mosquito (day 11–14);

⁵ The mean number of salivary gland sporozoites per mosquito (day 19–22);

⁶ Percentage of Dextran positive cells in Huh7 cell cultures 2h after post infection;

⁷ The percentage of intracellular sporozoites at 3 h post infection of Huh7 cell cultures;

⁸ The prepatent period (measured in days post sporozoite infection) is defined as the day when a blood stage infection with a parasitemia of 0.5–2% is observed. (+0 = similar to wild type; +1 = 1 day delay compared to wild type);

⁹ The developmental data for wild type parasites are shown as the range of mean values of > 10 experiments.

ND, not done; NA, not applicable.

* P<0.05, determined by student T-test as compared to wild type control run in parallel

role during liver stage development.

We generated one gene deletion mutant for *rom10* and analyzed this mutant throughout the entire life cycle. The phenotype of $\Delta rom10$ parasites was similar to that of wild type parasites in all developmental assays (Table 2), specifically *in vivo* asexual multiplication rate, *in vivo* gametocyte production, *in vitro* ookinete production, oocyst and sporozoite production and *in vivo* liver stage development. In addition, $\Delta rom10$ sporozoites showed normal rates of gliding (data not shown), *in vitro* hepatocyte invasion rate and prepatent period (Table 2). These results indicate that this protein is redundant and/or that its function can be fulfilled by other (rhomboid) proteases.

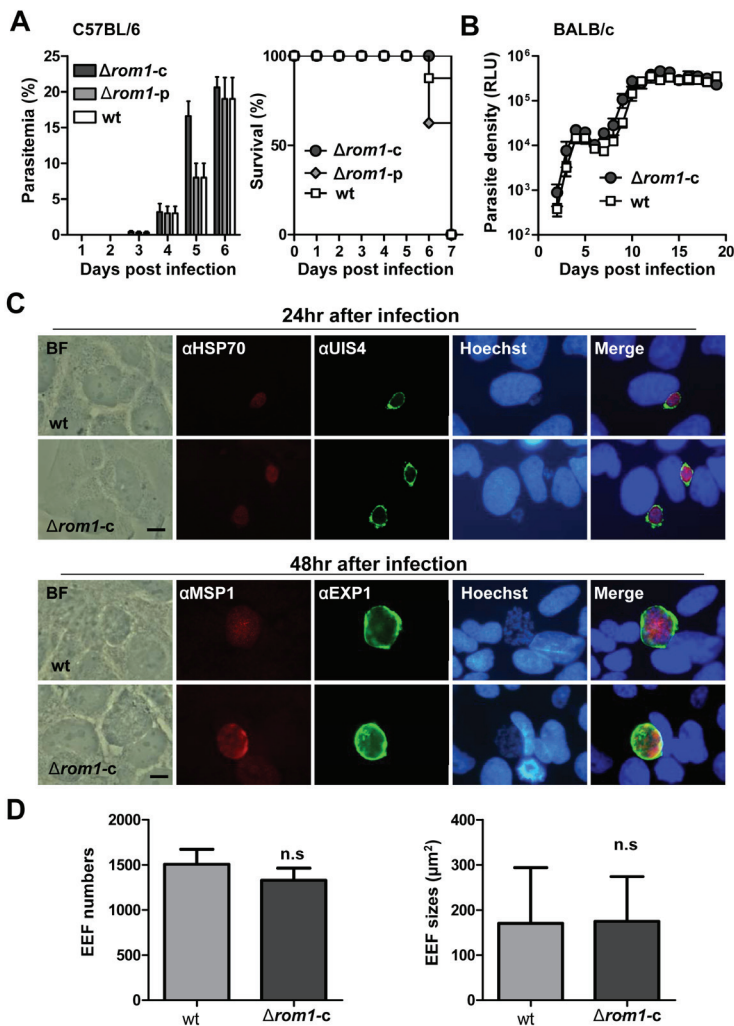


Figure 3. Liver stage development of $\Delta rom9$ parasites

A. Immunofluorescence assays of liver stages of $\Delta rom9$ and the wild type (wt) control *PbGFP-Luc_{schz}* at 24h and 48h after sporozoite infection of cultured Huh7 cells show a comparable morphology of $\Delta rom9$ and wild type parasites. Anti-HSP70 (red) antibody highlights the parasite's cytoplasm while anti-UIS4 (green) antibody decorates the parasitophorous vacuole membrane (PVM). Anti-MSP1 (red) antibody recognizes developing merozoites and anti-EXP1 (green) antibody the PVM. Nuclei were stained with Hoechst-33342 (Blue). BF, bright field; scale bars equals 10 μ m.

B. Parasite loads at 57h in cultured Huh7 cells after infection with 5×10^4 $\Delta rom9$ or wild type control *PbGFP-Luc_{schz}* sporozoites as determined by luciferase assay (left), qRT-PCR (middle) and FACS (right). All assays show a slight reduction of mutant parasite loads, however, only the relative infection value determined by qRT-PCR shows significant reduction (student T-test: n.s: not significant; *: $P < 0.5$).

C. Parasite loads in C57BL/6 mice at 53h after injection of 1×10^4 $\Delta rom9$ sporozoites or wild type control *PbGFP-Luc_{schz}* sporozoites as determined by *in vivo* imaging (left and middle) and qRT-PCR (right). Representative rainbow images of luminescence in livers of live mice (left) and the corresponding luminescence levels (photons/sec) of livers in whole mice (middle) are shown (student T-test: n.s: not significant). The lines indicate mean values and the error bars indicate standard deviations.

$\Delta rom1$ parasites have wild type blood-stage growth and virulence characteristics, but show delayed liver stage development

In the course of this study we generated two independent *P. berghei* $\Delta rom1$ mutants; the first mutant $\Delta rom1$ -p is a partial gene deletion lacking the 3rd and 4th exons of *rom1* that contain the catalytic diad (Fig. 1A&B); the second mutant $\Delta rom1$ -c lacks the entire open reading frame (Fig. 1A&B). Northern analyses of *rom1* transcripts in blood stages using two PCR-amplified probes specific to 3rd and 4th exons, or to the whole ORF, showed that $\Delta rom1$ -p lacks transcripts containing the 3rd and 4th exons but still produces stable, truncated transcripts consisting of the 1st and 2nd exons. As expected, $\Delta rom1$ -c had no detectable *rom1* transcripts (Fig. 1C). Both $\Delta rom1$ -p and $\Delta rom1$ -c showed *in vivo* multiplication rates were similar to wild type *P. berghei* parasites when analyzed in the cloning-assay (Table 2). To determine possible differences in growth rate and virulence during prolonged infections in mice, we analyzed the growth rate of $\Delta rom1$ and wild type parasites in C57BL/6 and in BALB/c mice (Fig. 4A&B). C57BL/6 mice are sensitive to experimental cerebral malaria (ECM) and cerebral complications develop 6–8 days post-infection with *P. berghei* ANKA parasites, whereas BALB/c mice are ECM-resistant and develop fulminating (and lethal) parasitemias peaking 2–3 weeks after infection. In both C57BL/6 and BALB/c mice $\Delta rom1$ parasites showed infection patterns that were highly similar to infections initiated with wild parasites (Fig. 4A&B); all $\Delta rom1$ infected C57BL/6 mice developed ECM symptoms at day 6 or 7 after infection (Fig. 4A).

$\Delta rom1$ parasites were next examined during mosquito and liver stage development. These parasites produced numbers of ookinetes, oocysts and salivary gland sporozoites similar to those of wild type parasites (Table 2). However, liver-stage development was reduced as shown by a 1-day extension of the prepatent period in mice following the inoculation

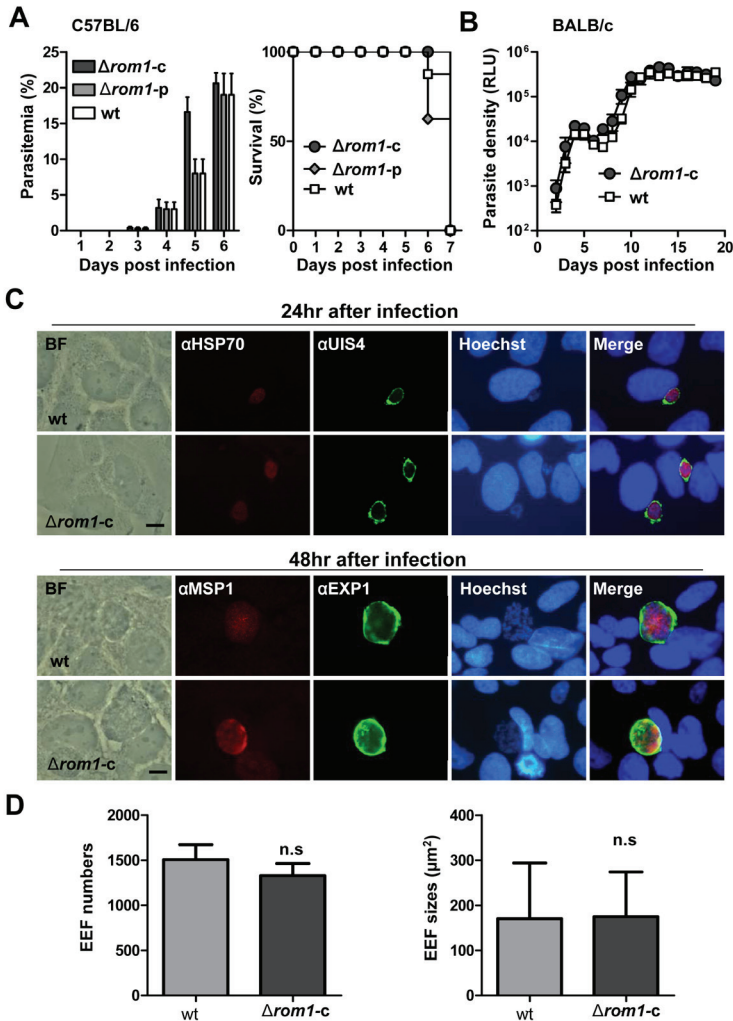


Figure 4. Blood and liver stage development of $\Delta rom1$ parasites.

A. The course of infection (left panel) and survival curve (right panel) in C57BL/6 mice ($n=6$) infected with 10^5 wild-type (wt, cl15cy1), $\Delta rom1$ -p or $\Delta rom1$ -c. The parasitemia developed in mice infected with wt, $\Delta rom1$ -p and $\Delta rom1$ -c parasites are highly comparable during the whole course of infection (left). All C57BL/6 mice infected with wild-type (wt, cl15cy1), $\Delta rom1$ -p and $\Delta rom1$ -c parasites developed ECM complications on day 6–7 as indicated by a drop in body temperature below 34°C ; mice were sacrificed at this point (right).

B. The course of infection in BALB/c mice ($n=6$) infected with 10^4 parasites of wild-type (wt, GFP-Luc_{con}) or $\Delta rom1$ -c parasites. Parasite densities were determined by measuring luciferase activity indicated as relative light unit (RLU) in the IVDL-assay. Error bars indicate standard deviations in A and B.

C. Immunofluorescence analyses of $\Delta rom1$ -c and the wild type (wt, GFP-Luc_{con}) exo-erythrocytic forms (EEF) at 24h and 48h after infection with 1×10^4 $\Delta rom1$ -c or wild type (GFP-Luc_{con}) parasites show normal development of $\Delta rom1$ -c parasites compared to wild type control. Anti-HSP70 (red) and anti-UIS4 (green) antibodies recognize the parasite's cytoplasm and the parasitophorous vacuole membrane (PVM). Anti-MSP1 (red) antibodies recognize developing merozoites and anti-EXP1 (green) antibodies stain the PVM. Nuclei were stained with

Hoechst-33342 (Blue). BF, bright field; scale bars equals 10µm.

D. EEF numbers per well of cultured Huh7 cells at 24hr (left) and the sizes of EEFs at 48hr (right) after sporozoite infection. The numbers of EEFs were determined by counting anti-UIS4 staining positive EEFs in the immunofluorescence assay, and the EEF sizes were determined by measuring the sizes of anti-Hsp70 staining positive parasites. The lines indicate mean values and the error bars indicate standard deviations.

with 10^4 purified sporozoites. While gliding motility (data not shown) and the rate of cell traversal of sporozoites were similar to wild type parasites (Table 2), we observed in two out of three experiments a reduction in sporozoite *in vitro* invasion rates (Table 2) that could explain (in part) the delay in the prepatent period. Immunofluorescence analyses of liver stage parasites stained with antibodies against markers for parasite development (HSP70), PVM (UIS4 and EXP1) and merozoite formation (MSP1), revealed no distinct differences in morphology and size between $\Delta rom1$ and wild type liver stages at 24h or 48h after sporozoite invasion (Fig. 4C). Although a significant reduction in parasite loads and expression of UIS4 have been reported for liver stages of *P. yoelii* mutants lacking expression of ROM1 [26], we only observed a slight, but not significant, reduction in numbers of liver stages as determined by anti-UIS4 antibody staining (Fig. 4D) and we did not observe that these mutants had unusual PVM morphology. Liver stages of $\Delta rom1$ and wild-type parasites were also comparable in size at 48 hrs post infection (Fig. 4D).

$\Delta rom3$ parasites establish oocysts but fail to produce sporozoites

Two independent gene-deletion mutants, $\Delta rom3$ -a and $\Delta rom3$ -b, were generated (Fig. 2B). Asexual blood stage multiplication rates of both mutants determined in the cloning assay were normal and $\Delta rom3$ parasites produced wild type levels of gametocytes, ookinetes and oocysts (Table 2). By light microscopy, $\Delta rom3$ ookinetes have the characteristics of fully mature wild-type ookinetes such as an elongated ‘banana’ shape, hemozoin clusters and a centrally located, enlarged nucleus and the $\Delta rom3$ and wild type ookinetes show a similar (tetraploid) DNA content (Fig. S3). In addition, by electron microscopy analyses we were unable to detect differences in the ultrastructural morphology of wild-type and $\Delta rom3$ ookinetes; with respect to the nucleus, crystalloid body and the structure of the apical complex (Fig. S5). All membranes of these organelles exhibit a normal structure and the apical complex of $\Delta rom3$ ookinetes had the characteristic features of abundant micronemes, and the presence of microtubules and the inner membrane complex.

However, no sporozoites were detected in salivary glands of mosquitoes infected with $\Delta rom3$ -a or $\Delta rom3$ -b in three independent experiments. Inspection of $\Delta rom3$ oocysts by light-microscopy revealed normal oocyst production but a complete absence of sporozoite formation; mature oocysts had clearly vacuolated cytoplasm and there were no signs

of sporulation (Fig. 5A). Western analysis of circumsporozoite protein (CSP) expression using anti-CSP antibody in oocysts-containing midguts at day 10 after infection, showed that CSP is almost absent in the $\Delta rom3$ oocysts (Fig. 5B). An indirect immunofluorescence assay (IFA) on wild type and $\Delta rom3$ oocysts confirmed the strongly reduced CSP levels in $\Delta rom3$ oocysts (Fig. 5C). There was also reduced intensity of Hoechst DNA-staining indicating decreased DNA replication in these oocysts (Fig. 5C). The crucial role of ROM3 in oocyst maturation/sporogony is unexpected given the high transcript levels detected in gametocytes (Table 1, Fig. S1B). When we analyzed ROM3::GFP expression in *rom3::gfp* parasites (with the endogenous *rom3* C-terminally tagged with GFP), we observed GFP signal in all female gametocytes (but not in male gametocytes) that persisted into mature ookinetes but was undetectable in oocysts (day 6-17) and sporozoites (Fig. 5D).

The normal development throughout the life cycle (Fig. 5D, Table 2) indicates that the C-terminal GFP-tag does not affect the essential function of ROM3 during sporozoite formation. We attempted to use the *rom3::gfp* parasites to gain a better understanding of the localization of ROM3 in female gametocytes and ookinetes. Specifically, we extracted soluble and insoluble protein fractions of *rom3::gfp* gametocytes and ookinetes and then examined the presence of ROM3 protein using antibodies against the GFP tag. Unfortunately, we were unable to unambiguously identify ROM3::GFP in either fraction, presumably due to the very low expression of ROM3 in these stages (data not shown).

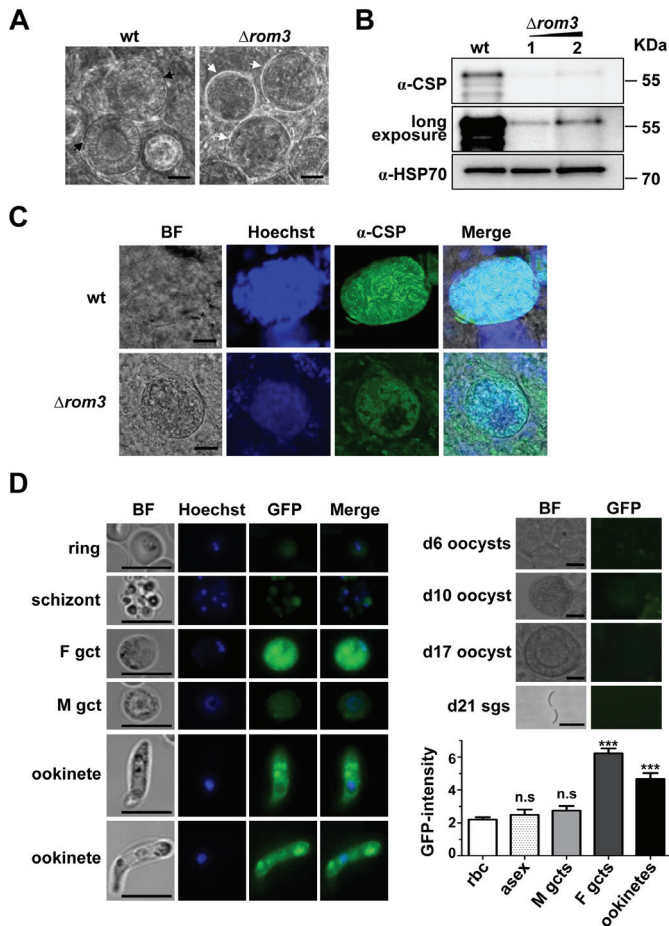


Figure 5. Rhomboid 3 is essential for sporozoite formation in oocysts.

A. Phase contrast microscopy of wild type and aberrant, vacuolated $\Delta rom3$ oocysts on day 12 after mosquito infection. Mutants lack any signs of sporozoite formation (white arrow) whereas wild type (wt) oocysts collected on the same day show clear sporulation (black arrow). Scale bar 10 μ m.

B. Western blot analysis of midguts from infected mosquitoes. Midguts from mosquitoes infected with $\Delta rom3$ (1 or 2 midguts, day 10) and wild-type (wt, day 10) were separated on SDS-PAGE and stained with anti-CSP and anti-HSP70 antibodies. A longer exposure of the anti-CSP blot is also shown.

C. Developmental defects of $\Delta rom3$ parasites examined by immunofluorescence assays. Compared to wild-type (wt), $\Delta rom3$ oocyst show decreased CSP expression as shown by staining oocysts with anti-CSP (green) antibody and reduced staining with the DNA-specific dye Hoechst-33342 (blue), indicating less DNA replication. BF, bright field. Scale bar 10 μ m.

D. All $rom3::gfp$ female gametocytes (F gct; n=50) and ookinetes (n >100) exhibited a GFP signal that was significantly above background values (**P<0.0001, student T-test). No GFP signals above background were detected in either male gametocyte (M gct; n=30) or asexual blood stages. In the mosquito vector no GFP signals were detected in either $rom3::gfp$ oocysts (6-17 days after mosquito infection) or in salivary gland sporozoites (sgs, day 21). Nuclei are stained with Hoechst-33342 (blue). BF, bright field. Scale bar 10 μ m. n.s., not significant, student T-test.

Discussion

The discovery of critical roles for certain rhomboid proteins in motility, host-cell invasion and pathogenesis of apicomplexan parasites has attracted considerable attention. However, ten years after their initial discovery, only two of the eight rhomboids of malaria parasites, ROM1 and ROM4, have been analyzed in more detail. Multiple roles have been suggested for ROM1 and ROM4: invasion of red blood cells (RBC) [22], sporozoite gliding motility [23] and the formation of the parasitophorous vacuole membrane (PVM) in infected hepatocytes [26]. In this study, we investigated expression patterns of all eight *P. berghei* rhomboids and examined the effects of rhomboid gene deletion across the entire lifecycle of the parasite in order to pinpoint additional, new role for this intramembrane protease family. In line with previously published work, our studies support the observations that ROM1 is dispensable for parasite development throughout the life cycle [25,26] and that ROM4 is essential for asexual blood stage development [22]. We identified 3 more rhomboids that are dispensable for asexual blood stage development: ROM3, ROM9 and ROM10. Mutants lacking expression of ROM9 and ROM10 can complete the entire life cycle without major developmental defects. These observations indicate functional redundancy for several rhomboids (ROM1, 9 and 10) and suggest that processing of essential substrates may be fulfilled by more than one protease. ROM4 and ROM1 are targeted to different cellular locations in the merozoite – surface and microneme [22] – making it unlikely that they process identical substrates that would allow ROM4 to compensate for ROM1 in the $\Delta rom1$ mutant, and clearly not vice versa.

The repeated failure to delete ROM4, ROM6, ROM7 and ROM8 genes indicate that these rhomboids play key and most likely independent roles during blood stage development that cannot be met by other proteins. Located on the merozoite surface, *P. falciparum* ROM4 is strongly implicated in the shedding of the erythrocyte binding antigen 175 (EBA175) during merozoite invasion [22]. Rodent malaria parasites lack EBA175 but express a homolog of EBA140 (BAEBL) which also belongs to the same EBL (erythrocyte-binding-like) TM protein family. Similar to EBA175, *P. falciparum* EBA140 is also an *in vitro* substrate of ROM4 [15], and in *P. yoelii* EBA140 (PY04764) is essential for RBC invasion [28]. Interestingly, in *P. berghei* the related protein, PBANKA_133270, also contains a putative cleavage site, similar to the one found in EBA140. Our successful C-terminal tagging of *P. berghei* ROM4 strengthens the notion that the failure to disrupt *rom4* is not due to inaccessibility of this specific locus to genetic modification, but is due to its key role in the enzymatic processing of surface molecules like EBA140. Combined these data suggest that ROM4 shares essential roles in both human and rodent malaria parasites

through cleavage of one or more merozoite surface proteins involved in RBC invasion, which cannot be compensated by other rhomboid or non-rhomboid proteases. ROM4 from another apicomplexan parasite, *T. gondii*, has been established as a sheddase during gliding motility and invasion [29]. In addition to ROM1 and ROM4, *P. falciparum* ROM7 and ROM8 are also expressed in merozoites [15]. It is however unlikely that these proteins process the same TM spanning proteins as ROM1 or ROM4, because they do not show the same *in vitro* substrate specificities as ROM1 or ROM4 [15]. *Plasmodium* ROM7 only has orthologs in the apicomplexan parasites, *Babesia bovis* and *Theileria annulata*, while ROM8 does not cluster with any other apicomplexan rhomboids [16].

Plasmodium ROM6 is the ortholog of *T. gondii* ROM6, which clusters with the PARL-like mitochondrial rhomboids and localizes to the single mitochondrion [16], however, a mitochondrial location in *Plasmodium* has yet to be confirmed. These ROM6 proteins share common features in their TM domains and catalytic sites, which are characteristic for PARL-type rhomboids [4], and contain predicted mitochondrial-targeting sequence [30]. Known conserved substrates of PARL-type rhomboids are dynamin-related proteins [12,14]. *Plasmodium* species express two conserved dynamins: DYN1 (PBANKA_090360) and DYN2 (PBANKA_052040). Interestingly, phylogenetic analyses show that *Plasmodium* DYN2 clusters with dynamins of other species that are mainly implicated in the division of the mitochondrial outer-membrane [31]. Attempts to disrupt the *dyn2* gene were unsuccessful (unpublished data, G.R.M. and C.J.J.; <http://www.pberghei.eu/index.php?rmgm=765>), suggesting its essential role in asexual stage parasites. Further research is needed to determine whether DYN2 is the substrate of ROM6 and protein localization studies with tagged proteins or antibodies may reveal whether both proteins are indeed located in the mitochondria in blood stages.

Although ROM1 is not essential for blood stage parasites, it has been reported that *P. berghei* and *P. yoelii* mutants lacking ROM1 exhibit a slight growth delay and appear less virulent in mice than wild type parasites [25,26]. In contrast, we were unable to detect either a growth or virulence-attenuation phenotype in experiments conducted with 2 independent *P. berghei* $\Delta rom1$ lines. The cause for these discrepancies in blood stage phenotypes between our and the *P. berghei* mutant reported by Srinivasan *et al.* [25] is unknown. In the study of Srinivasan *et al.* [25], the mutant clone examined was derived from a single transfection experiment that generated a 3' end truncation of the gene encoding ROM1, preserving a large part of the ROM1 protein. We were able to detect a stable, although truncated, transcript transcribed from the 5' end of the gene in the $\Delta rom1$ -p mutant; whether these are translated into stable, truncated proteins that are inserted into the membrane exerting a dominant-negative effect is unknown. Cloned

lines of wild type *P. berghei* ANKA parasites are known to differ in growth and virulence characteristics [32] and environmental factors have been shown to influence the course of infections in mice [33]; such differences between laboratories may influence the outcome of phenotypic analyses of genetically identical mutants. Therefore the reported growth and virulence phenotype may be unrelated to the disruption of *rom1*.

In contrast to normal blood stage infections of the mutants reported in this study, we found that $\Delta rom1$ parasites have a slight defect in liver stage development with a consistent delay of 1-day in blood stage patency following sporozoite infection. A prolonged prepatent period was also observed by Srinivasan *et al.* [25]. This finding was confirmed by a two-fold reduction in liver stage development of *P. yoelii* $\Delta rom1$ parasites [26]. It has been suggested that this reduction in *P. yoelii* liver development results from reduced cleavage of the PVM protein UIS4 (up-regulated in sporozoites 4) [26]. However, when we analyzed liver stage development of *P. berghei* $\Delta rom1$ parasites, we did not find evidence for the aborted liver stage development or parasites with unusual PVM morphology. In addition to the prolonged prepatent period, we did observe a decrease in sporozoite invasion rate in 2 out of 3 experiments. However, since there are discrepancies in $\Delta rom1$ -c sporozoite-hepatocyte invasion rates, we cannot conclude that a reduction in invasion is responsible for the delay in the prepatent period. Altogether, the phenotypic observations of different $\Delta rom1$ parasites prove that ROM1 is not essential throughout the complete life cycle in both *P. berghei* and *P. yoelii*. In addition to ROM1, our loss-of-function analyses indicate that there is large degree of functional redundancy of *Plasmodium* rhomboids. We identified two other rhomboids, ROM9 and ROM10, which are dispensable throughout the complete life cycle. Both rhomboids are exclusive to *Plasmodium* [16]. Interestingly, ROM9 carries a mitochondrial targeting sequence (MitoProtII <http://ihg.gsf.de/ihg/mitoprot.html>) but its predicted topology is atypical of mitochondrial PARL-like rhomboids [4]. ROM10 lacks key residues predicted to be critical to rhomboid proteolysis [4,15] and is therefore likely an inactive rhomboid. Although the expression of ROM10 was detected in multiple stages in *P. falciparum*, and our RT-PCR and Northern analyses also confirmed its expression in blood stage, the gene-deletion mutant showed no phenotypic defect throughout the entire life cycle.

In contrast to the $\Delta rom1$, $\Delta rom9$ and $\Delta rom10$ parasites, mutants lacking ROM3 expression exhibit a strong and distinct phenotype. The gene encoding ROM3 is highly transcribed in gametocytes and in the *rom3::gfp* mutant, the GFP signal was clearly observed in female gametocytes through to the ookinete stage but was absent from developing oocysts and sporozoites. *P. berghei* mutants lacking ROM3 are capable of producing normal numbers of oocysts; however, these oocysts show a complete absence of sporozoite formation.

This is the first apicomplexan rhomboid identified to play such a vital role in sporogony. Mutant oocysts show clear signs of stalled DNA replication and a failure to form individual sporozoites, and remain highly vacuolated. This 'delayed phenotype' in mutants which lack proteins normally expressed in female gametocytes/gametes but only manifest the consequences of the loss-of-function in maturing oocysts is not unique. Examples include several members of the LCCL/lectin adhesive-like protein (CCp/LAP) family with their distinct Lgl1(LCCL)-lectin adhesive domains [34]. Deletion of these also female gametocyte expressed genes produces a phenotype in maturing oocysts comparable to the one observed in the $\Delta rom3$ parasites; vacuolated oocysts and absence of sporozoite formation [34–36]. CCp/LAP proteins have no TM domains and therefore are unlikely ROM3 substrates. They are localized to the crystalloid body in ookinetes which has been postulated to constitute a reservoir of proteins synthesized by the gametocyte to be used during oocyst growth and sporozoite development [37–39]. However, ultrastructure analysis of the $\Delta rom3$ and wild-type ookinetes revealed no distinct differences with respect to their crystalloid bodies. In addition, although we observed a punctate location of ROM3::GFP in ookinetes, we did not observe the crystalloid-type location that was shown for LAP2 and LAP3 [39]. A failure of oocysts to sporulate also occurs in the absence of three other membrane-bound proteins: glycosyl phosphatidyl inositol (GPI) anchored CSP (PBANKA_040320) [40], or TM domain containing plasmepsin VI (PBANKA_040970) [35] and PBANKA_130960 [41]. CSP is localized on the oocyst plasma membrane and on the inner surface of the oocyst capsule; when budding begins, large amounts of CSP cover the surface of sporoblasts and sporozoites [42]. Our analyses of CSP expression and processing in $\Delta rom3$ parasites show that although CSP expression is strongly reduced (Fig. 5B and Fig. S4), processing appears to be normal (Fig. S4). Given that CSP contains a GPI anchor it is unlikely to be processed by ROM3. As most identified natural substrates of rhomboid proteases contain only a single transmembrane domain, it is questionable if PBANKA_130960 is a substrate since it has several putative transmembrane domains (www.plasmodb.org). In Table S5 we provide a list of putative substrates of ROM3, based on the published proteome data of oocysts and sporozoite proteins (www.plasmoDB.org), which are predicted to contain a single transmembrane domain and encode a signal peptide. Whether plasmepsin VI is the substrate of ROM3 and contributes to the phenotype observed in ROM3-deficient mutants remains to be investigated. Since we observe expression of ROM3 in gametocytes and ookinetes and not in developing and mature oocysts, it is very much possible that the ROM3 substrate(s) is (are) also present and cleaved in gametocytes/ookinetes.

In this study we have examined all eight rhomboid proteases encoded by *P. berghei* and found four of them (ROM4, 6, 7 and 8) to be critical for asexual development, and one

(ROM3) essential for mosquito development. While some member of these rhomboids may govern processes common to a large number of eukaryotic species (for example, the mitochondrial PARL-like rhomboid ROM6), most of them are unique to Apicomplexa and some unique to *Plasmodium*. These specific rhomboids and their substrates offer themselves as targets for anti-parasite interventions. While the exact nature of the function of most rhomboids and their substrate range remain to be elucidated, this study helps provide a clear framework of expression, function in parasite development and the specific and redundant enzymatic activities of this important class of proteases.

Experimental procedures

Experimental animals and *P. berghei* ANKA reference lines

Female C57BL/6, BALB/c and Swiss OF1 mice (6–8 weeks) and male C57BL/6 (6–8 weeks) from Charles River were used. All animal experiments performed at the LUMC were approved by the Animal Experiments Committee of the Leiden University Medical Center (DEC 07171; DEC 10099). The Dutch Experiments on Animal Act is established under European guidelines (EU directive no. 86/609/EEC regarding the Protection of Animals used for Experimental and Other Scientific Purposes). Animals used at the Instituto de Medicina Molecular, Faculdade de Medicina, Universidade de Lisboa, were housed in the Specific Pathogen Free facilities of the Institute. All experimental procedures were carried strictly within the rules of the Portuguese official Veterinary Directorate (Direcção Geral de Veterinária), which complies with the European Guideline 86/609/EC and follows the FELASA (Federation of European Laboratory Animal Science Associations) guidelines and recommendations concerning laboratory animal welfare.

Three reference *P. berghei* ANKA parasite lines were used for generation of the gene-deletion mutants and the transgenic parasites: the ‘wild type’ (wt) line cl15cy1 [43] and two reporter lines, i.e. *PbGFP-LUC_{con}* (line 676m1cl1; mutant RMgm-29; www.pberghei.eu) and *PbGFP-Luc_{schz}* (line 1037cl1; mutant RMgm-32; www.pberghei.eu). Both reporter lines were generated in the cl15cy1 parent line and express the fusion protein GFP-Luciferase either under the control of the constitutive *eef1α* promoter or the schizont-specific *ama1* promoter, respectively. The *gfp-luc* expression cassette is stably integrated into the *pb230p* locus without introduction of a drug-selectable marker [44,45].

RT-PCR analyses

To investigate the transcription pattern of the different rhomboid genes, RT-PCR was performed for each gene using cDNA from i) asexual blood stages of a non-gametocyte

producer *P. berghei* ANKA parasite line (HPE) [46], ii) purified gametocytes of wild type *P. berghei* ANKA (cl15cy1) parasites and iii) salivary gland sporozoites of wild type *P. berghei* ANKA (cl15cy1). Primers were designed specific to the ORF of each gene and across introns when possible in order to distinguish amplicons from gDNA and cDNA. Details of the primers and expected sizes are shown in Table S4.

Generation of gene deletion mutants

To disrupt the *rhomboid* genes, the following replacement constructs were generated. Plasmid constructs targeting *rom1*, *3*, *4*, and *10* were constructed in the generic plasmid pL0001 (www.mr4.com) which contains the pyrimethamine resistant *Toxoplasma gondii* (*tg*) dihydrofolate reductase-thymidylate synthase (*dhfr/ts*) as a selectable marker (SM) under the control of *P. berghei dhfr/ts* promoter. Targeting regions for homologous recombination were PCR-amplified from *P. berghei* ANKA (cl15cy1) genomic DNA using primers specific for the 5' or 3' ends of each *rhomboid* gene (see Table S2 for the primer sequences) and cloned in upstream and downstream, respectively of the SM; this allows integration of the construct into the targeting regions by double cross-over homologous recombination and complete replacement of the ORF. For transfection the gene-deletion constructs were linearized with the appropriate restriction enzymes (Table S2).

Constructs targeting *rom6*, *8* and *9* were generated using a modified two step PCR method [47]. Briefly, in the first PCR reaction two fragments of 5' and 3' targeting regions (TR) were amplified from *P. berghei* ANKA (cl15cy1) genomic DNA with the primer sets shown in Table S2. The reverse primers of 5'TR and the forward primers of 3'TR have 5' extensions homologous to the *hdhfr::yfcu* selectable marker cassette from pL0048. In the second PCR reaction, the 5'TR and 3'TR were annealed to either side of the selectable marker cassette, and the joint fragment was amplified by the external anchor-tag primers 4661/4662, resulting in the PCR-based targeting constructs. Before transfection, the PCR-based constructs were digested with *NruI* (as indicated in primer sequences in Table S2) to remove the 'anchor-tag' and with *DpnI* that digests any residual uncut pL0048 plasmid.

Transfection and selection of transformed parasites with pyrimethamine was performed using standard technology for the genetic modification of *P. berghei* [43]. All information on the generation of gene-deletion mutants (as well as unsuccessful disruption attempts), such as DNA constructs and primers, has been submitted to the RMgMDB database of genetically modified rodent malaria parasites (www.pberghei.eu).

Clonal parasite lines were obtained from all gene-deletion mutants by the method of limiting dilution. Correct integration of DNA constructs and disruption of the genes was

verified by diagnostic PCR analyses (see Table S3 for primers used) and Southern analyses of chromosomes separated by pulsed-field gel electrophoresis hybridized with probes specific for the selectable maker (see Table S3 for primers used) [43].

Generation and analyses of parasites expressing ROM3::GFP and ROM4::mCherry

To tag ROM3 C-terminally with GFP, 1.6 kb upstream of the stop codon of *rom3* containing the entire ORF were PCR-amplified from wild-type *P. berghei* ANKA genomic DNA, TOPO-cloned and sequence analyzed (see Table S2 for the primers). The fragment was released from pCR2.1-TOPO (Invitrogen) through digestion with *EcoRV* and *BamHI* and ligated into the generic GFP-tagging plasmid pL1200 [48], resulting in construct pL1079 containing the pyrimethamine resistant *tgdhfr/ts* as a selectable marker. To tag ROM4 with mCherry, the complete ORF of *rom4* (except the stop codon) was PCR-amplified from wild type *P. berghei* ANKA genomic DNA (see Table S2 for the primers used). This ORF was digested with *SpeI* and *BglII*, and ligated into *SpeI/BamHI* digested vector pL1646 (containing a C-terminal mCherry tag and the *tgdhfr/ts* selectable marker cassette), resulting in construct pL1920. Before transfection, pL1079 was linearized with *SpeI*, and pL1920 was linearized with *BamHI*. Transfection, selection and cloning of transgenic parasites with pyrimethamine was carried out as described above, generating the following transgenic lines, *rom3::gfp* (line 654cl1) and *rom4::mCherry* (line 2143cl1) that express endogenous C-terminally tagged ROM3 and ROM4, respectively. The live GFP or mCherry signals of parasites of the transgenic mutants were examined by fluorescence microscopy (Leica DM-IRBE Flu) after staining with Hoechst-33342 (2 $\mu\text{mol/L}$, Sigma, NL) for 15 min at room temperature. The fluorescence intensity was measured using ImageJ software.

Analysis of transcription of rhomboid genes in blood stages of wild type and gene-deletion parasites

Transcript levels were analyzed by standard Northern blot analyses. Total RNA was isolated from mixed blood stages or different stages of wild type *P. berghei* ANKA (cl15cy1), non-gametocyte producer line (HPE) and the different gene-deletion mutant lines. Northern blots were hybridised with probes specific for each rhomboid ORF, which had been PCR-amplified from wild-type *P. berghei* ANKA genomic DNA (primers shown in Table S3). As a loading control, Northern blots were hybridized with the oligonucleotide probe L644R that recognizes the large subunit ribosomal RNA [49].

***In vivo* multiplication rate of asexual blood stages**

The multiplication rate of asexual blood stages in mice is determined during the cloning procedure of each gene-deletion mutant [45] and is calculated as follows: the percentage of infected erythrocytes in Swiss OF1 mice injected with a single parasite is quantified at day 8 to 11 on Giemsa-stained blood films. The mean asexual multiplication rate per 24 hour is then calculated assuming a total of 1.2×10^{10} erythrocytes per mouse (2mL of blood). The percentage of infected erythrocytes in mice infected with reference lines of the *P. berghei* ANKA strain consistently ranges between 0.5–2% at day 8 after infection, resulting in a mean multiplication rate of 10 per 24h [45,50].

Course of parasitemia, virulence and experimental cerebral malaria in mice infected with $\Delta rom1$ parasites

The course of parasitemia was determined in BALB/c mice. Groups of 6 mice were intraperitoneally (i.p) infected with 10^4 $\Delta rom1$ -c parasites or equal numbers of the parental reporter line *PbGFP-LUC_{con}*. The course of parasitemia was determined in a luciferase assay (IVDL-assay) [51]; *in vivo* parasite growth in mice is quantified by measuring the luciferase activity of GFP-Luciferase expressing parasites in tail blood. The IVDL-assay generates growth-curves that are identical to those obtained by manual counting of parasites in Giemsa-stained smears. In brief, 10 μ L tail blood was collected daily from all mice using heparinized capillaries. Samples were stored at -80 °C in Eppendorf tubes till further processing for the luciferase assay. Luciferase activity (luminescence) in the samples was measured as described [51,52].

The capacity of $\Delta rom1$ to induce features of experimental cerebral malaria (ECM) was analyzed in C57BL/6 mice. Groups of 6 mice were infected with 10^5 *P. berghei* ANKA (cl15cy1), $\Delta rom1$ -p or $\Delta rom1$ -c parasites. Onset of ECM in *P. berghei* infection was determined by measurement of a drop in body temperature below 34°C [45]. The body temperature of infected mice was measured twice a day from day 5 to day 8 after infection using a laboratory thermometer (model BAT-12, Physitemp Instruments Inc., Clifton, NJ) with a rectal probe (RET-2) for mice. When infected mice showed a drop in temperature (below 34°C) the mice were sacrificed.

Gametocyte and ookinete production

Gametocyte production is defined as the percentage of ring forms developing into mature gametocytes during synchronized infections [53]. Ookinete production was determined in standard *in vitro* fertilization and ookinete maturation assays and is defined as the

percentage of female gametes that develop into mature ookinetes under standardized *in vitro* culture conditions [54]. Female gamete and mature ookinete numbers were determined in Giemsa-stained blood smears made 16–18 h post activation.

Electron microscopy

Ookinetes were cultured *in vitro* as previously described [54]; briefly, gametocytes for these assays were obtained from infected mice that had been pre-treated with phenylhydrazine and treated with the antimalarial drug sulfadiazine (dissolved in the drinking water at a concentration of 30 mg/L) to obtain highly pure gametocyte populations [55]. Ookinetes from these cultures were purified using a Nycodenz density gradient centrifugation. The purified ookinetes were diluted in RPMI medium (without serum) and fixed by resuspending them in an equal amount of 3% glutaraldehyde (Electron Microscopy Sciences, Hatfield, PA) in 0.2 M sodium cacodylate pH 7.4 (1h at RT), washed twice with cacodylate buffer (spinning for 2min at 425g), post-fixed with 1% osmium tetroxide (Electron Microscopy Sciences, Hatfield, PA) in cacodylate buffer (1h at RT), and washed again with cacodylate buffer. Subsequently, the samples were stained with an aqueous solution of 1% uranyl acetate for 40 min at RT, washed twice with demineralized water, re-suspended in 3% agar (Difco Laboratories, Detroit, Michigan; in demineralized water at 60°C), centrifuged (for 2min at 425g) and stored at 4°C until the agar became solid. The samples were dehydrated in series of washes 70% (overnight), 80% (10 min), 90% (10 min) and 100% ethanol (1h, refreshing 2 times), infiltrated with a 1:1 mixture of epon LX 112/propylene oxide (1h) and pure epon (3h), followed by embedding in epon and polymerization for 48h at 60°C. The samples were cut using a Leica UC6 ultramicrotome at RT into 100nm sections with a Diatome ultra 45°diamond knife (Diatome, Switzerland) at a cutting speed of 1 mm/s. The sections were attached to slot copper grids (Stork Veco BV, Eerbeek, The Netherlands), covered with 1% formvar film and a 7nm carbon layer; no post-staining was applied prior to data collection. Imaging was performed in a Tecnai 12 Twin transmission electron microscope (FEI Company). Transmission electron microscope was operated at an acceleration voltage of 80 kV, and binned images (2kx2k) were acquired with a FEI Eagle CCD camera (FEI Company).

Oocyst and sporozoite production in *Anopheles stephensi* mosquitoes

For mosquito transmission experiments female *A. stephensi* mosquitoes were fed on mice infected with wild-type parasites or mutants. Oocyst development, oocyst production and sporozoite production was monitored in infected mosquitoes as described [56]. Oocyst and sporozoites numbers were counted in infected mosquitoes at 11–14 days

and 19–22 days after infection, respectively. Salivary gland sporozoites were isolated and counted as described [57].

For Western Blot analysis of CSP expression in oocysts or sporozoites, we isolated oocysts containing midguts from infected mosquitoes, or 100,000 midgut sporozoites, and proteins were separated on 8% polyacrylamide gels and transferred to nitrocellulose membranes by electroblotting. CSP expression was detected by incubation of membranes with monoclonal anti-CSP antibody [58] followed by incubation with horseradish-peroxidase-conjugated anti-mouse antibody (Sigma). Immunostained protein complexes were visualized by enhanced chemiluminescence (Amersham). For the immunofluorescence assays (IFA), midguts of infected mosquitoes were isolated in RPMI-Medium and immobilised with 2% formaldehyde, 0.2% glutaraldehyde, 2mM magnesium chloride, 0.02% Triton-X 100 in phosphate buffered saline (PBS). Subsequently midguts were permeabilized, using 2% Saponin in PBS and oocysts stained with monoclonal anti-CSP antibody and monoclonal Alexa-Fluor® 488 goat anti-mouse antibody. DNA was stained with Hoechst-33342.

Sporozoite infectivity and liver stage development

Sporozoites were collected at day 19–25 after infection by hand-dissection of the salivary glands as described [57]. Gliding motility of sporozoites was determined in assays that were performed on anti-*P. berghei* CSP antibody (3D11, monoclonal mouse antibody 25 µg/ml, 100 µl/well) pre-coated 10 well cell-line diagnostic microscope slides (7mm, Thermo Scientific) to which 1×10^4 sporozoites were added [59]. After 30 min of incubation at 37°C sporozoites were fixed with 4% paraformaldehyde and after washing with PBS, the sporozoites and the trails ('gliding circles') were stained with anti-CSP-antiserum [60] and anti-rabbit IgG- secondary antibody (Alexa Fluor® 488 Goat Anti-rabbit IgG; Molecular Probes®, Invitrogen). Slides were mounted with Vectorshield (Vector Laboratories Inc) and 'gliding circles' were analyzed using a Leica DMR fluorescence microscope at 1000× magnification.

Huh-7 cells, a human hepatoma cell line, were used in *in vitro* analysis of sporozoite infectivity. Huh-7 cells were cultured in 'complete' RPMI 1640 medium supplemented with 10% (v/v) fetal bovine serum (FBS), 1% (v/v) penicillin-streptomycin, 1% (v/v) GultaMAX (Invitrogen), and maintained at 37°C with 5% CO₂. Sporozoite hepatocyte traversal was determined in assays as described previously [61]. Briefly, Huh-7 cells were suspended in 1mL of 'complete' medium and were seeded in 24 well plates (10^5 cells/mL). After the Huh7 monolayers were >80% confluent, 10^5 sporozoites were added with the addition of FITC- or Alexa-647-labeled dextran (Invitrogen, NL) for 2 h. No sporozoites were added

to the negative control wells. *In vitro* invasion rates of mutants lacking expression of rhomboids and wild type parasites were determined by the ratio between the number of sporozoites inside the cells and the total number of sporozoites (both inside and outside of cells). Huh-7 cells (5×10^4 cells per well) were seeded into coverslips in 24-well plates and on the following day, cells were infected with 5×10^4 sporozoites. Three hours after infection, cells were fixed with 4% paraformaldehyde in PBS for 20 min. For the double staining, cells were incubated for 30 min in blocking buffer (10% FBS in PBS) followed by 1 hour incubation with anti-CSP serum against *P. berghei* circumsporozoite protein (CSP) protein [60] diluted 1:500 in the same buffer. Cells were then washed with PBS and incubated for 45 min with a secondary antibody (anti-rabbit Alexa Fluor® 568) diluted 1:500 in blocking buffer. This procedure only stained the parasites outside the cells. After washing with PBS, cells were fixed with 4% paraformaldehyde in PBS for 30 min, then incubated in for 30 min in permeabilization buffer (1% Triton X-100 in PBS) followed by 1 h incubation with anti-CSP serum diluted 1:500 in the same buffer. Cells were then washed with PBS and incubated for 45 min with a secondary antibody (anti-rabbit Alexa Fluor® 488) diluted 1:500 in blocking buffer. This second staining allows visualization of all the parasites, whether inside or outside the cells. Nuclei were stained with Hoechst-33342. The parasites in both green and red channels were analyzed using a DM-IRBE Flu Leica fluorescence microscope.

For analysis of *in vitro* EEF (exo-erythrocytic form) development, 5×10^4 sporozoites were added to a monolayer of Huh7 cells on coverslips in 24 well plates in 'complete' RPMI 1640 (see above). At different time points after infection, cells were fixed with 4% paraformaldehyde, permeabilized with 0.5% Triton-X-100 in PBS, blocked with 10% FBS in PBS, and subsequently stained with primary and secondary antibodies for 2h and 1h, respectively. Primary antibodies used were anti-PbEXP1 (raised in chicken [62]) and anti-UIS4 (raised in rabbit [63]), detecting the PVM-resident proteins; anti-PbHSP70 (raised in mouse [59]), detecting the cytoplasmic heat shock protein 70 (PBANKA_081890); and anti-MSP1 (mouse; MRA-78 from MR4; www.MR4.org) detecting MSP1 of *P. yoelii* and *P. berghei*. Anti-mouse, -chicken and -rabbit secondary antibodies, conjugated to Alexa Fluor® 488 and 594, were used for visualization (Invitrogen). Nuclei were stained with Hoechst-33342. Cells were mounted in Vectashield (Vector Laboratories Inc) and examined using a DM-IRBE Flu Leica fluorescence microscope.

In addition, Intracellular parasite development was determined by measuring the area of the EEFs inside fixed Huh-7 hepatoma cells. Huh-7 cells (5×10^4 cells per well) were seeded into coverslips in 24-well plates and, the following day, cells were infected with 4×10^4 sporozoites. Forty-eight hours after infection, cells were fixed with 4% paraformaldehyde

in PBS for 20 min. Cells were stained by incubation for 30 min in blocking/permeabilization buffer (0.5% Triton X-100, 1% BSA in PBS) followed by 1 h incubation with monoclonal antibody 2E6 against *P. berghei* HSP70 diluted 1:500 in the same buffer. Cells were then washed with 0.5% Triton X-100 in PBS and incubated for 45 min with a secondary antibody (anti-mouse Alexa488) diluted 1:400 in blocking/permeabilization buffer. Nuclei were stained with DAPI. Images were acquired with a Zeiss Axiovert 200M widefield fluorescence microscope and processed using ImageJ.

Hepatocyte infection was determined by measuring the luminescence intensity in Huh-7 cells infected with either the firefly luciferase-expressing $\Delta rom9$ and the corresponding control line PbGFP-Luc_{schz}. Huh-7 cells infection and culture conditions were as described above. At 57 h after infection, 50 μ L of D-Luciferin (Firefly Luciferase Assay Kit, Biotium) were added to 30 μ L of lysed samples in white 96-well plates. Luminescence intensity of the samples was measured using a microplate reader (Tecan Infinite M200). The viability of Huh-7 cells was assessed by the AlamarBlue assay (Invitrogen, United Kingdom) according to the manufacturer's protocol.

To determine parasite loads by qRT-PCR, sporozoites (5×10^4) were added to a monolayer of Huh7 cells (seeded the day before with 10^5 cells) in 24 well plates in 'complete' DMEM (see above). At different time-points after adding the sporozoites, culture medium was removed, cells washed once with PBS, and cells were resuspended in 200 μ L of RLT buffer (Qiagen's MicroRNeasy kit). RNA from these samples was extracted following the manufacturer's instructions. The transcriptor first-strand cDNA synthesis kit (Roche) was used according to the manufacturer's recommendations to make single-stranded cDNA. Real time PCR analysis of *P. berghei* 18S rRNA and human β -actin was performed as described [64].

Flow cytometry analysis was used to determine the parasite load of $\Delta rom9$ in Huh-7 cell (57 h p.i) compared the wild type control (PbGFP-Luc_{schz}). The infection and culture condition was as described above. 57 h after infection, samples for were washed with PBS, incubated with trypsin for 5 min at 37°C and collected in 400 μ L of 10% v/v FBS in PBS. Cells were then centrifuged at 0.1 g for 5 min, resuspended in 300 μ L of 2% v/v FBS in PBS. All samples were analyzed on a LSR Fortessa cytometer with the appropriate settings for the fluorophores used. Data acquisition and analysis were carried out using the BD FACSDiva (BD Biosciences) and FlowJo (v6.4.7, FlowJo) software packages respectively.

To determine *in vivo* infectivity of sporozoites, Swiss OF1 mice were infected with 1×10^4 salivary gland sporozoites by intravenous injection, as previously described [56]. Blood stage infections were monitored by analysis of Giemsa-stained thin smears of tail blood collected on day 4–8 after inoculation of sporozoites. The prepatent period (measured in

days post sporozoite infection) is defined as the day when a blood stage infection with a parasitemia of 0.5–2% is observed. In addition we determined parasite loads in livers of infected mice by *in vivo* imaging as described [64]. In addition, a group of 10 male C57BL/6 mice were inoculated by i.v. injection of 1×10^4 freshly isolated sporozoites of *Δrom9* or its wild type control PbGFP-Luc_{schz}. Luciferase activity in the livers of the animals was visualized 44 hours after infection using an *in vivo* Imaging System (IVIS Lumina), following i.p injection of D-luciferin dissolved in PBS (100 mg/kg). Animals were kept under anesthesia during the measurements, which were performed within 3 to 5 min after the injection of D-luciferin. Bioluminescence imaging was acquired with a 10 cm field of view, medium binning factor and an exposure time of 180 seconds. Quantitative analysis of bioluminescence was performed by measuring the luminescence signal intensity using the ROI settings of the Living Image® 3.0 software. ROI measurements are expressed in total flux of photons. qRT-PCR is also used to determine the *in vivo* parasite load in liver. After measuring luminescence, livers from 5 mice were collected, homogenized in 4 mL denaturing solution (4 M guanidine thiocyanate; 25 mM sodium citrate pH 7, 0.5% sarcosyl and 0.7% β-Mercaptoethanol in DEPC-treated water) and total RNA was extracted using the RNeasy Mini kit (Qiagen). cDNA was obtained by reverse transcription (First-strand cDNA synthesis kit, Roche) and qRT-PCR using the SybrGreen method (DyNAmo™ HS SYBR® Green qPCR Kit, Finnzymes) was performed with primers specific for *P. berghei* 18S rRNA for quantification of parasite load in the liver of each mouse. Relative amounts of *P. berghei* mRNA were calculated against the Hypoxanthine Guanine Phosphoribosyl Transferase (HPRT) housekeeping gene [64].

Acknowledgements

We thank Inês S. Albuquerque and Hans Kroeze for technical assistance. Jing-wen Lin is supported by the China Scholarship Council-Leiden University Joint Program and Chris J Janse, Andy Waters, Kai Matuschewski by a grant of the European Community's Seventh Framework Programme (FP7/2007–2013) under grant agreement no. 242095. Gunnar Mair is supported by FCT (PTDC/BIA-BCM/ 105610/2008, PTDC/SAU-GMG/104392/2008 and PTDC/SAU-MIC/122082/2010), Patrícia Meireles by FCT grant SFRH/BD/71098/2010 and Miguel Prudêncio by FCT project grant PTDC/SAUMIC/117060/2010.

References

1. Freeman M (2004) Proteolysis within the membrane: rhomboids revealed. *Nat Rev Mol Cell Biol* 5: 188-197.
2. Urban S, Lee JR, Freeman M (2001) Drosophila rhomboid-1 defines a family of putative intramembrane serine proteases. *Cell* 107: 173-182.
3. Koonin EV, Makarova KS, Rogozin IB, Davidovic L, Letellier MC, Pellegrini L (2003) The rhomboids: a nearly ubiquitous family of intramembrane serine proteases that probably evolved by multiple ancient horizontal gene transfers. *Genome Biol* 4: R19.
4. Lemberg MK, Freeman M (2007) Functional and evolutionary implications of enhanced genomic analysis of rhomboid intramembrane proteases. *Genome Res* 17: 1634-1646.
5. Wang Y, Zhang Y, Ha Y (2006) Crystal structure of a rhomboid family intramembrane protease. *Nature* 444: 179-180.
6. Wu Z, Yan N, Feng L, Oberstein A, Yan H, Baker RP, *et al* (2006) Structural analysis of a rhomboid family intramembrane protease reveals a gating mechanism for substrate entry. *Nat Struct Mol Biol* 13: 1084-1091.
7. Ben-Shem A, Fass D, Bibi E (2007) Structural basis for intramembrane proteolysis by rhomboid serine proteases. *Proc Natl Acad Sci U S A* 104: 462-466.
8. Urban S, Schlieper D, Freeman M (2002) Conservation of intramembrane proteolytic activity and substrate specificity in prokaryotic and eukaryotic rhomboids. *Curr Biol* 12: 1507-1512.
9. Urban S, Lee JR, Freeman M (2002) A family of Rhomboid intramembrane proteases activates all Drosophila membrane-tethered EGF ligands. *EMBO J* 21: 4277-4286.
10. Sundaram MV (2004) Vulval development: the battle between Ras and Notch. *Curr Biol* 14: R311-R313.
11. Stevenson LG, Strisovsky K, Clemmer KM, Bhatt S, Freeman M, Rather PN (2007) Rhomboid protease AarA mediates quorum-sensing in *Providencia stuartii* by activating TatA of the twin-arginine translocase. *Proc Natl Acad Sci U S A* 104: 1003-1008.
12. McQuibban GA, Saurya S, Freeman M (2003) Mitochondrial membrane remodelling regulated by a conserved rhomboid protease. *Nature* 423: 537-541.
13. Cipolat S, Rudka T, Hartmann D, Costa V, Serneels L, *et al* (2006) Mitochondrial rhomboid PARL regulates cytochrome c release during apoptosis via OPA1-dependent cristae remodeling. *Cell* 126: 163-175.
14. Dowse TJ, Soldati D (2005) Rhomboid-like proteins in Apicomplexa: phylogeny and nomenclature. *Trends Parasitol* 21: 254-258.
15. Baker RP, Wijetilaka R, Urban S (2006) Two *Plasmodium* rhomboid proteases preferentially cleave different adhesins implicated in all invasive stages of malaria. *PLoS Pathog* 2: e113.
16. Santos M, Graindorge A, Soldati-Favre D (2011) New insights into parasite rhomboid proteases. *Mol Biochem Parasitol* . S0166-6851(11)00285-4

17. Freeman M (2009) Rhomboids: 7 years of a new protease family. *Semin Cell Dev Biol* 20: 231-239. S1084-9521(08)00115-8
18. Buguliskis JS, Brossier F, Shuman J, Sibley LD (2010) Rhomboid 4 (ROM4) affects the processing of surface adhesins and facilitates host cell invasion by *Toxoplasma gondii*. *PLoS Pathog* 6: e1000858.
19. Santos JM, Ferguson DJ, Blackman MJ, Soldati-Favre D (2011) Intramembrane cleavage of AMA1 triggers *Toxoplasma* to switch from an invasive to a replicative mode. *Science* 331: 473-477. science.1199284
20. Brossier F, Jewett TJ, Sibley LD, Urban S (2005) A spatially localized rhomboid protease cleaves cell surface adhesins essential for invasion by *Toxoplasma*. *Proc Natl Acad Sci U S A* 102: 4146-4151.
21. Brossier F, Starnes GL, Beatty WL, Sibley LD (2008) Microneme rhomboid protease TgROM1 is required for efficient intracellular growth of *Toxoplasma gondii*. *Eukaryot Cell* 7: 664-674.
22. O'Donnell RA, Hackett F, Howell SA, Trecek M, Struck N, Krnajski Z, *et al* (2006) Intramembrane proteolysis mediates shedding of a key adhesin during erythrocyte invasion by the malaria parasite. *J Cell Biol* 174: 1023-1033.
23. Ejigiri I, Ragheb DRT, Pino P, Coppi A, Bennett BL, *et al* (2012) Shedding of TRAP by a Rhomboid Protease from the Malaria Sporozoite Surface Is Essential for Gliding Motility and Sporozoite Infectivity. *PLoS Pathog* 8: e1002725.
24. Olivieri A, Collins CR, Hackett F, Withers-Martinez C, Marshall J, *et al* (2011) Juxtamembrane shedding of *Plasmodium falciparum* AMA1 is sequence independent and essential, and helps evade invasion-inhibitory antibodies. *PLoS Pathog* 7: e1002448.
25. Srinivasan P, Coppens I, Jacobs-Lorena M (2009) Distinct roles of *Plasmodium* rhomboid 1 in parasite development and malaria pathogenesis. *PLoS Pathog* 5: e1000262.
26. Vera IM, Beatty WL, Sinnis P, Kim K (2011) *Plasmodium* protease ROM1 is important for proper formation of the parasitophorous vacuole. *PLoS Pathog* 7: e1002197.
27. Khan SM, Franke-Fayard B, Mair GR, Lasonder E, Janse CJ, *et al* (2005) Proteome analysis of separated male and female gametocytes reveals novel sex-specific *Plasmodium* biology. *Cell* 121: 675-687.
28. Otsuki H, Kaneko O, Thongkukiatkul A, Tachibana M, Iriko H, *et al* (2009) Single amino acid substitution in *Plasmodium yoelii* erythrocyte ligand determines its localization and controls parasite virulence. *Proc Natl Acad Sci U S A* 106: 7167-7172. 0811313106
29. Parussini F, Tang Q, Moin SM, Mital J, Urban S, Ward GE (2012) Intramembrane proteolysis of *Toxoplasma* apical membrane antigen 1 facilitates host-cell invasion but is dispensable for replication. *Proc Natl Acad Sci U S A* 109: 7463-7468.
30. Verma R, Varshney GC, Raghava GP (2010) Prediction of mitochondrial proteins of malaria parasite using split amino acid composition and PSSM profile. *Amino Acids* 39: 101-110.
31. Charneau S, Bastos IM, Mouray E, Ribeiro BM, Santana JM, *et al* (2007) Characterization of PfDYN2, a dynamin-like protein of *Plasmodium falciparum* expressed in schizonts. *Microbes Infect* 9: 797-805.
32. Amani V, Boubou MI, Pied S, Marussig M, Walliker D, *et al* (1998) Cloned lines of *Plasmodium berghei* ANKA differ in their abilities to induce experimental cerebral malaria. *Infect Immun* 66: 4093-4099.
33. Levander OA, Fontela R, Morris VC, Ager AL, Jr. (1995) Protection against murine cerebral malaria by dietary-induced oxidative stress. *J Parasitol* 81: 99-103.
34. Raine JD, Ecker A, Mendoza J, Tewari R, Stanway RR, Sinden RE (2007) Female inheritance of malarial lap genes is essential for mosquito transmission. *PLoS Pathog* 3: e30.
35. Ecker A, Bushell ES, Tewari R, Sinden RE (2008) Reverse genetics screen identifies six proteins important for malaria development in the mosquito. *Mol Microbiol* 70: 209-220.
36. Lavazec C, Moreira CK, Mair GR, Waters AP, Janse CJ, Templeton TJ (2009) Analysis of mutant *Plasmodium berghei* parasites lacking expression of multiple PbCCp genes. *Mol Biochem Parasitol* 163: 1-7.
37. Garnham PC, Bird RG, Baker JR (1962) Electron microscope studies of motile stages of malaria parasites. III. The ookinetes of *Haemamoeba* and *Plasmodium*. *Trans R Soc Trop Med Hyg* 56: 116-120.
38. Garnham PC, Bird RG, Baker JR, Desser SS, el-Nahal HM (1969) Electron microscope studies on motile stages of malaria parasites. VI. The ookinete of *Plasmodium berghei yoelii* and its transformation into the early oocyst. *Trans R Soc Trop Med Hyg* 63: 187-194.
39. Saeed S, Carter V, Tremp AZ, Dessens JT (2010) *Plasmodium berghei* crystalloids contain multiple LCCL proteins. *Mol Biochem Parasitol* 170: 49-53.

40. Menard R, Sultan AA, Cortes C, Altszuler R, van Dijk MR, *et al* (1997) Circumsporozoite protein is required for development of malaria sporozoites in mosquitoes. *Nature* 385: 336-340.
41. Lasonder E, Janse CJ, van Gemert GJ, Mair GR, Vermunt AM, *et al* (2008) Proteomic profiling of *Plasmodium* sporozoite maturation identifies new proteins essential for parasite development and infectivity. *PLoS Pathog* 4: e1000195.
42. Thathy V, Fujioka H, Gantt S, Nussenzweig R, Nussenzweig V, Menard R (2002) Levels of circumsporozoite protein in the *Plasmodium* oocyst determine sporozoite morphology. *EMBO J* 21: 1586-1596.
43. Janse CJ, Ramesar J, Waters AP (2006) High-efficiency transfection and drug selection of genetically transformed blood stages of the rodent malaria parasite *Plasmodium berghei*. *Nat Protoc* 1: 346-356.
44. Janse CJ, Franke-Fayard B, Mair GR, Ramesar J, Thiel C, *et al* (2006) High efficiency transfection of *Plasmodium berghei* facilitates novel selection procedures. *Mol Biochem Parasitol* 145: 60-70.
45. Spaccapelo R, Janse CJ, Caterbi S, Franke-Fayard B, Bonilla JA, Syphard LM, *et al* (2010) Plasmepsin 4-deficient *Plasmodium berghei* are virulence attenuated and induce protective immunity against experimental malaria. *Am J Pathol* 176: 205-217. S
46. Janse CJ, Boersma EG, Ramesar J, van VP, van der MR, *et al* (1989) *Plasmodium berghei*: gametocyte production, DNA content, and chromosome-size polymorphisms during asexual multiplication *in vivo*. *Exp Parasitol* 68: 274-282.
47. Lin JW, Annoura T, Sajid M, Chevalley-Maurel S, Ramesar J, *et al* (2011) A Novel 'Gene Insertion/Marker Out' (GIMO) Method for Transgene Expression and Gene Complementation in Rodent Malaria Parasites. *PLoS One* 6: e29289.
48. Mair GR, Lasonder E, Garver LS, Franke-Fayard BM, Carret CK, *et al* (2010) Universal features of post-transcriptional gene regulation are critical for *Plasmodium* zygote development. *PLoS Pathog* 6: e1000767.
49. van Spaendonk RM, Ramesar J, van WA, Eling W, Beetsma AL, *et al* (2001) Functional equivalence of structurally distinct ribosomes in the malaria parasite, *Plasmodium berghei*. *J Biol Chem* 276: 22638-22647.
50. Janse CJ, Haghparast A, Speranca MA, Ramesar J, Kroeze H, *et al* (2003) Malaria parasites lacking eef1a have a normal S/M phase yet grow more slowly due to a longer G1 phase. *Mol Microbiol* 50: 1539-1551.
51. Franke-Fayard B, Djokovic D, Dooren MW, Ramesar J, Waters AP, *et al* (2008) Simple and sensitive antimalarial drug screening *in vitro* and *in vivo* using transgenic luciferase expressing *Plasmodium berghei* parasites. *Int J Parasitol* 38: 1651-1662.
52. Lin JW, Sajid M, Ramesar J, Khan SM, Janse CJ, Franke-Fayard B (2013) Screening Inhibitors of *P. berghei* Blood Stages Using Bioluminescent Reporter Parasites. *Methods Mol Biol* 923: 507-522.
53. Janse CJ, Waters AP (1995) *Plasmodium berghei*: the application of cultivation and purification techniques to molecular studies of malaria parasites. *Parasitol Today* 11: 138-143.
54. van Dijk MR, Janse CJ, Thompson J, Waters AP, Braks JA, *et al* (2001) A central role for P48/45 in malaria parasite male gamete fertility. *Cell* 104: 153-164.
55. Beetsma AL, van de Wiel TJ, Sauerwein RW, Eling WM (1998) *Plasmodium berghei* ANKA: purification of large numbers of infectious gametocytes. *Exp Parasitol* 88: 69-72.
56. Sinden R.E. (1997) Infection of mosquitoes with rodent malaria. In: Crampton J.M., Beard C.B., Louis C., editors. *Molecular biology of insect disease vectors: a method manual*. London, United Kingdom: Chapman and Hall. pp. 67-91.
57. Annoura T, Ploemen IH, van Schaijk BC, Sajid M, Vos MW, *et al* (2012) Assessing the adequacy of attenuation of genetically modified malaria parasite vaccine candidates. *Vaccine* 30: 2662-2670.
58. Potocnjak P, Yoshida N, Nussenzweig RS, Nussenzweig V (1980) Monovalent fragments (Fab) of monoclonal antibodies to a sporozoite surface antigen (Pb44) protect mice against malarial infection. *J Exp Med* 151: 1504-1513.
59. van Dijk MR, Douradinha B, Franke-Fayard B, Heussler V, van Dooren MW, *et al* (2005) Genetically attenuated, P36p-deficient malarial sporozoites induce protective immunity and apoptosis of infected liver cells. *Proceedings of the National Academy of Sciences of the United States of America* 102: 12194-12199.
60. Yoshida N, Nussenzweig RS, Potocnjak P, Nussenzweig V, Aikawa M (1980) Hybridoma produces protective antibodies directed against the sporozoite stage of malaria parasite. *Science* 207: 71-73.

61. Mota MM, Pradel G, Vanderberg JP, Hafalla JCR, Frevert U, Nussenzweig RS, Nussenzweig V, Rodriguez A (2001) Migration of *Plasmodium* sporozoites through cells before infection. *Science* 291: 141-144.
62. Sturm A, Amino R, van de SC, Regen T, Retzlaff S, Rennenberg A, *et al* (2006) Manipulation of host hepatocytes by the malaria parasite for delivery into liver sinusoids. *Science* 313: 1287-1290.
63. Mueller AK, Camargo N, Kaiser K, Andorfer C, Frevert U, *et al* (2005) *Plasmodium* liver stage developmental arrest by depletion of a protein at the parasite-host interface. *Proc Natl Acad Sci U S A* 102: 3022-3027. 0408442102
64. Ploemen IH, Prudencio M, Douradinha BG, Ramesar J, Fonager J, *et al* (2009) Visualisation and quantitative analysis of the rodent malaria liver stage by real time imaging. *PLoS ONE* 4: e7881.

Supplementary Material

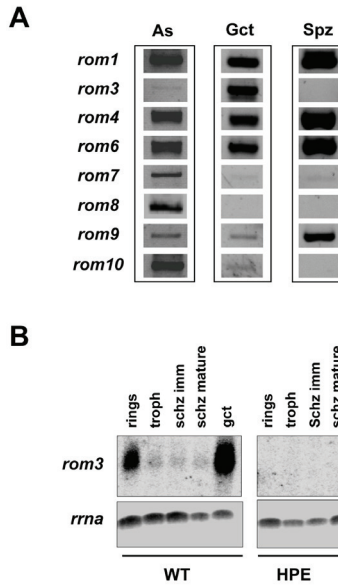


Figure S1. RT-PCR and Northern blot analyses of rhomboid transcription

A. Transcription patterns of different rhomboids as determined by RT-PCR using cDNA from i) asexual blood stages of a non-gametocyte producer *P. berghei* ANKA parasite line (HPE), ii) purified gametocytes of wild type *P. berghei* ANKA (cl15cy1) parasites and iii) salivary gland sporozoites of wild type *P. berghei* ANKA (cl15cy1). Details of the primers and expected sizes of the amplified products are shown in Table S4.

B. Northern analysis of *rom3* transcription. Total RNA was isolated from synchronized blood stages and purified gametocytes (gct) of wild type (WT) *P. berghei* ANKA (cl15cy1) and from blood stages of the non-gametocyte producer *P. berghei* ANKA parasite line (HPE). Transcripts were only detected in WT parasites with high level of expression in gametocytes. Signals in rings are the result of contamination with gametocytes in synchronized infections (Janse and Waters, 1995). Hybridization was performed using a PCR probe recognizing the *rom3* gene (primers 1812/1813). As a loading control, hybridization was performed with probe L644R that recognizes the large subunit ribosomal RNA (see Table S4 for primer sequences). Rings (5 h post invasion, hpi); troph (trphozoites, 16hpi); schz imm (immature schizonts; 20hpi); schz mature (mature schizonts 24hpi); gct (gametocytes).

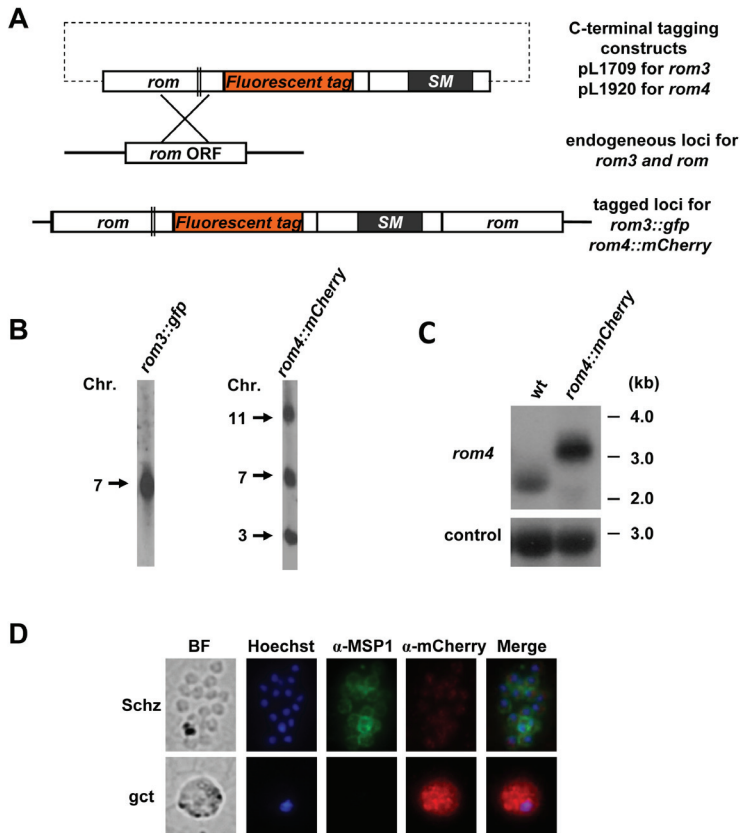


Figure S2. Generation of transgenic lines expressing C-terminally fluorescent-tagged ROM3 and ROM4.

A. Schematic representation of the tagging constructs pL1709 and pL1920 targeting *rom3* and *rom4* respectively by single cross-over homologous recombination, and the locus before and after tagging. The tagging constructs contain C-terminal fluorescent tag (orange boxes) and the *tgdhfr/ts* drug selectable marker cassette (SM; black boxes). The double lines indicate the enzyme site used for construct linearization.

B. Southern analyses of pulsed field gel-separated chromosomes confirm correct integration of the two tagging constructs. Chromosomes of *rom3::gfp* line (left) were hybridized using a *tgdhfr/ts* probe that recognizes the construct integrated into *rom3* locus on chromosome 7. Chromosomes of *rom4::mCherry* line were hybridized with a 3'UTR *pbdhfr* probe recognizing the tagging construct integrated into the *rom4* locus on chromosome 11, the endogenous *dhfr/ts* gene on chromosome 7 and the GFP-luciferase reporter cassette introduced in chromosome 3 (right).

C. Northern blot analysis showing transcription of *rom4::mCherry*. Hybridization was performed using a PCR probe recognizing the *rom4* gene (primers 6929/6930). As a loading control, hybridization was performed with probe L644R that recognizes the large subunit ribosomal RNA (see Table S3 for primer sequences and product sizes). wt, wild-type.

D. Immunofluorescence analyses of schizonts and gametocytes of *rom4::mCherry* using anti-mCherry antibody. Distinct mCherry staining was observed in gametocytes (gct) whereas in schizonts (schz) only weak signals (barely above background signals) were observed. Staining was performed using anti-mCherry (red) and anti-MSP1 (green) antibodies and the DNA dye Hoechst-33258 (blue). BF, bright field.

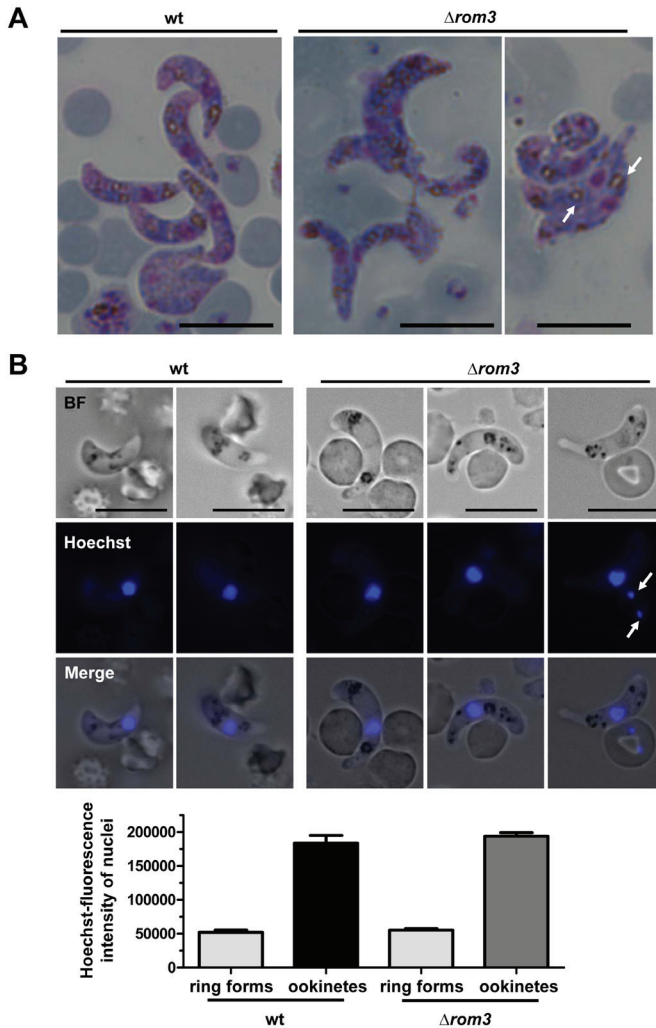


Figure S3. Morphology and nuclear DNA content of $\Delta rom3$ and wild type ookinetes analyzed by light and fluorescence microscopy.

A. Morphology of Giemsa stained *in vitro* cultured ookinetes. $\Delta rom3$ ookinetes have the characteristics of fully mature WT ookinetes such as an elongated ‘banana’ shape, hemozoin clusters (white arrows) and centrally located nucleus. Scale bar 10 μm .

B. Nuclear DNA content of $\Delta rom3$ and wild type live ookinetes as determined by Hoechst -fluorescence intensity measurements. The mean fluorescence intensity of haploid ring-form nuclei (white arrows) is 53632 (relative light intensity; RLI). The $\Delta rom3$ and wild type ookinetes show similar (tetraploid) DNA content and both have similarly enlarged nuclei, with RLI values of 193788 and 183668, respectively. BF: bright field. Scale bar 10 μm . Twenty parasites were measured and the means and SEM are shown in the graph, n=20.

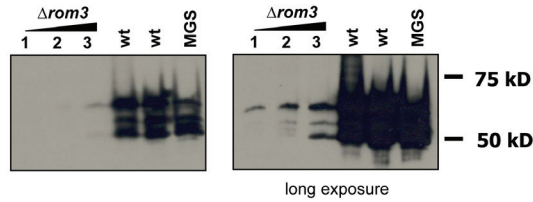


Figure S4. Circumsporozoite protein expression in $\Delta rom3$ and wild-type oocysts

Western blot analysis of proteins isolated from increasing numbers of midguts of $\Delta rom3$ infected mosquitoes. Midguts from mosquitoes infected with $\Delta rom3$ (1, 2 or 3 midguts, day 13) and wild-type (wt, day 13) were separated on SDS-PAGE and stained with anti-CS antibody. Purified 10^5 wt midgut sporozoites (MGS) were used as a control. Right hand panel shows a longer exposure of the blot on the left.

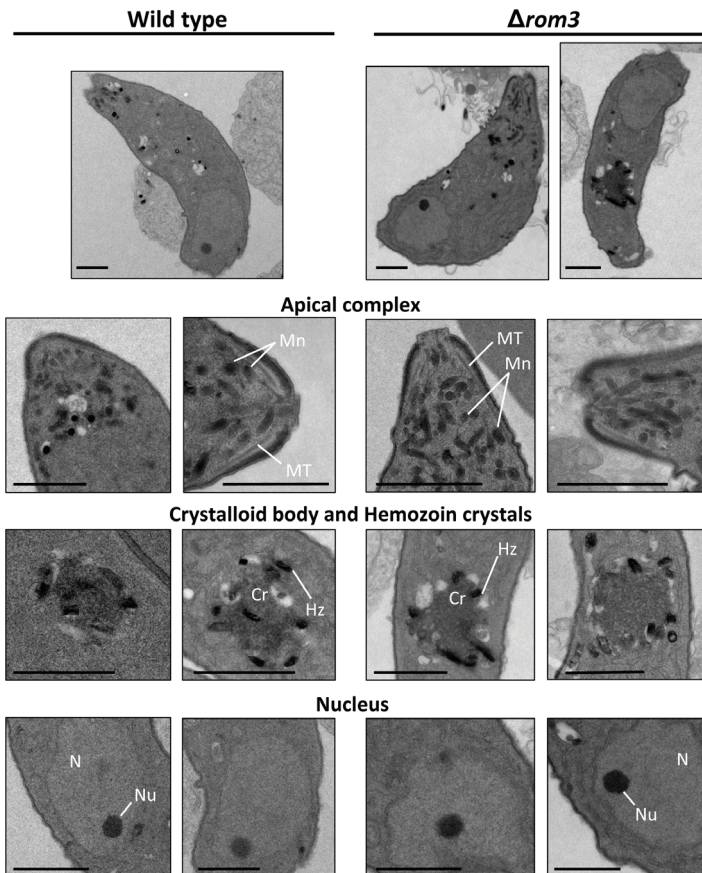


Figure S5. Ultrastructural analyses of wt and $\Delta rom3$ ookinetes.

Both wt and $\Delta rom3$ parasites produce normal ookinetes with respect to size, organelles and membrane morphology. No differences were observed in the apical complex which has a similar distribution and localization of micronemes (Mn), the arrangement of the subpellicular microtubules (MT), morphology of the crystalloid body (Cr) and hemozoin crystals (Hz). No differences were observed in the nucleus (N), the nuclear membrane, or in the nucleolus-like (Nu) structure between wt and $\Delta rom3$ ookinetes. Scale bar $1\mu\text{M}$.

Table S1. Gene deletion experiments to disrupt the *P. berghei* genes encoding rhomboid proteases

Gene name, Gene deletion mutant	Gene ID	DNA construct name	Experiment No., Mutant name ¹	Parent line ²	RMgmDB ID ³
Unsuccessful attempts					
<i>rom4</i>	PBANKA_110650	pL1078	653, 684, 695	cl15cy1	RMgm-187
<i>rom6</i>	PBANKA_135810	PCR1916	2118, 2119 2140	1037m1f1cl1 676m1cl1	RMgm-758
<i>rom7</i>	PBANKA_113460	PCR1917	2120, 2121 2141	1037m1f1cl1 676m1cl1	RMgm-759
<i>rom8</i>	PBANKA_103130	PCR1918	2122, 2123 2142	1037m1f1cl1 676m1cl1	RMgm-760
Mutants					
$\Delta rom1$ -p	PBANKA_093350	Mg031	538cl2	cl15cy1	RMgm-177
$\Delta rom1$ -c		pL1533	1496cl4	676m1cl1	RMgm-761
$\Delta rom3$ -a	PBANKA_070270	pL1097	430cl1	cl15cy1	RMgm-178
$\Delta rom3$ -b		pL1097	687cl1	cl15cy1	
$\Delta rom9$ -a	PBANKA_111470	PCR1919	2124cl1	1037m1f1cl1	RMgm-762
$\Delta rom9$ -b		PCR1919	2125cl1	1037m1f1cl1	
$\Delta rom10$	PBANKA_111780	Mg011	468cl2	cl15cy1	RMgm-179
Fluorescence-tagged mutants					
<i>rom3::gfp</i>	PBANKA_070270	pL1079	654cl1	cl15cy1	RMgm-763
<i>rom4::mCherry</i>	PBANKA_110650	pL1920	2143cl1	676m1cl1	RMgm-764

¹ Experiment number for independent transfection experiments: the unsuccessful attempts (x3) and the experiment number/clone of the gene deletion mutants

² Parent *P. berghei* ANKA line in which the genes were targeted for deletion

³ The ID number of the mutants (or of the unsuccessful attempts for gene deletion) in the RMgm database (www.pberghei.eu) of genetically modified rodent malaria parasites

Table S2. Targeting constructs and primers

Gene	Construct	Basic construct	No.	Sequences	Restriction sites	Description
<i>Gene deletion constructs</i>						
<i>rom1</i>	Mg031	pL0001	2082	AACAATGATTCGTTGTGAATATAATCAGG	MunI	5'-rom1 targeting region F
			2083	TFAAGCTTTCGATTCGGACACAAATTAATAC	HindIII	5'-rom1 targeting region R
			2086	AAGATATCAAGTTATAGTAATAATGCTTTGC	EcoRV	3'-rom1 targeting region F
			2087	TGGATCCCTATGTATATATCTTTGTACC	BamHI	3'-rom1 targeting region R
pL1533	pL0001	4718	GACGGGTACTATCGAGCAACAATGTCTG	Asp718I	5'-rom1 targeting region F	
		4937	CCCATCGATAAATAAGTCCAAACTCAAAGC	Clal	5'-rom1 targeting region R	
		4697	CCGGAATCAAGTTATAGTAATAATGCTTTGC	EcoRI	3'-rom1 targeting region F	
		2087	TGGATCCCTATGTATATATCTTTGTACC	BamHI	3'-rom1 targeting region R	
		1754	AAATCGATGAATTCACCAATGAATGTAATAAAGG	Clal, EcoRI	5'-rom3 targeting region F	
		1755	TFAAGCTTATGTCTATTTTGTTCACCTTG	HindIII	5'-rom3 targeting region R	
<i>rom3</i>	pL1097	pL0001	1756	AAGATATCAATTAAGTATATAGGATAAC	EcoRV	3'-rom3 targeting region F
			1757	TGGATCCACGAAGAAGTATTGACAC	BamHI	3'-rom3 targeting region R
			2408	AAAAGAATCTGCATGTATAAGTAATGTGC	EcoRI	5'-rom4 targeting region F
			2409	AAAAGCTTTCATTCAGAGAGTTGGAAC	HindIII	5'-rom4 targeting region R
<i>rom4</i>	pL1078	pL0001	2410	AAAAGATCCAATTAATGAAAGAAAAGGC	EcoRV	3'-rom4 targeting region F
			2411	AAAAGGATCCTTATATATCTTAAATGCGC	BamHI	3'-rom4 targeting region R
			7055	GAACTCGTACTCCTTGGTGACGTCGGACTATTTTTATAGGCACATTTTG	NruI	5'-rom6 targeting region F
			7056	CATCTACAAGCATCGTCGACCTCGTATAGGGTTTTTTTACAAATAGTG	NruI	5'-rom6 targeting region R
<i>rom6</i>	PCR1916	pL0048	7057	CCTTCAATTTTGGATCCACTAGAAAACATACACCACCAATGTC	EcoRV	3'-rom6 targeting region F
			7058	AGGTTGGTCATTGACACTCAGCTCGGACATCCCTTGTGCATACC	NruI	3'-rom6 targeting region R
			7063	GAACTCGTACTCCTTGGTGACGTCGGATGCTTTGTATTTTCAATGGAG	NruI	5'-rom7 targeting region F
			7064	CATCTACAAGCATCGTCGACCTCATGATGCTCTTTGATATATTC	NruI	5'-rom7 targeting region R
<i>rom7</i>	PCR1917	pL0048	7065	CCTTCAATTTTGGATCCACTAGATGCTGCCACATAATTTTG	EcoRV	3'-rom7 targeting region F
			7066	AGGTTGGTCATTGACACTCAGCTCGGATTCGGAATCCGAAGCATACATAAAG	NruI	3'-rom7 targeting region R
			7071	GAACTCGTACTCCTTGGTGACGTCGGAGTGAAGATTTTGAATAAATAGAAGAAG	NruI	5'-rom8 targeting region F
			7072	CATCTACAAGCATCGTCGACCTCATGCCAATTCACAAATAATGC	NruI	5'-rom8 targeting region R
<i>rom8</i>	PCR1918	pL0048	7073	CCTTCAATTTTGGATCCACTAGATGTTGATATACCCAGTATCC	EcoRV	3'-rom8 targeting region F
			7074	AGGTTGGTCATTGACACTCAGCTCGGATGCTTTCAACAATAATTTACAC	NruI	3'-rom8 targeting region R
			7079	GAACTCGTACTCCTTGGTGACGTCGGAAATAAGCGCATGTCATTTGTTG	NruI	5'-rom9 targeting region F
			7080	CATCTACAAGCATCGTCGACCTCGTAAAGAATAATGCTGGAATGG	NruI	5'-rom9 targeting region R

rom10	Mg011	7081	CCTTCAATTTCCGGATCCACTAGCTCTAGTCTATATGAACATAAAACTC	3'-rom9 targeting region F
		7082	AGGTTGGTCATTGACACTCAGCTCGCGATTTTCAGCAATAGAGAAACAAG	3'-rom9 targeting region R
		1774	AAAGGGCCCTCACATTTTCCCATCAGAG	5'-rom10 targeting region F
		1775	TTATCGATTCTGTCTATACATGCCCAAG	5'-rom10 targeting region R
		1776	AAAGATATCCATACGTAATATGTCTATGC	3'-rom10 targeting region F
1777	TTGGATCCAGTTATAACTGCACAGGTGTTCC	3'-rom10 targeting region R		
anchor-tag primers				
		4661	GAACTCGTACTCCTTGGTGACG	anchor-tag primer, F
		4662	AGGTTGGTCATTGACACTCAGC	anchor-tag primer, R
C-terminal tagging constructs				
rom3	pL1079	1754	AAATCGATGAATTCACACAATGAATGTAATAAAGG	rom3 ORF, F
		2415	AAAGGATCCAGCAAAATTCACATGGCATATTC	rom3 ORF, R
rom4	pL1920	7016	AGCACTAGTATGGAAAAACAAATAAACCCGAAAAGG	rom4 ORF, F
		7017	GGGAGATCTTTCCTTGCAATAATAATCAAATG	rom4 ORF, R

Red: restriction sites

Blue: 5'-extensions homologues to the *hdhfr::yfcu* selectable marker cassette from pL0048

Green: 5'-extensions homologues to the anchor tag primers 4661/4662

Table S3. Primers for genotyping

Genes	No.	Primer sequences	Description	Integration PCR Pair	Product size (bp)
Primers for PCR analyses					
rom1	4586	TTATGCATTGTATAACATCTCTG	<i>rom1</i> 5' in-F	695	1172
	5036	ACCATTATTTTTGTATGTAGTG	<i>rom1</i> 5' in-F	695	1138
	4587	CTGATGATATTATTAAGAGAACTG	<i>rom1</i> 3' in-R	4239	998
	2084	TGGAAATATACTATCATCTCTG	<i>rom1</i> ORF-F		501
	2085	ACAGCAAACAAAACAACAGTTGG	<i>rom1</i> ORF-R		
rom3	2389	GGTATAATTTTGTATTATC	<i>rom3</i> 5' in-F	695	867
	1886	CAACACTCTTGAAGGATGTC	<i>rom3</i> 3' in-R	4239	1024
	1812	TTATTGTATGGATTAGTTTTTCC	<i>rom3</i> ORF-F		787
	1813	TATCCCAAAAATTTGTATAATGG	<i>rom3</i> ORF-R		
rom4	2451	AGTTAATTATAAACATGC	<i>rom4</i> 5' in-F	695	1015
	2452	CACACATATTATCAGTGC	<i>rom4</i> 3' in-R	4239	787
	6929	ATTGCATACATTGCCATCTG	<i>rom4</i> ORF-F		973
	6930	TAACATCCGTTCTCTAATGTG	<i>rom4</i> ORF-R		
rom6	7059	CATATTTGTAATGCTCAAAATAGTG	<i>rom6</i> 5' in-F	4906	1211
	7060	ACGAAAAGGAAAGAAAAGATAATTAG	<i>rom6</i> 3' in-R	4239	1219
	7061	CCTTTTACCAAAGTGGTGAG	<i>rom6</i> ORF-F		1033
	7062	CACCTAAAAGTTGAGCATATCTG	<i>rom6</i> ORF-R		
rom7	7067	GAAGGGGAAATTTATGATATATGG	<i>rom7</i> 5' in-F	4906	1425
	7068	GTGACGATGAAAATTTGATG	<i>rom7</i> 3' in-R	4239	971
	7069	CGATTCAAAAATATAATAATGTAGAG	<i>rom7</i> ORF-F		787
	7070	GGCTAACATTTTCTAAAAGTAGAG	<i>rom7</i> ORF-R		
rom8	7075	CCCCCATTTTTTATTATTATAAC	<i>rom8</i> 5' in-F	4906	1364
	7076	GCTATAGAAAACGGGAAACATC	<i>rom8</i> 3' in-R	4239	1061
	7077	TAAATGGCAGTAAAGAATATGAC	<i>rom8</i> ORF-F		940
	7078	TTCCGAAATAAAAAGCATCGTC	<i>rom8</i> ORF-R		
rom9	7083	AATACAAATTCAGAGGATGAC	<i>rom9</i> 5' in-F	4906	1242
	7084	AAATAGGAATAAAGTGAGTAAGC	<i>rom9</i> 3' in-R	4239	940
	7085	GAATGAAATTTGGGGTAAGG	<i>rom9</i> ORF-F		970
	7086	GTATTGTGACTTATTATGTAGTTAC	<i>rom9</i> ORF-R		
rom10	6939	AGCAATATCTTATTGCTACATAC	<i>rom10</i> 5' in-F	4179	714
	2088	CATTATAGTACAATTATAGGTG	<i>rom10</i> 3' in-R	4239	1093
	6940	CATAACTGCAACATTAATTCATC	<i>rom10</i> ORF-F		989
	2066	CCGATATTTCCATAATGTTTC	<i>rom10</i> ORF-R		
Universal primers					
	695	AATATTCATAACACACTTTTAAGC	<i>5'pbdhfr/ts</i> R		
	4906	CGACTAGTTAATAAAGGGCAC	<i>5'pbeef1a</i> R		
	4179	CTATAGGGCGAATTGGAGCTC	<i>LacZ</i> R		
	4239	GATTTTTAAAATGTTTATAATATGATTAGC	<i>3'pbdhfr/ts</i> F		
	4598	GGACAGATTGAACATCGTCG	<i>tdghfr/ts</i> F		1059
	4599	GTGTAGTCTGTGTGCATGTC	<i>tdghfr/ts</i> R		
	4698	GTTTCGCTAAACTGCATCGTC	<i>hdhfr</i> F		787
	4699	GTTTGAGGTAGCAAGTAGACG	<i>yfcu</i> R		

Other Primers for generation of probes

692	CGCGGATCCATGCATAAACCGGTGTGTC	3' <i>pbdhfr</i> /ts F
693	CGCGGATCCGCTAGACAGCCATCTCCAT	3' <i>pbdhfr</i> /ts R
741	CGCGGATCCATGCATAAACCGGTGTGTC	<i>tgdhfr</i> /ts F
742	CGCGGATCCGCTAGACAGCCATCTCCAT	<i>tgdhfr</i> /ts R
2082	AACAATTGATTCGTTGTGAATATAATCAGG	<i>rom1</i> upst F
L644R	GGAAACAGTCCATCTATAATTG	<i>lsu rrna</i> (A-type)

pb = *P. berghei*, *tg* = *T. gondii*; h = human, y = yeast

5' in=5' integration PCR; 3' in=3' integration PCR

Table S4. Primers for RT-PCR analyses

Gene	No.	Sequences	Description	Expected gDNA (bp)	Expected cDNA (bp)	Across intron
<i>rom1</i>	2084	TGGAAATATACTATCATCATCTG	<i>rom1</i> ORF-F	501	368	yes
	2085	ACAGCAAACAAAACAACAGTTGG	<i>rom1</i> ORF-R			
<i>rom3</i>	1812	TTATTGTATGGATTAGTTTTTCC	<i>rom3</i> ORF-F	787	562	yes
	1813	TATCCAAAAAATTTGTATAATGG	<i>rom3</i> ORF-R			
<i>rom4</i>	42	AAATCTAGAGACAAAGGTCGATTAG	<i>rom4</i> ORF-F	510	510	no
	43	AAACCGCGGAGCATATCCTCGACCATC	<i>rom4</i> ORF-R			
<i>rom6</i>	470	GGGAATTCCATTGGCGGG	<i>rom6</i> ORF-F	506	506	no
	7062	CACTAAAAGTTGAGCATATCTG	<i>rom6</i> ORF-R			
<i>rom7</i>	7069	CGATTCAAAAAATAATAATGTAGAG	<i>rom7</i> ORF-F	787	787	no
	7070	GGCTAACATTTTCTAAAAGTAGAG	<i>rom7</i> ORF-R			
<i>rom8</i>	7408	TAATTATACACCACCTGAAAATG	<i>rom8</i> ORF-F	922	529	yes
	7409	CGATGAACTACTACTTTCTG	<i>rom8</i> ORF-R			
<i>rom9</i>	1107	AACAATTGTTTACTAAATACAATTC	<i>rom9</i> ORF-F	730	408	yes
	1108	TATTCGAAACTTTTATTAAC	<i>rom9</i> ORF-R			
<i>rom10</i>	6940	CATAACTGCAACATTAATTCATC	<i>rom10</i> ORF-F	989	363	yes
	2066	CCGATATTTCCCATAAATGTTTC	<i>rom10</i> ORF-R			

Table S5. Potential substrates of ROM3; *P. berghei* single transmembrane domain containing oocyst and sporozoite proteins

Gene ID (<i>P. berghei</i>)	Gene ID (<i>P. falciparum</i>)	# Unique Peptides ¹	# of Spectra ¹	Product Description	# TM Domains	SignalP Peptide	Deletion Attempted (RMgMDB ² #)	Phenotype ²
PBANKA_091500	PF3D7_1133400	2	4	apical membrane antigen 1 (AMA1)	1	HMM: MRKLYCVLLLSAFEFTYMINFGRGQ, NN: MRKLYCVLLLSAFEFTYMINFGRGQ	Yes (10)	Not possible to KO
PBANKA_100360	PF3D7_0405900	5	25	apical sushi protein (ASP)	1	HMM: MKIYIHILFLLHYNIKAK, NN: MKIYIHILFLLHYNIKAK	No	
PBANKA_081340	PF3D7_0912400	7	49	conserved <i>Plasmodium</i> protein, unknown function	1	HMM: MNTCKLFAFFIKYGRCO, NN: MNTCKLFAFFIKYGRCO	No	
PBANKA_094160	PF3D7_1105300	4	16	conserved <i>Plasmodium</i> protein, unknown function	1	HMM: MRKIIPLLYSVIIFFVKWSY, NN: MRKIIPLLYSVIIFFVKWSY	No	
PBANKA_081150	PF3D7_0910300	2	4	conserved <i>Plasmodium</i> protein, unknown function	1	HMM: MIFLRNGFFFLSVLTSCYINLFTQCLGE, NN: MIFLRNGFFFLSVLTSCYINLFTQCLGE	No	
PBANKA_144390	PF3D7_1229300	1	1	conserved <i>Plasmodium</i> protein, unknown function	1	HMM: MKLKYHLFLIIFIQDILCL, NN: MKLKYHLFLIIFIQDILCL	No	
PBANKA_090130.1	PF3D7_1147800.1	33	1089	merozoite adhesive erythrocytic binding protein (MAEBL)	1	HMM: MGVLKHFFFLFLYVNTSAL, NN: MGVLKHFFFLFLYVNTSAL	Yes (220)	Important for sporozoite invasion of Salivary glands
PBANKA_020920	PF3D7_0103900	5	25	parasite-infected erythrocyte surface protein (PIEPS15)	1	HMM: MRKTGRLVFYLCISWCLFVNICK, NN: MRKTGRLVFYLCISWCLFVNICK	Yes (90)	No clear phenotype, no phenotype in mosquito
PBANKA_131570	PF3D7_1452000	12	144	rhoptry neck protein 2 (RON2)	1	HMM: MLKFFIFILHIYIDISVSS, NN: MLKFFIFILHIYIDISVSS	Yes (214)	Not possible to KO
PBANKA_020910	PF3D7_0104000	1	1	thrombospondin-related sporozoite protein (TRSP)	1	HMM: MLMKISRFFLLYLKAKHLD, NN: MLMKISRFFLLYLKAKHLD	Yes (34)	Normal salivary gland sporozoite (SGS) numbers but hepatocyte invasion reduced
PBANKA_130650	PF3D7_1442600	20	400	TRAP-like protein, sporozoite-specific transmembrane protein S6 (TREP)	1	HMM: MNFFSIFILNFFMLSTSSIGN, NN: MNFFSIFILNFFMLSTSSIGN	Yes (145/159/305)	Normal oocyst derived sporozoite (ODS) numbers, but reduced SGS numbers; reduced motility of ODS

¹ Based on Lasander E *et al.* 2008 PLoS Pathogens 4(10): e1000195² Data on attempted and successful deletions of these genes available from the RMgM Database (database entry www.pbergeth.eu)

CHAPTER 5

Malaria Parasites Lacking Critical Proteases Involved In Hemoglobin Degradation Are Viable and Are Less Sensitive To Chloroquine

Jing-wen Lin¹, Roberta Spaccapelo², Evelin Schwarzer³, Mohammed Sajid¹, Takeshi Annoura¹, Blandine M.D. Franke-Fayard¹, Séverine Chevalley-Maurel¹, Jai Ramesar¹, Elena Aime², Barbara Capuccini², Anna M. Mommaas-Kienhuis⁴, Paolo Arese³, Katrien Deroost⁵, Tom O'Toole⁶, Frans Prins⁷, Abraham J. Koster⁴, Andrea Crisanti⁸, Philippe E. Van den Steen⁵, Hans J. Tanke⁷, Raimond B. G. Ravelli⁴, Chris J. Janse¹ and Shahid M. Khan¹

¹Leiden Malaria Research Group, Department of Parasitology, ⁴Section Electron Microscopy, Department of Molecular Cell Biology, ⁷Department of Pathology, Leiden University Medical Centre, Leiden, The Netherlands

²Department of Experimental Medicine, University of Perugia, Piazzale Gambuli , Perugia, Italy

³Department of Genetics, Biology, and Biochemistry, University of Torino Medical School, Torino, Italy

⁵Laboratory of Immunobiology, Rega Institute for Medical Research, University of Leuven, Leuven, Belgium

⁶Department of Molecular Cell Biology and Immunology, Vrije University Medical Center, 1007 MB Amsterdam, The Netherlands

⁸Department of Biological Sciences, Imperial College London, South Kensington Campus, SAF, London, SW7 2AZ, UK

Submitted manuscript

Abstract

Survival of *Plasmodium falciparum* parasites inside erythrocytes is considered to depend on hemoglobin digestion. This degradation occurs inside a specialized digestive vacuole (DV) by a number of functionally overlapping and redundant hemoglobinases including the endoproteases (plasmepsins and falcipains) that perform the initial cleavage of hemoglobin. To study *Plasmodium* hemoglobin proteolysis *in vivo*, we used the rodent parasite *P. berghei* that, like the human parasite *P. vivax*, has only one DV plasmepsin and is restricted to reticulocytes. Unexpectedly it was possible to create mutants lacking enzymes known to initiate hemoglobin digestion that can complete development in reticulocytes without hemozoin formation, a detoxification product of hemoglobin degradation. Furthermore, these mutants were more resistant to chloroquine but equally sensitive to artemisinin as compared to wild-type parasites. These observations have important implications for *Plasmodium* drug development and drug resistance, in particular for malaria parasites that preferentially develop inside reticulocytes.

Introduction

Clinical symptoms of malaria are associated with replication of *Plasmodium* parasites inside red blood cells (RBC). Human *P. falciparum* parasites ingest and catabolize more than half of the hemoglobin (Hb) present in the erythrocyte [1,2]. The amino acids derived from Hb proteolysis are used for protein synthesis and energy metabolism and, as malaria parasites have a limited capacity to synthesize amino acids *de novo*, digestion of Hb is believed to be essential for successful parasite replication [1,3,4]. However, human Hb is a poor source of methionine, cysteine, glutamine and glutamate and contains no isoleucine [5-7], and *P. falciparum* blood-stage parasite growth is most effective in culture medium supplemented with these amino acids, especially isoleucine [4-6]. These data indicate that *P. falciparum* parasites not only rely on Hb digestion to acquire amino acids, but also import exogenous amino acids [4,8]. However, growth of *P. falciparum* blood-stages in culture is completely interrupted when Hb proteolysis is blocked by specific inhibitors targeting *Plasmodium* proteases involved in this pathway [1,4]. This proteolysis of Hb is accompanied by the release of free heme, which is highly cytotoxic for the parasite, it is rapidly detoxified by dimerization and then crystallization into a product known as hemozoin (Hz). Therefore, both Hb degradation and heme detoxification are considered to be essential for *P. falciparum* survival [1,9].

The digestion of Hb is a conserved and semi-ordered process, which principally occurs within the acidic digestive vacuole (DV). The important initial cleavage of native Hb is mediated by aspartic and papain-like cysteine endoproteases. In the *P. falciparum* DV there are four aspartic proteases termed plasmepsins and two papain-like cysteine proteases termed falcipains capable of hydrolyzing host Hb [10-14]. After the first cleavage, Hb unfolds and becomes susceptible for further proteolysis by downstream proteases. Gene disruption studies of hemoglobinsases demonstrate that *P. falciparum* has developed redundant and overlapping enzymatic systems for Hb degradation. Specifically, the multiple *P. falciparum* plasmepsins and falcipains overlap in function and there is extensive functional redundancy within and between these 2 families [4,15-17]. Most studies on hemoglobinsases have been performed using *P. falciparum* blood-stages cultured *in vitro* and it remains to be proven that observations derived from loss-of-function assays in culture can also be directly translated to parasites replicating *in vivo*. Further, *P. falciparum* infects mature RBC and it is unknown whether the observations on Hb digestion made with *P. falciparum* in mature RBC also apply to *P. falciparum* and other *Plasmodium* species that can invade and develop inside young RBC, reticulocytes.

Here we studied the functional redundancy amongst the enzymes involved in Hb digestion both *in vivo* and *in vitro*, using the rodent malaria parasite *P. berghei* that, like the human

malaria parasite *P. vivax*, preferentially invades reticulocytes. Using a reverse genetics (loss-of-function) approach we demonstrate that 6 out of 8 genes predicted to encode *P. berghei* hemoglobinasases are dispensable, demonstrating a high level of functional redundancy of these enzymes *in vivo*. Surprisingly, we were able to generate a *P. berghei* double gene deletion mutant lacking both plasmepsin-4 (PM4), the syntenic ortholog of all four *P. falciparum* plasmepsins I-IV [18], and berghepain 2 (BP2), the syntenic ortholog of the DV falcipains (falcipain 2 and 3), i.e. the enzymes involved in the initial and critical cleavage of host Hb. These mutants were able to mature into schizonts inside reticulocytes without producing Hz. Furthermore, these parasites are less sensitive to the action of chloroquine, a drug that principally acts by inhibiting Hz formation, but retain sensitivity to artemisinin. Our observations thus demonstrate that malaria parasites can multiply in reticulocytes without producing Hz, which show increased resistance to antimalarials that target heme detoxification. Currently, targeting *Plasmodium* enzymes that interfere with heme detoxification mechanisms is a major focus of drug development (www.mmv.org) and our observations not only have important implications for development of novel antimalarials but also suggest alternative mechanisms of drug-resistance. This is especially true for parasites with a preference for reticulocytes, such as the important human parasite *P. vivax*, for which evidence exists that chloroquine resistance is different from that described in *P. falciparum* [19,20]. In addition, mutant parasites that produce little or no Hz are excellent tools to analyze both the mode of action of drugs targeting Hz formation and to examine the possible pathological role of Hz during infections *in vivo*.

Results

High degree of functional redundancy amongst *Plasmodium* hemoglobinasases

In order to gain an understanding on the essential nature of individual enzymes involved in *P. berghei* Hb digestion, we performed a systematic loss-of-function analysis on 8 predicted hemoglobinasases that are orthologs of *P. falciparum* proteases with a role in Hb digestion and/or located in the DV. These enzymes (Table 1) are: the aspartic protease PM4 which is the single syntenic ortholog of the four plasmepsins in *P. falciparum* (plasmepsin I-IV) [18]; the papain-like cysteine protease BP2, which is the single syntenic ortholog of the *P. falciparum* DV falcipains 2 and 3 [21]; the M16 metalloprotease *bergheilysin* (BLN), the ortholog of *P. falciparum* falcilysin [22]; the dipetidyl peptidase DPAP1 or cathepsin C [23]; and four aminopeptidases, i.e. aminopeptidase P (APP) [24,25], M1-family alanyl aminopeptidase (AAP, ortholog of *P. falciparum* M1AAP) [25,26], M17-family leucyl

aminopeptidase (LAP, ortholog of *P. falciparum* M17LAP) [25,27] and M18-family aspartyl aminopeptidase (DAP, ortholog of *P. falciparum* M18DAP) [25]. In addition, we performed gene loss-of-function analyses for the heme detoxification protein (HDP), which is involved in the conversion of heme into Hz [28], as well as for three enzymes that are related to some proteases of the DV, but that do not have a proven role in Hb digestion and of which the cellular location is unknown. These enzymes are berghepain 1 (BP1, the ortholog of *P. falciparum* falcipain 1, FP1) [29-31] and 2 dipeptidyl peptidases, DPAP2 and DPAP3 [32].

Table 1. Genes targeted in this study

Product name <i>P. falciparum</i> Gene ID	Localization (Pf)	Essential for blood stages (Pf)	product name <i>P. berghei</i> Gene ID	Essential for blood stages (Pb) *
aspartic endoprotease				
plasmepsin I (PM I) PF3D7_1407900	DV [13]	no [16,17,33,34]	-	-
plasmepsin II (PM II) PF3D7_1408000	DV [13,35]	no [16,17,33,34]	-	-
plasmepsin IV (PM IV) PF3D7_1407800	DV [13]	no [16,17,33,34]	plasmepsin 4 (PM4) PBANKA_103440	no, [18]
plasmepsin III (PM III) PF3D7_1408100	DV [13]	no [16,17,33,34]	-	-
papain-like cysteine endoprotease				
falcipain 2a (FP 2a) PF3D7_1115700	DV [36-38]	no [15,29]	berghepain-2 (BP2) PBANKA_093240	no
falcipain 2b (FP 2b) PF3D7_1115300	DV [38]	no [29]	-	-
falcipain 3 (FP 3) PF3D7_1115400	DV [36,38]	yes [29]	-	-
metallopeptidase				
falcilysin (FLN) PF3D7_1360800	DV, MT, AP [22]	yes [22]	<i>bergheilysin</i> (BLN) PBANKA_113700	yes
dipeptidyl aminopeptidase				
dipeptidyl aminopeptidase 1 (DPAP1) PF3D7_1116700	DV [23]	yes [23]	dipeptidyl aminopeptidase 1 (DPAP1) PBANKA_093130	no
aminopeptidases				
aminopeptidase P (APP) PF3D7_1454400	DV, CY [24,25]	yes [24,25]	aminopeptidase P (APP) PBANKA_131810	no
M1- family alanyl aminopeptidase (M1AAP) PF3D7_1311800	DV, NU [25,26]	yes [25]	M1- family alanyl aminopeptidase (AAP) PBANKA_141030	yes
M17-family leucyl aminopeptidase (M17LAP) PF3D7_1446200	DV [39], CY [25,27]	yes [25]	M17-family leucyl aminopeptidase (LAP) PBANKA_130990	no
M18-family aspartyl aminopeptidase (M18DAP) PF3D7_0932300	CY [25]	no [25]	M18-family aspartyl aminopeptidase (DAP) PBANKA_083310	no

heme detoxification protein				
heme detoxification protein (HDP) PF3D7_1446800	DV [28]	yes [28]	heme detoxification protein (HDP) PBANKA_131060	yes
papain-like cysteine proteases				
falcipain 1 (FP1) PF3D7_1458000	Apical end of merozoites [31]	no [29,30]	berghelain 1 (BP1) PBANKA_132170	no
dipeptidyl aminopeptidases				
dipeptidyl aminopeptidase 2 (DPAP2) PF3D7_1247800	-	-	dipeptidyl aminopeptidase 2 (DPAP2) PBANKA_146070	no
dipeptidyl aminopeptidase 3 (DPAP3) PF3D7_0404700	-	yes [32]	dipeptidyl aminopeptidase 3 (DPAP3) PBANKA_100240	no

DV: digestive vacuole; MT: mitochondrion; AP, apicoplast; CY, cytosol; NU, nucleus

*, the phenotype observed in this study.

-, no published data.

We used standard genetic modification technologies to delete the genes encoding above mentioned enzymes and successfully generated gene deletion mutants for *pm4*, *bp1*, *bp2*, *dpap1*, *dpap2*, *dpap3*, *app*, *lap* and *dap* (Figure S1–3), whereas multiple attempts to disrupt *bln*, *aap* and *hdp* were unsuccessful (Table S1). The successful selection of gene-deletion mutants for 6 out of 8 predicted hemoglobinases indicates a high level of redundancy amongst the *P. berghei* proteases involved in Hb digestion. We previously reported that disruption of *pm4* results in the lack of all aspartic protease activity in the DV [18]. Also in *P. falciparum* it has been shown that blood stages are able to survive without DV aspartic protease activity [16]. We were able to select mutants that lack genes encoding DPAP1, APP and LAP, which is unexpected since the *P. falciparum* orthologs of these genes have been reported to be refractory to targeted gene disruption (Table 1; [23,25]. We were unable to select parasites lacking expression of AAP, HDP and BLN and in *P. falciparum*, the orthologous genes of *aap*, *hdp* and *bln* have also been reported to be resistant to disruption [22,25,28].

Mutants lacking expression of PM4, DPAP1, BP1, LAP or APP exhibit a significant reduction in growth and of these $\Delta pm4$ and Δapp also produce less hemozoin

We determined the *in vivo* asexual multiplication rate, i.e. growth rate, for all nine gene-deletion mutants (Table 2). We previously reported that the growth rate of $\Delta pm4$ parasites was moderately but significantly reduced compared to wt parasites, with multiplication rates ranging from 5.8 to 7.7-fold per 24 hours compared to a consistent 10-fold in wt parasites [18]. These multiplication rates were calculated during the initial

phase of infection after mice had been infected with a single parasite. Parasites lacking the DV dipeptidyl aminopeptidase DPAP1 ($\Delta dpap1$) and BP1 ($\Delta bp1$) have a comparable reduction in growth with multiplication rates of 7.7 and 6.8, respectively, and growth rates of Δlap and Δapp were much more reduced with multiplication rates of only 3.3 and 4.6, respectively (Table 2). The $\Delta bp2$ and Δdap mutants had normal, wt-like growth rates and growth rates of $\Delta dpap2$ and $\Delta dpap3$ mutants were only slightly (but not significantly) reduced (Table 2).

Table 2. Blood-stage growth and virulence characteristics of gene-deletion mutants

Gene deletion mutant	Day to 0.5-2% parasitemia ¹	multiplication rate ²	H _z production ³
wt ⁴	8 (0.2), n=40	10.0 (0.7)	198.8 (69.8)
$\Delta pm4$ -a ⁵	9-11, n>10	5.8(0.5)-7.0 (1.0) ***	129.5 (41.7) ***
$\Delta pm4$ -b	9 (0), n=2	7.7 (0) ***	134.5 (47.6) ***
$\Delta bp2$ -a	8 (0), n=5	10.0 (0)	177.5 (45.1)
$\Delta bp2$ -b	8 (0), n=6	10.0 (0)	188.4 (71.5)
$\Delta dpap1$ -a	9.5 (0.7), n=2	7.0 (1.0) ***	174.6 (34.0)
$\Delta dpap1$ -b	9 (0), n=4	7.7 (0) ***	189.2 (62.7)
Δapp -a	12 (0), n=1	4.6 (0) ***	131.8 (50.5) ***
Δapp -b	12 (0), n=4	4.6 (0) ***	111.4 (49.7) ***
Δdap	8 (0), n=3	10.0 (0)	223.8 (65.7)
Δlap	15.5 (0.7), n=2	3.3 (0.2) ***	213.6 (78.7)
$\Delta bp1$ -a	9.7 (0.6), n=3	6.8 (0.8) ***	186.2 (49.2)
$\Delta bp1$ -b	9 (0), n=1	7.7 (0) ***	n.d
$\Delta dpap2$	8.3 (0.4), n=4	9.4 (1.0)	187.8 (64.6)
$\Delta dpap3$ -a	8.3 (0.6), n=3	9.2 (1.3)	184.5 (86.3)
$\Delta dpap3$ -b	8 (0), n=5	10.0 (0)	193.3 (46.8)
$\Delta pm4\Delta bp2$ -a	12, 16, 20, n=3	3.4 (1.1) ***	27.2 (36.5) ***
$\Delta pm4\Delta bp2$ -b	21, 24, n=2	2.3 (0.1) ***	46.1 (51.2) ***

n.d., not determined

¹ The day on which the parasitemia reach 0.5–2% in mice infected with a single parasite during cloning assays. The mean of one cloning experiment and standard deviation were shown. n, the number of mice tested. For the $\Delta pm4\Delta bp2$ mutants, due to large variation, the days of which individual clone were shown.

² The multiplication rate of asexual blood stages per 24 hours is determined as following: when one clone in infected mice takes 8 days to parasitemia reach 0.5–2%, the multiplication rate is determined as 10. Mean values and standard deviations of each line were shown, student T-test, ***, P<0.0001.

³ H_z production values were determined by relative light intensity of H_z crystals in individual schizont under polarized light microscopy (Figure 1). Mean values and standard deviations were shown, student T-test, ***, P<0.0001.

⁴ wt, wild type *P. berghei* ANKA lines, including cl15cy1, 676m1cl1, 1037m1f1cl1, the data were collected more than 10 independent experiments.

⁵ *pm4* gene deletion mutants generated in Spaccapelo, R. *et al*, 2010 (ref [18])

We next determined the amount of H_z generated in schizonts of all mutants as a measure of Hb digestion. The total amount of H_z was quantified in individual schizonts by measuring relative light intensity (RLI) in schizonts using reflection contrast polarized light microscopy [33,34]. Only schizonts containing 8–24 nuclei were selected, thereby

selecting those parasites that were fully mature and in the process of mitosis (Figure 1A).

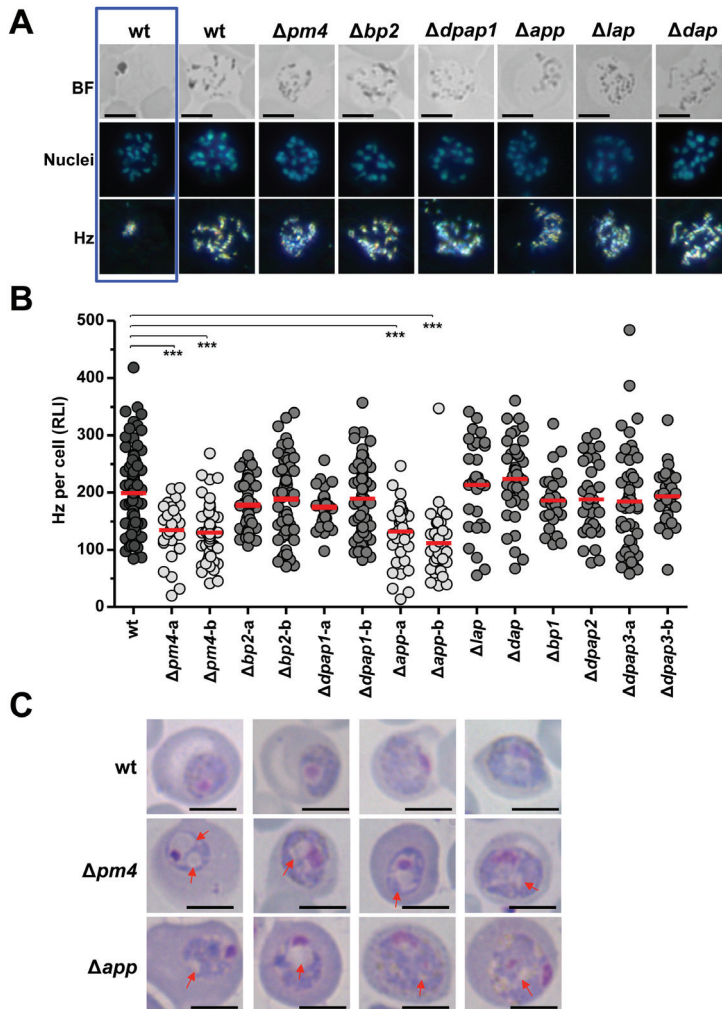


Figure 1. Hemozoin levels in parasite mutants lacking expression of enzymes involved in hemoglobin digestion

A. Hemozoin (Hz) crystals in schizonts as observed by light and reflection contrast polarized microscopy. Maturing schizonts were selected with scattered Hz that was not yet clustered into the characteristic single cluster that is observed only in fully segmented schizonts (boxed). Representative schizonts of wild-type (wt) and 6 mutants ($\Delta pm4$, $\Delta bp2$, $\Delta dap1$, Δapp , Δlap and Δdap) are shown. BF, bright-field; Nuclei, nuclei stained with Hoechst-33342.

B. The amount of Hz in individual schizonts ($n > 30$ /group) determined by measuring relative light intensity (RLI) of polarized light. The Hz level in mutants lacking expression of plasmepsin4 ($\Delta pm4$) and aminopeptidase P (Δapp) is significantly different from wt-schizonts (student T-test; *** $P < 0.0001$).

C. Aberrant morphology of $\Delta pm4$ and Δapp trophozoites exhibiting reduced Hz production and showing an accumulation of translucent vesicles (indicated by arrows) in their cytoplasm. Scale bars, 5 μm .

Compared to wt schizonts, only $\Delta pm4$ and Δapp mutants showed a clear and significant reduction in Hz production, whereas all the other 7 mutants produced similar levels of Hz compared to the wt parasite (Figure 1A&B, Table 2). The Hz reduction in Δapp mutants is unexpected since APP was shown to be involved in generating free amino acids from small peptides liberated from successive steps of hemoglobin digestion after heme is released from the initial cleavage of Hb. Trophozoites of Δapp and $\Delta pm4$ mutants have an aberrant morphology as visible on Giemsa stained blood smears, exhibiting an accumulation of translucent vesicles inside their cytoplasm (Figure 1C). These observations indicate that a number of gene-deletion mutants for *P. berghei* hemoglobinsases have reduced parasite multiplication rates, but only $\Delta pm4$ and Δapp mutants are impaired in Hz production.

Blood-stage mutant parasites lacking both PM4 and BP2 are viable but have a reduced rate of growth

We examined whether we could generate *P. berghei* parasites in which the genes encoding both PM4 and BP2 ($\Delta pm4\Delta bp2$) are deleted. The simultaneous absence of these two enzyme activities in *P. berghei* is expected to result in the absence of Hb hydrolysis in the DV, since in *P. berghei* PM4 is the only vacuolar aspartic protease, and BP2 is the single syntenic ortholog of the two cysteine endoproteases found in the DV of *P. falciparum* (falcipain 2 and 3). Unexpectedly, we were able to generate double gene-deletion mutants that lack expression of both PM4 and BP2 (Figure S4). Blood-stages of $\Delta pm4\Delta bp2$ have a strongly reduced growth rate in cloning assays with multiplication rates ranging from 2.2 to 4.6, which is significantly lower than wt ($P < 0.0001$) and $\Delta pm4$ parasites ($P < 0.0001$) (Table 2). In long-term infections in BALB/c and C57BL/6 mice, there is an initial slow rise in $\Delta pm4\Delta bp2$ parasite numbers. However, parasitemia can reach high levels (up to 50%) when these mice start to produce reticulocytes in response to the infection (Figure S5). In the infections with high parasitemias, mature schizonts were present in the peripheral blood circulation, most of which contained 8–12 merozoites (Figure S2A). Furthermore, in contrast to wt-infected mice (but similar to $\Delta pm4$ -infected mice) C57BL/6 mice infected with $\Delta pm4\Delta bp2$ did not develop symptoms of experimental cerebral malaria (ECM). In contrast to $\Delta pm4$ infections which can only be resolved by BALB/c mice [18], both C57BL/6 and BALB/c mice were able to resolve a $\Delta pm4\Delta bp2$ infection, resulting in undetectable parasitemias by microscopic analysis 3–6 weeks after infection (Figure S5).

Schizonts of $\Delta pm4\Delta bp2$ are smaller in size and produce fewer merozoites than wt-schizonts

Although wt *P. berghei* parasites preferentially invade reticulocytes, merozoites can also invade and develop in mature RBC producing mature schizonts both *in vivo* and *in vitro* [35]. Even though ring forms of $\Delta pm4\Delta bp2$ were observed in both mature RBC and reticulocytes, schizonts were exclusively found in reticulocytes as observed on Giemsa-stained slides (data not shown). This indicates that $\Delta pm4\Delta bp2$ parasites, while retaining their ability to invade mature RBC, are unable to develop into fully segmented schizonts in mature erythrocytes. Light microscopy examination of Giemsa-stained blood-stages showed that mature $\Delta pm4\Delta bp2$ -schizonts were small and left a large volume of the infected RBC (iRBC) unoccupied (occupying only 25–65%), whereas wt-schizonts occupied 60–90% of the host iRBC (Figure 2A). We also examined the sizes of live wt- and $\Delta pm4\Delta bp2$ -schizonts by imagestream flow cytometry. Both wt- and $\Delta pm4\Delta bp2$ -parasites express GFP under the control of the schizont/merozoite-specific *ama-1* promoter, therefore iRBCs with mature schizonts were selected based on their GFP and Hoechst fluorescence (Figure 2B). Analysis of the size of iRBCs and schizonts of $\Delta pm4\Delta bp2$ and wt parasites demonstrated that $\Delta pm4\Delta bp2$ -schizonts were significantly smaller than wt schizonts ($P < 0.0001$; Figure 2B). In addition, Giemsa-stained parasite analysis indicated that $\Delta pm4\Delta bp2$ -schizonts had fewer merozoites than wt-schizonts (Figure 2A). We therefore quantified the total DNA content of mature $\Delta pm4\Delta bp2$ -schizonts by measuring Hoechst fluorescence intensity using both standard and imagestream flow cytometry. Both methods demonstrated that mature $\Delta pm4\Delta bp2$ -schizonts have significantly less total DNA compared to wt-schizonts (55–60% of wt, $P < 0.0001$), indicating a significant reduction in the total number of merozoites per individual schizonts (Figure 2C). The reduction in the number of daughter merozoites was also reflected in the intensity of (*ama1* based) GFP expression levels in mature schizonts. In comparison to wt-schizonts, $\Delta pm4\Delta bp2$ -schizonts have a 40% reduction in GFP-intensity ($P < 0.0001$), which corresponds to the reduction in total DNA and therefore the number of merozoites per schizont (Figure 2C). Thus, parasites lacking both PM4 and BP2 develop into smaller schizonts and produce less daughter cells compared to wt-schizonts.

The $\Delta pm4\Delta bp2$ mutant can develop into mature schizonts in the absence of detectable hemozoin

Many trophozoites of $\Delta pm4\Delta bp2$, as observed by standard light microscopy, have an ‘amoeboid-like’ appearance, with many translucent vesicles inside the cytoplasm, similar to what we had observed for $\Delta pm4$ and Δapp mutants. Moreover, both $\Delta pm4\Delta bp2$

trophozoites and schizonts have strongly reduced or even no visible Hz (Figure 2 and Figure S5). To analyze these features in more detail we both quantified Hz levels in schizonts and analyzed the ultrastructure of $\Delta pm4\Delta bp2$ trophozoites. First, we determined the total

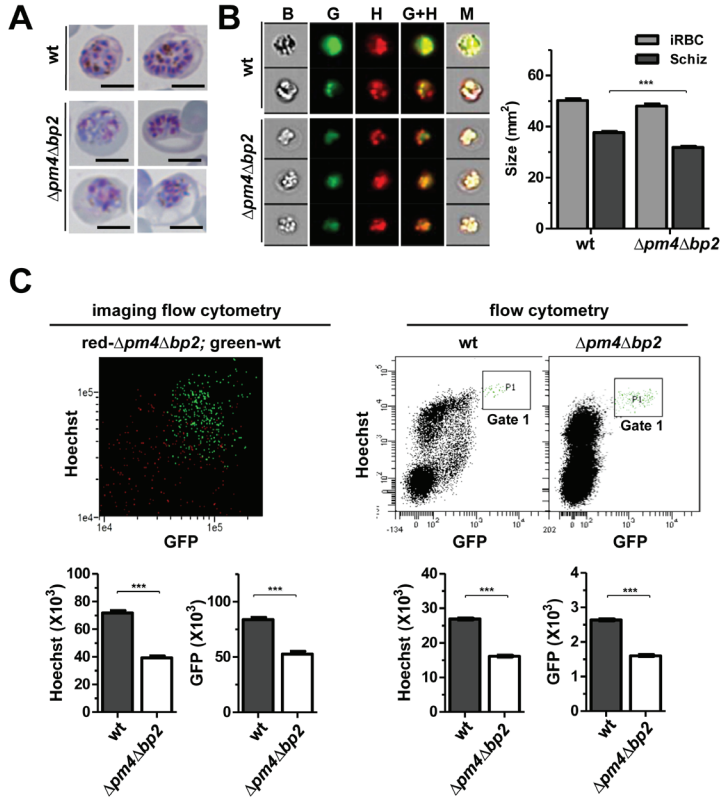


Figure 2. Schizonts of mutants lacking expression of PM4 and BP2 are smaller in size and have fewer merozoites

A. Giemsa-stained schizonts of wt and $\Delta pm4\Delta bp2$ -parasites. The $\Delta pm4\Delta bp2$ schizonts leave a large volume of the infected RBC unoccupied compared to wt schizonts. Scale Bar, 5 μm .

B. Images of mature schizonts and size measurement ($n > 250$) by imagestream flow cytometry (left and right panels). Both wt- and $\Delta pm4\Delta bp2$ -parasites express GFP under the control of the schizont/merozoite-specific *ama-1* promoter and their nuclei were stained with Hoechst-33342. Mature schizonts were selected on the basis of their GFP (G, green) and Hoechst (H, red) fluorescence intensity. The size of iRBCs containing schizonts was measured from the bright-field image (B) and the size of the schizonts was measured from the combined GFP and Hoechst images (G+H) (student T-test, *** $P < 0.0001$). M; all images merged.

C. Determination of the DNA content (Hoechst fluorescence intensity) and the GFP expression in wt and $\Delta pm4\Delta bp2$ -schizonts by imaging flow cytometry (left panel) and standard flow cytometry (right panel). Mature schizonts were selected based on their GFP- and Hoechst-fluorescence intensity. The dot plot (upper, left) shows the GFP- and Hoechst fluorescence intensity for individual schizonts in image stream flow cytometry. In standard flow cytometry (upper, right) schizonts were selected for measurement in Gate 1. Schizonts of $\Delta pm4\Delta bp2$ contained significantly less DNA and displayed reduced GFP expression (*** $P < 0.0001$, student T-test).

amount of Hz in individual schizonts using reflection contrast polarized light microscopy. Compared to wt-parasites the amount of Hz in schizonts of two independently derived $\Delta pm4\Delta bp2$ lines was strongly reduced (13–22% of the wt values, $p < 0.0001$; Figure 3A, Table 2). By polarized light microscopy we found that a large percentage (35–48%) of the $\Delta pm4\Delta bp2$ -schizonts were completely Hz-negative, whereas all wt-schizonts were Hz-positive (Figure 3A). The Hz-negative $\Delta pm4\Delta bp2$ -schizonts had relative light intensity (RLI) values similar to uninfected RBC. The presence of Hz-negative schizonts indicates that parasites can grow and multiply without Hb digestion. The strong reduction in Hz production per schizont was reflected in reduced Hz deposition in organs of $\Delta pm4\Delta bp2$ -infected mice compared to wt-infected mice. In wt-infected mice almost 95% of the Hz produced is deposited in the spleen and liver [36]. We compared Hz-levels in spleen, lungs and liver at different time points in mice infected with wt, $\Delta pm4$ or $\Delta pm4\Delta bp2$ parasites (Figure 3B). Mice infected with $\Delta pm4$ and $\Delta pm4\Delta bp2$ had significantly less Hz deposited in all organs examined compared to wt-infected mice at a comparable parasitemia (56% less, $P < 0.001$; and 87% less, $P < 0.0001$, respectively). In addition, organs of $\Delta pm4\Delta bp2$ -infected mice had significantly less Hz than $\Delta pm4$ -infected mice (72% less; $P < 0.001$) (Figure 3B). The relative differences in Hz deposition in organs of mice infected with the different parasite lines corresponds well with the differences in Hz levels found in schizonts of wt, $\Delta pm4$ and $\Delta pm4\Delta bp2$ parasites, as determined by polarized light microscopy (Figure 3A&B, Table 2). We also confirmed the reduction in Hz production in $\Delta pm4\Delta bp2$ trophozoites by quantifying the number of Hz crystals using electron microscopy (Figure 3C). The ultrastructural analysis showed that $\Delta pm4\Delta bp2$ trophozoites contained a higher number of cytotome or endocytic vesicles in comparison to wt trophozoites, which were filled with material that was structurally identical to erythrocyte cytoplasm (Figure 3C). Furthermore, in the cytoplasm of 37% of $\Delta pm4\Delta bp2$ -trophozoites we observed dark stained (electron dense) vesicles, which were completely absent in wt-parasites (Figure 3C and S6). The presence of increased numbers of these vesicles in the cytoplasm may explain the translucent vesicles observed in trophozoites on Giemsa-stained blood films (Figure S5).

Gametocytes of $\Delta pm4\Delta bp2$ are fertile despite their smaller size and reduced hemozoin production

In mice infected with $\Delta pm4\Delta bp2$ -parasites, uninuclear parasites with the characteristics of male and female gametocytes were readily detected (Figure S7). However, they were significantly smaller than wt-gametocytes (23% smaller, Figure S7), and their cytoplasm also have strongly reduced or no Hz crystals. Most $\Delta pm4\Delta bp2$ male gametocytes produced motile gametes ($79.3\% \pm 4.6$) and conversion rates of $\Delta pm4\Delta bp2$ female gametes into

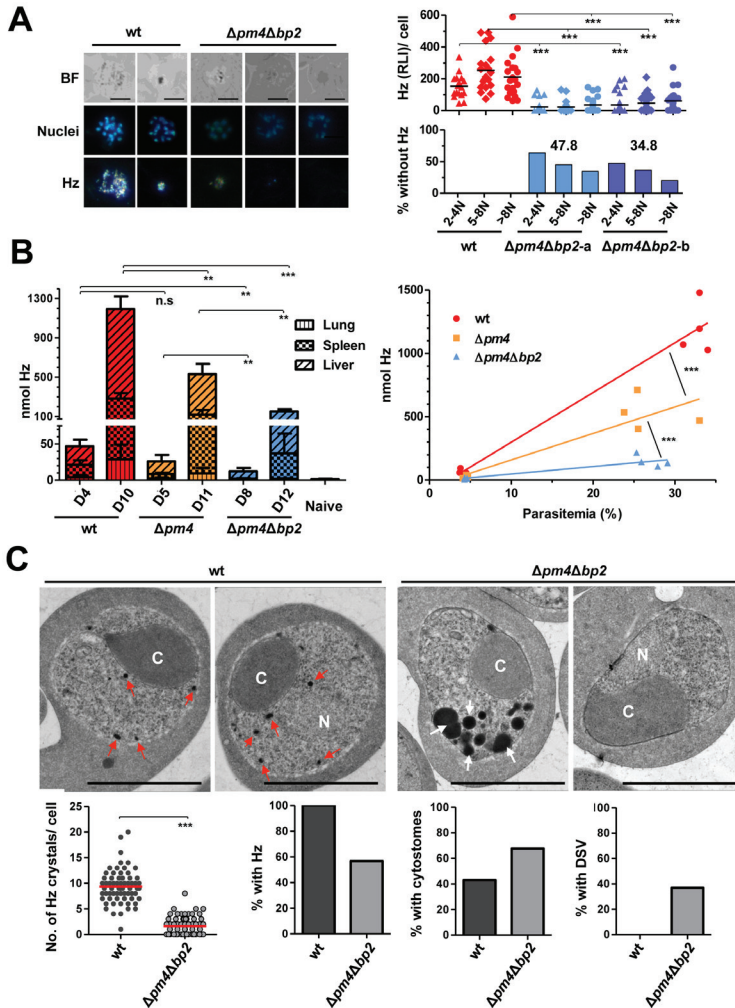


Figure 3. $\Delta pm4\Delta bp2$ mutant parasites can develop into mature schizonts with little or no detectable hemozoin

A. The amount of Hz in individual schizonts as determined by measuring relative light intensity (RLI) using reflection contrast polarized light-microscopy. Left panel: Hz crystals in schizonts as observed under polarized light. In $\Delta pm4\Delta bp2$ parasites Hz levels are either strongly reduced or absent. Right panel: Hz levels (RLI) in schizonts with 2–4, 5–8 or more than 8 nuclei (N) ($n > 20$ per category). The Hz level in two $\Delta pm4\Delta bp2$ -mutants is significantly less than in wt-schizonts across all categories (student T-test, *** $P < 0.0005$). Lower panel: a large proportion of $\Delta pm4\Delta bp2$ -schizonts have no detectable Hz crystals under polarized light with RLI levels similar to uninfected RBC. BF, bright field; Nuclei, nuclei stained with Hoechst-33342.

B. Hz levels in different organs of BALB/c mice infected with wt, $\Delta pm4$ or $\Delta pm4\Delta bp2$ -parasites at different days (D) after infection (left panel) and total Hz levels in function of peripheral parasitemia in infected mice (right panel). Not significant (ns), ** $p < 0.05$, *** $p < 0.0005$ (student T-test).

C. Quantification of Hz crystals, cytotomes (C) and dark-staining vesicles (DSV) in $\Delta pm4\Delta bp2$ - and wt-trophozoites. Upper panel: Electron micrographs of representative trophozoites of wt- and $\Delta pm4\Delta bp2$ -parasites. Red arrowheads denote pigment crystals (Hz) and white arrow indicate DSVs and light staining nuclei (N). Scale bars, 5 μm . Lower panel: quantification of Hz

crystals (student T-test, *** $P < 0.0005$), cytotomes and DSVs in randomly selected trophozoites ($n > 50$) from electron micrographs (see also Figure S6).

ookinetes were comparable to those of wt-parasites ($60.0\% \pm 6.1$; Figure S7). Analysis of Hz crystals in wt and $\Delta pm4\Delta bp2$ ookinetes revealed that these ookinetes had strongly reduced levels of Hz (57% reduction; Figure S7). These observations demonstrate that both asexual and sexual blood-stages can complete development in the absence of PM4 and BP2 to initiate Hb digestion.

The $\Delta pm4\Delta bp2$ parasites are more resistant to chloroquine but retain their sensitivity to artemisinin

We tested the sensitivity of the $\Delta pm4\Delta bp2$ -parasites to two antimalarial drugs known to interfere with Hb digestion and/or Hz formation, i.e. chloroquine (CQ) and artesunate (AS), an artemisinin derivative via different mechanisms [37,38]. As a control, we used sulfadiazine (SD), an inhibitor of folic acid synthesis with no known role in inhibiting Hb digestion [39]. BALB/c mice infected with either wt- or $\Delta pm4\Delta bp2$ -parasites were treated with these drugs when peripheral parasitemia was between 2 and 5%, i.e. at day 6 after infecting mice with 10^4 wt-parasites or at day 9 after infecting mice with 10^5 $\Delta pm4\Delta bp2$ -parasites. Treatment with SD as well as AS resulted in a rapid decrease in parasitemia with parasites being undetectable in peripheral blood 3–4 days after AS treatment and 4–5 days after SD treatment, and the profile of drug action being identical for both wt- and $\Delta pm4\Delta bp2$ -parasites (Figure 4C). In contrast, whereas wt-infected mice rapidly cleared their infection after CQ treatment with no parasites detectable in peripheral blood 3–4 days after the start of treatment, $\Delta pm4\Delta bp2$ infected mice maintained an increasing parasitemia for the first three days of treatment (Figure 4C). After this period, parasitemia started to decline but $\Delta pm4\Delta bp2$ -parasites with morphology similar to that of untreated parasites could still be observed by light microscopy (Figure S8A) up to 6 days after initiation of CQ treatment (Figure 4C). The parasitemia in CQ treated mice dropped to submicroscopic level after 7 days of CQ treatment (i.e. day 16 post infection). Interestingly, in untreated mice the $\Delta pm4\Delta bp2$ parasitemia similarly dropped around day 15–18 post-infection (Figure S8B), presumably due to an acquired immune response.

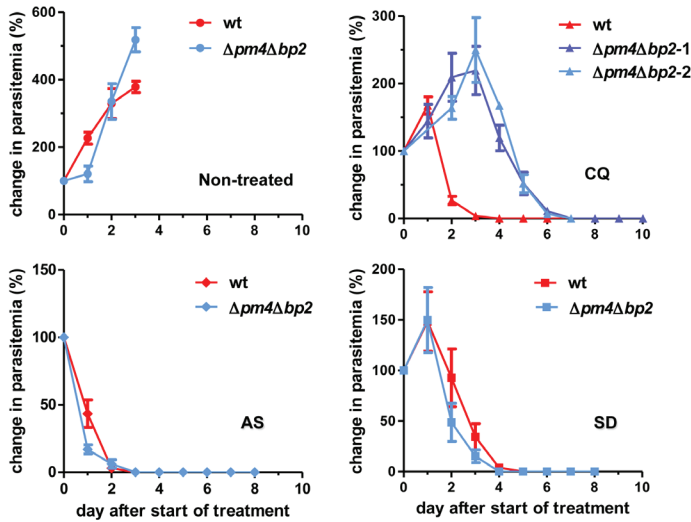


Figure 4. $\Delta pm4\Delta bp2$ -schizonts are less sensitive to chloroquine than wt-parasites

Change in parasitemia of mice (n=5) infected with wt- or $\Delta pm4\Delta bp2$ -parasites after treatment with chloroquine (CQ; 2 experiments), artesunate (AS) or sulfadiazine (SD). $\Delta pm4\Delta bp2$ parasites are less sensitive to CQ but retain the same sensitivity to AS and SD as wt parasites.

Discussion

P. falciparum growth in RBC is considered to be dependent on Hb digestion [40]. In addition to providing amino acids for growth it has been proposed that parasites digest Hb to maintain the intracellular osmolarity of the infected RBC, thereby preventing premature erythrocyte lysis [41], or to make space within the RBC as the parasite expands [42,43]. Our studies, however, provide evidence that *Plasmodium* blood stage parasites, both asexual and sexual forms, can fully mature with little or no Hz production when parasites invade and develop inside reticulocytes indicating that blood stages can grow without or with strongly reduced Hb digestion.

As has been previously reported in *P. falciparum*, we found that a large number of *P. berghei* enzymes predicted to have a role in Hb proteolysis are functionally redundant. The viability of mutant parasites lacking hemoglobinasen, indicates either that other enzymes can replace their function(s) or that *P. berghei* can obtain all amino acids from other sources, for example from the catabolism of proteins other than Hb or by scavenging free amino acids from the reticulocyte cytoplasm or serum. On the other

hand, the strong reduction in growth of $\Delta pm4\Delta bp2$ -parasites lacking both PM4 and BP2 enzymes, whose *P. falciparum* orthologs are responsible for the initial cleavage of Hb, suggests that Hb is an important amino acid source. The reduced growth rate might, however, also be attributed to the other features associated with reduced Hb digestion, such as limited space inside the RBC for growth resulting in smaller schizonts with fewer merozoites or the loss of parasites that invade mature RBC but are unable to fully mature.

We did not observe replicating $\Delta pm4\Delta bp2$ -parasites in mature RBC and in $\Delta pm4\Delta bp2$ infections, parasite numbers increased rapidly only when mice start to produce large numbers of reticulocytes, at which stage they can achieve parasitemias as high as 50%. Further, when $\Delta pm4\Delta bp2$ ring forms were transferred to culture less than 5% produced mature schizonts, in comparison more than 90% of wt ring forms can develop into fully mature schizonts (data not shown). This is most probably due to the accelerated maturation of reticulocytes in culture [44], which restricts the development of $\Delta pm4\Delta bp2$ schizonts. The ability of $\Delta pm4\Delta bp2$ -parasites to form merozoites only in reticulocytes is likely related to the greater abundance of amino acids and proteins other than Hb in the reticulocyte compared to mature RBC. Reticulocytes are known to accumulate amino acids for incorporation into Hb [45] and these may be available for direct utilization when the parasite ingests reticulocyte cytoplasm. The $\Delta pm4\Delta bp2$ -trophozoites show an increased number of cytosome-vesicles containing RBC cytoplasm, indicating that the absence of PM4 and BP2 does not affect Hb uptake. In addition to cytosomes, we found electron-dense dark-staining vesicles in a large proportion of $\Delta pm4\Delta bp2$ trophozoites. Interestingly, very similar vesicles have been observed in *P. falciparum* trophozoites when Hb digestion or Hb trafficking (cytosome formation) have been blocked by inhibitors [46,47]. It has been proposed that these vesicles are derived from the cytosomes and contain concentrated undigested or denatured Hb [47]. In addition to the increased numbers of vesicles in trophozoites, we found that mature $\Delta pm4\Delta bp2$ -schizonts and gametocytes have strongly reduced amounts or even no Hb in their cytoplasm, indicating that Hb digestion is strongly impaired. The presence of low Hb amounts in a proportion of $\Delta pm4\Delta bp2$ -parasites indicates that some heme is released from Hb in the absence of PM4 and BP2. However, whether this is mediated by a specific, but inefficient, compensatory enzymatic process or is the result of unspecific hemoglobin denaturation is unknown. In *P. berghei* PM4 is the only vacuolar aspartic protease and BP2 is the single syntenic ortholog of the two *P. falciparum* DV cysteine endopeptidases, falcipain-2 and 3. The other *Plasmodium* papain-like cysteine endoprotease (FP1 in *P. falciparum*; BP1 in *P. berghei*) is not located in the DV of *P. falciparum* but is located in merozoites and is involved RBC invasion [48]. While the cellular location of both BP1 in *P. berghei* blood stages is unknown, the BP1 ortholog of the closely related rodent parasite *P. yoelii*

(YP1) is also expressed in merozoites and is believed to have a role in RBC invasion [31], suggesting a similar function as FP1. It therefore seems unlikely that BP1 is involved in the initial phase of Hb digestion and release of heme in trophozoite-stage parasites. However, we cannot formally exclude a role for BP1, or indeed another endoprotease, in the initial step of Hb digestion, which would compensate, albeit poorly, for the loss of PM4 and/or BP2. Further research is needed to investigate whether the remaining low-level Hz formation in $\Delta pm4\Delta bp2$ -parasites is due to specific cleavage of Hb molecules by other enzymes or results from a non-specific disassembly of the Hb tetramer that may occur either the cytosomes or in the dark-staining vesicles which may be acidified and condensed cytosomes [47].

In *P. falciparum* the plasmepsins and falcipains overlap in function and there is extensive functional redundancy within and between these two protease classes, with the loss of an enzyme being not only being compensated by members of the same protease family but also between the two classes [4,15-17,49,50]. Recently a 200-kDa protein complex has been defined in *P. falciparum* that is required for Hb degradation and Hz formation in the food vacuole [51]. As expected, this protein complex contains the falcipains FP2/2' as well the plasmepsins II–IV in addition to HDP. Interestingly, evidence was provided that FP2 forms a complex with HDP and is involved in Hz formation. Our observations on Hz production in the single gene-deletion mutants $\Delta pm4$ and $\Delta bp2$ and the double gene-deletion mutant $\Delta pm4\Delta bp2$ indicate that also in *P. berghei* the aspartyl and cysteine endopeptidases overlap in their ability to cleave Hb. Interestingly, the $\Delta bp2$ mutant, which lacks the FP2 orthologs, has a normal growth rate and produces wt-levels of Hz, whereas $\Delta pm4$ parasites have a reduced growth and Hz production. These observations demonstrate that while PM4 is able to fully compensate for the function of BP2, BP2 can only partly compensate for the loss of PM4. Moreover, it suggests that BP2 is not necessary for the activation of PM4 as has been suggested previously [49].

The ability of *Plasmodium* parasites to produce mature schizonts without Hz formation may have important implications in the development of drugs that target Hb digestion and for understanding development of resistance against such drugs [40]. We found that $\Delta pm4\Delta bp2$ -parasites are less sensitive to chloroquine (CQ) *in vivo*. CQ directly interacts with free heme creating a heme-chloroquine complex that is highly toxic to the parasite [52] and therefore the increased in CQ resistance of $\Delta pm4\Delta bp2$ is consistent with our observations of reduced/absent Hb digestion. Interestingly, it has been previously reported that *P. berghei* lines that have been selected for CQ-resistance have a stronger preference for reticulocytes and produce less Hz [53-55]. It has been proposed that CQ-resistance in parasites with reduced Hz is due to detoxification of hemin by elevated

levels of glutathione in parasites that grow inside reticulocytes, thus precluding heme-polymerization and preventing the CQ activity [53,56]. However, our observations may provide a more direct explanation for CQ-resistance and reduced Hz production in these parasites, namely that these parasites digest less Hb in reticulocytes like $\Delta pm4\Delta bp2$ -parasites. Despite the reduced sensitivity to CQ, we found that $\Delta pm4\Delta bp2$ -parasites disappeared from the blood of mice during continuous CQ treatment (from day 16 after infection with 10^5 parasites). This may be due a combination of factors that characterize $\Delta pm4\Delta bp2$ infections in mice. CQ may eliminate the proportion of parasites that still produce (low levels) of Hz thereby slowing the multiplication rate of $\Delta pm4\Delta bp2$ parasites and in addition immune responses will limit parasite multiplication in mice. Interestingly, untreated mice also resolve infections between day 15–18, through the removal of iRBC by host immunity. Therefore the eventual drop in a $\Delta pm4\Delta bp2$ parasitemia in the CQ-treated mice may not result from CQ action, but from an effectively deployed acquired immune response.

We have been unable to more precisely determine the increase in CQ-resistance of $\Delta pm4\Delta bp2$ -parasites *in vitro* since the ring forms of this mutant do not mature into schizonts in culture (see above). While $\Delta pm4\Delta bp2$ parasites have an increased resistance to CQ they retain the same sensitivity to artesunate (AS). Although the precise and critical mode of action of artemisinin and related-derivatives remains contentious, most studies concur that their activity results from activation by reduced heme iron in the DV [57,58]. Our results show that compared to wt parasites, $\Delta pm4\Delta bp2$ -parasites have a reduced sensitivity to CQ but are equally sensitive to AS. This would suggest that additional, non-heme based, modes of AS action are equally or more effective at targeting *P. berghei* parasites *in vivo*. Therefore, as $\Delta pm4\Delta bp2$ -parasites produce little or no Hz they may be useful tools to analyze mode/s of drug action, for example, how inhibitory compounds target and interact with molecules either critical to or result from Hb digestion. The observations on the acquisition of CQ-resistance when parasites develop in reticulocytes with little or no Hz formation may have relevance for *P. vivax*, which is restricted for growth in reticulocytes. Interestingly mechanisms of CQ-resistance in *P. vivax* appear to be different from those in *P. falciparum* [20,59] and no clear association has been found between CQ-resistance in *P. vivax* and mutations associated with CQ-resistance in *P. falciparum*, such as *pfprt* or *pfmdr1* [20]. Studies into *P. vivax* suggest that development of CQ-resistance also confers cross-resistance to amodiaquine, an anti-malarial that also exercises its effects by complexing with heme [60-62]. Based on our observations, we hypothesize that *P. vivax* may acquire resistance to CQ (and other drugs targeting Hb digestion) by selecting for parasites that have ‘switched’ to a development mode where they are less dependent on Hb digestion for growth. This ‘switching’ could be dependent

on genetic (and/or epigenetic) changes that, for example, reduce Hb digestion or increase uptake of amino acids (from the reticulocyte and serum) and thus are unrelated to the genetic changes that influence CQ transport in *P. falciparum* resistant lines [63]. Such ‘switching’ may only be possible for those *Plasmodium* species that can infect and develop in reticulocytes. It would therefore be of great interest to analyze whether in ‘hotspots’ of *P. vivax* CQ-resistance parasites have reduced Hz formation.

The ability of *Plasmodium* parasites to develop inside reticulocytes with severely impaired Hb digestion and Hz formation was unexpected given the multiple proposed important roles of Hb digestion for survival in the blood. Our findings support the notion that *Plasmodium* parasites retain multiple modes of development and survival during blood stage development, which has important implications for the development of drugs targeting the *Plasmodium* Hb digestion or Hz formation as well as indicating alternative modes of drug resistance that require further investigation.

Materials and methods

Experimental animals and reference *P. berghei* ANKA lines

Female C57BL/6, BALB/c and Swiss OF1 mice (6–8 weeks old; Charles River/Janvier) were used. All animal experiments performed at the LUMC were approved by the Animal Experiments Committee of the Leiden University Medical Center (DEC 10099; 12042; 12120). All animal experiments performed at the University of Perugia were approved by Ministry of Health under the guidelines D.L. 116/92). The Dutch and Italian Experiments on Animal Act were established under European guidelines (EU directive no. 86/609/EEC regarding the Protection of Animals used for Experimental and Other Scientific Purposes).

Two reference *P. berghei* ANKA parasite lines were used: line cl15cy1 (wt) and reporter line 1037cl1 (wt-GFP-Luc_{schiz}; mutant RMgm-32; www.pberghei.eu). This reporter line contains the fusion gene *gfp-luc* gene under control of the schizont-specific *ama1* promoter integrated into the silent *230p* gene locus (PBANKA_030600) and does not contain a drug-selectable marker [18].

Generation of single gene deletion mutants and genotype analyses

Most DNA constructs used to disrupt genes were based on the standard plasmids: plasmid pL0001 (MRA-770, www.mr4.org) and pLTgDFHR both containing the pyrimethamine resistant *Toxoplasma gondii* (*Tg*) dihydrofolate reductase-thymidylate synthase (*dhfr/ts*) as a selectable marker (SM) under the control of the *P. berghei dhfr/ts* promoter;

and plasmid pL0035 (MRA-850, www.mr4.org) containing the *hdhfr::yfcu* SM under the control of the *eef1α* promoter [64]. Targeting sequences for homologous recombination were PCR amplified from *P. berghei* ANKA (cl15cy1) genomic DNA using primers specific for the 5' or 3' end of each gene (see Table S1 for the primer sequences). The PCR-amplified target sequences were cloned either upstream or downstream of the SM to allow for integration of the construct into the targeting regions by homologous recombination. The DNA construct targeting *bp1* was kindly provided by Dr. Photini Sinnis (Johns Hopkins University). The DNA deletion constructs were linearized with the appropriate restriction enzymes (Table S1) before transfection.

Several gene deletion constructs were generated by a modified two step PCR method [65]. Briefly, in the first PCR reaction two fragments (5'- and 3'-targeting sequences) of the targeted gene were amplified from *P. berghei* ANKA genomic DNA with the primer sets P1/P2 and P3/P4 (Table S1). Primers P2 and P3 have 5' extensions homologous to the SM cassette. The SM cassette (*eef1α-hdhfr::yfcu-3'dhfr/ts*) was excised by digestion from plasmid pL0048 with *XhoI* and *NotI* [65] or the SM cassette (*eef1α-hdhfr-3'dhfr/ts*) from plasmid pL0040 with *XhoI* and *NotI*. Primers P1 and P4 have 5' terminal extensions with an anchor-tag suitable for the second PCR reaction. In the second PCR reaction, the amplified 5' and 3' targeting sequences were annealed to either side of the SM cassette, and the joint fragment was amplified by the external anchor-tag primers L4661/L4662, resulting in the PCR-based gene deletion constructs. Before transfection, constructs were digested with appropriate restriction enzymes (in primers P1 and P4, respectively) to remove the 'anchor-tag', and with *DpnI* to digest any residual plasmids.

Transfection and selection of transformed parasites was performed using standard genetic modification technologies for *P. berghei* [66]. In Table S1 details of all gene-deletion experiments are given such as experiment number, deletion construct and parasite background for transfection. Cloned parasites were obtained from all gene-deletion mutants by the method of limiting dilution. Correct integration of DNA constructs and disruption of genes was verified by diagnostic PCR analyses (see Table S2 for primers) and Southern analyses of chromosomes separated by pulsed-field gel electrophoresis [66]. All information on successfully generated gene deletion mutants and the failed attempts to disrupt genes, including DNA constructs and primers, have been submitted to the RMgMDB database of genetically modified rodent malaria parasites (www.pberghei.eu). The loss of transcripts in gene-deletion mutants was analyzed by standard Northern blot analyses or RT-PCR. Total RNA was isolated from mixed blood-stages of wt *P. berghei* ANKA (cl15cy1) and the different gene-deletion mutant lines. Northern blots were hybridised with probes specific for the open reading frame (ORF) of each gene after PCR

amplification from wt *P. berghei* ANKA genomic DNA (primers shown in Table S2.b). As a loading control, Northern blots were hybridized with the oligonucleotide probe L644R that recognizes the large subunit ribosomal RNA (rRNA) [67]. For RT-PCR primers were designed to amplify a small fragment in the ORF of each gene (primers and product size are shown in Table S3). Amplification of *Pbtub* from cDNA was used as a control (primers and product size are shown in Table S3).

Generation of double gene-deletion mutants and genotype analysis

The $\Delta bp2$ -b mutant was generated using construct pL1602, which contains the *hdhfr::yfcu* SM flanked by two identical 3'UTR *dhfr* sequences [64]. A recombination event between the two 3'UTR *dhfr* sequences results in the removal of the *hdhfr::yfcu* SM. Negative selection with 5-fluorocytosine (5-FC) was used to select for parasites that have removed the SM cassette. Mice infected with $\Delta bp2$ -b parasites were treated with a daily single dose of 0.5 mL of 20 mg/mL drug/day for a period of 4 days starting at a peripheral parasitemia of 0.1–0.5%. Resistant parasites were collected between day 5 and 7 after initiation of the 5-FC treatment, and cloned parasites were obtained by the method of limiting dilution. The genotype of mutant $\Delta bp2$ -bsm was analyzed by diagnostic Southern analysis to confirm removal of the *hdhfr::yfcu* SM (Figure S4). The gene encoding PM4 was subsequently targeted in this line by standard transfection and drug selection procedures as mentioned above (Figure S4).

In vivo asexual multiplication (growth) rate and virulence of blood-stage parasites

The multiplication (growth) rate of asexual blood-stages in mice was determined during cloning of the gene-deletion mutants as described before [18] and was calculated as follows: the percentage of infected erythrocytes (parasitemia) in Swiss OF1 mice injected with a single parasite was determined by counting Giemsa-stained blood films when parasitemias reach 0.5–2%. The mean asexual multiplication rate per 24 hours was then calculated assuming a total of 1.2×10^{10} erythrocytes per mouse (2mL of blood). The percentage of infected erythrocytes in mice infected with reference lines of the *P. berghei* ANKA strain consistently ranged between 0.5–2% at day 8 after infection, resulting in a mean multiplication rate of 10 per 24 hours [68].

The development of experimental cerebral malaria (ECM) was analyzed in C57BL/6 mice and the course of parasitemia was determined in both BALB/c and C57BL/6 mice. Groups of 5–6 mice were injected intraperitoneally (i.p.) with 10^4 – 10^5 wt-iRBCs or with 10^5 – 10^6 mutant-iRBCs (see Results section). The onset of ECM was determined by observation of

clinical signs such as ruffled fur, hunching, wobbly gait, limb paralysis, convulsion, and coma and by measuring the drop in body temperature [18] at day 5 to 8 after infection at 6 hour intervals. The body temperature of infected mice was measured using a laboratory thermometer (model BAT-12, Physitemp Instruments Inc., Clifton, NJ) with a rectal probe (RET-2) for mice. The experiments were terminated when infected mice showed a drop in body temperature below 34°C or showed signs of cerebral complications.

Sizes measurements of parasites inside iRBCs

To measure the sizes of schizonts and gametocytes, tail or cardiac blood containing schizonts was collected from infected BALB/c mice with a high parasitemia (10–30%). Blood was collected in complete RPMI-1640 culture medium. The size of schizonts was determined in fixed iRBC on Giemsa-stained smears and by imagestream flow cytometry of live iRBCs. For the Giemsa-stained smears, pictures were taken using a Leica microscope (1000x magnification; oil immersion) from randomly chosen fields of 300–400 RBCs, and all schizonts and gametocytes were measured in these fields. The sizes of iRBCs and the parasites were measured by ImageJ by gating on the areas of parasites and iRBC. For imagestream flow cytometry analysis, iRBCs containing schizonts of wt-GFP-Luc_{schiz} and $\Delta pm4\Delta bp2$ -parasites were first enriched by Nycodenz density centrifugation [66]. Purified parasites were then collected in complete RPMI-1640 culture medium and stained with Hoechst-33258 (2 $\mu\text{mol/L}$, Sigma, NL) for 1 hour at room temperature. Cultured, mature schizonts of wt *P. berghei* ANKA (cl15cy1) were used as non-staining control; Hoechst stained cl15cy1 (Hoechst only) and non-stained wt-GFP-Luc_{schiz} (GFP only) were used as single-color controls. The analyses were performed using an Amnis ImageStream X imaging cytometer (Amnis Corp.) and images were analyzed using the IDEAS® image analysis software.

Electron microscopy analysis

For electron microscopy analyses, infected blood was collected from wt or $\Delta pm4\Delta bp2$ parasite infected BALB/c mice by heart puncture. Infected RBCs were enriched by Nycodenz centrifugation [66]. iRBC (10^7 – 10^8) were collected and fixed overnight in 2 mL of 1.5% glutaraldehyde in 0.1 M sodium cacodylate. After centrifugation, the pellet was rinsed twice with 0.1M sodium cacodylate, and postfixed with 1% osmium tetroxide in 0.1 M sodium cacodylate. After rinsing, samples were dehydrated in a graded ethanol series up to 100% and embedded in Epon. 110-nm sections were cut with a microtome and transferred onto standard grids and post-stained with uranyl acetate and lead citrate. Transmission electron microscopy (TEM) data were collected on a FEI Tecnai microscope

at 120 kV with a FEI Eagle CCD camera. Virtual slides [69] consisting of 759 and 729 unbinned 4kx4k images were collected for the WT and $\Delta pm4\Delta bp2$ sample respectively. The magnification at the detector plane was, in both cases, 12930: the pixel size 1.2 nm square. The resulting slides cover an area of $10^9 \times 10^5 \mu\text{m}^2$ and $10^5 \times 10^5 \mu\text{m}^2$ for the respective samples. The virtual slides were analyzed by Aperio ImageScope software (www.aperio.com). All statistical tests were performed using GraphPad Prism.

Quantification of hemozoin in schizonts-iRBC

Hz was quantified in schizonts using different methods. Hz was quantified by measuring the relative light intensity (RLI) of Hz crystals in schizonts by reflection contrast polarized light microscopy [33,70,71]. Schizonts were either collected from overnight *in vitro* blood-stage cultures or directly from tail blood when schizonts were present in the peripheral circulation. For the cultures, infected tail blood (10 μL) with a parasitemia between 0.5 and 1% was cultured overnight in 1mL complete RPMI-1640 culture medium at 37°C under standard conditions for the culture of *P. berghei* blood-stages [35]. Thin blood smears were made from cultured parasites or from tail blood and stained with Hoechst-33342 (2 $\mu\text{mol/L}$, Sigma, NL) for 20 min. Schizonts (8-24 nuclei) were selected on blood smears based on the Hoechst-stained nuclei and pictures were taken with a LeicaDM/RB microscope (1000x magnification, oil RC immersion objective; Leica, Wetzlar, Germany) which was adapted for RCM as described by Cornetese-ten Velde *et al.* [72]. The RLI of Hz crystals in the schizonts was measured using Image J software.

Quantification of hemozoin in organs

To quantify Hz deposition in organs of infected mice, groups of 8 BALB/c mice were i.p. infected with 10^5 wt, $\Delta pm4$ or $\Delta pm4\Delta bp2$ parasites. At different peripheral parasitemias, mice were sacrificed and systemically perfused with 20 mL PBS to remove circulating iRBC from the organs. Livers, spleens and lungs were removed, weighed and stored at -80°C until further analysis. The Hz extraction from these organs and quantification was performed using an optimized method for Hz quantification in tissues as described [36].

Gametocyte and ookinete production

Gametocyte production is defined as the percentage of ring forms developing into mature gametocytes during synchronized infections [35]. Ookinete production was determined in standard *in vitro* fertilization and ookinete maturation assays and is defined as the

percentage of female gametes that develop into mature ookinetes under standardized *in vitro* culture conditions [73]. Female gamete and mature ookinete numbers were determined on Giemsa-stained blood smears made 16–18 hours post-activation.

Measurement of drug-sensitivity of blood-stage parasites

Groups of 5 BALB/c mice were i.p. infected with either 10^4 wt- or 10^5 $\Delta pm4\Delta bp2$ -parasites. At a peripheral parasitemia of 2–5%, mice were treated with artesunate [AS; Pharbaco, Vietnam, 60 mg powder (a kind gift from Dafra Pharma)], chloroquine (CQ; Sigma) or sulfadiazine (SD; Sigma) and peripheral parasitemia was monitored daily by counting Giemsa-stained blood films of tail blood. AS treatment was performed by i.p. injection of 6.25mg/mL in 5% NaHCO_3 as a single dose for 4 consecutive days. CQ and SD were provided in the drinking water for a period of 7 days. CQ was provided at a concentration of 288mg/L with 15g/L glucose [74] and SD at a concentration of 35mg/L [75].

Acknowledgements

We would like to thank Dr. Photini Sinnis for providing us with a *P. berghei bp1* gene-deletion construct, and Guido de Roo for assistance with flow cytometry experiments. Jing-wen Lin is supported by the China Scholarship Council-Leiden University Joint Program and Chris J. Janse by a grant of the European Community's Seventh Framework Programme (FP7/2007–2013) under grant agreement no. 242095.

References

1. Goldberg DE (2005) Hemoglobin degradation. *Curr Top Microbiol Immunol* 295: 275-291.
2. Esposito A, Tiffert T, Mauritz JM, Schlachter S, Bannister LH, *et al.* (2008) FRET imaging of hemoglobin concentration in *Plasmodium falciparum*-infected red cells. *PLoS One* 3: e3780.
3. Sherman IW (1977) Amino acid metabolism and protein synthesis in malarial parasites. *Bull World Health Organ* 55: 265-276.
4. Liu J, Istvan ES, Gluzman IY, Gross J, Goldberg DE (2006) *Plasmodium falciparum* ensures its amino acid supply with multiple acquisition pathways and redundant proteolytic enzyme systems. *Proc Natl Acad Sci U S A* 103: 8840-8845.
5. Divo AA, Geary TG, Davis NL, Jensen JB (1985) Nutritional requirements of *Plasmodium falciparum* in culture. I. Exogenously supplied dialyzable components necessary for continuous growth. *J Protozool* 32: 59-64.
6. Francis SE, Gluzman IY, Oksman A, Knickerbocker A, Mueller R, *et al.* (1994) Molecular characterization and inhibition of a *Plasmodium falciparum* aspartic hemoglobinase. *EMBO J* 13: 306-317.
7. Babbitt SE, Altenhofen L, Cobbold SA, Istvan ES, Fennell C, *et al.* (2012) *Plasmodium falciparum* responds to amino acid starvation by entering into a hibernatory state. *Proc Natl Acad Sci U S A* 109: E3278-3287.
8. Elliott DA, McIntosh MT, Hosgood HD, 3rd, Chen S, Zhang G, *et al.* (2008) Four distinct pathways of hemoglobin uptake in the malaria parasite *Plasmodium falciparum*. *Proc Natl Acad Sci U S A* 105: 2463-2468.
9. Francis SE, Sullivan DJ, Jr., Goldberg DE (1997) Hemoglobin metabolism in the malaria parasite *Plasmodium falciparum*. *Annu Rev Microbiol* 51: 97-123.
10. Goldberg DE, Slater AF, Beavis R, Chait B, Cerami A, *et al.* (1991) Hemoglobin degradation in the human malaria pathogen *Plasmodium falciparum*: a catabolic pathway initiated by a specific aspartic protease. *J Exp Med* 173: 961-969.
11. Gluzman IY, Francis SE, Oksman A, Smith CE, Duffin KL, *et al.* (1994) Order and specificity of the *Plasmodium falciparum* hemoglobin degradation pathway. *J Clin Invest* 93: 1602-1608.
12. Wyatt DM, Berry C (2002) Activity and inhibition of plasmepsin IV, a new aspartic proteinase from the malaria parasite, *Plasmodium falciparum*. *FEBS Lett* 513: 159-162.
13. Banerjee R, Liu J, Beatty W, Pelosof L, Klemba M, *et al.* (2002) Four plasmepsins are active in the *Plasmodium falciparum* food vacuole, including a protease with an active-site histidine. *Proc Natl Acad Sci U S A* 99: 990-995.
14. Subramanian S, Hardt M, Choe Y, Niles RK, Johansen EB, *et al.* (2009) Hemoglobin cleavage site-specificity of the *Plasmodium falciparum* cysteine proteases falcipain-2 and falcipain-3. *PLoS One* 4: e5156.
15. Sijwali PS, Rosenthal PJ (2004) Gene disruption confirms a critical role for the cysteine protease falcipain-2 in hemoglobin hydrolysis by *Plasmodium falciparum*. *Proc Natl Acad Sci U S A* 101: 4384-4389.
16. Bonilla JA, Bonilla TD, Yowell CA, Fujioka H, Dame JB (2007) Critical roles for the digestive vacuole plasmepsins of *Plasmodium falciparum* in vacuolar function. *Mol Microbiol* 65: 64-75.

17. Omara-Opyene AL, Moura PA, Sulsona CR, Bonilla JA, Yowell CA, *et al.* (2004) Genetic disruption of the *Plasmodium falciparum* digestive vacuole plasmepsins demonstrates their functional redundancy. *J Biol Chem* 279: 54088-54096.
18. Spaccapelo R, Aime E, Caterbi S, Arcidiacono P, Capuccini B, *et al.* (2011) Disruption of plasmepsin-4 and merozoites surface protein-7 genes in *Plasmodium berghei* induces combined virulence-attenuated phenotype. *Sci Rep* 1: 39.
19. Baird JK (2004) Chloroquine resistance in *Plasmodium vivax*. *Antimicrob Agents Chemother* 48: 4075-4083.
20. Baird KJ, Maguire JD, Price RN (2012) Diagnosis and treatment of *Plasmodium vivax* malaria. *Adv Parasitol* 80: 203-270.
21. Singh A, Walker KJ, Sijwali PS, Lau AL, Rosenthal PJ (2007) A chimeric cysteine protease of *Plasmodium berghei* engineered to resemble the *Plasmodium falciparum* protease falcipain-2. *Protein Eng Des Sel* 20: 171-177.
22. Ponpuak M, Klemba M, Park M, Gluzman IY, Lamppa GK, *et al.* (2007) A role for falcilysin in transit peptide degradation in the *Plasmodium falciparum* apicoplast. *Mol Microbiol* 63: 314-334.
23. Klemba M, Gluzman I, Goldberg DE (2004) A *Plasmodium falciparum* dipeptidyl aminopeptidase I participates in vacuolar hemoglobin degradation. *J Biol Chem* 279: 43000-43007.
24. Ragheb D, Bompiani K, Dalal S, Klemba M (2009) Evidence for catalytic roles for *Plasmodium falciparum* aminopeptidase P in the food vacuole and cytosol. *J Biol Chem* 284: 24806-24815.
25. Dalal S, Klemba M (2007) Roles for two aminopeptidases in vacuolar hemoglobin catabolism in *Plasmodium falciparum*. *J Biol Chem* 282: 35978-35987.
26. Ragheb D, Dalal S, Bompiani KM, Ray WK, Klemba M (2011) Distribution and biochemical properties of an M1-family aminopeptidase in *Plasmodium falciparum* indicate a role in vacuolar hemoglobin catabolism. *J Biol Chem* 286: 27255-27265.
27. Stack CM, Lowther J, Cunningham E, Donnelly S, Gardiner DL, *et al.* (2007) Characterization of the *Plasmodium falciparum* M17 leucyl aminopeptidase. A protease involved in amino acid regulation with potential for antimalarial drug development. *J Biol Chem* 282: 2069-2080.
28. Jani D, Nagarkatti R, Beatty W, Angel R, Slebodnick C, *et al.* (2008) HDP-a novel heme detoxification protein from the malaria parasite. *PLoS Pathog* 4: e1000053.
29. Sijwali PS, Koo J, Singh N, Rosenthal PJ (2006) Gene disruptions demonstrate independent roles for the four falcipain cysteine proteases of *Plasmodium falciparum*. *Mol Biochem Parasitol* 150: 96-106.
30. Sijwali PS, Kato K, Seydel KB, Gut J, Lehman J, *et al.* (2004) *Plasmodium falciparum* cysteine protease falcipain-1 is not essential in erythrocytic stage malaria parasites. *Proc Natl Acad Sci U S A* 101: 8721-8726.
31. Kumar A, Kumar K, Korde R, Puri SK, Malhotra P, *et al.* (2007) Falcipain-1, a *Plasmodium falciparum* cysteine protease with vaccine potential. *Infect Immun* 75: 2026-2034.
32. Arastu-Kapur S, Ponder EL, Fonovic UP, Yeoh S, Yuan F, *et al.* (2008) Identification of proteases that regulate erythrocyte rupture by the malaria parasite *Plasmodium falciparum*. *Nat Chem Biol* 4: 203-213.
33. Maude RJ, Buapetch W, Silamut K (2009) A simplified, low-cost method for polarized light microscopy. *Am J Trop Med Hyg* 81: 782-783.
34. Lawrence C, Olson JA (1986) Birefringent hemozoin identifies malaria. *Am J Clin Pathol* 86: 360-363.
35. Janse CJ, Waters AP (1995) *Plasmodium berghei*: the application of cultivation and purification techniques to molecular studies of malaria parasites. *Parasitol Today* 11: 138-143.
36. Deroost K, Lays N, Noppen S, Martens E, Opendakker G, *et al.* (2012) Improved methods for haemozoin quantification in tissues yield organ- and parasite-specific information in malaria-infected mice. *Malar J* 11: 166.
37. Egan TJ, Koch KR, Swan PL, Clarkson C, Van Schalkwyk DA, *et al.* (2004) *In vitro* antimalarial activity of a series of cationic 2,2'-bipyridyl- and 1,10-phenanthrolineplatinum(II) benzoylthiourea complexes. *J Med Chem* 47: 2926-2934.
38. Klonis N, Crespo-Ortiz MP, Bottova I, Abu-Bakar N, Kenny S, *et al.* (2011) Artemisinin activity against *Plasmodium falciparum* requires hemoglobin uptake and digestion. *Proc Natl Acad Sci U S A* 108: 11405-11410.
39. Kinnamon KE, Ager AL, Orchard RW (1976) *Plasmodium berghei*: combining folic acid antagonists for potentiation against malaria infections in mice. *Exp Parasitol* 40: 95-102.

40. Tilley L, Dixon MW, Kirk K (2011) The *Plasmodium falciparum*-infected red blood cell. *Int J Biochem Cell Biol* 43: 839-842.
41. Lew VL, Tiffert T, Ginsburg H (2003) Excess hemoglobin digestion and the osmotic stability of *Plasmodium falciparum*-infected red blood cells. *Blood* 101: 4189-4194.
42. Krugliak M, Zhang J, Ginsburg H (2002) Intraerythrocytic *Plasmodium falciparum* utilizes only a fraction of the amino acids derived from the digestion of host cell cytosol for the biosynthesis of its proteins. *Mol Biochem Parasitol* 119: 249-256.
43. Ginsburg H (1990) Some reflections concerning host erythrocyte-malarial parasite interrelationships. *Blood Cells* 16: 225-235.
44. Koury MJ, Koury ST, Kopsombut P, Bondurant MC (2005) *In vitro* maturation of nascent reticulocytes to erythrocytes. *Blood* 105: 2168-2174.
45. Allen DW (1960) Amino acid accumulation by human reticulocytes. *Blood* 16: 1564-1571.
46. Vaid A, Ranjan R, Smythe WA, Hoppe HC, Sharma P (2010) Pfl3K, a phosphatidylinositol-3 kinase from *Plasmodium falciparum*, is exported to the host erythrocyte and is involved in hemoglobin trafficking. *Blood* 115: 2500-2507.
47. Fitch CD, Cai GZ, Chen YF, Ryerse JS (2003) Relationship of chloroquine-induced redistribution of a neutral aminopeptidase to hemoglobin accumulation in malaria parasites. *Arch Biochem Biophys* 410: 296-306.
48. Greenbaum DC, Baruch A, Grainger M, Bozdech Z, Medzihradsky KF, et al. (2002) A role for the protease falcipain 1 in host cell invasion by the human malaria parasite. *Science* 298: 2002-2006.
49. Drew ME, Banerjee R, Uffman EW, Gilbertson S, Rosenthal PJ, et al. (2008) *Plasmodium* food vacuole plasmepsins are activated by falcipains. *J Biol Chem* 283: 12870-12876.
50. Rosenthal PJ, McKerrow JH, Aikawa M, Nagasawa H, Leech JH (1988) A malarial cysteine proteinase is necessary for hemoglobin degradation by *Plasmodium falciparum*. *J Clin Invest* 82: 1560-1566.
51. Chugh M, Sundararaman V, Kumar S, Reddy VS, Siddiqui WA, et al. (2013) Protein complex directs hemoglobin-to-hemozoin formation in *Plasmodium falciparum*. *Proc Natl Acad Sci U S A* 110: 5392-5397.
52. Fitch CD (1986) Antimalarial schizontocides: ferriprotoporphyrin IX interaction hypothesis. *Parasitol Today* 2: 330-331.
53. Platel DF, Mangou F, Tribouley-Duret J (1999) Role of glutathione in the detoxification of ferriprotoporphyrin IX in chloroquine resistant *Plasmodium berghei*. *Mol Biochem Parasitol* 98: 215-223.
54. Peters W (1968) The chemotherapy of rodent malaria. VII. The action of some sulphonamides alone or with folic reductase inhibitors against malaria vectors and parasites, 2: schizontocidal action in the albino mouse. *Annu Rev Pharmacol* 64: 488-494.
55. Peters W (1968) The chemotherapy of rodent malaria. V. Dynamics of drug resistance. I. Methods for studying the acquisition and loss of resistance to chloroquine by *Plasmodium berghei*. *Ann Trop Med Parasitol* 62: 277 -287.
56. Fidock M, DeSilva B (2012) Bioanalysis of biomarkers for drug development. *Bioanalysis* 4: 2425-2426.
57. Eastman RT, Fidock DA (2009) Artemisinin-based combination therapies: a vital tool in efforts to eliminate malaria. *Nat Rev Microbiol* 7: 864-874.
58. Olliaro PL, Haynes RK, Meunier B, Yuthavong Y (2001) Possible modes of action of the artemisinin-type compounds. *Trends Parasitol* 17: 122-126.
59. Suwanarusk R, Russell B, Chavchich M, Chalfein F, Kenangalem E, et al. (2007) Chloroquine resistant *Plasmodium vivax*: *in vitro* characterisation and association with molecular polymorphisms. *PLoS One* 2: e1089.
60. Hasugian AR, Tjitra E, Ratcliff A, Siswantoro H, Kenangalem E, et al. (2009) *In vivo* and *in vitro* efficacy of amodiaquine monotherapy for treatment of infection by chloroquine-resistant *Plasmodium vivax*. *Antimicrob Agents Chemother* 53: 1094-1099.
61. Hasugian AR, Purba HL, Kenangalem E, Wuwung RM, Ebsworth EP, et al. (2007) Dihydroartemisinin-piperaquine versus artesunate-amodiaquine: superior efficacy and posttreatment prophylaxis against multidrug-resistant *Plasmodium falciparum* and *Plasmodium vivax* malaria. *Clin Infect Dis* 44: 1067-1074.
62. Russell B, Chalfein F, Prasetyorini B, Kenangalem E, Piera K, et al. (2008) Determinants of *in vitro* drug susceptibility testing of *Plasmodium vivax*. *Antimicrob Agents Chemother* 52: 1040-1045.

63. Ecker A, Lehane AM, Clain J, Fidock DA (2012) PfCRT and its role in antimalarial drug resistance. *Trends Parasitol* 28: 504-514.
64. Braks JA, Franke-Fayard B, Kroeze H, Janse CJ, Waters AP (2006) Development and application of a positive-negative selectable marker system for use in reverse genetics in *Plasmodium*. *Nucleic Acids Res* 34: e39.
65. Lin JW, Annoura T, Sajid M, Chevalley-Maurel S, Ramesar J, *et al.* (2011) A novel 'gene insertion/marker out' (GIMO) method for transgene expression and gene complementation in rodent malaria parasites. *PLoS One* 6: e29289.
66. Janse CJ, Ramesar J, Waters AP (2006) High-efficiency transfection and drug selection of genetically transformed blood stages of the rodent malaria parasite *Plasmodium berghei*. *Nat Protoc* 1: 346-356.
67. van Spaendonk RM, Ramesar J, van Wigcheren A, Eling W, Beetsma AL, *et al.* (2001) Functional equivalence of structurally distinct ribosomes in the malaria parasite, *Plasmodium berghei*. *J Biol Chem* 276: 22638-22647.
68. Janse CJ, Haghparast A, Speranca MA, Ramesar J, Kroeze H, *et al.* (2003) Malaria parasites lacking eef1a have a normal S/M phase yet grow more slowly due to a longer G1 phase. *Mol Microbiol* 50: 1539-1551.
69. Faas FG, Avramut MC, van den Berg BM, Mommaas AM, Koster AJ, *et al.* (2012) Virtual nanoscopy: generation of ultra-large high resolution electron microscopy maps. *J Cell Biol* 198: 457-469.
70. Prins FA, van Diemen-Steenvoorde R, Bonnet J, Cornelese-ten Velde I (1993) Reflection contrast microscopy of ultrathin sections in immunocytochemical localization studies: a versatile technique bridging electron microscopy with light microscopy. *Histochemistry* 99: 417-425.
71. Prins FA, Velde IC, de Heer E (2006) Reflection contrast microscopy: The bridge between light and electron microscopy. *Methods Mol Biol* 319: 363-401.
72. Cornelese-ten Velde I, Bonnet J, Tanke HJ, Ploem JS (1988) Reflection contrast microscopy. Visualization of (peroxidase-generated) diaminobenzidine polymer products and its underlying optical phenomena. *Histochemistry* 89: 141-150.
73. van Dijk MR, Janse CJ, Thompson J, Waters AP, Braks JA, *et al.* (2001) A central role for P48/45 in malaria parasite male gamete fertility. *Cell* 104: 153-164.
74. Lewis MD, Pfeil J, Mueller AK (2011) Continuous oral chloroquine as a novel route for *Plasmodium* prophylaxis and cure in experimental murine models. *BMC Res Notes* 4: 262.
75. Beetsma AL, van de Wiel TJ, Sauerwein RW, Eling WM (1998) *Plasmodium berghei* ANKA: purification of large numbers of infectious gametocytes. *Exp Parasitol* 88: 69-72.
76. Liu J, Gluzman IY, Drew ME, Goldberg DE (2005) The role of *Plasmodium falciparum* food vacuole plasmepsins. *J Biol Chem* 280: 1432-1437.
77. Bonilla JA, Moura PA, Bonilla TD, Yowell CA, Fidock DA, *et al.* (2007) Effects on growth, hemoglobin metabolism and paralogous gene expression resulting from disruption of genes encoding the digestive vacuole plasmepsins of *Plasmodium falciparum*. *Int J Parasitol* 37: 317-327.
78. Klemba M, Beatty W, Gluzman I, Goldberg DE (2004) Trafficking of plasmepsin II to the food vacuole of the malaria parasite *Plasmodium falciparum*. *J Cell Biol* 164: 47-56.
79. Dahl EL, Rosenthal PJ (2005) Biosynthesis, localization, and processing of falcipain cysteine proteases of *Plasmodium falciparum*. *Mol Biochem Parasitol* 139: 205-212.
80. Dasaradhi PV, Korde R, Thompson JK, Tanwar C, Nag TC, *et al.* (2007) Food vacuole targeting and trafficking of falcipain-2, an important cysteine protease of human malaria parasite *Plasmodium falciparum*. *Mol Biochem Parasitol* 156: 12-23.
81. Rosenthal PJ (2011) Falcipains and other cysteine proteases of malaria parasites. *Adv Exp Med Biol* 712: 30-48.
82. Lamarque M, Tastet C, Poncet J, Demettré E, Jouin P, *et al.* (2008) Food vacuole proteome of the malarial parasite *Plasmodium falciparum*. *Proteomics Clin Appl* 2: 1361-1374.

Supplementary Material

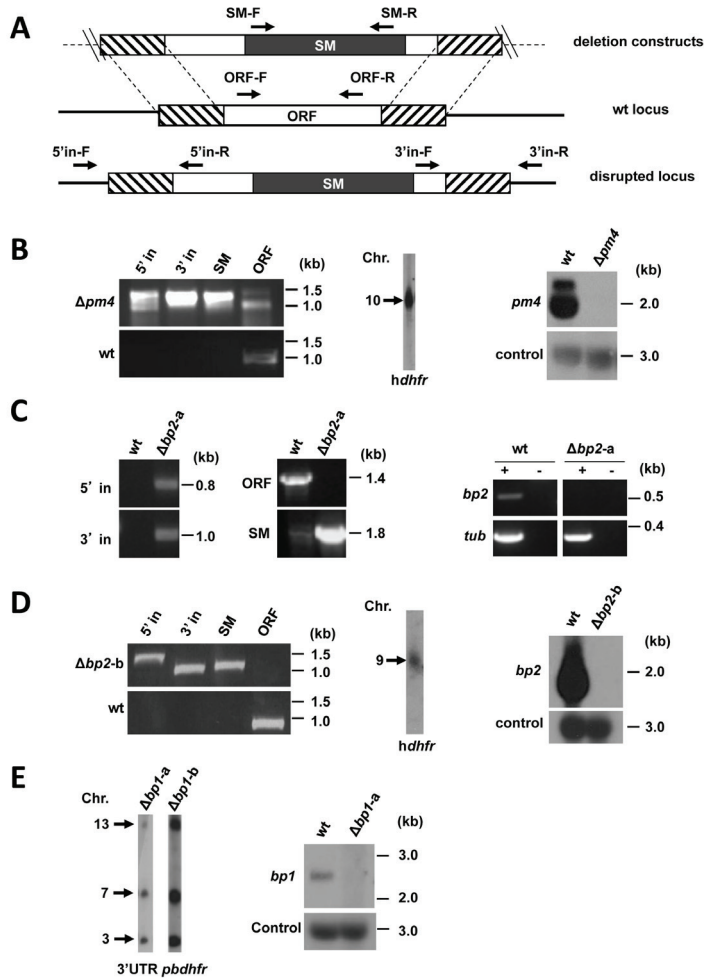


Figure S1. Generation of the *P. berghei* mutants $\Delta pm4$, $\Delta bp1$ and $\Delta bp2$.

A. Schematic representation of gene-deletion constructs targeting the open reading frame (ORF) of genes expressing plasmepsin 4 (*pm4*), berghepains 2 (*bp2*) or berghepains 1 (*bp1*) by double cross-over homologous recombination, and wild-type (wt) gene loci before and after disruption. The constructs contain a drug-selectable marker cassette (SM; black box) and gene target regions (hatched boxes). See Table S2 for primer sequences used to amplify the target regions. Primer positions (arrows) for diagnostic PCRs are shown (see Table S3 for primer sequences and expected product sizes).

B. Diagnostic PCR (left) and Southern analysis of pulsed field gel-separated chromosomes (center) confirm correct disruption of *pm4* in mutant $\Delta pm4$ -b. Northern analysis of blood-stage mRNA (right) confirms the absence of *pm4* transcripts in the $\Delta pm4$ -b mutant. The following primers were used for diagnostic PCRs: 5' integration (5' in): L5516/L4096; 3' integration: (3' in) L1662/L5517; SM (*hdhfr::yfcu*): L4698/L4699; *pm4* ORF: L5518/L5519. Separated chromosomes were hybridized using an *hdhfr* probe that recognizes the DNA-construct integrated into the *pm4* locus on chromosome 10. Northern blot was hybridized using a PCR probe

recognizing the *pm4* ORF (primers L5518/L5519) and with an oligonucleotide probe L644R recognizing the large subunit rRNA (as loading control).

C. Diagnostic PCR (left) confirms the correct deletion of the *bp2* gene in mutant $\Delta bp2$ -a. RT-PCR analysis of blood stage mRNA (right) shows the absence of *bp2* transcription in $\Delta bp2$ -a blood-stages. The following primer pairs were used for diagnostic PCR analyses: 5' in, RS835/RS32; 3' in, RS110/RS836; SM (*tgdhfr/ts*), RS404/RS405; *bp2* ORF, RS514/RS515. For RT-PCR the following primers were used: tub (*tubulin*), RS782/RS783 and *bp2*, RS515/RS516.

D. Diagnostic PCR (left) and Southern analysis of pulsed field gel-separated chromosomes (center) confirm the correct disruption of the *bp2* gene in mutant $\Delta bp2$ -b. Northern blot analysis of blood stage mRNA (right) confirms the absence of *bp2* transcripts in $\Delta bp2$ -b. The following primers were used for diagnostic PCRs: 5' in, L5024/L3211; 3' in, L5025/L1662; SM (*hdhfr::yfcu*), L4698/L4699; *bp2* ORF, L5026/L5027. Separated chromosomes were hybridized using an *hdhfr* probe that recognizes the DNA-construct integrated into the *bp2* locus on chromosome 9. Northern blot was hybridized using a PCR probe recognizing the *bp2* ORF (primers L5026/L5027) and with an oligonucleotide probe L644R recognizing the large subunit rRNA (as loading control).

E. Southern analysis of pulsed field gel-separated chromosomes (left) confirms the correct disruption of *bp1* in mutant $\Delta bp1$ -a and $\Delta bp1$ -b. Northern analysis of blood-stage mRNA (right) confirms the absence of *bp1* transcripts in mutant $\Delta bp1$ -a. Separated chromosomes were hybridized using an 3'UTR *pbdhfr* probe that recognizes the DNA-construct integrated into the *bp1* locus on chromosome 13, the endogenous *dhfr/ts* on chromosome 7 and the GFP-luciferase reporter cassette in the *230p* locus on chromosome 3. Northern blot was hybridized using a PCR probe recognizing the *bp1* ORF (primers L7422/L7423) and with an oligonucleotide probe L644R recognizing the large subunit rRNA (as loading control). See Table S3 for primers used for generation of probes.

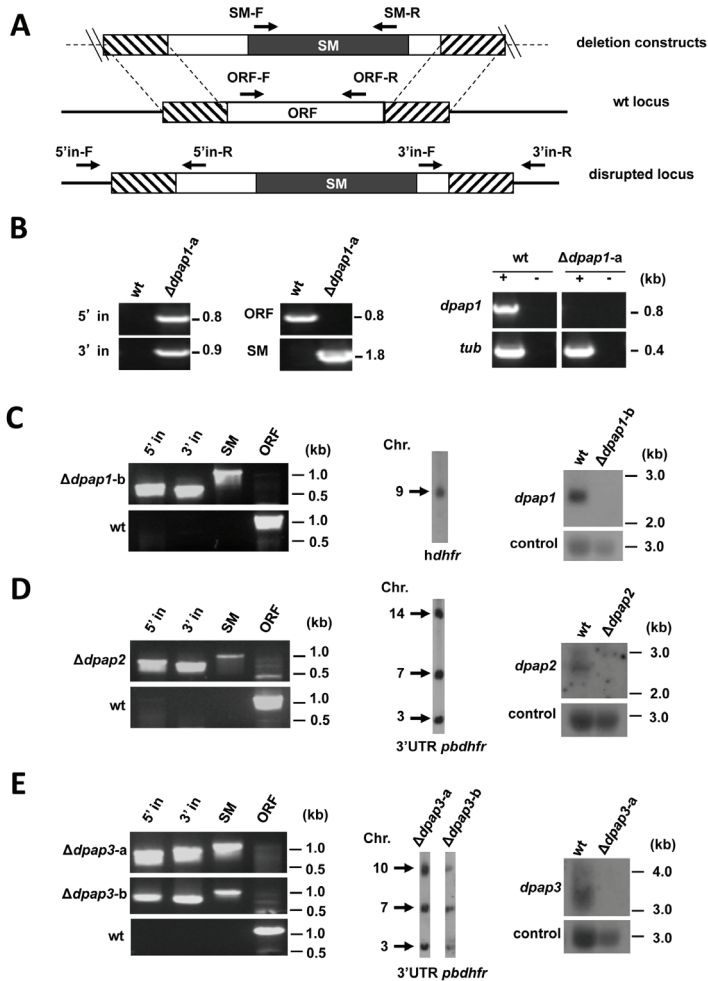


Figure S2. Generation of the *P. berghei* mutants $\Delta dpap1$, $\Delta dpap2$ and $\Delta dpap3$.

A. Schematic representation of the gene-deletion constructs targeting the ORF of genes expressing dipeptidyl peptidases 1-3 (*dpap1-3*) by double cross-over homologous recombination and the wt gene loci before and after disruption. The constructs contain a drug-selectable marker cassette (SM; black box) and gene target regions (hatched boxes). See Table S2 for primer sequences used to amplify the target regions. Primer positions (arrows) for diagnostic PCRs are shown (see Table S3 for primer sequences and expected product sizes).

B. Diagnostic PCR (left, center) and RT-PCR (right) analysis confirm correct disruption of *dpap1* in $\Delta dpap1-a$. For diagnostic PCRs, the following primers were used: 5' in, RS672/RS32; 3' in, RS110/RS673; SM (*tgdhfr/ts*), RS404/RS405; *dpap1* ORF, RS582/RS583. For RT-PCR the following primers were used: *tub* (*tubulin*), RS782/RS783 and *dpap1*, RS582/RS583.

C. Diagnostic PCR (left) and Southern analysis of pulsed field gel-separated (center) confirm correct disruption of *dpap1* in $\Delta dpap1-b$. Northern analysis of blood-stage mRNA (right) confirms the absence of *dpap1* transcripts in the $\Delta dpap1-b$ mutant. The following primers were used for diagnostic PCRs: 5' integration (5' in), L6204/L4770; 3' integration (3' in), L4771/L6205; SM (*hdhfr::yfcu*), L4698/L4699; *dpap1* ORF, L6206/L6207. For Southern analysis, separated chromosomes were hybridized using an *hdhfr* probe that recognizes the construct integrated into the *dpap1* locus on chromosome 9. Northern blot was hybridized using a PCR probe recognizing

the *dpap1* ORF (primers L6206/L6207). As a loading control, hybridization was performed with oligonucleotide probe L644R that recognizes the large subunit rRNA.

D. Diagnostic PCR (left) and Southern analysis of pulsed field gel-separated chromosomes (center) confirms correct disruption of *dpap2* in mutant $\Delta dpap2$. Northern analysis of blood-stage mRNA (right) confirms the absence of *dpap2* transcripts in the $\Delta dpap2$ mutant. The following primers were used for diagnostic PCRs: 5' in, L6935/L4770; 3' in, L4771/L6936; SM (*hdhfr::yfcu*), L4698/L4699; *dpap2* ORF, L6937/L6938. Separated chromosomes were hybridized using a 3'UTR *pbdhfr* probe that recognizes the construct integrated into *dpap2* on chromosome 14, the endogenous *dhfr/ts* on chromosome 7 and the GFP-luciferase reporter cassette in the *230p* locus on chromosome 3. Northern blot was hybridized using a PCR probe recognizing the *dpap2* ORF (primers L6937/L6938) and with an oligonucleotide probe L644R recognizing the large subunit rRNA (as loading control).

E. Diagnostic PCR (left) and Southern analysis of pulsed field gel-separated chromosomes (center) confirm correct disruption of *dpap3* in $\Delta dpap3$ -a and $\Delta dpap3$ -b. Northern analysis of blood-stage mRNA (right) confirms the absence of *dpap3* transcripts. The following primers were used for diagnostic PCRs: 5' in, L6941/L4770; 3' in, L4771/L6942; SM (*hdhfr::yfcu*), L4698/L4699; *dpap3* ORF, L6943/L6944. Separated chromosomes were hybridized using a 3'UTR *pbdhfr* probe that recognizes the construct integrated into *dpap3* on chromosome 10, the endogenous *dhfr/ts* on chromosome 7 and the GFP-luciferase reporter cassette in the *230p* locus on chromosome 3. Northern blot was hybridized using a PCR probe recognizing the *dpap3* ORF (primers L6943/L6944) and with an oligonucleotide probe L644R recognizing the large subunit rRNA (as loading control). See Table S3 for primers used for generation of probes.

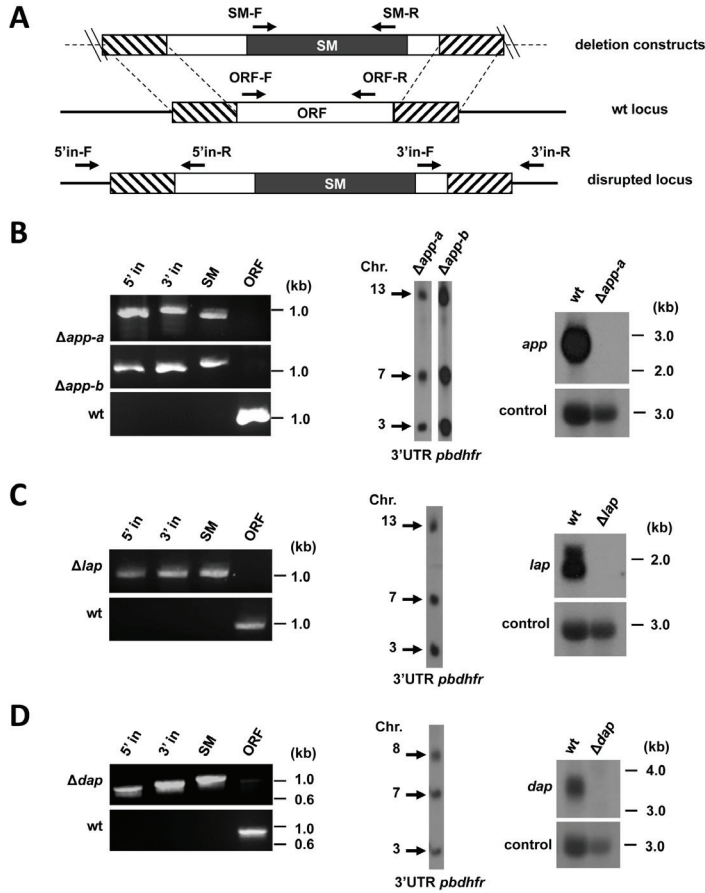


Figure S3. Generation of *P. berghei* mutants Δapp , Δlap and Δdap .

A. Schematic representation of the gene-deletion constructs targeting the ORF of genes expressing aminopeptidase P (*app*), leucyl aminopeptidase (*lap*) and aspartyl aminopeptidase (*dap*) by double cross-over homologous recombination and the wt gene loci before and after disruption. The constructs contain a drug-selectable marker cassette (SM; black box) and gene target regions (hatched boxes). See Table S2 for primer sequences used to amplify the target regions. Primer positions (arrows) for diagnostic PCRs are shown (see Table S3 for primer sequences and expected product sizes).

B. Diagnostic PCR (left) and Southern analysis of pulsed field gel-separated chromosomes (center) confirm correct disruption of *app* in $\Delta app-a$ and $\Delta app-b$. Northern analysis of blood-stage mRNA (right) confirms the absence of the *app* transcripts in the Δapp mutants. The following primers were used for diagnostic PCRs: 5' integration (5' in): L7107/L4770; 3' integration (3' in): L4771/L7108; SM (*dhfr::yfcu1*): L4698/L4699; *app* ORF: L7109/L7110. Separated chromosomes of $\Delta app-a$ and $\Delta app-b$ were hybridized using a 3'UTR *pbdhfr* probe that recognizes the construct integrated into the *app* locus on chromosome 13, the endogenous *dhfr/ts* on chromosome 7 and the GFP-luciferase reporter cassette in the *230p* locus on chromosome 3. Northern blot was hybridized using a PCR probe recognizing the *app* ORF (primers L7109/L7110) and with an oligonucleotide probe L644R recognizing the large subunit rRNA (as loading control).

C. Diagnostic PCR (left) and Southern analysis of separated chromosomes (center) confirm correct disruption of *lap* in mutant Δlap . Northern analysis of blood-stage mRNA (right) confirms the absence of *lap* transcripts in

the Δlap mutant. The following primers were used for diagnostic PCRs: 5' in, L6967/L4770; 3' in, L4771/L6968; SM (*hdfhr::yfcu*), L4698/L4699; *lap* ORF, L6969/L6970. Separated chromosomes were hybridized using a 3'UTR *pbdhfr* probe that recognizes the construct integrated into *lap* on chromosome 13, the endogenous *dhfr/ts* on chromosome 7 and the GFP-luciferase reporter cassette in the *230p* locus on chromosome 3. Northern blot was hybridized using a PCR probe recognizing *lap* ORF (primers L6969/L6970) and with an oligonucleotide probe L644R recognizing the large subunit rRNA (as loading control).

D. Diagnostic PCR (left) and Southern analysis of pulsed field gel-separated chromosomes (center) confirm correct disruption of *dap* in Δdap . Northern analysis of blood-stage mRNA (right) confirms the absence of the *dap* transcripts in the Δdap mutant. The following primers were used for diagnostic PCRs: 5' in, L6975/L4770; 3' in, L4771/L6976; SM (*hdfhr::yfcu*), L4698/L4699; *dap* ORF, L6977/L6978. Separated chromosomes were hybridized using a 3'UTR *pbdhfr* probe that recognizes the construct integrated into *dap* on chromosome 8, the endogenous *dhfr/ts* on chromosome 7 and the GFP-luciferase reporter cassette in the *230p* locus on chromosome 3. For Northern blot was hybridized using a PCR probe recognizing *dap* ORF (primers L6977/L6978) and with an oligonucleotide probe L644R recognizing the large subunit rRNA (as loading control). See Table S3 for primers used for generation of probes.

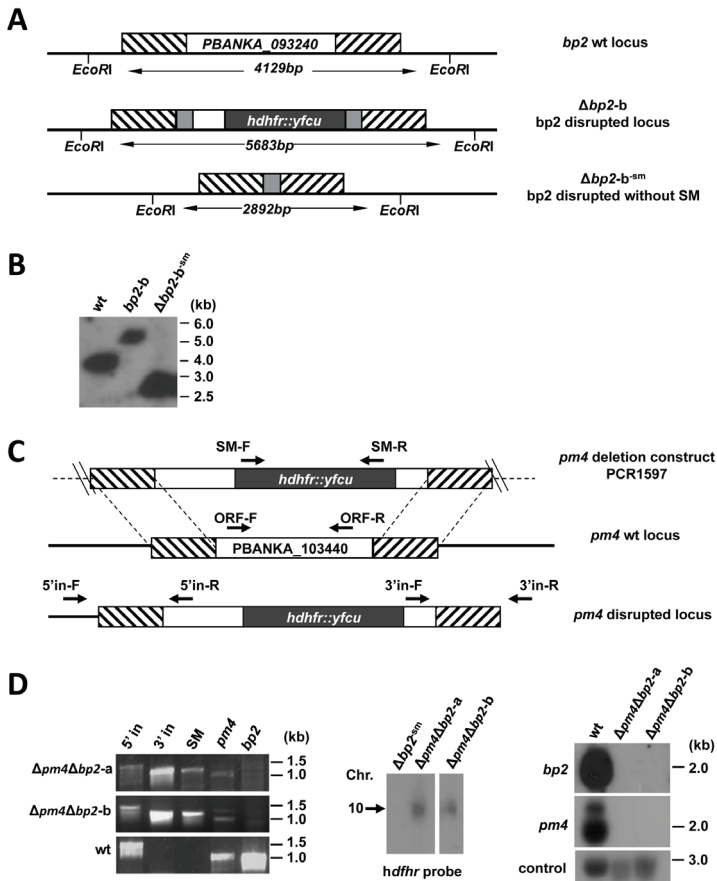


Figure S4. Generation of two independent *P. berghei* $\Delta pm4\Delta bp2$ mutants

A. Schematic representation of the wt berghepain 2 (*bp2*) gene locus, the disrupted *bp2* locus in mutant

deletion $\Delta bp2$ -b and the locus of $\Delta bp2$ -bsm. In the $\Delta bp2$ -bsm the drug selectable marker (SM, black) has been removed by negative selection using 5-FC. Construct pL1602, used to generate mutant $\Delta bp2$ -b, targets *bp2* by double cross-over homologous recombination at the target regions (hatched boxes) and contains a positive-negative SM (*hdhfr::yfcu*) flanked on both sides by 3' *pbdhfr* sequences (grey boxes). The application of negative selection (5-FC) on $\Delta bp2$ -b parasites permits the selection of $\Delta bp2$ -bsm parasites without the SM that has been excised from the genome as a result of a recombination event between the two 3' *pbdhfr* sequences. Restriction sites and size of the expected fragments in Southern analysis (see B) are shown.

B. Southern analysis of *EcoRI* digested DNA of wt, $\Delta bp2$ -b and $\Delta bp2$ -bsm parasites, confirming correct integration of construct pL1602 in $\Delta bp2$ -b and the subsequent removal of the SM cassette in $\Delta bp2$ -bsm after negative selection (see A for the expected sizes of the *EcoRI* fragments). Hybridization was performed using a probe recognizing 3' UTR of *bp2* (primers L5460/L5461).

C. Schematic representation of the gene-deletion construct targeting the ORF of plasmepsin 4 (*pm4*) by double cross-over homologous recombination and the wt gene locus before and after disruption. The constructs contain a drug-selectable marker cassette (SM; black box) and gene target regions (hatched boxes). See Table S2 for primer sequences used to amplify the target regions. Primer positions (arrows) for diagnostic PCRs are shown. See Table S3 for primer sequences and expected product sizes.

D. Diagnostic PCR (left) and Southern analysis of separated chromosomes (center) confirm correct disruption of *pm4* and *bp2* in $\Delta pm4\Delta bp2$ -a and $\Delta pm4\Delta bp2$ -b. Northern analysis of blood-stage mRNA (right) confirms the absence of transcripts of *pm4* and *bp2* in the mutants. The following primers were used for diagnostic PCRs: 5' integration (5' in): L5516/L4096; 3' integration (3' in): L1662/L5517; SM (*hdhfr::yfcu*): L4698/L4699; *pm4* ORF: L5518/L5519; *bp2* ORF: L5026/L5027. Separated chromosomes were hybridized using an *hdhfr* probe that recognizes the construct integrated into *pm4* on chromosome 10. Northern blots were hybridized using a PCR probe recognizing the *bp2* ORF (primers L5026/L5027) or the *pm4* ORF (primers L5518/L5519) and with an oligonucleotide probe L644R recognizing the large subunit rRNA (as loading control). See Table S3 for primers used for generation of the probes.

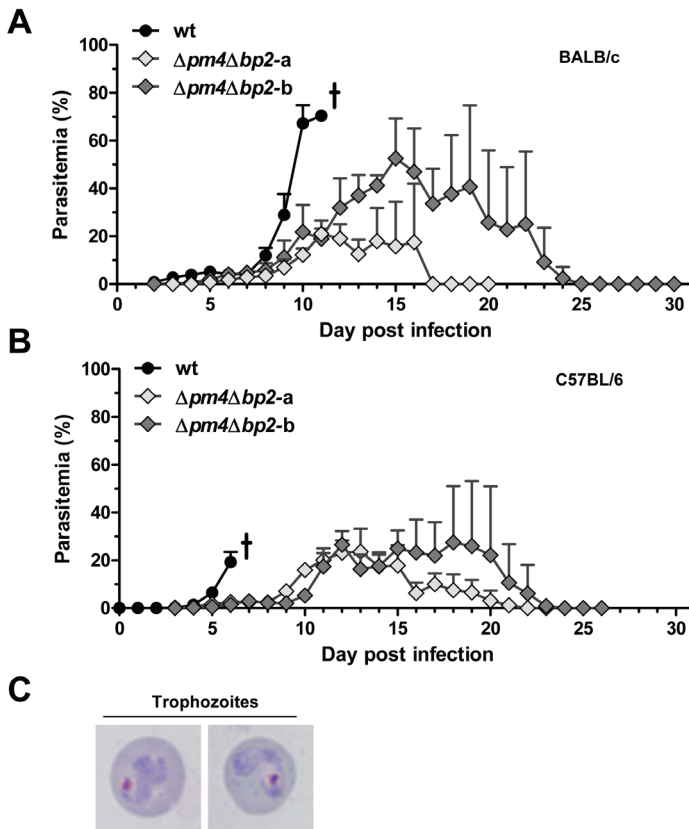


Figure S5. $\Delta pm4\Delta bp2$ parasites cause self-resolving blood infections in both C57BL/6 and BALB/c mice

A. Course of parasitemia in BALB/c mice. Mice (n=6) were intraperitoneally (i.p) infected with 10^5 wt, 10^5 $\Delta pm4\Delta bp2-a$ or 10^6 $\Delta pm4\Delta bp2-b$ parasites. Wt-infected mice developed hyperparasitemia and severe anemia in the second week post infection (p.i) and were sacrificed on day 10-11 p.i. Mice infected with $\Delta pm4\Delta bp2$ -parasites resolved infections resulting in undetectable parasitemia by microscopic analysis between day 17 and 25 after infection.

B. Course of parasitemia in C57BL/6 mice. Mice (n=6) were i.p infected with 10^5 wt, 10^5 $\Delta pm4\Delta bp2-a$ or 10^6 $\Delta pm4\Delta bp2-b$ parasites. All wt-infected mice developed cerebral complications at day 6 after infection, whereas none of the mice infected with $\Delta pm4\Delta bp2-a$ or $\Delta pm4\Delta bp2-b$ parasites developed ECM. Mice infected with $\Delta pm4\Delta bp2$ parasites resolved infections resulting in undetectable parasitemia by microscopic analysis between day 22 and 24 after infection.

C. Trophozoites of $\Delta pm4\Delta bp2$ -parasites on Giemsa-stained blood smears showing translucent vesicles in the cytoplasm and the absence of hemozoin pigment.

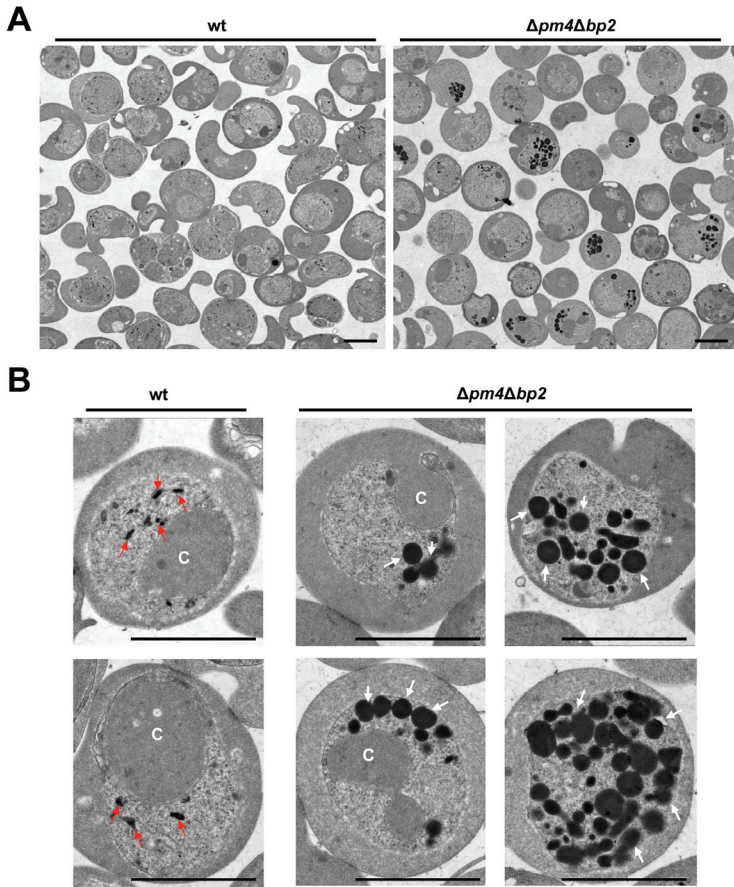


Figure S6. Ultrastructural analysis of wt- and $\Delta pm4\Delta bp2$ -trophozoites

A. Electron micrographs of red blood cells infected with wt- or $\Delta pm4\Delta bp2$ -trophozoites showing differences in the number, morphology and electron-dense staining of intracellular vesicles within their cytoplasm. Scale bars, 5 μm .

B. Hz crystals (red arrow heads) and cytosomes (C) in both wt- and $\Delta pm4\Delta bp2$ -trophozoites. The presence and accumulation of dark-staining vesicles (DSV, white arrow heads) is only visible in $\Delta pm4\Delta bp2$ -trophozoites. Scale bars, 5 μm .

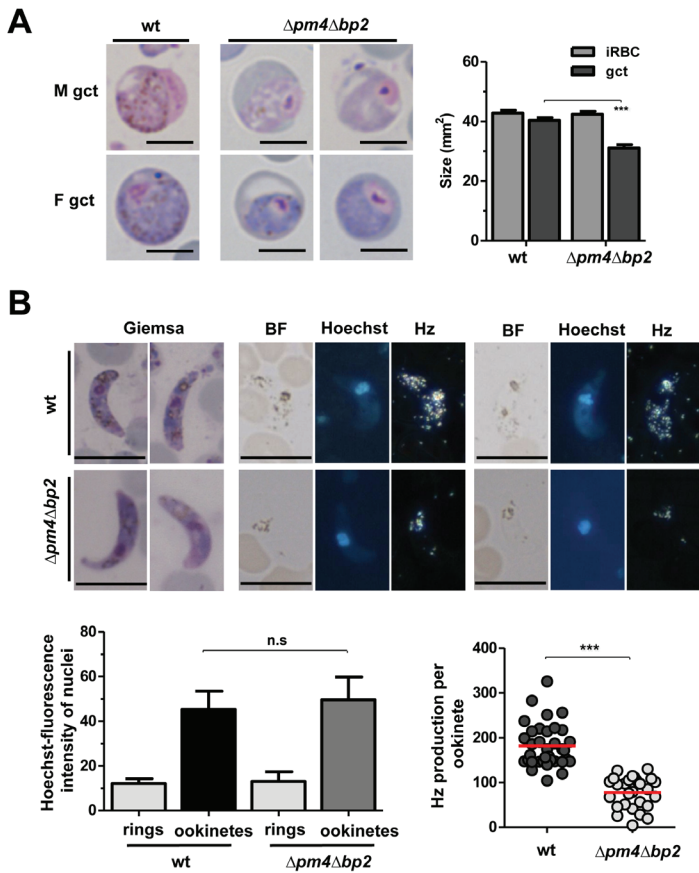


Figure S7. Gametocytes of $\Delta pm4\Delta bp2$ are fertile despite their smaller size and reduced hemozoin production

A. $\Delta pm4\Delta bp2$ -parasites produce gametocytes with a smaller size compared to wt-gametocytes. Mature wt male (M) and female (F) gametocytes (gct) usually occupy the entire volume of the iRBC and are characterized by abundant Hz crystals scattered throughout the cytoplasm, a single excentric located nucleus that is enlarged in male gametocytes, dark blue stained cytoplasm in females and pink stained cytoplasm in males. Uninuclear parasites with characteristics of mature male and female gametocytes (excentric nucleus, blue or pink stained cytoplasm) were readily detected on Giemsa-stained smears of tail blood obtained from mice infected with $\Delta pm4\Delta bp2$ -parasites (left panel). Size measurements of gametocytes in Giemsa-stained smears showed a significant reduction in size of the $\Delta pm4\Delta bp2$ gametocytes (right panel). Scale bars, 5 μm .

B. Female $\Delta pm4\Delta bp2$ gametes are fertilized and develop into ookinetes with the same characteristics as wt-ookinetes, including a banana shaped morphology and a centrally located, enlarged nucleus. However, the $\Delta pm4\Delta bp2$ -ookinetes show strongly reduced or absent Hz clusters. BF, bright-field.

C. Normal DNA content and reduced Hz levels in $\Delta pm4\Delta bp2$ -ookinetes.

Nuclear DNA content of $\Delta pm4\Delta bp2$ - and wt-ookinetes as determined by Hoechst-fluorescence intensity measurements. The mean fluorescence intensity of haploid ring-form nuclei (white arrows) of $\Delta pm4\Delta bp2$ and wt are 13.0 and 12.1 RLI (relative light intensity), respectively. The $\Delta pm4\Delta bp2$ and wt ookinetes show similar (tetraploid) DNA content and both have similarly enlarged nuclei, with RLI values of 49.6 and 45.3, respectively (n.s, student T-test, not significant, n>25). The amount of Hz in individual ookinetes (n>25) is determined by

measuring relative light intensity (RLI) of polarized light. The Hz level in $\Delta pm4\Delta bp2$ parasites ookinetes is significantly lower (57% less) than wt ookinetes (***) $P < 0.0001$, student T-test).

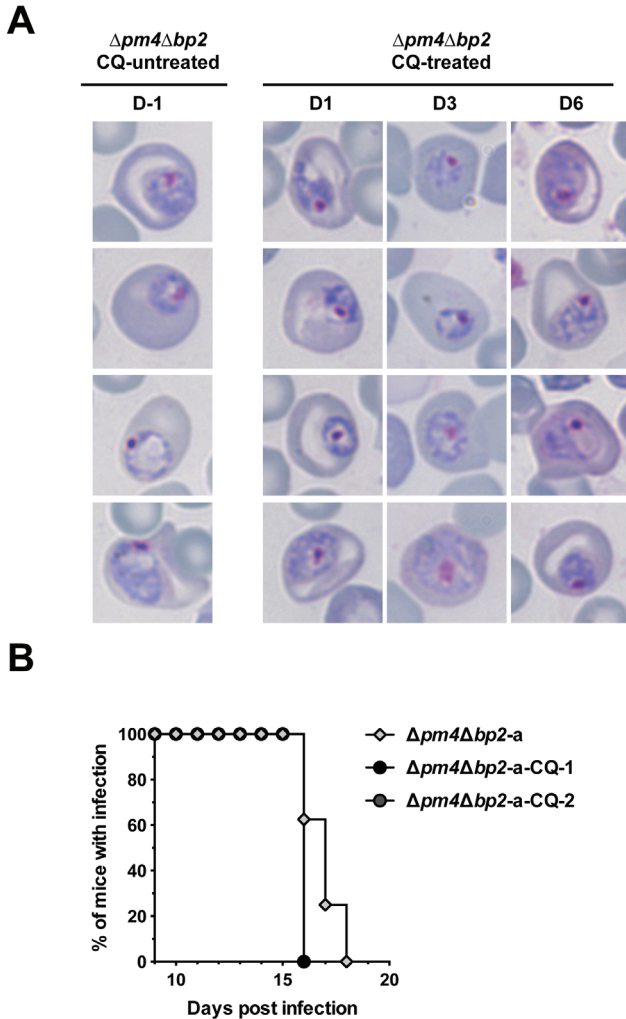


Figure S8. Chloroquine treatment of $\Delta pm4\Delta bp2$ -infected BALB/c mice

A. Trophozoites of $\Delta pm4\Delta bp2$ -parasites before chloroquine (CQ) treatment and at different days after start of CQ treatment. Untreated $\Delta pm4\Delta bp2$ -parasites 1 day before CQ treatment (D-1) show an identical morphology to $\Delta pm4\Delta bp2$ -parasites at day 1, 3 and 8 (D1, D3, D6) during CQ treatment with respect to size, absence of Hz pigment granules, accumulation of intracellular vacuoles and amoeboid morphology (see Figure S5).

B. Clearance of $\Delta pm4\Delta bp2$ -parasites in infected mice that were treated (CQ-1,2) or non-treated (NT) with CQ. In 2 experiments, $\Delta pm4\Delta bp2$ -parasites were cleared in all mice (n=10) to undetectable levels (as examined by microscopy) on day 16 post-infection in CQ-treated mice (7 days after CQ treatment). In non-treated mice (n=8), parasites were cleared between 16-18 days post-infection.

Table S1. Gene deletion experiments to disrupt the *P. berghei* genes encoding hemoglobins

Gene deletion mutant	Gene name	Gene ID	DNA construct name	Experiment No., Mutant name ¹	Parent line ²	RMgmDB ID ³
Unsuccessful attempts						
-	bergelysin (bin)	PBANKA_1113700	PCR1541 pL1557 pL1glysin	1502 1543 lysinko 1-2-3	676m1c1 676m1c1 676m1c1	RMgm-804
-	M1- family alanyl Aminopeptidase (aap)	PBANKA_141030	PCR1877 pL1gAPN	2058, 2087, 2111 aapko 1-2-3	1037m1f1c1, 820d1m1d1 676m1c1	RMgm-806
-	Heme detoxification protein (hdp)	PBANKA_131060	PCR1690 PCR1762 pPhHDP	1748, 1778, 2212 2208, 2213 hdpko 1-2-3	676m1c1 ci15 cy1, 676m1c1 ci15cy1	RMgm-807
Mutants						
$\Delta pm4$	plasmepsin 4	PBANKA_103440	PCR1597	1688c11	1037m1f1c1	RMgm-808
$\Delta bp2$ -a	berghepain-2	PBANKA_093240	pL1gPain2 pL1602	Pain2c8 1619c11	1037m1f1c1 1037m1f1c1	RMgm-809
$\Delta dpap1$ -a	dipeptidyl aminopeptidase 1	PBANKA_093130	pLDPA PCR1833	DPAkocl5 1962c11	1037m1f1c1 ci15cy1	RMgm-810
$\Delta dpap2$	dipeptidyl aminopeptidase 2	PBANKA_146070	PCR1875	2056c11	1037m1f1c1	RMgm-811
$\Delta dpap3$ -a	dipeptidyl aminopeptidase 3	PBANKA_100240	PCR1876	2057c11 2110c11	1037m1f1c1 1037m1f1c1	RMgm-812
Δapp -a	aminopeptidase P	PBANKA_131810	PCR1924	2129c12 2248c11	1037m1f1c1 1037m1f1c1	RMgm-813
Δlap	M17-family leucyl aminopeptidase	PBANKA_130990	PCR1878	2112c13	1037m1f1c1	RMgm-814
Δdap	M18-family aspartyl aminopeptidase	PBANKA_083310	PCR1879	2060c11	1037m1f1c1	RMgm-815
$\Delta bp1$	berghepain-1	PBANKA_132170	pL1976_3	2250c11	1037m1f1c1	RMgm-816
$\Delta pm4\Delta bp2$ -a	plasmepsin 4	PBANKA_103440	PCR1597	1863c11	$\Delta bp2$ -b sm	RMgm-817
$\Delta pm4\Delta bp2$ -b	berghepain-2	PBANKA_093240	PCR1597	1864c11	$\Delta bp2$ -b sm	RMgm-817

¹ Experiment number for independent transfection experiments: the unsuccessful attempts (3 times) and the experiment number/clone of the gene deletion mutants

² Parent *P. berghei*/ANKA line in which the genes were targeted for deletion

³ The ID number of the mutants (or of the unsuccessful attempts for gene deletion) in the RMgm database (www.pberghel.eu)

Table S2. Targeting constructs and primers

Gene	DNA Construct	Basic construct	Description	No.	Primer sequences *	Restriction sites	Localization
<i>plasmepsin 4</i> (<i>pm4</i>)	pL1873	pL0048	P1	L6861	GAAC TG TACTCCTGGT GAGC TCCGGAC CTTGTCCGGGGTACTCAG	NruI	pm4 5'-targeting sequence, F pm4 5'-targeting sequence, R pm4 3'-targeting sequence, F pm4 3'-targeting sequence, R
			P2	L6862	CATCTACAAGCATCGTCAGCCTCAAGCTCCCAATCTCTTTAATAAGG		
			P3	L6863	CCTTCAATTTCCGGATCCACTAGACAGCTACATAAACATGC		
			P4	L6864	AGGTTGGTCATTGACACTCAGCTCGGATTCCTACAAAATCAATATCAG		
<i>bergheipain 2</i> (<i>bp2</i>)	pLigPain2-a	pLigDHFR	P1	RS443	CGGGCCCGGGGGTTTCTATCTATATTTATTTCTCG	ApaI	bp2 5'-targeting sequence, F bp2 5'-targeting sequence, R bp2 3'-targeting sequence, F bp2 3'-targeting sequence, R
			P2	RS444	CCATCGATTTATGTTTCATGTTAATTTTTTTTTGG		
			P3	RS445	GGAATTCAAATAATATTATGATACCGATAGG		
			P4	RS446	CGGGATCCTGGAATCGCCCTTTTAAATGC		
<i>bergheylisin</i> (<i>bln</i>)	PCR1541	pL0035	P1	L5458	GAAC TG TACTCCTGGT GAGC AGCTT TATATCGTATACCCTGC	HindIII KspI Asp718I EcoRI	bp2 5'-targeting sequence, F bp2 5'-targeting sequence, R bp2 3'-targeting sequence, F bp2 3'-targeting sequence, R
			P2	L5459	CAGATCTATCGATCCGCGG CCGCGG ACATACAATTTAGTGCATGG		
			P3	L5460	CGATATCTGATCACCCGGGG GTAC CATAGTTGCACCTTATGGAGC		
			P4	L5461	AGGTTGGTCATTGACACTCAG CGAAATC GAAAGGATTAAGTCTACAGAC		
<i>bergheylisin</i> (<i>bln</i>)	pL1557	pL0048	P1	L5101	GAAC TG TACTCCTGGT GAGC GGTACC CAATATGCTAAGCATTACAC	Asp718I	bln5'-targeting sequence, F bln5'-targeting sequence, R bln3'-targeting sequence, F bln3'-targeting sequence, R
			P2	L5102	CATCTACAAGCATCGTGCACCTCTTCCACATATTCACCTTGAC		
			P3	L5103	CCTTCAATTTCCGGATCCACTAGACAATGATAGACCTAGAAGAG		
			P4	L5104	AGGTTGGTCATTGACACTCAG CGACTG TTCATACAATGAGTACTC		
<i>dipeptidyl peptidase 1</i> (<i>dpap1</i>)	pLigLysin	pLigDHFR	P1	RS447	CGGGCCCGGGAAATATGTTCCAACTTAAATTTAAAGG	ApaI	dpap1 5'-targeting sequence, F dpap1 5'-targeting sequence, R dpap1 3'-targeting sequence, F dpap1 3'-targeting sequence, R
			P2	RS448	CCATCGATTTATTAICTGCACATATAAAAAATGC		
			P3	RS449	GGAATTCGTTTTTGTTCACCTCTTTTACATATAAAC		
			P4	RS450	CGGGATCCCAAAATGAGATACTCTCAAAAAATTTG		
<i>dipeptidyl peptidase 1</i> (<i>dpap1</i>)	pLigdpap1a	pLigDHFR	P1	RS578	CGGGCCCGGGGCATGTAATCGGTATATTCG	ApaI	dpap1 5'-targeting sequence, F dpap1 5'-targeting sequence, R dpap1 3'-targeting sequence, F dpap1 3'-targeting sequence, R
			P2	RS579	CCATCGATCGAATTTTGGGGTTAATATATCC		
			P3	RS580	GGGGTACCAGATATATGCTTTTCATGGAAATG		
			P4	RS581	CGGGATCCTCAATAITTCATTAATAAAAAATGATATTAAG		

PCR1833	pL0048	P1	L6855	GAACCTGTA	CTCCTTG	TGACG	TCGGC	AGCATG	TAATCG	TATATTCG	<i>dpap1</i> 5'-targeting sequence, F		
		P2	L6856	CATCTACA	AGCATCG	TGACCTC	GAATTT	TTGGGG	TTAA	TATATATCC	<i>dpap1</i> 5'-targeting sequence, R		
		P3	L6857	CCTCAAA	TTTCGG	ATCCACT	AGTATAT	GCTTTC	ATGGA	AATGTTG	<i>dpap1</i> 3'-targeting sequence, F		
		P4	L6858	AGGTGGT	CATTG	ACACTC	AGCTCG	CGA	TAATTC	ATAAAG	TATATAAGAG	<i>dpap1</i> 3'-targeting sequence, R	
dipeptidyl peptidase 2 (<i>dpap2</i>)	pL0048	P1	L6925	GAACCTG	TACTCCT	TGGTG	ACG	TCGGC	AAATTT	TGGTG	TACAATGTG	<i>dpap2</i> 5'-targeting sequence, F	
		P2	L6926	CATCTACA	AGCATCG	TGACCTC	ATAA	TATAT	ATATG	CCACTG	CTC	<i>dpap2</i> 5'-targeting sequence, R	
		P3	L6927	CCTCAAA	TTTCGG	ATCCACT	AGTAT	TATG	CTTTC	CGCC	CTTTTC	<i>dpap2</i> 3'-targeting sequence, F	
		P4	L6928	AGGTTGG	TCAATG	ACACTC	AGCTCG	CGA	ATAA	ATAA	TGCTATATGCAG	<i>dpap2</i> 3'-targeting sequence, R	
dipeptidyl peptidase 3 (<i>dpap3</i>)	pL0048	P1	L6931	GAACCTG	TACTCCT	TGGTG	ACG	TCGGC	AAATTT	TAGG	CGGAGTG	<i>dpap3</i> 5'-targeting sequence, F	
		P2	L6932	CATCTACA	AGCATCG	TGACCTC	GA	AAACG	GA	TATATATG	TG	<i>dpap3</i> 5'-targeting sequence, R	
		P3	L6933	CCTCAAA	TTTCGG	ATCCACT	AGTAT	TATG	CTTTC	AGCTG	TAGCTG	<i>dpap3</i> 3'-targeting sequence, F	
		P4	L6934	AGGTGGT	CATTG	ACACTC	AGCTCG	CGA	TAATTC	ATAA	TTTTTAATGAG	<i>dpap3</i> 3'-targeting sequence, R	
Aminopeptidase P (<i>app</i>)	pL0048	P1	7103	GAACCTG	TACTCCT	TGGTG	ACG	TCGGC	AAATTT	TACACA	TAAGGG	CTGAATG	<i>app5'</i> -targeting sequence, F
		P2	7104	CATCTACA	AGCATCG	TGACCTC	ATA	TATG	GCATAT	TATATACATAC		<i>app5'</i> -targeting sequence, R	
		P3	7105	CCTCAAA	TTTCGG	ATCCACT	AGTAT	TATG	CTTTC	AGCTG	TAGCTG		<i>app3'</i> -targeting sequence, F
		P4	7106	AGGTTGG	TCAATG	ACACTC	AGCTCG	CGA	AAACG	TA	ATAA	TATCAACA	AAG
pLTgAPP	pLTgDHR	P1	RS695	GGGGGG	CGCC	CGGG	CGCA	ATAT	CATA	TATATATCTTC	<i>app5'</i> -targeting sequence, F		
		P2	RS696	GGGGAT	CGATG	TTTGC	ATA	TATA	AGCG	AAATTTATA	ACC	<i>app5'</i> -targeting sequence, R	
		P3	RS697	GGGGAA	ATTTCT	AGAA	TTTTG	TATAT	ATG	ATTTAG	TTGA	<i>app3'</i> -targeting sequence, F	
		P4	RS698	AAGGAA	AAAA	GGCG	CGCC	CAAA	ACTA	GACAAA	GAA	AACC	<i>app3'</i> -targeting sequence, R
M11-family alanyl aminopeptidase (<i>aap</i>)	pL0048	P1	L6945	GAACCTG	TACTCCT	TGGTG	ACG	TCGGC	AAATTT	TAGTATA	AAAGG	GAATATATG	<i>aap</i> 5'-targeting sequence, F
		P2	L6946	CATCTACA	AGCATCG	TGACCTC	ATA	ATA	TATAC	ATG	TATATTC		<i>aap</i> 5'-targeting sequence, R
		P3	L6947	CCTCAAA	TTTCGG	ATCCACT	AGTAT	TATG	CTTTC	CACTT	TGC		<i>aap</i> 3'-targeting sequence, F
		P4	L6948	AGGTGGT	CATTG	ACACTC	AGCTCG	CGA	TAATTC	ATAA	TTTTGTTTCC		<i>aap</i> 3'-targeting sequence, R
pLTgAPN	pLTgDHR	P1	RS715	GGGGGG	CGCC	CGGG	CGCT	TATG	TATC	CTCTGG	CATTG	<i>aap5'</i> -targeting sequence, F	
		P2	RS716	GGGGAT	CGATG	TTTGC	ATA	TATA	AGCG	AAATTTATA	ACC	<i>aap5'</i> -targeting sequence, R	
		P3	RS717	GGGGAA	ATTTCT	AGAA	TTTTG	TATAT	ATG	ATTTAG	TTAC	<i>aap3'</i> -targeting sequence, F	
		P4	RS718	AAGGAA	AAAA	GGCG	CGCC	CAAA	ACTA	GACAAA	TCC	ATAA	GAAG
M17-family leucyl aminopeptidase (<i>lap</i>)	pL0048	P1	L6963	GAACCTG	TACTCCT	TGGTG	ACG	TCGGC	AAATTT	TAAG	AGATG	ATCGTAGTG	<i>lap</i> 5'-targeting sequence, F
		P2	L6964	CATCTACA	AGCATCG	TGACCTC	ATA	TATG	GCACAAA	TG	AAAA	AATAC	<i>lap</i> 5'-targeting sequence, R

Table S3. Primers for genotyping

Genes	No.	Primer sequences	Description	Integration PCR pair	Product size (bp)
Primers for PCR analyses					
<i>pm4</i>	L5516	TTATGGGGATCCATATTTAC	<i>pm4</i> 5' in-F	L4906	1364
	L5517	CATGCGAATAAATGCTCAG	<i>pm4</i> 3' in-R	L1662	1122
	L5518	TCCGAATATTTAACAATTCGTG	<i>pm4</i> ORF-F		869
	L5519	ATGAAAGGACTGGAATACTC	<i>pm4</i> ORF-R		
<i>bp2</i>	RS835	TCTACAAGAATAAAAAGTTTCC	<i>bp2</i> -a 5' in-F	RS32	879
	RS836	TATTACATCTATATAAGAATCATGC	<i>bp2</i> -a 3' in-R	RS110	1075
	RS514	CACCATGAATTACCATTCTAGCCATCATATTAGAC	<i>bp2</i> -a ORF-F		1407
	RS515	TTATTCAAATTATAGGAGCATAACCTTGTC	<i>bp2</i> -a ORF-R		
	RS516	TTAAGTGAACAACAATTAGTTGATTGTGC	<i>bp2</i> -a ORF-F		516
	L5024	ATTGTTTATCGAGGAATTCG	<i>bp2</i> -b 5' in-F	L3211	1299
	L5025	TGGATATTCACGATTACC	<i>bp2</i> -b 3' in-R	L1662	1009
	L5026	GTATGTTTGGTTTTACCGTC	<i>bp2</i> -b ORF-F		1108
	L5027	CACATAAACCATCCATGTC	<i>bp2</i> -b ORF-R		
	<i>bln</i>	L5105	TGTTACATATTATGGCATTCC	<i>bln</i> 5' in-F	L4770
L5106		GCCAACTAGTACAAATATACAC	<i>bln</i> 3' in-R	L4771	990
L5107		GACCCATTAGATGCTGAG	<i>bln</i> ORF-F		694
L5108		GTCCACAGCATCATCTC	<i>bln</i> ORF-R		
<i>dap1</i>	RS672	CAACATACAAAAATAAACACC	<i>dap1</i> -a 5'in-F	RS32	875
	RS673	TGTTATAATCCCTTATATGT	<i>dap1</i> -a 3'in-R	RS110	903
	RS582	CACCGATAATGAACACAGAGAAAATTGGAAC	<i>dap1</i> -a ORF-F		856
	RS583	TTACATTTGAGATGCAATATAACATGAACC	<i>dap1</i> -a ORF-R		
	L6204	GCTGTTTTTATTTCCCTTATTTTAC	<i>dap1</i> -b 5' in-F	L4770	875
	L6205	GAGTAATGTTATAATCCCTTATATGTG	<i>dap1</i> -b 3' in-R	L4771	903
	L6206	GTTGTTTTTATGCTGAAAAATACG	<i>dap1</i> -b ORF-F		856
	L6207	AGTACATTTTTGGCATGTG	<i>dap1</i> -b ORF-R		
<i>dap2</i>	L6935	ATTCTCAACAATGGGGCAACTG	<i>dap2</i> 5' in-F	L4770	853
	L6936	TCTTTAAACTCGACATTTTTTCC	<i>dap2</i> 3' in-R	L4771	951
	L6937	CTCCCTATTCTGCTCTTATGG	<i>dap2</i> ORF-F		922
	L6938	CTACAATACTTGGACATTCCTC	<i>dap2</i> ORF-R		
<i>dap3</i>	L6941	CAATGCAAGTAGCAGAGAATG	<i>dpap3</i> 5' in-F	L4770	893
	L6942	CTTCATTACGAGATTAATAATTCAC	<i>dpap3</i> 3' in-R	L4771	819
	L6943	ATCCCTGTTCAATTGCTTGAG	<i>dpap3</i> ORF-F		1181
	L6944	AGTATCTGCATTAACATCTAGAG	<i>dpap3</i> ORF-R		
<i>app</i>	L7107	AAGTATTATAAAAATTAGCGAAAACAG	<i>app</i> 5' in-F	L4770	1003
	L7108	TCATTTTGCTTTATTTCTCTTTTG	<i>app</i> 3' in-R	L4771	1009
	L7109	ATGCGTATAAATTCGCTTATATATG	<i>app</i> ORF-F		996
	L7110	CAAAGAATCTACATCAGGGTTCTC	<i>app</i> ORF-R		
<i>aap</i>	L6949	TGTGAATTTGCGGAGATGTTG	<i>aap</i> 5' in-F	L4770	928
	L6950	AATTATTAGTAAAAATGCGAAAGG	<i>aap</i> 3' in-R	L4771	1068
	L6951	AGAACAGATTACAACCAAGTG	<i>aap</i> ORF-F		912
	L6952	ACCAATATAGTTATGAAAATATTCG	<i>aap</i> ORF-R		
<i>lap</i>	L6967	AAGTAATGCTTTTACCCTTTCTG	<i>lap</i> 5' in-F	L4770	1051
	L6968	ATATATACTCCCTTATACCACGTC	<i>lap</i> 3' in-R	L4771	1088

	L6969	AAAACAATTACAATAGTGATTGTC	<i>lap</i> ORF-F		
	L6970	GGATACATACTACCTTTTCTACTG	<i>lap</i> ORF-R		988
<i>dap</i>	L6975	TATGGGTGTCTAATTTTAACTG	<i>dap</i> 5' in-F	L4770	880
	L6976	AGTTAATCGAAAGCACTGATAC	<i>dap</i> 3' in-R	L4771	893
	L6977	GATAAAAAGGCACGAGAATATG	<i>dap</i> ORF-F		1037
	L6978	AAACTTCCATATATTTTCATCTACTG	<i>dap</i> ORF-R		
Universal primers					
	L695	AATATTCATAACACACTTTTAAGC	5' <i>pbdhfr</i> /ts R		
	L3211	GCACACAACATACACATTTTACAG	3' <i>pbdhfr</i> /ts R		
	L4906	CGACTAGTTAATAAAGGGCAC	5' <i>pbeef1a</i> R		
	L1662	GATTCATAAATAGTTGGACTTG	3' <i>pbdhfr</i> /ts F		
	L4770	CATCTACAAGCATCGTCGACCTC	anchor-tag R		
	L4771	CCTTCAATTCGGATCCACTAG	anchor-tag F		
	L4598	GGACAGATTGAACATCGTCG	<i>tgdhfr</i> /ts F		1059
	L4599	GTGTAGTCTGTGTCATGTC	<i>tgdhfr</i> /ts R		
	RS1900	CGGGATCCATGCATAAACCGGTGTGTC	<i>tgdhfr</i> /ts F		1850
	RS1901	CGGGATCCAAGCTTCTGTATTTCCGC	<i>tgdhfr</i> /ts R		
	L4698	GTTCGCTAAACTGCATCGTC	<i>hdhfr</i> F		787
	L4699	GTTTGAGGTAGCAAGTAGACG	<i>yfcu</i> R		
Primers for PCR probes and RT-PCR					
	L692	CGCGGATCCATGCATAAACCGGTGTGTC	3' <i>pbdhfr</i> /ts F		404
	L693	CGCGGATCCGCTAGACAGCCATCTCCAT	3' <i>pbdhfr</i> /ts R		
	L886	GGAAGATCTATGTTGGTTCGCTAAACTGCATCG	<i>hdhfr</i> F		582
	L887	GGAAGATCTTTAATCATTCTTCTCATATACTTC	<i>hdhfr</i> R		
	L644	GGAAACAGTCCATCTATAATTG	<i>lsu</i> rrna (A-type)		
	RS32	CAAACATACAAAAATAAACACC	5' <i>pbdhfr</i> /ts R		
	RS110	CTTTATGTCCACAACATCATC	3' <i>pbdhfr</i> /ts F		
	RS782	TGGAGCAGGAAATAACTGGG	<i>pbTub</i> F		402
	RS783	ACCTGACATAGCGGCTGAAA	<i>pbTub</i> R		
	7422	AACATTACCACAAGCAGTATCG	<i>bp1</i> ORF-F		1001
	7423	CCATCACATCCAAAATTGTAC	<i>bp1</i> ORF-R		

pb = *P. berghei*, *tg* = *T. gondii*; h = human, y = yeast

5' in = 5' integration PCR; 3' in = 3' integration PCR

CHAPTER 6

Generation of Growth- and Virulence-Attenuated Blood-stage Malaria Parasites

Jing-wen Lin¹, Séverine Chevalley-Maurel¹, Mohammed Sajid¹, Blandine Franke-Fayard¹,
Jai Ramesar¹, Hans Kroeze¹, Roberta Spaccapelo², John H. Adams³, Gordon Langsley⁴,
Chris J. Janse¹, Shahid M. Khan¹

¹Leiden Malaria Research Group, Department of Parasitology, Leiden University Medical Centre, 2333 ZA Leiden, The Netherlands

²Department of Experimental Medicine, University of Perugia, Piazzale Gambuli, Perugia, Italy

³Department of Global Health, College of Public Health, University of South Florida, College of Public Health, Tampa, Florida

⁴Institut Cochin (INSERM U1016), Université Paris Descartes, Sorbonne Paris Cité, CNRS (UMR 8104), 75014 Paris, France

Abstract

Immunization with killed or attenuated *Plasmodium* blood-stage parasites, or with live parasites under curative chemotherapy, can induce protective immunity against a malaria infection. Such infection-based immunization is being pursued not only to characterize potential live-attenuated blood-stage vaccines, but also to identify the critical host and pathogen components involved in development of protective immunity and pathology. We targeted 41 *Plasmodium berghei* genes for disruption in order to generate genetically modified blood stage parasites (GAP_{BS}) that are growth- and virulence- attenuated and that may serve as immunogens and as tools to study protective immunity. Using mutants generated in this and in previous studies, we examined their infection and virulence characteristics by assessing experimental cerebral malaria (ECM) in C57BL/6 mice and the development of hyper-parasitemia in BALB/c mice. Blood stage infections of 9 mutants showed significant reduction in *in vivo* growth rates. Seven of these 9 growth-attenuated mutants did not induce ECM in C57BL/6 mice. Two single-gene deletion mutants, lacking expression of either aminopeptidase P or leucyl aminopeptidase and a double gene-deletion mutant that lacks expression of both plasmepsin-4 and berghepain-2, did not induce hyper-parasitemia in the majority of BALB/c mice. These mice resolved the infection and the convalescent mice were protected against infections with wild type parasites.

Introduction

Licensed human vaccines available today principally belong to three categories – live attenuated microbes (e.g. measles, mumps), killed/inactivated microbes (e.g. Polio, rabies) or protein subunit/conjugate (e.g. Hepatitis B, HPV) (<http://www.cdc.gov/vaccines/>). A large number of subunit-vaccine candidates against malaria parasites, *Plasmodium*, have been tested in animal models and humans, mainly as a protein (antigen) formulation, or expressed by a (DNA or viral) vector system in order to generate protective immunity [1]. Most malaria antigens that have been selected as subunit-vaccine candidates have been characterized as targets of natural immunity, most often associated with strong antibody responses [2]. However, the most advanced leading subunit pre-erythrocytic vaccine candidate RTS,S showed only limited efficacy as in Phase 3 testing with clinical malaria episodes in children being reduced by only 30–50% [3,4]. Clinical trials of erythrocytic (blood stage) subunit-vaccines have also shown modest protection; the testing of more than 10 candidate subunit vaccines targeting *Plasmodium* blood stages have not progressed to or further than Phase 2 trials, with only three candidates having reached Phase 2b trials [5]. The limited success with subunit-vaccine development has renewed interest in developing vaccines consisting of whole, killed or attenuated parasites [6]. While sustained and sterile immunity has been achieved using live *Plasmodium* liver stage parasites attenuated by radiation or genetic modification or administered under curative doses of chemoprophylaxis [7–9], full protective immunity to malaria with either killed sporozoites or killed blood stage parasites have so far been unsuccessful [7,10].

Whole *Plasmodium* blood-stage formulations used in immunization studies usually consist of infected red blood cells (iRBC). These formulations have included killed parasites in adjuvant, radiation-attenuated iRBC, or infection with wild-type iRBC administered under curative doses of chemotherapy and these have been used to immunize both rodents and primate models of malaria [6,10–12]. The results of these immunizations, while varied in their protective efficacies for the different combinations, have demonstrated protective immunity including complete protection against a challenge with wild type parasites (for a review see [10]). Furthermore, in a small immunization study of humans, evidence was found for the generation of complete protective immunity against *P. falciparum* that was achieved through repeated inoculations of very low numbers of iRBC (~30) resulting in sub-patent infections that were controlled using curative dose of chemotherapy [13]. These studies were remarkable in that they showed that not only immunization with whole blood stages can induce complete protective immunity in humans, but also that protective immunity could be achieved using only limited amounts of parasite material and in the absence of a major antibody response [6].

Currently practical limitations exist for immunization strategies that require humans be infected with parasites inside red blood cells, either killed or attenuated, for example it is unclear if regulatory authorities would approve, as part of a mass vaccination program, the intravenous administration of infected red blood cells to humans [2,6]. Nonetheless, such immunization studies can provide important insights into how protective immune responses can be induced and maintained against *Plasmodium* blood stages [14,15]. Similar to immunization studies using genetically attenuated parasites that arrest in the liver (GAP_{LS}) [8], studies into blood-stage immunization would clearly benefit from creating genetically attenuated blood stage parasites (GAP_{BS}) in animal models that induce limited, self-resolving infections that are virulence-attenuated and that can provoke strong and long-lasting immunity without the induction of malarial symptoms or additional pathologies. Such parasites can be instrumental tools to uncover important correlates of protection, to both better understand how iRBC are detected and eliminated by the host immune response, and also to identify correlates of disease.

A number of gene-deletion mutants generated in both rodent and human parasites have been reported to exhibit moderate to severe reduction in their blood-stage multiplication rates. However, the first growth- and virulence-attenuated GAP_{BS} was only recently reported for the rodent model malaria parasite *P. yoelii* YM (a lethal strain) [16]. This GAP_{BS}, which lacks the gene encoding purine nucleoside phosphorylase (PNP), is virulence-attenuated and produces a self-resolving infection in mice. Importantly, after a single infection with this parasite, all convalescent mice were protected against subsequent wild-type parasite challenge for prolonged periods (>5 months) [16]. Since then, other rodent malaria GAP_{BS} have been also reported, which show growth- and virulence-attenuation and induce self-resolving infections after which mice are protected against wild type challenge. This includes the GAP_{BS} that lacks genes encoding for nucleotide transporter 1 (NT1) [17] which was based on a study performed in *P. falciparum*, where an equivalent gene-deletion created parasites that grow only when purines are provided at supra-physiological concentrations to the culture medium and has been proposed as a potential *P. falciparum* GAP_{BS} candidate [18]. Others GAP_{BS} characterized in the rodent system include GAP_{BS} lacking expression of rhomboid 1 [19], plasmepsin-4 (PM4) [20], and a GAP_{BS} that lacks both PM4 and MSP7, a merozoite-specific protein [21]. The GAP_{BS} that have been created in *P. berghei* ANKA do not cause experimental cerebral malaria (ECM) in ECM-susceptible mice as wild type parasite do. These studies show that not only is it possible to generate growth- and virulence-attenuated blood stages parasites by targeting specific genes in the parasite genome, but also that strong and long-lasting protective immune responses can be induced in mice that have resolved their infections. However, despite growth- and virulence-attenuation, most of the reported GAP_{BS} still

produce infections with relatively high parasitemias (parasite loads). An ideal GAP_{BS} should result in infections with low level parasitemias that spontaneously resolve shortly after the parasites are introduced into the blood. An infection with low (sub-patent) parasitemias was only achieved by the $\Delta nt1$ mutant generated in non-lethal *P. yoelii* XNL when infected with low dose of parasites [17]. These sub-patent, self-resolving, infections generated strong cellular and humoral immune responses that provided complete protection in BALB/c, C57BL/6 and Swiss mice [17]. However, this GAP_{BS} was created in a virulent rodent parasite line (i.e. *P. yoelii* YM or *P. berghei* ANKA), where the kinetics and virulence phenomena of a gene-deletion mutant might be substantially different. We have targeted 41 genes for targeted disruption in the virulent rodent parasite *P. berghei* ANKA in order to generate GAP_{BS} that are both growth- and virulence-attenuated and can serve as protective immunogens. Specifically we aimed to create virulence-attenuated GAP_{BS}, which induce short-term blood infections with low parasitemias that are resolved by the host and induce protective immunity. The genes selected for targeted disruption were based on published roles of their encoding proteins in blood stages, or based on a reported delay in growth phenotype in *P. falciparum* mutants [22]. From the 41 genes selected 19 were refractory to targeted disruption. We generated 7 single gene-deletion mutants and 2 double gene-deletion mutants that showed significant reduction in blood stage asexual multiplication rates. From these mutants we identified seven GAP_{BS} that were both growth- and virulence-attenuated and 3 of these mutants did not generate hyper-parasitemia in BALB/c mice. These mice were able to resolve their infection and were protected against an infection with wild type parasites.

Results

Selection of genes for analysis by targeted gene deletion

For the generation of mutant blood stage parasites that are growth- and/or virulence-attenuated we selected a total of 41 genes for analysis by targeted deletion (Table 1). The first group consists of 8 genes encoding all *Plasmodium* rhomboid proteases ('rhomboid genes'). We chose the genes coding for these proteins, because of the critical roles identified for several rhomboid proteases in host cell invasion and pathogenesis of apicomplexan parasites [23,24]. In addition, it has been shown that *P. berghei* and *P. yoelii* mutants lacking rhomboid 1 show a reduction in their blood stage growth rates [19,25]. Gene targeting experiments for the 8 rhomboids, generation and characterization of mutants lacking expression of rhomboid proteases has been described in Chapter 4. In Table 1 we show an overview of all the gene deletion experiments performed and in Table 2 we show growth- and virulence-characteristics of the mutants that we were able

to generate.

The second group (consisting of 12 genes) constitutes genes encoding 8 putative hemoglobinas and 4 other enzymes possibly involved in the *Plasmodium* hemoglobin (Hb) digestion ('hemoglobin digestion genes'). We chose genes coding for these proteins, because of the important role Hb digestion has in parasite growth [26]. In addition, gene disruption studies of hemoglobinas in *P. falciparum* demonstrate that this system is redundant and the enzymes have overlapping activities in Hb degradation [27–32]. Mutants lacking expression of certain hemoglobinas, while viable, show reduced growth rates and the equivalent mutants in *P. berghei* are both growth- and virulence-attenuated [20,30]. Gene targeting experiments for 12 genes and the generation and characterization of mutants lacking expression of hemoglobinas has been described in Chapter 5. Here, we analyse the growth rates of all mutants (Table 2) and provide data on the virulence-characteristics of these mutants (see below and Table 2).

The third group (of 8 genes) was selected based on *P. falciparum* mutants that exhibited a growth-delay phenotype ('*P. falciparum* growth-related genes'). These mutants were generated in a forward genetic screen based on random *piggyBac* mutagenesis ([22] and J.H. Adams unpublished observations).

The last group (consisting of 13 genes) is a heterogeneous group, which encode a variety of proteins expressed in asexual blood stages ('other genes'). These have been selected based on a proven, or putative effect on growth of *Plasmodium* blood stages. It includes 3 members of Rab GTPase family. Rab GTPases are key regulators of vesicular traffic in eukaryotic cells and in *Plasmodium* 11 *rab* genes have been identified of which 10 are transcribed in the iRBC and they possibly have overlapping functions [33]. Two genes were selected that encode enzymes involved in carbon metabolism: phosphoenolpyruvate carboxylase (PEPC) and carbonic anhydrase (CA). Carbon dioxide (CO₂) is thought to be essential for the growth of intraerythrocytic malaria parasites in order to synthesize pyrimidine through CO₂ fixation and to regulate the intracellular pH of the parasite [34]. PEPC is thought to catalyse CO₂ fixation with phosphoenolpyruvate in the absence of pyruvate carboxylase in *Plasmodium* and thereby supplying the cytosol with oxaloacetate (OAA) [34]. *P. falciparum* mutants lacking expression of PEPC showed a strong reduction in growth of trophozoites and mutants could only be selected by supplying additional malate to cultures of the blood stages [34]. Carbonic anhydrase (CA) facilitates CO₂ transport across the plasma membrane and inhibitors of *Plasmodium* CA affect the growth of *P. falciparum* blood stages [35,36]. Two genes were selected that encode putative transporters, putative amino acid transporter (AAT) and nucleoside transporter 1 (NT1). NT1 is a plasmamembrane permease which is involved in uptake of

purines [37,38] and asexual blood stages of *P. yoelli* and *P. berghei* NT1-deficient mutants show a very reduced growth in mice [17,39]. Three genes were selected that play a role in the Kennedy phospholipid biosynthesis pathway, choline kinase (*ct*), choline/ethanolaminephosphotransferase (*cept*) and a putative ethanolamine kinase (*ek*). It was unclear at the initiation of these studies if the generation of *Plasmodium* phospholipids were only derived by *de novo* synthesis, or could be also derived from an alternative scavenging pathway. If the parasite would make use of both systems, deletion of one of these genes may not have a deleterious effect, but may affect growth rate of the parasites [40]. We also targeted the gene encoding a putative hemolysin, as it is implicated to play a role in parasite egress from the RBC [41,41]. As multiple genes are important for parasitophorous vacuole (PV) formation and since *P. berghei* liver stages can survive and replicate inside a hepatocyte with a compromised/absent PV [42], we attempted to delete the PV resident protein hepatocyte erythrocyte protein 17 kDa (*hep17*; also known as exported protein 1) [43]. Finally, we attempted to disrupt a gene encoding a putative DNA (cytosine-5)-methyltransferase (*dnmt2*). DNA methylation plays an important role in gene silencing/activation, deletion of the equivalent gene (*pmt1*) in yeast resulted in decreased rates of vegetative growth [44].

Genes which were refractory to targeting deletion

A total of 19 out of the 41 genes were refractory to targeting deletion in multiple transfection experiments (Table 1). The multiple unsuccessful attempts to disrupt these genes indicate that these have a critical function for asexual blood stage growth, although a failure to disrupt a gene is not an unequivocal proof that the encoded protein is essential for blood stage multiplication.

These genes include 4 'rhomboid genes' (*rom4*, 6, 7 and 8; see Chapter 4) and 3 'hemoglobin digestion genes' (*bln*, *aap*, *hdp*; see Chapter 5). Four out of 8 '*P. falciparum* growth-related genes' were refractory to gene deletion in *P. berghei* (i.e. *caf1*, *pp2c*, *ApiAP2* and PBANKA_020890). The unsuccessful attempts to disrupt one of these genes, *caf1* encoding CCR4-associated factor 1 (PBANKA_142620), has been published [45]. Of the 'other genes', the 3 *rab* genes were refractory to deletion and attempts to delete *ck*, *cept* and *ek*, were also unsuccessful, and this was supported by a recent study that also showed that genes of the Kennedy phospholipid biosynthesis pathway were refractory to genetic disruption in *P. berghei* [40]. The genes encoding hemolysin, and HEP17 were also refractory to disruption. See Table 1 and Table S1 for details of these unsuccessful gene-deletion attempts and primers used to amplify the targeting sequences, generate the gene-deletion constructs and for genotyping. Information on failed attempts to disrupt

genes including DNA constructs and primers have been submitted to the RMgMDB database of genetically modified rodent malaria parasites (www.pberghei.eu).

Table 1. Selected genes for analysis by targeted gene deletion

Gene name	<i>P. berghei</i> Gene ID	<i>P. falciparum</i> Gene ID	Product name in PlasmoDB	Successful targeting deletion?	DNA construct name	Experiment No. Mutant name ¹	RMgMDB ID ²
Genes that encode rhomboid proteases (8 genes)							
<i>rom1</i>	PBANKA_093350	PF3D7_1114100	rhomboid protease ROM1	yes	Mg031 pL1533	538cl2 1496cl4	RMgm-177 RMgm-761
<i>rom3</i>	PBANKA_070270	PF3D7_0828000	rhomboid protease, putative	yes	pL1097	430cl1, 687cl1	RMgm-178
<i>rom4</i>	PBANKA_110650	PF3D7_0506900	rhomboid protease, putative (ROM4)	no	pL1078	653, 684, 695	RMgm-187
<i>rom6</i>	PBANKA_135810	PF3D7_1345200	rhomboid protease ROM6, putative	no	PCR1916	2118, 2119, 2140	RMgm-758
<i>rom7</i>	PBANKA_113460	PF3D7_1358300	rhomboid protease ROM7, putative	no	PCR1917	2120, 2121, 2141	RMgm-759
<i>rom8</i>	PBANKA_103130	PF3D7_1411200	rhomboid protease, putative	no	PCR1918	2122, 2123, 2142	RMgm-760
<i>rom9</i>	PBANKA_111470	PF3D7_0515100	rhomboid protease, putative	yes	PCR1919	2124cl1, 2125cl1	RMgm-762
<i>rom10</i>	PBANKA_111780	PF3D7_0618600	rhomboid protease ROM10, putative	yes	Mg011	468cl2	RMgm-179
Genes that encode enzymes involved in hemoglobin digestion pathway (12 genes)							
<i>pm4</i>	PBANKA_103440	PF3D7_1407800	plasmepsin 4	yes	PCR1597	1688cl1	RMgm-808
<i>bp2</i>	PBANKA_093240	PF3D7_1115700	berghepain-2	yes	pLTgPain2 pL1602	Pain2cl8 1619cl1	RMgm-809
<i>bln</i>	PBANKA_113700	PF3D7_1360800	bergheylisin	no	PCR1541 pL1557 pLTgLysin	1502 1543 lysinko 1-2-3	RMgm-804
<i>dpap1</i>	PBANKA_093130	PF3D7_1116700	dipeptidyl aminopeptidase 1	yes	pLDPA PCR1833	DPAkocI5 1962cl1	RMgm-810
<i>app</i>	PBANKA_131810	PF3D7_1454400	aminopeptidase P	yes	PCR1924	2129cl2, 2248cl1	RMgm-813
<i>aap</i>	PBANKA_141030	PF3D7_1311800	M1- family alanyl aminopeptidase	no	PCR1877 pLTgAPN	2058, 2087, 2111 aapko 1-2-3	RMgm-806
<i>lap</i>	PBANKA_130990	PF3D7_1446200	M17-family leucyl aminopeptidase	yes	PCR1878	2112cl3	RMgm-814
<i>dap</i>	PBANKA_083310	PF3D7_0932300	M18-family aspartyl aminopeptidase	yes	PCR1879	2060cl1	RMgm-815
<i>hdp</i>	PBANKA_131060	PF3D7_1446800	heme detoxification protein	no	PCR1690 PCR1762 pPhHDP	1748, 1778, 2212 2208, 2213 hdpko 1-2-3	RMgm-807

<i>bp1</i>	PBANKA_132170	PF3D7_1458000	berghepain 1	yes	pL1976	2250cl1	RMgm-816
<i>dpap2</i>	PBANKA_146070	PF3D7_1247800	dipeptidyl aminopeptidase 2	yes	PCR1875	2056cl1	RMgm-811
<i>dpap3</i>	PBANKA_100240	PF3D7_0404700	dipeptidyl aminopeptidase 3	yes	PCR1876	2057cl1, 2110cl1	RMgm-812

Genes selected based on *P. falciparum* piggyBac insertion mutants with a growth phenotype (8 genes)

<i>caf1</i>	PBANKA_142620	PF3D7_0811300	CCR4-associated factor 1	no	PCR1518 PCR1585	1463, 1489 1591, 1615	RMgm-639
<i>cdc25</i>	PBANKA_140400	PF3D7_1305500	conserved <i>Plasmodium</i> protein, unknown function	yes	PCR1524	1492cl1	RMgm-829
<i>pp2c</i>	PBANKA_123070	PF3D7_0615900	conserved <i>Plasmodium</i> protein, unknown function	no	PCR1699 PCR1827	1782 1957	RMgm-827
<i>ApiAP2</i>	PBANKA_135600	PF3D7_1342900	transcription factor with AP2 domain(s), putative (ApiAP2)	no	PCR1831	2007, 2330, 2337	RMgm-913
	PBANKA_020890	PF3D7_0104200	conserved <i>Plasmodium</i> protein, unknown function	no	PCR1691 PCR1774	1799 1893	RMgm-828
	PBANKA_112890	PF3D7_0630100	conserved <i>Plasmodium</i> protein, unknown function	yes	PCR1830	2329cl1	RMgm-860
	PBANKA_030100	PF3D7_0203000	conserved <i>Plasmodium</i> protein, unknown function	yes	PCR1883	2331cl1	RMgm-861
<i>Rpus</i>	PBANKA_111100	PF3D7_0511500	RNA pseudouridylate synthase, putative, fragment	yes	PCR1775	1894cl1	RMgm-830

Other genes (13 genes)

<i>rab5a</i>	PBANKA_030800	PF3D7_0211200	Rab5a, GTPase, putative	no	PCR1548	1526, 1587, 1608, 1647, 1648, 1680, 1681	RMgm-821
<i>rab5b</i>	PBANKA_140910	PF3D7_1310600	Rab5b, GTPase, putative	no	PCR1709	1785, 1786	RMgm-822
<i>rab11b</i>	PBANKA_135410	PF3D7_1340700	Rab GTPase 11b	no	PCR1710	1787, 1788	RMgm-823
<i>ck</i>	PBANKA_104010	PF3D7_1401800	choline kinase	no	PCR1549	1527, 1609, 1649, 1682	RMgm-818
<i>cept</i>	PBANKA_112700	PF3D7_0628300	choline/ethanolamine-phosphotransferase	no	PCR1550	1528, 1610, 1650, 1683	RMgm-819
<i>ek</i>	PBANKA_092370	PF3D7_1124600	ethanolamine kinase, putative	no	PCR1643	1673, 1695	RMgm-820
<i>nt1</i>	PBANKA_136010	PF3D7_1347200	nucleoside transporter 1	yes	PCR1693 PCR1776	1781cl1 1912	RMgm-831
<i>aat</i>	PBANKA_112830	PF3D7_0629500	amino acid transporter, putative	yes	PCR1925	2130cl1	RMgm-832
<i>pepc</i>	PBANKA_101790	PF3D7_1462700	phosphoenolpyruvate carboxylase	yes	PCR1777	1895cl1	RMgm-833
<i>ca</i>	PBANKA_090900	PF3D7_1140000	carbonic anhydrase, putative	yes	PCR1881	2114cl1	RMgm-834

<i>hemolysin</i>	PBANKA_131910	PF3D7_1455400	hemolysin, putative	no	PCR1591	1594, 1618	RMgm-824
<i>hep17</i>	PBANKA_092670	PF3D7_1121600	circumsporozoite-related antigen	no	PCR1555	1542, 1611	RMgm-825
<i>dnmt2</i>	PBANKA_021140	PF3D7_0727300	DNA (cytosine-5)-methyltransferase, putative (DNMT2)	yes	pL1789	1935cl1, 1965cl1	RMgm-835

¹ Experiment number for independent transfection experiments: the unsuccessful attempts (X3) and the experiment number/clone of the gene deletion mutants

² The ID number of the mutants (or of the unsuccessful attempts for gene deletion) in the RMgmDB database (www.pberghei.eu) of genetically modified rodent malaria parasites

Successfully generated gene deletion mutants and analysis of growth- and virulence- attenuation

Successful gene deletion mutants were generated for 22 out of the 41 genes (Table 1). Successful deletion of these genes demonstrates that they are not essential for asexual blood stage growth under the conditions used for selection of the gene-deletion mutants. These genes include 4 ‘rhomboïd genes’ (*rom1*, 3, 9, 10; see Chapter 4) and 9 ‘hemoglobin digestion genes’ (*pm4*, *bp2*, *dpap1*, *app*, *dap*, *lap*; *bp1*, *dpap2*, *dpap3*; see Chapter 5). Four out of 8 ‘*P. falciparum* growth-related genes’, were successfully deleted (*cdc25*, PBANKA_030100, PBANKA_112890 and *Rpus*) (Figure S1). In addition, for five out of 13 ‘other genes’ (*nt1*, *aat*, *pepc*, *ca*, *dnmt2*), it was possible to generate deletion mutants (Figure S2). In addition to these single gene-deletion mutants, we also generated two ‘double’ gene-deletion mutants. In one mutant ($\Delta pm4\Delta bp2$) both plasmepsin-4 (*pm4*) and berghepain-2 (*bp2*) were sequentially deleted. The proteins encoded by these genes are responsible for initial cleavage of native hemoglobin (Chapter 5). In the second double gene-deletion mutant ($\Delta pm4\Delta smac$), both plasmepsin-4 (*pm4*) and the gene *smac* were deleted (Figure S2). The *smac* gene encodes SMAC (schizont membrane-associated cytoadherence protein, PBANKA_010060), which is involved in *P. berghei* ANKA schizont sequestration [46]. See Table 1 and Table S1 for details of the successful gene-deletion mutant generation and primers used to amplify the targeting sequences, generate the gene-deletion constructs and for genotyping. All information on the gene deletion mutants, including DNA constructs and primers, has been submitted to the RMgmDB database of genetically modified rodent malaria parasites (www.pberghei.eu).

For all gene-deletion mutants, we confirmed the correct integration of the constructs and the successful disruption of the gene by diagnostic PCR and/or Southern analyses of separated chromosomes (Figures S1-2). For all mutants we determined the *in vivo* asexual multiplication rates (i.e. growth rate), which is calculated during the initial phase of infection after mice are infected with a single parasite and is defined as the daily-fold increase in parasite numbers [20] (Table 2). When mutants were observed to have

a significantly reduced growth rate we also confirmed the lack of transcription of the disrupted genes by Northern analyses of blood stage mRNA from the mutant parasites (Figures S2). In addition, for mutants with a significant growth defect (see below; 9 out of 22 mutants), we determined their virulence characteristics in C57BL/6 and BALB/c mice. In C57BL/6 mice we determined whether the mutant parasites induce experimental cerebral malaria (ECM). *P. berghei* ANKA is a frequently used model to study ECM in C57BL/6 mice. When these mice are infected with 10^4 to 10^5 wild type (wt) *P. berghei* ANKA parasites, more than 90% of mice develop features of ECM between day 6 and 9 after infection [47]. In BALB/c mice we determined the development of hyper-parasitemia. BALB/c mice infected with wt *P. berghei* ANKA do not develop ECM, but succumb to hyper-parasitemia (>50%), anemia and general organ failure in the second or third week after infection [48].

Gene-deletion mutants that exhibit normal growth rates

Wild-type *P. berghei* ANKA parasites have a consistent 10-fold increase in parasitemia per 24 hour [20], and we observed that 15 out of 22 single gene-deletion mutants we generated had no significant reduction in their asexual multiplication rates (Table 2). The '*P. falciparum* growth-related gene mutants' $\Delta cdc25$, $\Delta PBANKA_030100$, $\Delta PBANKA_112890$ and $\Delta Rpus$ have wt multiplication rates (Table 2), which are different from the reduced growth rates of their corresponding *P. falciparum* piggyBac insertion mutants. The cell cycle of mutant *Pf* $\Delta cdc25$ is prolonged by 10% (J. H. Adams, unpublished data); mutants $\Delta PF3D7_0630100$ (ortholog of PBANKA_030100), $\Delta PF3D7_0203000$ (ortholog of PBANKA_112890) and *Pf* $\Delta Rpus$ exhibit 45–65% reduction in RBC invasion compared to wt *P. falciparum* NF54 [22]. Other mutants with wt growth rates were 4 'rhomboid gene mutants' ($\Delta rom1$, $\Delta rom3$, $\Delta rom9$, $\Delta rom10$; Chapter 4, Table 2), 4 'hemoglobin digestion gene mutants' ($\Delta bp2$, Δdap , $\Delta dpap2$, $\Delta dpap3$; Chapter 5, Table 2) and 3 'other gene mutants' (Δaat , Δca and $\Delta dnmt2$). The wt-like growth of $\Delta rom1$ and Δca mutants is unexpected. In other studies it has been found that *P. berghei* and *P. yoelii* mutants lacking rhomboid 1 show a reduction in their blood stage growth rates [19,25]. The normal growth rate of Δca is also unexpected, given CA has been considered a potential drug target and the antimalarial activity of CA inhibitors against both *P. falciparum* and *P. berghei* has been reported [35,36].

Gene-deletion mutants that exhibit significant reduced growth rates

In infections of mice, 7 out of 22 single gene-deletion mutants show a reduction in their growth rates and have a significantly lower than the 10-fold increase in parasitemia per 24 hour observed in wt *P. berghei* ANKA infections. Specifically, 5 'hemoglobin digestion

gene mutants' ($\Delta pm4$, $\Delta dpap1$, Δapp , Δlap and $\Delta bp1$; Chapter 5, Table 2) and 2 'other gene mutants' ($\Delta nt1$ and $\Delta pepc$) (Table 2). Recent analyses of the growth of *P. yoelli* and *P. berghei* mutants lacking expression of NT1 show a reduction in asexual blood stages growth rate [17,39], which is similar to that we report in this study (Table 2). The reduced growth rate of the *P. berghei* $\Delta pepc$ corresponds to the reduced growth of *P. falciparum* blood stages lacking expression of PEPC [34]. In addition to the 7 single gene-deletion mutants, the two double gene-deletion mutants, $\Delta pm4\Delta smac$ and $\Delta pm4\Delta bp2$, showed a strong reduction in their multiplication/growth rates (Table 2).

Table 2. Growth and virulence characteristics of blood stages of gene deletion mutants.

Mutant	Day to 0.5-2% parasitemia ¹	Multiplication rate ²	ECM in C57BL/6 ³	Self-resolving in C57BL/6 ⁴	Hyper-parasitemia in BALB/c ⁵	Self-resolving in BALB/c ⁴
wt ⁷	8 (0.2), n=40	10.0 (0.7)	6/6	0/6	6/6	0/6
Mutants without significant reduction in asexual multiplication rates (15 mutants)						
$\Delta rom1$ -p	8 (0), n=2	10.0 (0.0)	6/6	0/6	6/6	0/6
$\Delta rom1$ -c	8 (0), n=3	10.0 (0.0)	6/6	0/6	6/6	0/6
$\Delta rom3$	8 (0), n=3	10.0 (0.0)	n.d	n.d	n.d	n.d
$\Delta rom9$	8 (0), n=4	10.0 (0.0)	n.d	n.d	n.d	n.d
$\Delta rom10$	8 (0), n=4	10.0 (0.0)	n.d	n.d	n.d	n.d
$\Delta bp2$ -a	8 (0), n= 5	10.0 (0.0)	6/6	0/6	6/6	0/6
$\Delta bp2$ -b	8 (0), n=6	10.0 (0.0)	6/6	0/6	n.d	n.d
Δdap	8 (0), n=3	10.0 (0.0)	6/6	0/6	n.d	n.d
$\Delta dpap2$	8.3 (0.4), n=4	9.4 (1.0)	n.d	n.d	n.d	n.d
$\Delta dpap3$ -a	8.3 (0.6), n=3	9.2 (1.3)	n.d	n.d	n.d	n.d
$\Delta dpap3$ -b	8 (0), n=5	10.0 (0.0)	n.d	n.d	n.d	n.d
$\Delta cdc25$	8 (0), n=4	10.0 (0.0)	n.d	n.d	n.d	n.d
$\Delta PBANKA_030100$	8.2 (0.4), n=5	9.5 (1.0)	n.d	n.d	n.d	n.d
$\Delta PBANKA_112890$	8 (0), n=4	10.0 (0.0)	n.d	n.d	n.d	n.d
$\Delta Rpus$	8 (0), n=7	10.0 (0.0)	n.d	n.d	n.d	n.d
Δaat	8 (0), n=5	10.0 (0.0)	n.d	n.d	n.d	n.d
Δca	8 (0), n=4	10.0 (0.0)	n.d	n.d	n.d	n.d
$\Delta dnmt2$ -a	8.4 (0.5), n=5	9.1 (1.2)	5/5	0/5	n.d	n.d
$\Delta dnmt2$ -b	8 (0), n=3	10.0 (0.0)	n.d	n.d	n.d	n.d
Mutants with significant reduction in asexual multiplication rates (7 mutants)						
$\Delta pm4$	9 (0), n=2	7.7 (0.0) ***	0/6	0/6	6/6	0/6
$\Delta dpap1$ -a	9.5 (0.7), n=2	7.0 (1.0) ***	yes ⁶	none ⁷	6/6	n.d
$\Delta dpap1$ -b	9 (0), n=4	7.7 (0.0) ***	6/6	0/6	n.d	n.d
Δapp -a	12 (0), n=1	4.6 (0.0) ***	0/6	3/6	0/6	6/6
Δapp -b	12 (0), n=4	4.6 (0.0) ***	0/6	6/6	n.d	n.d
Δlap	15.5 (0.7), n=2	3.3 (0.2) ***	0/6	6/6	0/6	6/6
$\Delta bp1$	9.7 (0.6), n=3	6.8 (0.8) ***	0/6	0/6	n.d	n.d

<i>Δnt1</i>	9.8 (0.5), n=4	6.7 (0.7) ***	0/5	0/5	6/6	n.d
<i>Δpepc</i>	13.7 (0.6), n=3	3.9 (0.2) ***	6/6	0/6	6/6	n.d
Double gene-deletion mutants (2 mutants)						
<i>Δpm4Δsmac</i>	13.5 (0.7), n=2	3.9 (0.3) ***	0/6	5/6	5/5	n.d
<i>Δpm4Δbp2-a</i>	12, 16, 20, n=3	3.4 (1.1) ***	0/6	6/6	2/12	10/10
<i>Δpm4Δbp2-b</i>	21, 24, n=2	2.3 (0.1) ***	0/6	6/6	3/6	3/3

n.d, not determined

¹ The day on which the parasitemia reach 0.5–2% in mice infected with a single parasite during cloning assays. The mean of one cloning experiment and standard deviation are shown. n, the number of mice tested. For the *Δpm4Δbp2* mutants, due to large variation, the days of the individual clone are shown.

² The multiplication rate of asexual blood stages per 24 hours as determined in the cloning assays. Mean values and standard deviations of each line were shown, student T-test, *, P<0.01; ***, P<0.0001.

³ Development of symptoms of experimental cerebral malaria (ECM)

⁴ Mice with parasitemias <50% that resolving infections in C57BL/6 or BALB/c.

⁵ Hyper-parasitemia infections in BALB/c mice is defined as a parasitemia > 50%.

⁶ Spaccapelo R, *et al*, 2011 (ref[21])

⁷ Spaccapelo R, unpublished data

Gene-deletion mutants that exhibit normal growth and virulence characteristics

We tested 3 out of 15 mutants with normal (wt) growth rates for their ability of inducing ECM in C57BL/6 mice (i.e. *Δrom1*, *Δbp2* and *Δdap*). It has been reported that *P. berghei* and *P. yoelii* mutants lacking rhomboid 1 exhibit a slightly reduced growth rate and are less virulent in mice than wt parasites [19,25]. In particular, the *P. berghei Δrom1* mutant as reported by Srinivasan *et al.* did not cause ECM in Swiss mice [19]. We therefore determined the virulence of two independent *Δrom1* mutants (Chapter 4) in C57BL/6 mice. We found that both mutants induced ECM at day 5–6 as wt *P. berghei* ANKA parasites (Chapter 4, Table 2).

Gene-deletion mutants that exhibit reduced growth rates but still cause ECM

Infections with 2 of the 9 growth-attenuated mutants, *Δdpap1* and *Δpepc*, still induced ECM in C57BL/6 mice. The *Δdpap1-b* mutant caused ECM on day 7–9 post infection in mice infected with 10⁵ parasites; in comparison, a wt infection initiated with the same number of parasites produced a higher parasitemia and mice succumbed to ECM 1 or 2 days earlier (i.e. day 6–7; Figure 1A). Most mice infected with *Δdpap1-a* developed ECM (R. Spaccapelo, unpublished data). Interestingly, while we observed *Δpepc* infections have a strong reduction in growth when infections are initiated with a single parasite, the growth rates in mice infected with 10⁵ parasites (intraperitoneally) was, unexpectedly, not strongly reduced compared to a wt infection in 2 independent experiments and all

mice developed ECM (Figure 1B). Unfortunately, we have been unable to select a second independent $\Delta pepc$ mutant yet, despite 6 separate transfection experiments targeting *pepc*. Confirmation of the effects on parasite growth rates in mice when infected with different parasite numbers awaits either the generation/characterization of a second independent mutant or restoration of the wt phenotype when *pepc* gene is re-introduced into the $\Delta pepc$ genome (i.e. genetic complementation).

Gene-deletion mutants that exhibit reduced growth rates and reduced virulence

Infections with 7 out of 9 growth-attenuated mutants also showed virulence-attenuation, with respect to ECM. Specifically, $\Delta pm4$, Δapp , Δlap , $\Delta bp1$, $\Delta nt1$, $\Delta pm4\Delta bp2$ and $\Delta pm4\Delta smac$ did not induce ECM in C57BL/6 (Table 2). Furthermore, C57BL/6 mice infected with four of these mutants were able to spontaneously resolve infections to different degrees (Table 2): 3 out of 6 mice survived a Δapp -a infections, while all (6/6) mice resolved infections with either with Δapp -b or Δlap (Table 2). Whereas $\Delta pm4$ -infected C57BL/6 were not able to resolve infections [20], 12 out of 12 mice resolved infections with the double gene-deletion mutants $\Delta pm4\Delta bp2$ -a or $\Delta pm4\Delta bp2$ -b and 4 of these resolved infections without developing hyper-parasitemia (Figure 1C). For the double gene-deletion mutant $\Delta pm4\Delta smac$, 5/6 mice resolved the infection and these mice cleared parasites in 3 weeks before parasitemia reaching 20%. One of the six mice did not control the infection and developed hyper-parasitemia (>50%) (Figure 1C).

In addition to virulence characteristics in C57BL/6 mice we analysed the growth (parasitemia and self-resolving infections) of 6 growth-attenuated mutants in BALB/c mice ($\Delta pm4$, $\Delta dpap1$ -a, Δapp , Δlap , $\Delta pm4\Delta smac$ and $\Delta pm4\Delta bp2$; Table 2). BALB/c mice infected with wt *P. berghei* ANKA do not succumb to ECM, but still are unable to resolve the infection and mice die of sustained hyper-parasitemia (>50%) and anemia. Mutants $\Delta pm4$ and $\Delta dpap1$ -a induced parasitemias in excess of 50% in BALB/c mice, as did the double gene-deletion mutant $\Delta pm4\Delta smac$ that had shown reduced parasitemias in C57BL/6 mice which could resolve the infections. As mice were sacrificed at parasitemias between 50 and 70%, we did not determine whether these mice were able to resolve the infections as had previously shown with $\Delta pm4$ infections [20]. All BALB/c mice (n=6) infected with 10^5 Δapp or 10^5 Δlap parasites, and 13 out of 18 BALB/c mice infected with the 10^5 or even 10^6 $\Delta pm4\Delta bp2$ mutants did not develop hyper-parasitemias and resolved their infections (Figure 2).

All mice that had resolved their infections (both C57BL/6 and BALB/c) were challenged with 10^5 wt parasites by intraperitoneal (i.p) injection, at least 1 month after clearance of

the parasites. All mice are protected against wild type *P. berghei* ANKA challenge (data not shown).

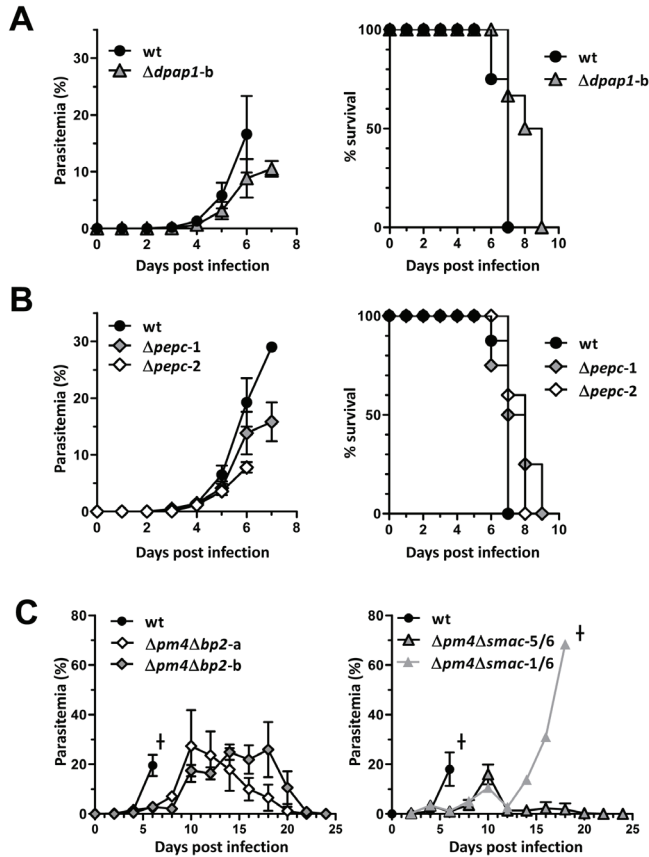


Figure 1. The course of infection of wild type and mutant *P. berghei* parasites in C57BL/6 mice.

A. The course of infection (left panel) and survival curve (right panel) in C57BL/6 mice (n=6) i.p infected with 10^5 wild-type (wt, cl15cy1) or $\Delta dpap1-b$ parasites. $\Delta dpap1-b$ infection produced a lower parasitemia and mice succumbed to ECM 1 or 2 days later compare to wt parasites.

B. The course of infection (left panel) and survival curve (right panel) in C57BL/6 mice (n=6) i.p infected with 10^5 wt (cl15cy1) or $\Delta pepc$ parasites in 2 independent experiments. $\Delta pepc$ infection produced a lower parasitemia compared wt infection, but still caused ECM on day 6-9 after infection.

C. Course of parasitemia in C57BL/6 mice. Mice (n=6) were i.p infected with 10^5 wt (cl15cy1), 10^5 $\Delta pm4\Delta bp2-a$, 10^5 $\Delta pm4\Delta bp2-b$ (left panel) or 10^5 $\Delta pm4\Delta smac$ parasites (right panel). All wt-infected mice developed cerebral complications at day 6 after infection, whereas none of the mice infected with $\Delta pm4\Delta bp2$ or $\Delta pm4\Delta smac$ parasites developed ECM. All mice infected with $\Delta pm4\Delta bp2$ parasites resolved infections resulting in undetectable parasitemia by microscopic analysis between day 22 and 24 post infection. Five out of 6 mice infected $\Delta pm4\Delta smac$ parasites resolved infections in 3 weeks with peak parasitemia less than 25%. One mouse developed hyper-parasitemia (>50%).

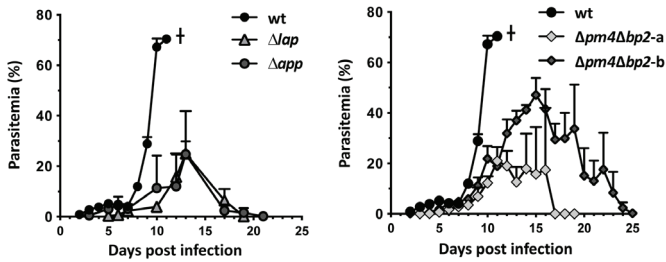


Figure 2. The course of infection of wild type and mutant *P. berghei* parasites in BALB/c mice.

Mice (n=6) were i.p infected with 10^5 wt (c15cy1), 10^5 Δlap , 10^5 Δapp (left panel); 10^5 $\Delta pm4\Delta bp2-a$ (n=12) or 10^6 $\Delta pm4\Delta bp2-b$ (n=6) (right panel). All wt-infected mice developed hyper-parasitemia on day 10-11 after infection, whereas none of the mice infected with Δlap or Δapp parasites developed hyperparasitemia and resolved infections resulting in undetectable parasitemia by microscopic analysis between day 20 and 22 post infection (p.i). Ten out of 12 mice infected with 10^5 $\Delta pm4\Delta bp2-a$ parasites and 3 out of 6 mice infected with 10^6 $\Delta pm4\Delta bp2-b$ resolved infections without developing hyperparasitemia.

Discussion

In this study we examined *P. berghei* gene-deletion mutants in order to identify genetically attenuated blood stage parasites (GAP_{BS}), specifically, mutants that are both growth- and virulence-attenuated and that may serve as immunizing agents and as tools to study correlates of disease and protection. Using mutants generated in this and previous studies, we first examined their growth characteristics and established the multiplication rates for blood stages of each mutant in cloning assays. For those mutants with a significant reduction in growth, we examined their virulence by assessing experimental cerebral malaria (ECM) in C57BL/6 mice and for a number of these mutants we also examined if the infection in BALB/c mice resulted in hyper-parasitemia (i.e. >50%). We analysed the course of parasitemia in both C57BL/6 and BALB/c mice as we aimed to identify GAP_{BS} that induce only low-parasitemia, self-resolving infections that are cleared soon after parasites are introduced into the blood. Until now, most of the reported virulence-attenuated GAP_{BS} that do not induce ECM in C57BL/6 mice, still produce infections in BALB/c with relatively high parasitemias [20,21]. We identified 9 mutants that had a strongly reduced asexual multiplication rate (>20% reduction compared to wt). Seven of these mutants did not induce ECM, suggesting that the growth rate of blood stages is an important factor for inducing ECM. The absence of ECM in mice infected with the double gene-deletion mutants $\Delta pm4\Delta bp2$ and $\Delta pm4\Delta smac$ was expected, since mice infected with $\Delta pm4$ parasites also do not develop ECM [20]. Interestingly, while it has been reported that C57BL/6 mice infected with $\Delta pm4$ cannot resolve their infections

and die from hyper-parasitemia [20], we found that all C57BL/6 mice infected with $\Delta pm4\Delta bp2$, and most mice (5/6) infected with $\Delta pm4\Delta smac$ can resolve their infections. These results demonstrate that it is possible to generate further virulence-attenuated parasites through the deletion of multiple genes, as was also reported by Spaccapelo *et al.* [21] with mutants that lack expression of both PM4 and MSP7. The $\Delta pm4\Delta bp2$ mutant lacks PM4 and BP2, the two key enzymes involved in hemoglobin digestion, as described in Chapter 5. This mutant has a further reduced multiplication rate compared to $\Delta pm4$, which may contribute to the capacity of C57BL/6 mice to resolve infections with this mutant. The $\Delta pm4\Delta smac$ mutant lacks in addition to plasmepsin-4, expression of SMAC, a parasite protein involved in the adherence of *P. berghei* schizonts (in a CD36-dependent manner) to host endothelium [46]. It has been shown that the reduced growth of parasites lacking SMAC is in large part due to the clearance of unsequestered SMAC-deficient schizonts by the spleen. We found that the growth rate of $\Delta pm4\Delta smac$ is strongly reduced compared to either $\Delta pm4$ or $\Delta smac$, which may explain why C57BL/6 mice are able to resolve infections.

While 7 of the 9 'slow-growing' mutants were virulence-attenuated, two of these mutants ($\Delta dpap1$ and $\Delta pepc$) still induced ECM in mice, suggesting that factors other than a delay in growth contribute to induction of ECM. We found that all mutants (i.e. $\Delta pm4$, Δapp , $\Delta pm4\Delta bp2$ and $\Delta pm4\Delta smac$) that had reduced hemozoin (Hz) production (data shown in Chapter 5) do not induce ECM. Hz is released into the circulation at schizont rupture and it is rapidly removed by phagocytosis mainly in the liver and spleen. Upon phagocytosis Hz cannot be further degraded and persists for prolonged periods in host tissue and has long been considered as a virulence factor. It has been shown that the number of Hz-containing leukocytes in the peripheral blood correlates with disease severity in *P. falciparum*-infected patients [49,50]. Several inflammatory and immune-modulatory effects of Hz have been reported (reviewed in [51,52]). Therefore, the amount of Hz that is released by the parasite may play a critical role in both inducing inflammatory responses and severe pathology in the host. Since induction of ECM correlates with pro-inflammatory status of the host [53], Hz may be a critical factor involved in inducing ECM. However, the amount of Hz, like growth, may not be the only factor responsible for inducing ECM, since blood stages of several growth-attenuated mutants ($\Delta nt1$, Δlap and $\Delta bp1$) have normal Hz production and do not induce ECM (Chapter 5, Table 2; unpublished results). However, the absence of ECM in these mutants could still be related to reduced amounts of Hz released in the circulation early in an infection. Mice infected with slow-growing parasites can be expected to release less Hz compared to wt parasites and therefore the Hz levels may be below the threshold that is required to induce inflammatory responses during the acute phase of the infection necessary to

produce ECM. Clearly, further research is required to unravel the relative contributions of the critical parasite (and host) factors that result in severe disease and protection. So far we have been unable to select mutants that do not induce ECM, but that have both a normal growth rate and Hz production. The selection of such mutants would indicate that other factors in addition to growth rate and Hz levels contribute to ECM. Despite reduced growth rates and lack of ECM in C57BL/6 mice, the $\Delta pm4$, $\Delta nt1$ and $\Delta pm4\Delta smac$ mutants produced hyper-parasitemia infections in BALB/c mice. However, we found that BALB/c infected with three mutants, Δlap , Δapp and $\Delta pm4\Delta bp2$, are able to resolve without developing hyper-parasitemias.

Combined, our results show that it is possible to generate mutants with strongly reduced growth rates that do not induce ECM and that through the deletion of one or multiple genes it is possible to create mutants that produce self-resolving infections in mice without producing hyper-parasitemia. However, mice infected with these mutants still develop parasitemias ranging between 10–50%. Up to now we have not yet been able to generate mutants that produce ‘low-level’ infections that resolve shortly after parasite inoculation into the blood and without developing high parasitemias. Even with parasites that have strongly reduced growth rates, both C57BL/6 and BALB/c mice are unable to rapidly mount an effective immune response that can control an acute infection. It is, however, important to note that in all our experiments, the mice were infected with relatively high numbers of parasites (10^5 – 10^6). It is possible that starting infection with lower numbers of parasites would allow the mice to control infections before developing high parasitemias, or would lead to infections with very low or even sub-patent parasitemias [17]. For *P. falciparum*, it has been postulated that infection with low numbers of infected RBC (under curative chemotherapy) generates protective immune responses that are defined by the absence, or low levels of antibodies and strong cell-mediated responses, including upregulation of nitric oxide synthase, CD4+/CD8+ proliferative T-cell and INF- γ responses [13,54,55]. Protective immunity with *P. berghei* infections in mice have been mainly reported from immunization requiring repeated, prolonged infections cleared by drug treatment, or after a self-resolving and sustained infection with an avirulent parasite line [10,16,20,56–59]. The protective immune responses in these mice are largely antibody-dependent, where the iRBC of wt challenge are opsonized and then removed in the spleen by phagocytosis [20,60,61]. These studies and those of experimental *P. falciparum* infections in humans, where protective cellular immune responses are induced with low numbers of iRBC, would suggest that the induction of protective immunity might require different parasite loads depending on the nature of the immune (cellular or humoral) responses required. Clearly, further research is required to determine both the parasite and host factors that can induce protective immune responses against blood stages.

The use of attenuated blood stage parasites can be extremely useful tools to better understand induced rather than acquired immunity against *Plasmodium* and may help to create an effective and the boardest anti-parasite vaccine.

Material and Methods

Animals and parasites

Female C57BL/6, BALB/c and Swiss OF1 mice (6–8 weeks old; Charles River/Janvier) were used. All animal experiments of this study were approved by the Animal Experiments Committee of the Leiden University Medical Center (DEC 10099; 12042; 12120). The Dutch Experiments on Animal Act is established under European guidelines (EU directive no. 86/609/EEC regarding the Protection of Animals used for Experimental and Other Scientific Purposes).

Three reference *P. berghei* ANKA parasite lines were used for generation of the gene-deletion mutants and the transgenic parasites: the ‘wild type’ (wt) line cl15cy1 [62] and two reporter lines, i.e. *PbGFP-LUC_{con}* (line 676m1cl1; mutant RMgm-29; www.pberghei.eu) and *PbGFP-Luc_{schiz}* (line 1037cl1; mutant RMgm-32; www.pberghei.eu). Both reporter lines were generated in the cl15cy1 parent line and express the fusion protein GFP-Luciferase either under the control of the constitutive *eef1α* promoter or the schizont-specific *ama1* promoter, respectively. The *gfp-luc* expression cassette is stably integrated into the *pb230p* locus without introduction of a drug-selectable marker [20,63].

Generation of gene-deletion mutants

To generate targeted gene deletion mutants, the replacement constructs (Table S1) were generated using conventional cloning method or a modified two step PCR method [64]. Plasmid construct pL1789 targeting *dnmt2* was constructed in plasmid pL0035 (www.mr4.com), which contains the *hdhfr::yfcu* selectable marker (SM) under the control of the *eef1α* promoter [65]. The *hdhfr::yfcu* marker is a fusion gene of the positive selection marker human *dihydrofolate reductase* and the negative selection marker, which is a fusion gene of yeast *cytosine deaminase* and *uridyl phosphoribosyl transferase* [65]. The 5'- and 3'- targeting regions (TR) of *dnmt2* were amplified from wild type *P. berghei* ANKA (cl15cy1) genomic DNA (primers used were shown in Table S1) and cloned into restriction sites of *HindIII*/ *SacII* and *XhoI*/*EcoRV* of plasmid pL0035. Prior to transfection the DNA-construct was linearized with *HindIII* and *EcoRV*. Constructs targeting *rab5a*, *rab5b* and *rab11b* were kindly provided by Dr. Gordon Langsley (Faculte de Medecine, Universite

Paris Descartes) as a collaborative project. Other replacement constructs were generated by the modified two step PCR method (Figure S1A). Briefly, in the first PCR reaction two fragments of 5'- and 3'-TR were amplified from wild type genomic DNA with the primer sets P1/P2 and P3/P4 respectively (primers sequences shown in Table S1). The reverse primers of 5' TR (P2) and the forward primers of 3' TR (P3) have 5' extensions homologous to the *hdhfr* SM from pL0040 or to *hdhfr::yfcu* SM from pL0048. In the second PCR reaction, the 5'- and 3'-TR were annealed to either side of the selectable marker cassette, and the joint fragment was amplified by the external anchor-tag primers 4661/4662, resulting in the PCR-based targeting constructs. Before transfection, the PCR-based constructs were digested with appropriate restriction sites (as indicated in primer sequences in Table S1) to remove the 'anchor-tag' and with *DpnI* that digests any residual uncut plasmids (Figure S1A).

Transfection and selection of transformed parasites with pyrimethamine was performed using standard technology for the genetic modification of *P. berghei* [62]. All information on the generation of gene-deletion mutants (as well as unsuccessful disruption attempts), such as DNA constructs and primers, has been submitted to the RMgmdB database of genetically modified rodent malaria parasites (www.pberghei.eu).

Clonal parasite lines were obtained from all gene-deletion mutants by the method of limiting dilution. Correct integration of DNA constructs and disruption of the genes was verified by diagnostic PCR analyses (see Table S2 for primers used) and/or Southern analyses of chromosomes separated by pulsed-field gel electrophoresis hybridized with probes specific for the selectable marker [62]. See Table S2 for primers used.

Northern analysis of blood stage mRNA were performed to confirm absence of transcripts. Total RNA was isolated from mixed blood-stages of wild type *P. berghei* ANKA (cl15cy1) and the different gene-deletion mutant lines. Northern blots were hybridized with probes specific for the open reading frame (ORF) of each gene after PCR amplification from wt *P. berghei* ANKA genomic DNA (primers shown in Table S2). As a loading control, Northern blots were hybridized with the oligonucleotide probe L644R that recognizes the large subunit ribosomal RNA (rRNA) [66].

The double gene-deletion mutant $\Delta pm4\Delta smac$ which lacks expression of both PM4 and SMAC (schizont membrane-associated cytoadherence protein, PBANKA_010060) was generated by targeting *pm4* using construct PCR1597 in mutant $\Delta smac3^{-sm}$, which lacks expression of SMAC and is free of SM (the generation of $\Delta smac3^{-sm}$ is described in [46]).

The generation of the double gene-deletion mutant $\Delta pm4\Delta bp2$ (lacking genes coding PM4 and BP2) is described in Chapter 5 using the same method as described for $\Delta pm4\Delta smac$.

Analysis of growth-attenuation

To determine growth-attenuation of the mutants, we determined their growth rate (multiplication rate) of asexual blood stages in mice. The multiplication rate of asexual blood stages in mice is determined during the cloning procedure [20] and is calculated as follows: the percentage of infected erythrocytes in Swiss OF1 mice injected with a single parasite is quantified at day 8 to 11 on Giemsa-stained blood films. The mean asexual multiplication rate per 24 hour is then calculated assuming a total of 1.2×10^{10} erythrocytes per mouse (2mL of blood). The percentage of infected erythrocytes in mice infected with reference lines of the *P. berghei* ANKA strain consistently ranges between 0.5–2% at day 8 after infection, resulting in a mean multiplication rate of 10 per 24 hour [20,67].

Analysis of Virulence-attenuation

The capacity of mutants to induce ECM was analysed in C57BL/6 mice. Groups of 6 mice were intraperitoneally (i.p) infected with 10^5 – 10^6 wild type *P. berghei* ANKA, or different mutant parasites. Onset of ECM in *P. berghei* infection was determined by measurement of a drop in body temperature below 34°C [20]. The body temperature of infected mice was measured twice a day from day 5 to day 8 after infection using a laboratory thermometer (model BAT-12, Physitemp Instruments Inc., Clifton, NJ) with a rectal probe (RET-2) for mice. When infected mice showed a drop in temperature (below 34°C), the mice were sacrificed. In addition to ECM in C57BL/6 mice we determined the course of parasitemia in BALB/c mice. Groups of 5–6 BALB/c mice were i.p infected with 10^4 – 10^6 mutants or wild type parasites. The course of parasitemia was determined by Giemsa-staining of blood smears once in every two days or every day during acute and peak infection. When mice developed high parasitemias (50–70%), the mice were sacrificed.

References

1. Anders RF, Adda CG, Foley M, Norton RS (2010) Recombinant protein vaccines against the asexual blood stages of *Plasmodium falciparum*. *Hum Vaccin* 6: 39-53.
2. Anders RF (2011) The case for a subunit vaccine against malaria. *Trends Parasitol* 27: 330-334.
3. Agnandji ST, Lell B, Soulanoudjingar SS, Fernandes JF, Abossolo BP, *et al* (2011) First results of phase 3 trial of RTS,S/AS01 malaria vaccine in African children. *N Engl J Med* 365: 1863-1875.
4. Agnandji ST, Lell B, Fernandes JF, Abossolo BP, Methogo BG, *et al* (2012) A phase 3 trial of RTS,S/AS01 malaria vaccine in African infants. *N Engl J Med* 367: 2284-2295.
5. Schwartz L, Brown GV, Genton B, Moorthy VS (2012) A review of malaria vaccine clinical projects based on the WHO rainbow table. *Malar J* 11: 11. 1475-2875-11-11
6. Good MF (2011) A whole parasite vaccine to control the blood stages of *Plasmodium*: the case for lateral thinking. *Trends Parasitol* 27: 335-340.
7. Nussenzweig R, Vanderberg J, Most H (1969) Protective immunity produced by the injection of x-irradiated sporozoites of *Plasmodium berghei*. IV. Dose response, specificity and humoral immunity. *Mil Med* 134: 1176-1182.
8. Khan SM, Janse CJ, Kappe SH, Mikolajczak SA (2012) Genetic engineering of attenuated malaria parasites for vaccination. *Curr Opin Biotechnol* 23(6):908-16.
9. Roestenberg M, Teirlinck AC, McCall MB, Teelen K, Makamdop KN, *et al* (2011) Long-term protection against malaria after experimental sporozoite inoculation: an open-label follow-up study. *Lancet* 377: 1770-1776.
10. McCarthy JS, Good MF (2010) Whole parasite blood stage malaria vaccines: a convergence of evidence. *Hum Vaccin* 6: 114-123.
11. Renia L, Gruner AC, Mauduit M, Snounou G (2006) Vaccination against malaria with live parasites. *Expert Rev Vaccines* 5: 473-481.
12. Amante FH, Engwerda CR, Good MF (2011) Experimental asexual blood stage malaria immunity. *Curr Protoc Immunol* Chapter 19: Unit. 10.1002/0471142735.im1904s93 [doi].
13. Pombo DJ, Lawrence G, Hirunpetchcharat C, Rzepczyk C, Bryden M, *et al* (2002) Immunity to malaria after administration of ultra-low doses of red cells infected with *Plasmodium falciparum*. *Lancet* 360: 610-617.
14. Engwerda CR, Minigo G, Amante FH, McCarthy JS (2012) Experimentally induced blood stage malaria infection as a tool for clinical research. *Trends Parasitol* 28: 515-521.
15. Woodberry T, Minigo G, Piera KA, Amante FH, Pinzon-Charry A, *et al* (2012) Low-level *Plasmodium falciparum* blood-stage infection causes dendritic cell apoptosis and dysfunction in healthy volunteers. *J Infect Dis* 206: 333-340.
16. Ting LM, Gissot M, Coppi A, Sinnis P, Kim K (2008) Attenuated *Plasmodium yoelii* lacking purine nucleoside phosphorylase confer protective immunity. *Nat Med* 14: 954-958.
17. Aly AS, Downie MJ, Mamoun CB, Kappe SH (2010) Subpatent infection with nucleoside transporter 1-deficient *Plasmodium* blood stage parasites confers sterile protection against lethal malaria in mice. *Cell Microbiol* 12: 930-938.
18. El BK, Downie MJ, Kim SK, Horowitz M, Carter N, *et al* (2008) Genetic evidence for the essential role of PfNT1 in the transport and utilization of xanthine, guanine, guanosine and adenine by *Plasmodium falciparum*. *Mol Biochem Parasitol* 161: 130-139.
19. Srinivasan P, Coppens I, Jacobs-Lorena M (2009) Distinct roles of *Plasmodium* rhomboid 1 in parasite development and malaria pathogenesis. *PLoS Pathog* 5: e1000262.
20. Spaccapelo R, Janse CJ, Caterbi S, Franke-Fayard B, Bonilla JA, Syphard LM, Di CM, Dottorini T, Savarino A, Cassone A, Bistoni F, Waters AP, Dame JB, Crisanti A (2010) Plasmeprin 4-deficient *Plasmodium berghei* are virulence attenuated and induce protective immunity against experimental malaria. *Am J Pathol* 176: 205-217.
21. Spaccapelo R, Aime E, Caterbi S, Arcidiacono P, Capuccini B, *et al* (2011) Disruption of plasmeprin-4 and merozoites surface protein-7 genes in *Plasmodium berghei* induces combined virulence-attenuated phenotype. *Sci Rep* 1: 39.
22. Balu B, Singh N, Maher SP, Adams JH (2010) A genetic screen for attenuated growth identifies genes crucial for intraerythrocytic development of *Plasmodium falciparum*. *PLoS One* 5: e13282.

23. Freeman M (2009) Rhomboids: 7 years of a new protease family. *Semin Cell Dev Biol* 20: 231-239.
24. Santos M, Graindorge A, Soldati-Favre D (2011) New insights into parasite rhomboid proteases. *Mol Biochem Parasitol* 182(1-2):27-36.
25. Vera IM, Beatty WL, Sinnis P, Kim K (2011) *Plasmodium* protease ROM1 is important for proper formation of the parasitophorous vacuole. *PLoS Pathog* 7: e1002197.
26. Goldberg DE (2005) Hemoglobin degradation. *Curr Top Microbiol Immunol* 295: 275-291.
27. Omara-Opyene AL, Moura PA, Sulsona CR, Bonilla JA, Yowell CA, *et al* (2004) Genetic disruption of the *Plasmodium falciparum* digestive vacuole plasmepsins demonstrates their functional redundancy. *J Biol Chem* 279: 54088-54096.
28. Liu J, Gluzman IY, Drew ME, Goldberg DE (2005) The role of *Plasmodium falciparum* food vacuole plasmepsins. *J Biol Chem* 280: 1432-1437.
29. Bonilla JA, Moura PA, Bonilla TD, Yowell CA, Fidock DA, *et al* (2007) Effects on growth, hemoglobin metabolism and paralogous gene expression resulting from disruption of genes encoding the digestive vacuole plasmepsins of *Plasmodium falciparum*. *Int J Parasitol* 37: 317-327.
30. Bonilla JA, Bonilla TD, Yowell CA, Fujioka H, Dame JB (2007) Critical roles for the digestive vacuole plasmepsins of *Plasmodium falciparum* in vacuolar function. *Mol Microbiol* 65: 64-75.
31. Sijwali PS, Rosenthal PJ (2004) Gene disruption confirms a critical role for the cysteine protease falcipain-2 in hemoglobin hydrolysis by *Plasmodium falciparum*. *Proc Natl Acad Sci U S A* 101: 4384-4389.
32. Sijwali PS, Koo J, Singh N, Rosenthal PJ (2006) Gene disruptions demonstrate independent roles for the four falcipain cysteine proteases of *Plasmodium falciparum*. *Mol Biochem Parasitol* 150: 96-106.
33. Quevillon E, Spielmann T, Brahim K, Chattopadhyay D, Yeremian E, *et al* (2003) The *Plasmodium falciparum* family of Rab GTPases. *Gene* 306: 13-25.
34. Storm J, Müller S (2010) The phenotype of a *Plasmodium falciparum* phosphoenolpyruvate carboxylase null mutant. *Malaria Journal* 9 (Suppl 2): P49.
35. Reungprapavut S, Krungkrai SR, Krungkrai J (2004) *Plasmodium falciparum* carbonic anhydrase is a possible target for malaria chemotherapy. *J Enzyme Inhib Med Chem* 19: 249-256.
36. Krungkrai J, Krungkrai SR, Supuran CT (2008) Carbonic anhydrase inhibitors: inhibition of *Plasmodium falciparum* carbonic anhydrase with aromatic/heterocyclic sulfonamides-*in vitro* and *in vivo* studies. *Bioorg Med Chem Lett* 18: 5466-5471.
37. Downie MJ, Kirk K, Mamoun CB (2008) Purine salvage pathways in the intraerythrocytic malaria parasite *Plasmodium falciparum*. *Eukaryot Cell* 7: 1231-1237.
38. Rager N, Mamoun CB, Carter NS, Goldberg DE, Ullman B (2001) Localization of the *Plasmodium falciparum* PfNT1 nucleoside transporter to the parasite plasma membrane. *J Biol Chem* 276: 41095-41099.
39. Niikura M, Inoue SI, Mineo S, Yamada Y, Kaneko I, *et al* (2013) Experimental cerebral malaria is suppressed by disruption of nucleoside transporter 1 but not purine nucleoside phosphorylase. *Biochem Biophys Res Commun* . S0006-291X(13)00227-1.
40. Dechamps S, Wengelnik K, Berry-Sterkers L, Cerdan R, Vial HJ, *et al* (2010) The Kennedy phospholipid biosynthesis pathways are refractory to genetic disruption in *Plasmodium berghei* and therefore appear essential in blood stages. *Mol Biochem Parasitol* 173: 69-80.
41. Roggwiler E, Blisnick T, Braun BC (1998) A *Plasmodium falciparum* hemolytic activity. *Mol Biochem Parasitol* 94: 303-307.
42. Ploemen IH, Croes HJ, van Gemert GJ, Wijers-Rouw M, Hermesen CC, *et al* (2012) *Plasmodium berghei* Deltap52&p36 parasites develop independent of a parasitophorous vacuole membrane in Huh-7 liver cells. *PLoS One* 7: e50772.
43. Doolan DL, Hedstrom RC, Rogers WO, Charoenvit Y, Rogers M, *et al* (1996) Identification and characterization of the protective hepatocyte erythrocyte protein 17 kDa gene of *Plasmodium yoelii*, homolog of *Plasmodium falciparum* exported protein 1. *J Biol Chem* 271: 17861-17868.
44. Yoshikawa K, Tanaka T, Ida Y, Furusawa C, Hirasawa T, *et al* (2011) Comprehensive phenotypic analysis of single-gene deletion and overexpression strains of *Saccharomyces cerevisiae*. *Yeast* 28: 349-361.
45. Balu B, Maher SP, Pance A, Chauhan C, Naumov AV, *et al* (2011) CCR4-associated factor 1 coordinates the expression of *Plasmodium falciparum* egress and invasion proteins. *Eukaryot Cell* 10: 1257-1263.

46. Fonager J, Pasini EM, Braks JA, Klop O, Ramesar J, *et al* (2012) Reduced CD36-dependent tissue sequestration of *Plasmodium*-infected erythrocytes is detrimental to malaria parasite growth *in vivo*. *J Exp Med* 209: 93-107.
47. Elliott SR, Spurck TP, Dodin JM, Maier AG, Voss TS, *et al* (2007) Inhibition of dendritic cell maturation by malaria is dose dependent and does not require *Plasmodium falciparum* erythrocyte membrane protein 1. *Infect Immun* 75: 3621-3632.
48. Moumaris M, Sestier C, Miltgen F, Halbreich A, Gentilini M, *et al* (1995) Effect of fatty acid treatment in cerebral malaria-susceptible and nonsusceptible strains of mice. *J Parasitol* 81: 997-999.
49. Nguyen PH, Day N, Pram TD, Ferguson DJ, White NJ (1995) Intraleucocytic malaria pigment and prognosis in severe malaria. *Trans R Soc Trop Med Hyg* 89: 200-204.
50. Amodu OK, Adeyemo AA, Olumese PE, Gbadegesin RA (1998) Intraleucocytic malaria pigment and clinical severity of malaria in children. *Trans R Soc Trop Med Hyg* 92: 54-56.
51. Hanscheid T, Egan TJ, Grobusch MP (2007) Haemozoin: from melatonin pigment to drug target, diagnostic tool, and immune modulator. *Lancet Infect Dis* 7: 675-685.
52. Shio MT, Kassa FA, Bellemare MJ, Olivier M (2010) Innate inflammatory response to the malarial pigment hemozoin. *Microbes Infect* 12: 889-899.
53. Grau GE, Craig AG (2012) Cerebral malaria pathogenesis: revisiting parasite and host contributions. *Future Microbiol* 7: 291-302.
54. Elliott SR, Kuns RD, Good MF (2005) Heterologous immunity in the absence of variant-specific antibodies after exposure to subpatent infection with blood-stage malaria. *Infect Immun* 73: 2478-2485.
55. Pinzon-Charry A, McPhun V, Kienzel V, Hirunpetcharat C, Engwerda C, McCarthy J, Good MF (2010) Low doses of killed parasite in CpG elicit vigorous CD4+ T cell responses against blood-stage malaria in mice. *J Clin Invest* 120: 2967-2978.
56. Celluzzi CM, Liem PL, van de WT, Eling WM (1995) Attenuated immunogenic parasites are essential in the transfer of immunity to virulent *Plasmodium berghei*. *Immunology* 85: 509-515.
57. Eling W, Jerusalem C (1977) Active immunization against the malaria parasite *Plasmodium berghei* in mice: sulfathiazole treatment of a *P. berghei* infection and development of immunity. *Tropenmed Parasitol* 28: 158-174.
58. Schettters TP, van Run-van Breda JH, van de WT, Hermsen CC, Curfs J, Eling WM (1989) Impaired immune responsiveness in *Plasmodium berghei* immune mice. *Parasite Immunol* 11: 519-528.
59. Miyagami T, Igarashi I, Suzuki M (1987) *Plasmodium berghei*: long lasting immunity induced by a permanent attenuated mutant. *Zentralbl Bakteriol Mikrobiol Hyg A* 264: 502-512.
60. Yoneto T, Waki S, Takai T, Tagawa Y, Iwakura Y, *et al* (2001) A critical role of Fc receptor-mediated antibody-dependent phagocytosis in the host resistance to blood-stage *Plasmodium berghei* XAT infection. *J Immunol* 166: 6236-6241.
61. Inoue S, Niikura M, Takeo S, Mineo S, Kawakami Y, *et al* (2012) Enhancement of dendritic cell activation via CD40 ligand-expressing gammadelta T cells is responsible for protective immunity to *Plasmodium* parasites. *Proc Natl Acad Sci U S A* 109: 12129-12134.
62. Janse CJ, Ramesar J, Waters AP (2006) High-efficiency transfection and drug selection of genetically transformed blood stages of the rodent malaria parasite *Plasmodium berghei*. *Nat Protoc* 1: 346-356.
63. Janse CJ, Franke-Fayard B, Mair GR, Ramesar J, Thiel C, *et al* (2006) High efficiency transfection of *Plasmodium berghei* facilitates novel selection procedures. *Mol Biochem Parasitol* 145: 60-70.
64. Lin JW, Annoura T, Sajid M, Chevalley-Maurel S, Ramesar J, *et al* (2011) A Novel 'Gene Insertion/Marker Out' (GIMO) Method for Transgene Expression and Gene Complementation in Rodent Malaria Parasites. *PLoS One* 6: e29289.
65. Braks JA, Franke-Fayard B, Kroeze H, Janse CJ, Waters AP (2006) Development and application of a positive-negative selectable marker system for use in reverse genetics in *Plasmodium*. *Nucleic Acids Res* 34: e39.
66. van Spaendonk RM, Ramesar J, van WA, Eling W, Beetsma AL, *et al* (2001) Functional equivalence of structurally distinct ribosomes in the malaria parasite, *Plasmodium berghei*. *J Biol Chem* 276: 22638-22647.
67. Janse CJ, Haghparast A, Speranca MA, Ramesar J, Kroeze H, *et al* (2003) Malaria parasites lacking eef1a have a normal S/M phase yet grow more slowly due to a longer G1 phase. *Mol Microbiol* 50: 1539-1551.

Supplementary Material

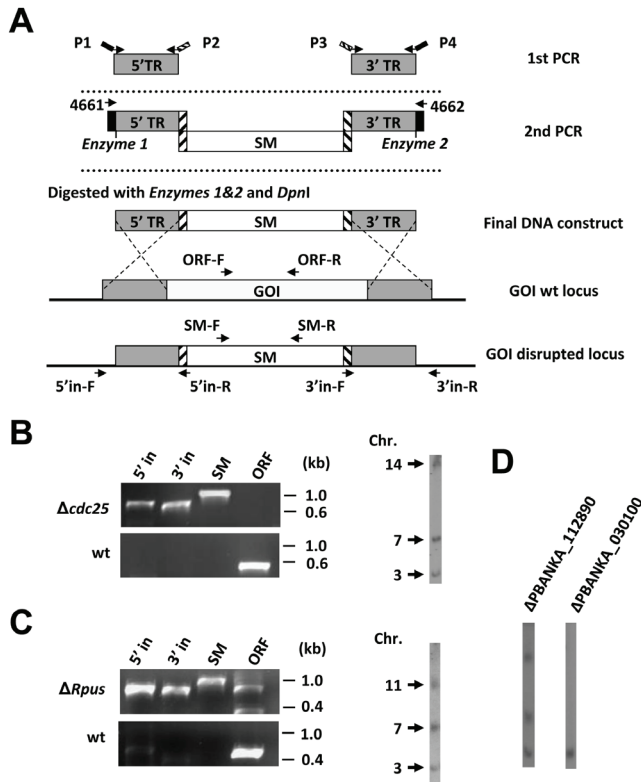


Figure S1. Generation of the *P. berghei* mutants $\Delta cdc25$, $\Delta Rpus$, $\Delta PBANKA_{112890}$ and $\Delta PBANKA_{030100}$.

A. Schematic representation of the double cross-over gene-deletion constructs generated using a modified two-step PCR method and the wild type (wt) loci of the gene of interest (GOI) before and after disruption. In the first PCR reaction, 5'- and 3'- targeting region (TR, grey boxes) of the gene of interest (GOI) were amplified from *P. berghei* ANKA genomic DNA with the primer sets P1/P2 and P3/P4. Primers P2 and P3 have 5'- extensions homologues to the selectable marker cassette (SM) (hatched boxes). This SM cassette was excised from plasmid pL0040 (*hdhfr*) or pL0048 (*hdhfr::yfcu*) digested with *XhoI* and *NotI*. Primers P1 and P4 have 5'-terminal extensions (black boxes) for the second PCR reaction. In the second PCR reaction, the 5'- and 3'- targeting sequences annealed to either side of the SM, and the joint fragment was amplified by the external anchor-tag primers 4661/4662. Before transfection, the PCR construct was digested with 1 (or 2) restriction enzymes that were introduced in primers P1 and P4 to remove the anchor-tag and with *DpnI* to digest any residual plasmid. See Table S1 for primer sequences used to amplify the target regions. Primer positions (arrows) for diagnostic PCRs are shown (see Table S2 for primer sequences and expected product sizes).

B. Diagnostic PCRs (left) and Southern analysis of pulsed field gel-separated chromosomes (right) confirm correct disruption of *cdc25* in mutant $\Delta cdc25$. The following primers were used for diagnostic PCRs: 5' integration (5' in): 5033/4770; 3' integration (3' in): 4771/5100; SM (*hdhfr*): 307C/3187; *cdc25* ORF: 5034/5035. Separated chromosomes were hybridized using a 3'UTR *pbdhfr* probe that recognizes the DNA-construct integrated into the *cdc25* locus on chromosome 14, the endogenous *dhfr/ts* on chromosome 7 and the GFP-luciferase cassette in the *230p* locus on chromosome 3.

C. Diagnostic PCRs (left) and Southern analysis of pulsed field gel-separated chromosomes (right) confirm

correct disruption of *Rpus* in mutant $\Delta Rpus$. The following primers were used for diagnostic PCRs: 5' in: 5880/4770; 3' in: 4771/5881; SM (*hdfhr::yfcu*): 4698/4699; *Rpus* ORF: 5882/5883. Separated chromosomes were hybridized using a 3'UTR *pbdhfr* probe that recognizes the DNA-construct integrated into the *Rpus* locus on chromosome 11, the endogenous *dhfr/ts* on chromosome 7 and the GFP-luciferase reporter cassette in the *230p* locus on chromosome 3.

D. Southern analyses of pulsed field gel-separated chromosomes confirm correct disruption of PBANKA_112890 and PBANKA_030100 in Δ PBANKA_112890 and Δ PBANKA_030100, respectively. Separated chromosomes of Δ PBANKA_112890 were hybridized using a 3'UTR *pbdhfr* probe that recognizes the DNA-construct integrated into the PBANKA_112890 locus on chromosome 11, the endogenous *dhfr/ts* on chromosome 7 and the GFP-luciferase reporter cassette in the *230p* locus on chromosome 3. Separated chromosomes of Δ PBANKA_030100 were hybridized using an *hdfhr* probe that recognizes the DNA-constructs integrated into the PBANKA_030100 locus on chromosome 3.

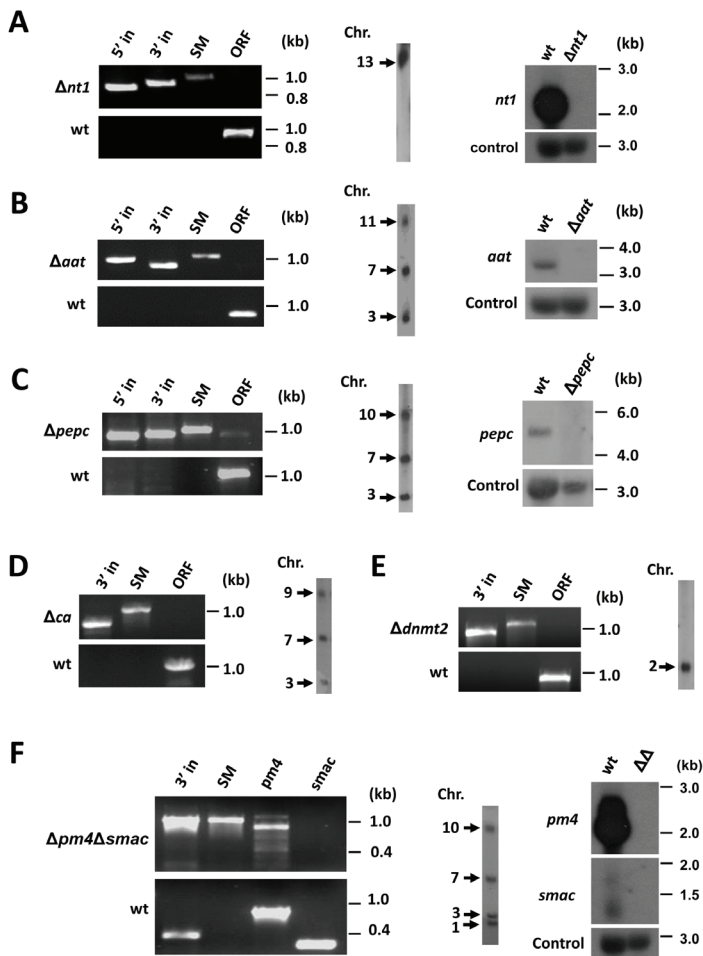


Figure S2. Genotype analysis of the *P. berghei* mutants $\Delta nt1$, Δaat , $\Delta pepc$, Δca , $\Delta dnmt2$ and $\Delta pm4\Delta smac$
 A. Diagnostic PCRs (left) and Southern analysis of pulsed field gel-separated chromosomes (center) confirm

correct disruption of *nt1* in mutant $\Delta nt1$. Northern analysis of blood-stage mRNA (right) confirms the absence of *nt1* transcripts in $\Delta nt1$. The following primers were used for diagnostic PCRs: 5' integration (5' in): 5855/4770; 3' integration: (3' in) 4771/5856; SM (*hdhfr*): 307C/3187; *nt1* ORF: 5857/5858. Separated chromosomes were hybridized using an *hdhfr* probe that recognizes the DNA-construct integrated into the *nt1* locus on chromosome 13. Northern blot was hybridized using a PCR probe recognizing the *nt1* ORF (primers 5857/5858) and with an oligonucleotide probe L644R that recognizes the large subunit ribosomal RNA (as loading control).

B. Diagnostic PCR (left) and Southern analysis of pulsed field gel-separated chromosomes (center) confirms correct disruption of *aat* in mutant Δaat . Northern analysis of blood-stage mRNA (right) confirms the absence of *aat* transcripts in the Δaat . The following primers were used for diagnostic PCRs: 5' in: 7115/4770; 3' in: 4771/7116; SM (*hdhfr::yfcu*): 4698/4699; *aat* ORF: 7117/7118. Separated chromosomes were hybridized using a 3'UTR *pbdhfr* probe that recognizes the construct integrated into the *aat* locus on chromosome 11, the endogenous *dhfr/ts* on chromosome 7 and the GFP-luciferase reporter cassette in the *230p* locus on chromosome 3. Northern blot was hybridized using a PCR probe recognizing the *aat* ORF (primers 7117/7118) and with an oligonucleotide probe L644R recognizing the large subunit rRNA (as loading control).

C. Diagnostic PCR (left) and Southern analysis of pulsed field gel-separated chromosomes (center) confirms correct disruption of *pepc* in mutant $\Delta pepc$. Northern analysis of blood-stage mRNA (right) confirms the absence of *pepc* transcripts in the $\Delta pepc$. The following primers were used for diagnostic PCRs: 5' in: 5977/4770; 3' in: 4771/5978; SM (*hdhfr::yfcu*): 4698/4699; *pepc* ORF: 5979/5980. Separated chromosomes were hybridized using a 3'UTR *pbdhfr* probe that recognizes the construct integrated into the *pepc* locus on chromosome 10, the endogenous *dhfr/ts* on chromosome 7 and the GFP-luciferase reporter cassette in the *230p* locus on chromosome 3. Northern blot was hybridized using a PCR probe recognizing the *pepc* ORF (primers 5979/5980) and with an oligonucleotide probe L644R recognizing the large subunit rRNA (as loading control).

D. Diagnostic PCRs (left) and Southern analysis of pulsed field gel-separated chromosomes (right) confirm correct disruption of *ca* in mutant Δca . The following primers were used for diagnostic PCRs: 3' in: 4771/6984; SM (*hdhfr::yfcu*): 4698/4699; *ca* ORF: 6985/6986. Separated chromosomes were hybridized using a 3'UTR *pbdhfr* probe that recognizes the DNA-construct integrated into the *ca* locus on chromosome 9, the endogenous *dhfr/ts* on chromosome 7 and the GFP-luciferase reporter cassette in the *230p* locus on chromosome 3.

E. Diagnostic PCRs (left) and Southern analysis of pulsed field gel-separated chromosomes (right) confirm correct disruption of *dnmt2* in mutant $\Delta dnmt2$. The following primers were used for diagnostic PCRs: 3' in: 4239/5990; SM (*hdhfr::yfcu*): 4698/4699; *dnmt2* ORF: 5373/5374. Separated chromosomes were hybridized using an *hdhfr* probe that recognizes the DNA-construct integrated into the *dnmt2* locus on chromosome 2.

F. Diagnostic PCRs (left) and Southern analysis of pulsed field gel-separated chromosomes (middle) confirm correct disruption of *pm4* in the $\Delta smac3^{sm}$ mutant background. Northern analysis of blood-stage mRNA (right) confirms the absence of *pm4* and *smac* transcripts in the mutant $\Delta pm4\Delta smac$. The following primers were used for diagnostic PCRs: 3' in: 1662/5517; SM (*hdhfr::yfcu*): 4698/4699; *pm4* ORF: 5518/5519; *smac* ORF: 4204/4205. Separated chromosomes were hybridized using a 3'UTR *pbdhfr* probe that recognizes the DNA-construct integrated into the *pm4* locus on chromosome 10, the endogenous *dhfr/ts* on chromosome 7, the GFP-luciferase reporter cassette in the *230p* locus on chromosome 3 and the 3'*pbdhfr* sequence in the disrupted *smac* locus on chromosome 1. Northern blot was hybridized using a PCR probe recognizing the *pm4* ORF (primers 5518/5519) or the *smarc* ORF (4204/4205) and with an oligonucleotide probe L644R recognizing the large subunit rRNA (as loading control). See Table S2 for primers used for generation of the probes.

Table S1. Targeting constructs and primers

Gene	Construct	Basic construct	Descrip- tion	No.	Sequences	Restriction sites	Description
<i>caf1</i>	PCR1518	pL0040	P1	4674	GAACCTGTA	Asp718I	5'- <i>caf1</i> targeting region F
			P2	4762	CTTTCAATTT		5'- <i>caf1</i> targeting region R
	PCR1585	pL0040	P1	5342	GAACCTGTA	Asp718I	5'- <i>caf1</i> targeting region F
			P2	5343	CATCTACA		5'- <i>caf1</i> targeting region R
<i>pp2c</i>	PCR1699	pL0040	P3	4727	CTTCAATTT	ScaI	3'- <i>caf1</i> targeting region F
			P4	4675	AGTTGGT		3'- <i>caf1</i> targeting region R
	PCR1827	pL0048	P1	5844	GAACCTGTA	Asp718I	5'- <i>pp2c</i> targeting region F
			P2	5845	CATCTACA		5'- <i>pp2c</i> targeting region R
<i>ApiAP2</i>	PCR1831	pL0048	P3	4725	CTTCAATTT	ScaI	3'- <i>pp2c</i> targeting region F
			P4	4673	AGTTGGT		3'- <i>pp2c</i> targeting region R
	PCR1831	pL0048	P1	5999	GAACCTGTA	Asp718I	5'- <i>ApiAP2</i> targeting region F
			P2	6000	CATCTACA		5'- <i>ApiAP2</i> targeting region R
PBANKA_020890	PCR1691	pL0040	P3	6001	CTTCAATTT	ScaI	3'- <i>ApiAP2</i> targeting region F
			P4	6002	AGTTGGT		3'- <i>ApiAP2</i> targeting region R
	PCR1774	pL0048	P1	5868	GAACCTGTA	Asp718I	5'-PBANKA_020890 targeting region F
			P2	5869	CATCTACA		5'-PBANKA_020890 targeting region R
PBANKA_112890	PCR1830	pL0048	P3	5870	CTTCAATTT	HindIII	3'-PBANKA_020890 targeting region F
			P4	5871	AGTTGGT		3'-PBANKA_020890 targeting region R
	PCR1830	pL0048	P1	6672	GAACCTGTA	SacII	5'- PBANKA_112890 targeting region F
			P2	6673	CATCTACA		5'- PBANKA_112890 targeting region R
PBANKA_030100	PCR1883	pL0048	P3	6674	CTTCAATTT	EcoRI	3'- PBANKA_112890 targeting region F
			P4	6675	AGTTGGT		3'- PBANKA_112890 targeting region R
	PCR1883	pL0048	P1	6731	GAACCTGTA	HindIII	5'- PBANKA_030100 targeting region F
			P2	6732	CATCTACA		5'- PBANKA_030100 targeting region R
<i>cdc25</i>	PCR1524	pL0040	P3	6733	CTTCAATTT	KpnI	3'- PBANKA_030100 targeting region F
			P4	6734	AGTTGGT		3'- PBANKA_030100 targeting region R
	PCR1524	pL0040	P1	4676	GAACCTGTA	Asp718I	5'- <i>cdc25</i> targeting region F

<i>Rpus</i>	P2	4728	CATCTACAAGCATCGTGGACCTCAATAATATTTTGGGATGCTTCTG	5'-cdc25 targeting region R
	P3	4729	CCTTCAATTTCCGATCCACTAGCATTTTGAAGTTCCAAATATGTC	3'-cdc25 targeting region F
	P4	4677	AGGTTGGTCATTGACACTAGCAGTACTGTTATCCAGGACAATTTGC	3'-cdc25 targeting region R
	PCR1775	pl0048		Scal
<i>Rpus</i>	P1	5876	GAACTCGTACTCCTTGGTGACGGGTACCTTCATGATTTGTACCTAATCTC	5'-Rpus targeting region F
	P2	5877	CATCTACAAGCATCGTGGACCTCTTGTTTCCCTCCTAATAGG	5'-Rpus targeting region R
	P3	5878	CCTTCAATTTCCGATCCACTAGTAGATAACGCAATCCCTCATG	3'-Rpus targeting region F
	P4	5879	AGGTTGGTCATTGACACTCAGCGGTACCCCTAATGTTTCAATGATTTCC	3'-Rpus targeting region R
<i>ck</i>	P1	5193	GAACTCGTACTCCTTGGTGACGGGTACCAATATTAGATCTTGTACAATTATAATTC	5'-ck targeting region F
	P2	5194	CATCTACAAGCATCGTGGACCTCACTTGAGATTTTTTATTTTGTATATG	5'-ck targeting region R
	P3	5195	CCTTCAATTTCCGATCCACTAGTCTATTGATTTACTACAGACAC	3'-ck targeting region F
	P4	5196	AGGTTGGTCATTGACACTAGCAGTACTATATAATTTCAAATGTTTGAAGTG	3'-ck targeting region R
<i>cept</i>	P1	5205	GAACTCGTACTCCTTGGTGACGGGTACCCATTTTCATAAATGCATAACTG	5'-cept targeting region F
	P2	5206	CATCTACAAGCATCGTGGACCTCTTTCATAACTTGCATTTCTC	5'-cept targeting region R
	P3	5207	CCTTCAATTTCCGATCCACTAGGAGGGTAAATATACATCG	3'-cept targeting region F
	P4	5208	AGGTTGGTCATTGACACTCAGCAGTACTGATCATTAGCATTTATGGTGTG	3'-cept targeting region R
<i>ek</i>	P1	5794	GAACTCGTACTCCTTGGTGACGGGTACCCGATCAATTTCCCTTATCG	5'-ek targeting region F
	P2	5795	CATCTACAAGCATCGTGGACCTCAACGGTAAATGCAATTTCCAG	5'-ek targeting region R
	P3	5796	CCTTCAATTTCCGATCCACTAGTCCCAACGTTTATAATTTACTG	3'-ek targeting region F
	P4	5797	AGGTTGGTCATTGACACTAGCAGTACTGGCCAAATGAACAGCTC	3'-ek targeting region R
<i>nt1</i>	P1	5851	GAACTCGTACTCCTTGGTGACGGGTACCTGTCCATCGTTATATTTATCC	5'-nt1 targeting region F
	P2	5852	CATCTACAAGCATCGTGGACCTCTTTATGAAAAATGGAGAATTCG	5'-nt1 targeting region R
	P3	5853	CCTTCAATTTCCGATCCACTAGATAAATAAATCAATGTGTGCCTC	3'-nt1 targeting region F
	P4	5854	AGGTTGGTCATTGACACTCAGCAGTACTATCTCGAATGGCTATTCG	3'-nt1 targeting region R
<i>amino acid transporter</i>	P1	7111	GAACTCGTACTCCTTGGTGACGGTCCGGATGCTGCTGTATTTTATTCTGG	5'-aat targeting region F
	P2	7112	CATCTACAAGCATCGTGGACCTCAATAGATAGCAATCATTATACACC	5'-aat targeting region R
	P3	7113	CCTTCAATTTCCGATCCACTAGGAAGTGTCTTTTACTTTATACC	3'-aat targeting region F
	P4	7114	AGGTTGGTCATTGACACTCAGCTCCGATGCAATTTATAAGCCGAGCTTG	3'-aat targeting region R
<i>pepc</i>	P1	5973	GAACTCGTACTCCTTGGTGACGGGTACCGATAATGCTACTTTTTCTTTTG	5'-pepc targeting region F
	P2	5974	CATCTACAAGCATCGTGGACCTCTATATAGCTGTCTTGAGACAC	5'-pepc targeting region R
	P3	5975	CCTTCAATTTCCGATCCACTAGGCAAAATACCGGATAACTC	3'-pepc targeting region F
	P4	5976	AGGTTGGTCATTGACACTCAGCGGTACCTTTAGGAAACCAATCAAAGAG	3'-pepc targeting region R

ca	PCR1881	pL0048	P1	6979	GAAC T CGTACTCCTTGGT G ACG T CG G ACCTTTGGATATTACAACATATTATAC	<i>Nru</i> I	5'- <i>ca</i> targeting region F
			P2	6980	CATCTACAAGCAGCTCGACCTCGAATTACAAAACCTGGATAATCAC		5'- <i>ca</i> targeting region R
			P3	6981	CCTTCAATTTCCGATCCACTAGTTTTTTTGGTGAATGATTAGG		3'- <i>ca</i> targeting region F
			P4	6982	AGTTGGTCATTGACACTAGCTCG G ACTGGACATATTTCAATATTAC	<i>Nru</i> I	3'- <i>ca</i> targeting region R
hemolysin	PCR1591	pL0040	P1	5386	GAAC T CGTACTCCTTGGT G ACG G AT C CTCTCTAAAATCCCATATACAC	<i>Bam</i> HI	5'- <i>hemolysin</i> targeting region F
			P2	5387	CATCTACAAGCAGCTCGACCTCCTTTGGGGTTTTATGTGAG		5'- <i>hemolysin</i> targeting region R
			P3	5388	CCTTCAATTTCCGATCCACTAGATATGTCCCAATCAAATACAC		3'- <i>hemolysin</i> targeting region F
			P4	5389	AGTTGGTCATTGACACTAGCTAG T ACTATTACTTGAACATAGGCAC	<i>Sca</i> I	3'- <i>hemolysin</i> targeting region R
hep17	pL1415	pL0037	P1	3953	ATGCTCGT G ACATATTGTACATAAGCCCAATTTGGC	<i>Sal</i> I	5'- <i>hep17</i> targeting region F
			P2	3955	ATGCTCAAGCTTAGGCCATGAAAAGGAGGAGC	<i>Hind</i> III	5'- <i>hep17</i> targeting region R
			P3	3596	ATGCTCGAA T TCGTAGCCTTACTAAGGTCATGCG	<i>Eco</i> RI	3'- <i>hep17</i> targeting region F
			P4	3597	ATGCTCCCGGGTGTATCTCTTATATCGATTGTGCG	<i>Xma</i> I	3'- <i>hep17</i> targeting region R
PCR1555	pL0040	P1	5213	GAAC T CGTACTCCTTGGT G ACG G TAC C TATTTTATGTAGCTCCTCC	<i>Asp</i> 718I	5'- <i>hep17</i> targeting region F	
			P2	5214	CATCTACAAGCAGCTCGACCTCAGAAAATAGTGTATATGTG		5'- <i>hep17</i> targeting region R
			P3	5215	CCTTCAATTTCCGATCCACTAGTATCATAAAAAGTTTCGACTC		3'- <i>hep17</i> targeting region F
			P4	5216	AGTTGGTCATTGACACTAG T ACTTTAATGTCCCAATTATGG	<i>Sca</i> I	3'- <i>hep17</i> targeting region R
dnm12	pL1789	pL0035	P1	6468	GCCC A AGCTTATAAGCCGTGGAAAGG T G	<i>Hind</i> III	5'- <i>dcm</i> targeting region F
			P2	6469	TTC C CGGGGCCCCATAATATACAAAG T GC	<i>Sac</i> II	5'- <i>dcm</i> targeting region R
			P3	6373	CCG T CGAGAGCTTTAAACACACAGTTAAGAAA T TG	<i>Xho</i> I	3'- <i>dcm</i> targeting region F
			P4	6374	GCGGG A TATCGTTAAATACTAGCATGTAA T TGG	<i>Eco</i> RV	3'- <i>dcm</i> targeting region R
pm4	pL1873	pL0048	P1	L6861	GAAC T CGTACTCCTTGGT G ACG T CG G ACCTGTCCGGGTACTCAG	<i>Nru</i> I	<i>pm4</i> 5'-targeting sequence, F
			P2	L6862	CATCTACAAGCAGCTCGACCTCAAGCTTCCCAATCTCTTAA T AAGG		<i>pm4</i> 5'-targeting sequence, R
			P3	L6863	CCTTCAATTTCCGATCCACTAGACAGCTACCATAA C ATCG		<i>pm4</i> 3'-targeting sequence, F
			P4	L6864	AGTTGGTCATTGACACTAG T ACTTCTCAAAATCAAATAT C AGG	<i>Nru</i> I	<i>pm4</i> 3'-targeting sequence, R
anchor-tag primers							
				4661	GAAC T CGTACTCCTTGGT G ACG		anchor-tag primer, F
				4662	AGTTGGTCATTGACACT C AGC		anchor-tag primer, R

Red: restriction sites

Blue: 5'- extensions homologues to the *hdf1r::yfcu* selectable marker cassette from pL0048

Green: 5'- extensions homologues to the anchor tag primers 4661/4662

Table S2. Primers for genotyping

Genes	No.	Primer sequences	Description	Integration PCR Pair	Expected product size (bp)
Primers for PCR analyses					
caf1	5029	CATGTATGGATACAATTTAATCG	<i>caf1</i> 5' in-F for pL1518	4770	801
	2849	aaacaattgAAAATCGTAGATGTATGG	<i>caf1</i> 5' in-F for pL1585	4770	788
	5030	GTTTACATCACTTCCATAGTC	<i>caf1</i> 3' in-R	4771	837
	5031	GTTGTTAGTATTGGCACAC	<i>caf1</i> ORF-F		578
	5032	TTCATAGCACAAATTGTTACTC	<i>caf1</i> ORF-R		
pp2c	5846	AGATTGGTGTATATAAAAGACTG	<i>pp2c</i> 5'in-F	4770	932
	4978	CCGATTAATGATATGCGTG	<i>pp2c</i> 3'in-R	4771	853
	5847	CGGCATTTTAGAATGTATGAC	<i>pp2c</i> ORF-F		1022
	4980	GGAACCTCCGGTATTTGAG	<i>pp2c</i> ORF-R		
ApiAP2	6003	GCGAATGGTTATTATACATGC	<i>ApiAP2</i> 5'in-F	4770	859
	6004	TGTAAC TATTGTTCTGTTTCC	<i>ApiAP2</i> 3'in-R	4771	877
	6005	GTGATAAATTTCCATGAATTGC	<i>ApiAP2</i> ORF-F		850
	6006	AGAGGTTAGATGATTGATGTG	<i>ApiAP2</i> ORF-R		
PBANKA_020890	5872	TCGAAAATTAGCATATGAAGG	PBANKA_020890 5'in-F	4770	870
	5873	CCAATTACACCAAAATTTAC	PBANKA_020890 3'in-R	4771	610
	5874	ATATTAGAAGAAGCACTTATGG	PBANKA_020890 ORF-F		618
	5875	TTCATAAGGAGCATCATGAC	PBANKA_020890 ORF-R		
cdc25	5033	TCTACTATTTCTCATTTCTTCAC	<i>cdc25</i> 5' in-F	4770	893
	5100	TAATGTGAAGCCACATCC	<i>cdc25</i> 3' in-R	4771	835
	5034	GGAAAATAACAGCGTCAG	<i>cdc25</i> ORF-F		567
	5035	CCTACATAGACGTTGTCCAC	<i>cdc25</i> ORF-R		
Rpus	5880	ACGTGTAATGTATTATATACC	<i>Rpus</i> 5' in-F	4770	856
	5881	TTAATTGAAATCGAACATTTGG	<i>Rpus</i> 3' in-R	4771	831
	5882	CCCCAAAGATTCTCACAC	<i>Rpus</i> ORF-F		597
	5883	CCAGCATTTTCGTTAACTC	<i>Rpus</i> ORF-R		
Rab5a	5348	CCAGCAAATATCATATGGAG	<i>rab5a</i> 5'in-R	3189	1193
	5349	CATGAATCCAAGTATTATGTG	<i>rab5a</i> 3'in-F	4239	1015
	5350	AATAATAATAACGGTGATAATCG	<i>rab5a</i> ORF-R		506
	5351	TTTGTTTTTTGTGTTTTTCAC	<i>rab5a</i> ORF-F		
Rab5b	6909	TTAAATTTGTTAGTTGCTTTGTG	<i>rab5b</i> 5'in-F	3189	1221
	6910	TATGCCAAATTAATAGAAAATTCAG	<i>rab5b</i> 3'in-R	4239	1015
	6911	GCAGCTTTTTGCACCATAC	<i>rab5b</i> ORF-F		555
	6912	TTACCTCTGAATTTATTTTTGTG	<i>rab5b</i> ORF-R		
Rab11b	6297	CTTTACCAATTTTGCTAAATAAGG	<i>rab11b</i> 5'in-F	3189	853
	6298	TCTATTTCAAAGGTGCAAGAG	<i>rab11b</i> 3'in-R	4239	896
	6299	CCAGGTAACAACATTTATTGTG	<i>rab11b</i> ORF-F		992
	6300	GCACCTTTCATATGTTTCATGAC	<i>rab11b</i> ORF-R		
ck	5840	GCATTTGTTTATATATCACAGAG	<i>ck</i> 5' in-F	4770	640
	5197	GTAGCATGGAATAATGTTCTC	<i>ck</i> 3' in-R	4771	786
	5198	TGAAGTATATGAAACGATGAG	<i>ck</i> ORF-F		474
	5199	GTAGCTATGAAATTATATCCAG	<i>ck</i> ORF-R		
cept	5972	TTATCATAATAAAGGCATCTACC	<i>cept</i> 5' in-F	4770	942
	5210	TGATGATCTCGAATATACAG	<i>cept</i> 3' in-R	4771	726

	5211	TTATGCGAACCGTATTGG	<i>cept</i> ORF-F		
	5212	AAACGTAAGTAATTGC	<i>cept</i> ORF-R		546
ek	5836	TTGTTTATTTAAGCACTTTCC	<i>ek</i> 5' in-F	4770	917
	5837	GATGCACAAAATGATGCAG	<i>ek</i> 3' in-R	4771	759
	5838	ATACAGAAATTCAGAAAAACG	<i>ek</i> ORF-F		
	5839	CGGGTTGGTATTAATTTCC	<i>ek</i> ORF-R		1042
nt1	5855	CGTCAACTTAAAAATTGTATGC	<i>nt1</i> 5' in-F	4770	791
	5856	TGTTTTACGGATTAAGATCAC	<i>nt1</i> 3' in-R	4771	883
	5857	CTGTTTTAGCCCTTTTCG	<i>nt1</i> ORF-F		
	5858	GTATAAGCATGTGGTTAGC	<i>nt1</i> ORF-R		995
aat	7115	AAAATGAAATTAATCCAAAACAATAC	<i>aat</i> 5' in-F	4770	1034
	7116	ATTATACCCATAGCAAGAATTGTG	<i>aat</i> 3' in-R	4771	885
	7117	TGATGTGGTTCAAAATATAGTG	<i>aat</i> ORF-F		
	7118	TAATGGGAGCACTAATAAGC	<i>aat</i> ORF-R		883
pepc	5977	GGGCTTTATACTATTTTTTTGTC	<i>pepc</i> 5' in-F	4770	954
	5978	TATCGTGGTAGAGTAAAACG	<i>pepc</i> 3' in-R	4771	997
	5979	CATGATTTATCCGAAAAATATAGTG	<i>pepc</i> ORF-F		
	5980	GTGCTTTATATACATATACAACAC	<i>pepc</i> ORF-R		1003
ca	6983	ACCCCACTTATTTAAAGATAG	<i>ca</i> 5' in-F	4770	798
	6984	CAAAGATTCGATTATTTCAAAGAG	<i>ca</i> 3' in-R	4771	836
	6985	AGAGCGAATATTTGAATTGC	<i>ca</i> ORF-F		
	6986	CATAATCATAGATCTCATTAGTACTG	<i>ca</i> ORF-R		1013
hemolysin	5390	ACTGTATATGGATGCATGG	<i>hemolysin</i> 5' in-F	4770	810
	5391	AATTTCTTTGGGTTGACG	<i>hemolysin</i> 3' in-R	4771	734
	5392	ATGAAAAAACGCTGCTGAG	<i>hemolysin</i> ORF-F		
	5393	TGAGGAAATAAGACATACCAG	<i>hemolysin</i> ORF-R		561
hep17	4355	ttgcatactcgagCAAACCCGAGAATAAAATTAATTTCC	<i>hep17</i> 5' in-F	4770	1121
	4356	aataaactcgagCAAATGGTGATCCAAATATAAAGGCC	<i>hep17</i> 3' in-R	4771	899
	3942	CGATTCAAAAAATATAAATGTAGAG	<i>hep17</i> ORF-F		
	3911	GGCTAACATTTCTAAAAGTAGAG	<i>hep17</i> ORF-R		476
dnmt2	5990	ATTACTATTTACAACGGATGC	<i>dcm</i> 3' in-R	4239	953
	5373	TGATTCGGAGGAAAATTCAC	<i>dcm</i> ORF-F		
	5374	TGCTTGAAATTAATTACCACC	<i>dcm</i> ORF-R		936
pm4	5517	CATGCGAATAAATGTCTCAG	<i>pm4</i> 3' in-R	1662	1122
	5518	TCCGAATATTTAACAATTCGTG	<i>pm4</i> ORF-F		
	5519	ATGAAAGGTACTGGAATACTC	<i>pm4</i> ORF-R		869
smac	4204	CACCATGGATAAATACGATAACAATGGAAAATCATTGG	<i>smac</i> ORF-F		
	4205	AATGATCTTAGAATTATGTCTTAGCCTTTCC	<i>smac</i> ORF-R		328
Universal primers					
	4770	CATCTACAAGCATCGTCGACCTC	<i>5'pbeef1a</i> R, 5'in-R		
	4771	CCTTCAATTCGGATCCACTAG	<i>3'pbdhfr/ts</i> F, 3'in-F		
	3189	CTGGTGCTTTGAGGGGTG	<i>5'eef1a</i> R, 5'in-R		
	4239	GATTTTTAAATGTTTATAATATGATTAGC	<i>3'pbdhfr/ts</i> F, 3'in-F		
	1662	GATTCATAAATAGTTGGACTTG	<i>3'pbdhfr/ts</i> F		
	307C	GCTTAATCTTTTCGAGCTC	<i>hdhfr</i> F, SM-F		
	3187	GTGTAGTCTGTGTCATGTC	<i>3'pbdhfr/ts</i> R, SM-R		1009
	4698	GTTTCGTAACCTGCATCGTC	<i>hdhfr</i> F, SM-F		
	4699	GTTTGAGGTAGCAAGTAGACG	<i>yfcu</i> R, SM-R		1108

Other Primers for generation of probes

692	CTTATATATTATACCAATTG	3' <i>pbdhfr</i> /ts F	404
693	GTTTTTTTTTAATTTTCAAC	3' <i>pbdhfr</i> /ts R	
886	GGAAGATCTATGGTTGGTTCGCTAAACTGCATCG	<i>hdhfr</i> F	582
887	GGAAGATCTTTAATCATTCTTCTCATATACTTC	<i>hdhfr</i> R	
L644R	GAAACAGTCCATCTATAATTG	<i>lsu rrna</i> (A-type)	

pb = *P. berghei*, h = human, y = yeast

5' in=5' integration PCR; 3' in=3' integration PCR

CHAPTER 7

Conclusions and Discussion

The principal aim of the studies described in this thesis was to generate growth- and virulence-attenuated blood stage parasites in the rodent malaria model *P. berghei*, which may serve as immunizing agents and as tools to study correlates of disease and protection. Specifically, we aimed to create genetically attenuated blood stage parasites that induce low parasitemia, self-resolving short-term blood infections, which induce protective immunity. In order to screen a large number of potential genetically attenuated (blood stage) parasites (GAP_{BS}), we developed methods to improve both transfection technology to generate GAP and for analysing GAP growth-characteristics during a blood stage development.

1. Progress in genetic modification technology for *Plasmodium* rodent malaria parasites

Genetic modification of the rodent malaria parasites, *P. berghei* and *P. yoelii*, is limited by the paucity of drug-selection markers that permit the selection of transformed mutants, and this in turn also hampers multiple genetic modifications in the same mutant. The novel GIMO-transfection method described in Chapter 2 permits the generation of mutants that stably express heterologous proteins and are free of drug-selectable markers in their genome, thereby facilitating further genetic modification of the transgenic parasites. In addition, it provides a fast and simple way to ‘gene complement’ gene deletion/mutation mutants (i.e. restoring the wt phenotype upon restoration of the disrupted gene). The GIMO method not only simplifies and speeds up both the generation of marker-free transgenic parasites and gene complementation experiments, the application of this method also greatly reduces the numbers of animals required to generate and complement mutants.

GIMO transfection uses negative selection to remove the positive-negative selectable marker cassette, *hdhfr::yfcu* and thereby generate transgenic mutants ready for subsequent modifications. Since GIMO-transfection is a simple, fast and efficient approach to generate mutants permissive to further genetic modification, we recommend that, where possible, transfection of *P. berghei* and *P. yoelii* parasites be performed with DNA-constructs that contain the *hdhfr::yfcu* selectable marker cassette. A recent study has reported a ‘recombineering’ system for high-throughput, genome wide and efficient generation of gene targeting constructs for *P. berghei* [1]. This development can be partnered with GIMO transfection by ensuring all the targeting constructs have a positive-negative (*hdhfr::yfcu*) selectable marker cassette. Consequently all resulting mutants would be receptive to GIMO-transfection thereby permitting further modification (e.g.

reporter protein expression) and complementation. In addition to the use of the GIMO-transfections described in this thesis, we have generated a wide variety of new transgenic *P. berghei* reporter parasites that express fluorescent- and luminescent-markers under the control of different *Plasmodium* promoters, all of which do not contain a drug-selectable marker (data not shown). In addition, we have generated *P. berghei* parasites expressing the (immunological) reference protein ovalbumin (OVA) under the control of different promoters (data not shown), as such parasites are excellent tools to further unravel (protective) immune responses induced by growth- and virulence-attenuated GAP_{BS} as described in Chapter 6.

2. Generation of growth- and virulence-attenuated attenuated blood stage parasites (GAP_{BS}) by targeted gene deletion

In this study, we targeted 41 genes for targeted disruption in the virulent rodent parasite, *P. berghei* ANKA, in order to generate GAP_{BS} that are both growth- and virulence-attenuated and can serve as protective immunogens. Specifically, we aimed to create virulence-attenuated GAP_{BS} that induce short-term blood infections with low parasitemias and are resolved by the host and induce protective immunity. The genes we targeted for deletion were selected either based on the published roles of their encoding proteins as being important for blood stage development, or based on *P. falciparum* studies where effecting their encoded protein expression produces a growth delay phenotype.

2.1 Genes encoding rhomboid proteases

We included all 8 genes encoding *Plasmodium* rhomboids for targeted deletion because of important roles that several of rhomboid proteases have in host cell invasion and pathogenesis in *Plasmodium* and *Toxoplasma* infections [2,3]. In addition, it has been shown that *P. berghei* and *P. yoelii* mutants lacking rhomboid 1 (ROM1) show a reduction in their blood stage growth rates [4,5]. In Chapter 4, we show successful generation of gene-deletion mutants for *rom1*, 3, 9 and 10, while multiple attempts to disrupt *rom4*, 6, 7 and 8 were unsuccessful. However, blood stages of all 4 gene-deletion mutants showed normal growth and virulence characteristics, indicating that these proteins are redundant and/or that their functions can be fulfilled by other (possibly rhomboid) proteases. It had been reported that *P. berghei* and *P. yoelii* mutants lacking ROM1 exhibit a slight growth defect and are less virulent in mice than wild type parasites [4,5]. In contrast, we were unable to detect either a growth or virulence phenotype of two independent *P. berghei*

Δrom1 lines. The cause for these discrepancies in blood stage phenotypes between our and the *P. berghei* mutant reported by Srinivasan *et al.* [4] is unknown. Cloned lines of wild type *P. berghei* ANKA parasites can differ in their growth and virulence characteristics [6] and environmental factors have been shown to influence the course of infections in mice [7]. It is therefore possible that the growth and virulence phenotype of the single *Δrom1* mutant reported by Srinivasan *et al.* [4] may be unrelated to the disruption of *rom1*. The interclonal and environmental induced differences in growth and virulence characteristics of *P. berghei* blood stages emphasize the importance to analyse the phenotype of at least two independently-derived mutants in gene-deletion studies, and/or to perform gene complementation.

Interestingly, mutants lacking rhomboid 3 (ROM3) expression exhibit a strong and clear phenotype during mosquito-stage development. While *P. berghei* mutants lacking ROM3 are capable of producing normal numbers of oocysts, these oocysts show a complete absence of sporozoite formation. This is the first apicomplexan rhomboid identified to play such a vital role in sporogony. Mutant oocysts show clear signs of stalled DNA replication and fail to form individual sporozoites, and remain highly vacuolated. Further research is needed to identify the substrates of ROM3 in oocysts. We identified a number of possible substrates of ROM3, based on the published proteome data of oocysts and sporozoite proteins (www.plasmodb.org), which are predicted to contain a single transmembrane domain and encode a signal peptide. However, since we observed the expression of ROM3 in gametocytes and ookinetes, but not in developing and mature oocysts, it is very much possible that the ROM3 substrate(s) is (are) also present and cleaved in gametocytes/ookinetes.

2.2 Genes encoding hemoglobinsases

We chose to target 12 *P. berghei* genes that encode proteins with predicted or possible roles in hemoglobin (Hb) digestion because of the importance that Hb digestion has in parasite blood stage development [8]. Further, it has been shown that *P. berghei* and *P. falciparum* mutants lacking expression of certain hemoglobinsases, while viable, exhibit reduced growth rates, and some mutants in *P. berghei* are both growth and virulence attenuated [9,10]. As shown in Chapter 5, we were able to successfully generate gene deletion mutants for 9 of the 12 'hemoglobin digestion genes', which indicates a high level of redundancy in the Hb degradation pathway. The viability of mutant parasites lacking hemoglobinsases, indicates either that other enzymes can compensate their function(s) or that *P. berghei* can obtain necessary amino acids from other sources, for example, from the catabolism of proteins other than Hb or by scavenging free amino acids from

the reticulocyte cytoplasm or serum (see also below). Four of the nine mutants showed normal growth characteristics in mice, whereas 5 mutants showed a significantly reduced growth rate compared to wild type parasites. Four of these 5 mutants are reduced in their virulence, specifically, do not induce experimental cerebral malaria (ECM) in susceptible mice. In addition to these single gene-deletion mutants, we also generated a double gene-deletion mutant, $\Delta pm4\Delta bp2$, lacking two hemoglobinases plasmepsin-4 (PM4) and berghepain-2 (BP2). The 2 endoproteases are responsible for initial and critical cleavage of the native Hb and it was therefore highly unexpected to be able to generate this double gene-deletion mutant, since it indicates that $\Delta pm4\Delta bp2$ parasites may survive inside reticulocytes without Hb digestion. The initial cleavage of native Hb is mediated by aspartic and papain-like cysteine endoproteases in digestive vacuole (DV). In the *P. falciparum* DV, there are four aspartic proteases termed plasmepsins and two papain-like cysteine proteases termed falcipains capable of hydrolyzing native Hb [11–15]. In *P. berghei* PM4 is the syntenic ortholog of all four *P. falciparum* plasmepsins I-IV [10] and berghepain 2 (BP2) is the syntenic ortholog of the DV falcipains (falcipain 2 and 3) (www.plasmodb.org). The simultaneous absence of these two enzyme activities in *P. berghei* was therefore expected to result in the absence of Hb proteolysis in the DV. We show that $\Delta pm4\Delta bp2$ parasites can complete asexual development in reticulocytes without hemozoin (Hz) formation, a detoxification product of Hb degradation. These observations have important implications for *Plasmodium* drug development and drug resistance, in particular for human malaria parasites (e.g. *P. vivax*) that can develop inside reticulocytes in which Hb digestion may not be essential (see below). The presence of low Hz amounts in a proportion of $\Delta pm4\Delta bp2$ parasites indicates that Hb can still be degraded to some degree in the absence of PM4 and BP2. At present we cannot formally exclude a role of other *P. berghei* proteases in the initial step of Hb digestion, which would compensate (albeit poorly) for the loss of PM4 and/or BP2. Further research is needed to investigate whether the remaining low-level of Hz formation in $\Delta pm4\Delta bp2$ parasites is due to specific cleavage of some Hb molecules by other enzymes or results from a non-specific disassembly of the Hb tetramer.

Interestingly, while it has been reported that C57BL/6 mice infected with $\Delta pm4$ cannot resolve their infections and die from hyper-parasitemia [10], we found that all C57BL/6 mice infected with $\Delta pm4\Delta bp2$ resolve their infections. In addition, we found that BALB/c infected with $\Delta pm4\Delta bp2$ can resolve this infection without developing hyper-parasitemias (i.e. >50%) when i.p infected with 10^5 parasites. These results demonstrate that it is possible to generate further virulence-attenuated parasites through the deletion of multiple genes, as was also reported by Spaccapelo *et al.* [17] with mutants that lack expression of both PM4 and MSP7. Below we discuss in more detail the future research

on these growth- and virulence-attenuated parasites in identifying the critical host and pathogen components inducing (protective) immunity and virulence, and to better understand the differences in induced rather than acquired immune responses against a *Plasmodium* infection and this may help to create an effective and the broadest possible anti-parasite vaccine.

3. Future research on growth- and virulence-attenuated *P. berghei* mutants

3.1 Analysis of immune responses induced by infection with growth- and virulence-attenuated parasites

Our studies show that it is possible to generate mutants with strongly reduced growth rates that do not induce ECM, and that through the deletion of multiple genes it is possible to create mutants that produce self-resolving infections in mice without producing hyper-parasitemia (Chapter 6). However, mice infected with these mutants can still develop high parasitemias ranging between 10–50%. Till now, we have not yet been able to generate mutants that produce low-level infections that resolve shortly after parasite inoculation into the blood and without developing high parasitemias (<10%). Even with parasites that have strongly reduced growth rates, both C57BL/6 and BALB/c mice are unable to rapidly mount an effective immune response that can control an acute infection. It is, however, important to note that in all our experiments the mice were infected with relatively high numbers of parasites ($10^5 - 10^6$). It is possible that starting infection with lower numbers of parasites would allow the mice to control infections before developing high parasitemias or would lead to infections with very low or even sub-patent parasitemias [18]. For *P. falciparum* it has been postulated that infection with low numbers of infected red blood cells (iRBC) under curative chemotherapy generates protective immune responses that are marked by absent or low levels of antibodies and strong cell-mediated responses, including upregulation of nitric oxide synthase, CD4+/CD8+ proliferative T-cell and INF- γ responses [19–21]. Protective immunity with *P. berghei* infections in mice have been mainly reported from immunization requiring repeated, prolonged infections cleared by drug treatment or after a self-resolving and sustained infection with an avirulent parasite line [10,22–27]. The protective immune responses in these mice are largely antibody-dependent, where the iRBC of wt challenge are opsonized and then removed in the spleen by phagocytosis [10,28,29]. These studies, and studies of experimental *P. falciparum* infections in humans where protective cellular immune responses are induced with low numbers of iRBC, would suggest that the induction of

protective immunity might require different parasite loads depending on the nature of the (cellular or humoral) immune responses required.

When studying host-cell interaction, pathology and immunity induced by *Plasmodium* infections in rodents, the differences between the rodent and human host have to be taken into consideration. Differences in both host physiologies and host immune responses to infections, will strongly influence both how a host copes with an infection and how a malarial disease will manifest. Clearly, further research is required to determine both parasite and host factors that can induce protective immune responses against blood stage infection and to understand the critical differences in protective immunity induced by *P. falciparum* infections in humans and rodent *Plasmodium* infection in mice. Notwithstanding these considerations, I believe that the use of attenuated blood stage parasites generated in this, and in future studies, can be very useful tools to better understand induced protective immunity against *Plasmodium* blood stages and may help to create an effective anti-parasite vaccine.

3.2 Defining the parasite factors that induce ECM

We found that all mutants that have reduced Hz production do not induce ECM (Chapter 6). Hz is released into the circulation at schizont rupture and it is rapidly removed by phagocytosis mainly in the spleen and liver. Upon phagocytosis, Hz cannot be further degraded and persists for prolonged periods in host tissues and has long been considered as a virulence factor. It has been shown that the number of Hz-containing leukocytes in the peripheral blood correlates with disease severity in *P. falciparum*-infected patients [30,31]; and several inflammatory and immune-modulatory effects of Hz have been reported (reviewed in [32,33]). Therefore, the amount of Hz that is released by the parasite in the host may play a critical role in both inducing inflammatory responses and severe pathology in the host. Since induction of ECM is correlated with pro-inflammatory status of the host [34], Hz may be a critical factor involved in inducing ECM. However, the amount of Hz, like growth rates of the parasites, may not be the only factor responsible for inducing ECM, since blood stages of several growth-attenuated mutants (*Δnt1*, *Δlap* and *Δbp1*) have normal Hz production but do not induce ECM (Chapter 6; unpublished results). However, the absence of ECM-inducing capacity of these mutants could still be related to reduction in amounts of released Hz in the circulation in the early phase of an infection. Mice infected with slow-growing parasites can be expected to release less Hz compared to wt parasites and therefore the Hz levels may be below the threshold that is required to induce inflammatory responses causing ECM. So far we have been unable to select mutants that have both a normal growth rate and Hz production, but do not

induce ECM. The successful selection of such mutants would indicate that other factors contribute to ECM in addition to growth rate and Hz levels.

Further research is required to unravel the relative contributions and relationship between the critical parasite and host factors that cause severe disease and elicit protective immunity. I believe that the mutants produced in this study, with their different phenotypes and properties, may help shed light on parasite factors involved in ECM induction. Such knowledge may be critical in evaluating the value of the *P. berghei* ANKA infections in C57BL/6 mouse as an experiment model of cerebral malaria for understanding human cerebral malaria, since the similarities of induced immunopathology between humans and rodent infections is under considerable debate [35,36].

3.3 Drug development and drug resistance of drugs that target hemoglobin digestion

The ability of *Plasmodium* parasites to invade RBC and produce infectious merozoites without Hz formation may have important implications for development of drugs that target Hb digestion and/ or Hz formation and in understanding the development of resistance against such drugs. We found that $\Delta pm4\Delta bp2$ parasites that lack expression of PM4 and BP2 can grow with little or no Hz production, and importantly, are less sensitive to chloroquine (CQ) treatment *in vivo*. CQ directly interacts with free heme creating a heme-chloroquine complex that is highly toxic for the parasite [37], and therefore the increased CQ resistance of $\Delta pm4\Delta bp2$ is consistent with our observations of severely reduced/ absent Hz formation. Interestingly, it has been previously reported that *P. berghei* lines that have been selected for CQ-resistance have a stronger preference for reticulocytes and produce less Hz [38,39]. It has been proposed that CQ-resistance in parasites with reduced Hz is due to detoxification of heme by elevated levels of glutathione in parasites that grow inside reticulocytes, thus precluding heme-polymerization and preventing the CQ activity [39,40]. However, our observations may provide a more direct explanation for CQ-resistance and reduced Hz production in these parasites, namely that these parasites hydrolyse less Hb in reticulocytes like the $\Delta pm4\Delta bp2$ -parasites. While $\Delta pm4\Delta bp2$ parasites have an increased resistance to CQ, they retain the same sensitivity to artesunate (AS). Although the precise and critical mode of action of artemisinin and related-derivatives remains contentious, most studies concur that their activity results from activation by reduced heme iron in the DV [41,42]. Our results showing that $\Delta pm4\Delta bp2$ -parasites are more resistant to CQ but not AS, would suggest that additional, non-heme based, modes of AS action are equally, or even more effective at targeting *P. berghei* parasites *in vivo*. Therefore, the $\Delta pm4\Delta bp2$ -parasites that grow with little or no Hz formation may

be useful tools to further analyse the mode of drug action, for example, how they target and interact with molecules critical to or result from Hb digestion.

Our results on the acquisition of CQ-resistance when parasites develop in reticulocytes with limited or no Hz production may have relevance for *P. vivax*, which is restricted for growth in reticulocytes. Interestingly, mechanisms of CQ-resistance in *P. vivax* appears to be different from those in *P. falciparum* [43]. Based on our observations, we hypothesize that some *P. vivax* parasites may acquire resistance to CQ (and other drugs targeting Hb digestion) by preferentially 'switching' to a development mode where they are less dependent on Hb digestion for growth. Such 'switching' may only be possible for those *Plasmodium* species that can infect and develop in reticulocytes. It would therefore be of great interest to analyse whether in 'hotspots' of *P. vivax* CQ-resistance parasites develop inside the RBC with reduced Hz formation. I believe that mutants with reduced Hz production are not only useful tools to analyse the influence of Hz in inducing pathology (as explained above), but also useful tools to analyse drug activities where Hb digestion/ Hz formation is believed to be critical for their mode of actions.

References

1. Pfander C, Anar B, Schwach F, Otto TD, Brochet M, *et al* (2011) A scalable pipeline for highly effective genetic modification of a malaria parasite. *Nat Methods* 8(12):1078-82
2. Freeman M (2009) Rhomboids: 7 years of a new protease family. *Semin Cell Dev Biol* 20: 231-239.
3. Santos M, Graindorge A, Soldati-Favre D (2011) New insights into parasite rhomboid proteases. *Mol Biochem Parasitol* 182(1-2):27-36.
4. Srinivasan P, Coppens I, Jacobs-Lorena M (2009) Distinct roles of *Plasmodium* rhomboid 1 in parasite development and malaria pathogenesis. *PLoS Pathog* 5: e1000262.
5. Vera IM, Beatty WL, Sinnis P, Kim K (2011) *Plasmodium* protease ROM1 is important for proper formation of the parasitophorous vacuole. *PLoS Pathog* 7: e1002197.
6. Amani V, Boubou MI, Pied S, Marussig M, *et al* (1998) Cloned lines of *Plasmodium berghei* ANKA differ in their abilities to induce experimental cerebral malaria. *Infect Immun* 66: 4093-4099.
7. Levander OA, Fontela R, Morris VC, Ager AL, Jr. (1995) Protection against murine cerebral malaria by dietary-induced oxidative stress. *J Parasitol* 81: 99-103.
8. Goldberg DE (2005) Hemoglobin degradation. *Curr Top Microbiol Immunol* 295: 275-291.
9. Bonilla JA, Bonilla TD, Yowell CA, Fujioka H, Dame JB (2007) Critical roles for the digestive vacuole plasmepsins of *Plasmodium falciparum* in vacuolar function. *Mol Microbiol* 65: 64-75.
10. Spaccapelo R, Janse CJ, Caterbi S, Franke-Fayard B, Bonilla JA, *et al* (2010) Plasmepsin 4-deficient *Plasmodium berghei* are virulence attenuated and induce protective immunity against experimental malaria. *Am J Pathol* 176: 205-217.
11. Goldberg DE, Slater AF, Beavis R, Chait B, Cerami A, *et al* (1991) Hemoglobin degradation in the human malaria pathogen *Plasmodium falciparum*: a catabolic pathway initiated by a specific aspartic protease. *J Exp Med* 173: 961-969.
12. Wyatt DM, Berry C (2002) Activity and inhibition of plasmepsin IV, a new aspartic proteinase from the malaria parasite, *Plasmodium falciparum*. *FEBS Lett* 513: 159-162.
13. Gluzman IY, Francis SE, Oksman A, Smith CE, Duffin KL, *et al* (1994) Order and specificity of the *Plasmodium falciparum* hemoglobin degradation pathway. *J Clin Invest* 93: 1602-1608.
14. Banerjee R, Liu J, Beatty W, Pelosof L, Klemba M, *et al* (2002) Four plasmepsins are active in the *Plasmodium falciparum* food vacuole, including a protease with an active-site histidine. *Proc Natl Acad Sci U S A* 99: 990-995.
15. Subramanian S, Hardt M, Choe Y, Niles RK, Johansen EB, *et al* (2009) Hemoglobin cleavage site-specificity of the *Plasmodium falciparum* cysteine proteases falcipain-2 and falcipain-3. *PLoS One* 4: e5156.
16. Spaccapelo R, Janse CJ, Caterbi S, Franke-Fayard B, Bonilla JA, *et al* (2010) Plasmepsin 4-deficient *Plasmodium berghei* are virulence attenuated and induce protective immunity against experimental malaria. *Am J Pathol* 176: 205-217.
17. Spaccapelo R, Aime E, Caterbi S, Arcidiacono P, Capuccini B, Di CM, Dottorini T, Rende M, Bistoni F, Crisanti A (2011) Disruption of plasmepsin-4 and merozoites surface protein-7 genes in *Plasmodium berghei* induces combined virulence-attenuated phenotype. *Sci Rep* 1: 39.
18. Aly AS, Downie MJ, Mamoun CB, Kappe SH (2010) Subpatent infection with nucleoside transporter 1-deficient *Plasmodium* blood stage parasites confers sterile protection against lethal malaria in mice. *Cell Microbiol* 12: 930-938.
19. Pombo DJ, Lawrence G, Hirunpetcharot C, Rzepczyk C, Bryden M, *et al* (2002) Immunity to malaria after administration of ultra-low doses of red cells infected with *Plasmodium falciparum*. *Lancet* 360: 610-617.
20. Elliott SR, Kuns RD, Good MF (2005) Heterologous immunity in the absence of variant-specific antibodies after exposure to subpatent infection with blood-stage malaria. *Infect Immun* 73: 2478-2485.
21. Pinzon-Charry A, McPhun V, Kienzle V, Hirunpetcharot C, Engwerda C, *et al* (2010) Low doses of killed parasite in CpG elicit vigorous CD4+ T cell responses against blood-stage malaria in mice. *J Clin Invest* 120: 2967-2978.
22. Celluzzi CM, Liem PL, van de WT, Eling WM (1995) Attenuated immunogenic parasites are essential in the transfer of immunity to virulent *Plasmodium berghei*. *Immunology* 85: 509-515.

23. Eling W, Jerusalem C (1977) Active immunization against the malaria parasite *Plasmodium berghei* in mice: sulfathiazole treatment of a *P. berghei* infection and development of immunity. *Tropenmed Parasitol* 28: 158-174.
24. Schetters TP, van Run-van Breda JH, van de WT, Hermsen CC, Curfs J, Eling WM (1989) Impaired immune responsiveness in *Plasmodium berghei* immune mice. *Parasite Immunol* 11: 519-528.
25. Miyagami T, Igarshi I, Suzuki M (1987) *Plasmodium berghei*: long lasting immunity induced by a permanent attenuated mutant. *Zentralbl Bakteriell Mikrobiol Hyg A* 264: 502-512.
26. Ting LM, Gissot M, Coppi A, Sinnis P, Kim K (2008) Attenuated *Plasmodium yoelii* lacking purine nucleoside phosphorylase confer protective immunity. *Nat Med* 14: 954-958.
27. McCarthy JS, Good MF (2010) Whole parasite blood stage malaria vaccines: a convergence of evidence. *Hum Vaccin* 6: 114-123.
28. Yoneto T, Waki S, Takai T, Tagawa Y, Iwakura Y, *et al* (2001) A critical role of Fc receptor-mediated antibody-dependent phagocytosis in the host resistance to blood-stage *Plasmodium berghei* XAT infection. *J Immunol* 166: 6236-6241.
29. Inoue S, Niikura M, Takeo S, Mineo S, Kawakami Y, *et al* (2012) Enhancement of dendritic cell activation via CD40 ligand-expressing gammadelta T cells is responsible for protective immunity to *Plasmodium* parasites. *Proc Natl Acad Sci U S A* 109: 12129-12134.
30. Nguyen PH, Day N, Pram TD, Ferguson DJ, White NJ (1995) Intraleucocytic malaria pigment and prognosis in severe malaria. *Trans R Soc Trop Med Hyg* 89: 200-204.
31. Amodu OK, Adeyemo AA, Olumese PE, Gbadejesin RA (1998) Intraleucocytic malaria pigment and clinical severity of malaria in children. *Trans R Soc Trop Med Hyg* 92: 54-56.
32. Hanscheid T, Egan TJ, Grobusch MP (2007) Haemozoin: from melatonin pigment to drug target, diagnostic tool, and immune modulator. *Lancet Infect Dis* 7: 675-685.
33. Shio MT, Kassa FA, Bellemare MJ, Olivier M (2010) Innate inflammatory response to the malarial pigment hemozoin. *Microbes Infect* 12: 889-899.
34. Grau GE, Craig AG (2012) Cerebral malaria pathogenesis: revisiting parasite and host contributions. *Future Microbiol* 7: 291-302.
35. Craig AG, Grau GE, Janse C, Kazura JW, Milner D, Barnwell JW, Turner G, Langhorne J (2012) The role of animal models for research on severe malaria. *PLoS Pathog* 8: e1002401.
36. Langhorne J, Buffet P, Galinski M, Good M, Harty J, Leroy D, Mota MM, Pasini E, Renia L, Riley E, Stins M, Duffy P (2011) The relevance of non-human primate and rodent malaria models for humans. *Malar J* 10: 23. 1475-2875-10-23.
37. Fitch CD (1986) Antimalarial schizontocides: ferriprotoporphyrin IX interaction hypothesis. *Parasitol Today* 2: 330-331.
38. Peters W (1968) The chemotherapy of rodent malaria. V. Dynamics of drug resistance. I. Methods for studying the acquisition and loss of resistance to chloroquine by *Plasmodium berghei*. *Ann Trop Med Parasitol* 62: 277-287.
39. Platel DF, Mangou F, Tribouley-Duret J (1999) Role of glutathione in the detoxification of ferriprotoporphyrin IX in chloroquine resistant *Plasmodium berghei*. *Mol Biochem Parasitol* 98: 215-223.
40. Fidock M, DeSilva B (2012) Bioanalysis of biomarkers for drug development. *Bioanalysis* 4: 2425-2426.
41. Eastman RT, Fidock DA (2009) Artemisinin-based combination therapies: a vital tool in efforts to eliminate malaria. *Nat Rev Microbiol* 7: 864-874.
42. Olliaro PL, Haynes RK, Meunier B, Yuthavong Y (2001) Possible modes of action of the artemisinin-type compounds. *Trends Parasitol* 17: 122-126.
43. Baird KJ, Maguire JD, Price RN (2012) Diagnosis and treatment of *Plasmodium vivax* malaria. *Adv Parasitol* 80: 203-270.

Summary

Despite intense efforts over the past 50 years to develop a vaccine, there is currently no licensed malaria vaccine available. Optimism that a first-generation malaria (subunit) vaccine based on the *Plasmodium* circumsporozoite protein, RTS,S, would soon be licensed has been dampened by the interim results of the ongoing Phase 3 trials in Africa, which indicate that this vaccine confers only around 30% protection against severe malaria in young children and infants, and that the protection generated is only short-lived (<6 months). The limited success achieved in inducing long-lasting effective protective immunity against malaria using subunit vaccines has led to renewed interest in whole-parasite vaccination strategies, which while hard to formulate and administer, have been shown to confer long-lasting sterile immunity in humans. The aim of the work described in this thesis was to genetically engineer and characterize growth- and virulence-attenuated blood stage parasites (GAP_{BS}) in the rodent malaria model, *P. berghei*. Specifically, GAP_{BS} that produce only short-lived low-parasitemia self-resolving blood infections and provoke strong protective immune responses. In order to screen a large number of potential GAP_{BS}, we first improved both transfection methods to generate these GAP_{BS} and methods to analyse their blood stage growth-characteristics.

In **Chapter 2**, I describe the development of a novel genetic modification method in two rodent malaria parasites, *P. yoelii* and *P. berghei*, which helps overcome the problem of limited number of selectable markers that can be effectively used to select for *Plasmodium* mutants. This 'gene insertion/marker out' (GIMO) method uses negative selection to rapidly generate transgenic mutants that are free of drug selectable markers and therefore ready for subsequent modifications. This method can also be used to rapidly and more easily generate 'reporter parasites', which are useful for phenotype characterization of mutants and facilitate the generation of parasites expressing multiple transgenes and/ or lacking multiple genes. In addition, it provides a fast and simple way to 'gene complement' gene deletion/mutation mutants (i.e. restoring the wt phenotype upon restoration of the disrupted gene). The GIMO method not only simplifies and speeds up both the generation of marker-free transgenic parasites and gene complementation experiments, but the application of this method also greatly reduces the numbers of animals required to generate and complement mutants.

We also improved the existing methods to analyse both *in vitro* and *in vivo* the growth kinetics of GAP_{BS} that have been created in luciferase-expressing background parasite lines and also described how luciferase-expressing reporter parasites can be used in drug screening assays both *in vitro* and *in vivo*. These improved protocols are described in **Chapter 3**.

In order to generate a GAP_{BS}, I targeted 41 genes in the virulent *P. berghei* ANKA line, to specifically identify mutants that are both growth- and virulence-attenuated and that can serve as protective immunogens. The selection of these genes was mainly based on their predicted roles in parasite blood stage development or based on *P. falciparum* piggyBac random mutagenesis studies, where a growth defect was observed in mutants with a piggyBac gene-insertion. Specifically, we targeted the 8 genes encoding *Plasmodium* rhomboid proteases, because critical roles were published for several rhomboid proteases in host cell invasion and pathogenesis. However, we found a high degree of redundancy in this family; 4 of them (ROM1, 3, 9 and 10) were dispensable for parasite blood stage development, with no alteration in growth or virulence. We also examined the phenotype of these gene-deletion mutants throughout the complete lifecycle including development in the mosquito and in the liver (**Chapter 4**). We found that *P. berghei* mutants lacking ROM3, although producing normal numbers of oocysts in the mosquito, show a complete absence of sporozoite formation within the oocysts. This is the first apicomplexan rhomboid identified to play a vital role in sporogony.

In addition to the rhomboid proteases, we selected 12 genes with predicted or possible roles in the hemoglobin degradation pathway for targeted disruption (**Chapter 5**), as hemoglobin catabolism is believed to be essential for parasite blood-stage development, and a mutant lacking expression of one of the hemoglobinases, plasmepsin-4, was shown to be growth- and virulence-attenuated. We were able to successfully generate gene-deletion mutants for 9 out of the 12 selected genes, indicating a high level of redundancy also amongst *P. berghei* hemoglobinases. Four of the 9 mutants showed normal growth characteristics in mice, whereas 5 mutants showed a significantly reduced growth rate compared to wild type parasites. Unexpectedly, we were able to generate a double gene-deletion mutant lacking expression of both plasmepsin-4 and berghepains-2, the only 2 enzymes reported to initiate hemoglobin digestion. This double gene-deletion mutant was restricted to growth in young red blood cells, reticulocytes, where parasites were able to develop without any detectable hemozoin formation. Hemozoin is the detoxified byproduct of hemoglobin degradation and its absence indicates that this mutant is able to develop inside red blood cells with little or no hemoglobin digestion, and is supported by the observation that these parasites are more resistant to chloroquine compared to wild-type parasites. Chloroquine directly interacts with heme that is liberated upon hemoglobin degradation, creating a complex highly toxic to the parasite; and therefore the increase in chloroquine resistance of the double gene-deletion parasites is consistent with our observations of reduced/absent hemozoin production. These observations have important implications for *Plasmodium* drug development and drug resistance, in particular for malaria parasites (e.g. *P. vivax*) that can develop inside reticulocytes where

hemoglobin digestion may not be essential.

From the 41 genes targeted, we generated 22 single gene-deletion mutants and 2 double gene-deletion mutants, one already described above lacks expression of both plasmepsin-4 and berghepain-2 ($\Delta pm4\Delta bp2$), and another lacks expression of both plasmepsin-4 and SMAC (schizont membrane-associated cytoadherence protein, $\Delta pm4\Delta smac$). The growth and virulence characterization of these 24 mutants is presented in **Chapter 6**. Nine of these mutants showed significant reduction in *in vivo* multiplication rates, and 7 of the 9 growth-arrested mutants did not induce experimental cerebral malaria (ECM) in ECM-sensitive (C57BL/6) mice. All 4 mutants that produce significantly reduced amounts of hemozoin fail to induce ECM. The mutants Δlap , Δapp and $\Delta pm4\Delta bp2$ were able to produce self-resolving infections in C57BL/6 and ECM-resistant BALB/c mice.

Our studies show that it is possible to generate mutants with strongly reduced growth rates that do not induce ECM and that through the deletion of multiple genes it is possible to create mutants that produce self-resolving infections in mice without producing hyperparasitemia. However, even with parasites that have strongly reduced growth rates, both C57BL/6 and BALB/c mice are unable to rapidly mount an effective immune response that can control an acute infection at low parasitemias. It is, however, important to note that in all our experiments the mice were infected with relatively high numbers of parasites ($10^5 - 10^6$). It is possible that starting infection with lower numbers of parasites would allow the mice to control infections before developing high parasitemias, or would lead to infections with very low or even sub-patent parasitemias. These studies and those of experimental *P. falciparum* infections in humans, where protective cellular immune responses are induced with low numbers of infected red blood cells, would suggest that the induction of protective immunity might require different parasite loads depending on the nature of the immune (cellular or humoral) responses required. Clearly, further research is required to determine both the parasite and host factors that can induce protective immune responses against blood stages. The use of attenuated blood stage parasites can be an extremely useful tool to better understand induced rather than acquired immunity against *Plasmodium* and may help to create the most effective and broadest anti-malaria vaccine.

Samenvatting

Ondanks vele inspanningen de afgelopen 50 jaar voor het ontwikkelen van een vaccin is er tot op heden geen geregistreerd malariavaccin beschikbaar. Optimistische geluiden omtrent een mogelijke registratie van een eerste-generatie malaria subunit vaccin, gebaseerd op het *Plasmodium* circumsporozoïte eiwit – RTS,S – zijn gedempt door de voorlopige resultaten van de nog lopende fase 3 trials in Afrika welke laten zien dat dit vaccin bij kinderen en zuigelingen slechts 30% bescherming genereert tegen gecompliceerde malaria en dat de geïnduceerde bescherming een kortstondig effect heeft van minder dan 6 maanden. De tegenvallende successen met betrekking tot het induceren van een langdurige, effectieve immuunreactie tegen malaria met subunit vaccins heeft er toe geleid dat het gebruik van verzwakte parasieten, een beproefde strategie voor het induceren van langdurige steriele immuniteit in de mens, opnieuw in de belangstelling staat. Het doel van het onderzoek beschreven in dit proefschrift was het genereren en karakteriseren van genetisch gemodificeerde, groei- en virulentieverzwakte, bloedstadium malariaparasieten in het *Plasmodium berghei* knaagdier-malariamodel. Dit geldt in het bijzonder voor ‘genetisch geattenuerde bloedstadium parasieten’ (GAP_{BS}) die alleen een infectie opwekken met een kortstondige, lage infectiegraad (parasitemie) en die zichzelf niet kunnen handhaven in het bloed maar wel een krachtige, beschermende immuunreacties opwekken. Om het screenen van een groot aantal potentiële GAP_{BS} mogelijk te maken werden zowel de transfectiemethodes voor het genereren van de GAP_{BS} en de methodes die het mogelijk maken de groei- en virulentie-karakteristieken in het bloedstadium te analyseren verbeterd.

In **Hoofdstuk 2** beschrijf ik de ontwikkeling van een nieuwe methode voor genetische modificatie die toegepast kan worden op de knaagdier-malariaparasieten *P. berghei* en *P. yoelii* waarvan de toepassing niet wordt gelimiteerd door het beperkte aantal effectieve selectiemarkers dat beschikbaar is voor het selecteren van malariaparasiet mutanten. Deze ‘gene insertion/marker out’ (GIMO) methode maakt gebruik van negatieve selectie om snel en effectief transgene mutanten te genereren zonder selectiemarker die geschikt zijn voor verdere genetische modificatie. Deze methode kan ook worden toegepast voor het genereren van zogenaamde transgene reporterparasieten die reporter eiwitten tot expressie brengen (bijvoorbeeld fluorescerende eiwitten). Reporterparasieten faciliteren het fenotypisch karakteriseren van mutanten en het genereren van transgene parasieten die meerdere heterologe genen tot expressie brengen dan wel meerdere gen deleties kennen. Daarnaast is het mogelijk om mutanten met gen deleties of mutanten die gemuteerde genen tot expressie brengen genetische te complementeren, ofwel het herstellen van het oorspronkelijke fenotype door de genetische modificatie ongedaan te maken. De GIMO methode maakt het niet alleen mogelijk sneller en eenvoudiger transgene parasieten zonder selectiemarker te genereren en mutaties te complementeren, ook

het aantal proefdieren nodig voor het genereren/complementeren van mutanten wordt sterk gereduceerd.

We hebben ook de bestaande methodes voor *in vitro* en *in vivo* analyse van de groeikinetiek van malaria parasieten vereenvoudigd door gebruik te maken van reporterparasieten die luciferase tot expressie brengen. Deze methoden zijn gebruikt voor het analyseren van de groei- en virulentie eigenschappen van GAP_{BS} en beschrijven hoe deze reporterparasieten toegepast kunnen worden in *in vitro* en *in vivo* drug screening assays. Deze verbeterde methodieken worden beschreven in **Hoofdstuk 3**.

Voor het genereren van een GAP_{BS} heb ik 41 genen in de virulente *P. berghei* ANKA lijn geselecteerd voor mijn zoektocht naar groei- en virulentie-verzwakte mutanten (GAP_{BS}) die kunnen dienen als beschermend immunogen. De selectie van deze genen was voornamelijk gebaseerd op hun vermeende rol bij de ontwikkeling van de parasiet in het bloedstadium of gebaseerd op *P. falciparum piggyBac* random mutagenese studies waarbij mutanten met een groeidefect zijn gegenereerd door middel van van een *piggyBac* gen insertie. Acht genen coderend voor *Plasmodium* rhomboid proteasen werden specifiek geselecteerd vanwege publicaties waaruit is gebleken dat verschillende rhomboid proteasen een essentiële rol vervullen bij invasie van de gastheercel en bij de pathogenese. Toch hebben we binnen deze familie van proteasen geconstateerd dat 4 van hen (ROM1, 3, 9 en 10) niet noodzakelijk zijn voor de ontwikkeling van de parasiet in het bloedstadium en geen effect hebben op de groei en virulentie van de parasiet. Het fenotype van de knock-out mutanten is gedurende de hele levenscyclus geanalyseerd inclusief de ontwikkeling in de muskiet en lever (**Hoofdstuk 4**). Hieruit is gebleken dat oocysten van *P. berghei* mutanten deficiënt voor ROM3, ondanks het feit dat ze in normale hoeveelheden in de muskiet worden geproduceerd, geen sporozoieten vormen. Dit is het eerste geïdentificeerde rhomboid eiwit die een essentiële rol speelt in sporogenese binnen de groep van organismen die behoren tot de Apicomplexa.

Behalve de rhomboid proteasen hebben we 12 additionele genen geselecteerd met een vermeende rol bij de afbraak van hemoglobine voor deletie/knock-out (**Hoofdstuk 5**). Men vermoedt dat omzetting van hemoglobine essentieel is voor de ontwikkeling van de bloedstadia van malaria parasieten. Het is aangetoond dat een mutant waarin een gen coderend voor één van de eiwitten betrokken bij hemoglobinedigestie (plasmepsin -4) is uitgeschakeld een verzwakte groei en virulentie laat zien. Voor 9 van de 12 genen hebben we met succes knock-out mutanten gegenereerd waarmee tevens is aangetoond dat de afzonderlijke *P. berghei* hemoglobinasen in het algemeen niet essentieel zijn voor de parasiet om te overleven. Vergeleken met wildtype parasieten vertoonden 4 van de 9 mutanten normale groei-eigenschappen. Van de overige 5 mutanten was de groeisnelheid

significanter gereduceerd. Opmerkelijk genoeg zijn we in staat geweest een mutant te maken die deficiënt is voor zowel plasmepsin-4 als berghepain-2, de enige twee enzymen waarvan bekend is dat ze betrokken zijn bij de initiatie van hemoglobinedigestie. Groei van deze mutant was beperkt tot de jonge rode bloedcellen, de reticulocyten, alwaar de parasiet in staat was zich te ontwikkelen zonder waarneembare vorming van hemozoin. Hemozoin is het gedetoxificeerde bijproduct van hemoglobine degradatie en afwezigheid van hemozoin toont aan dat deze mutant in staat is zich in de rode bloedcel te ontwikkelen met weinig of geen hemoglobine digestie. Deze bevinding wordt gestaafd door de observatie dat deze parasiet minder gevoelig is voor chloroquine vergeleken met wildtype parasieten. Chloroquine gaat een directe interactie aan met hem dat vrijkomt bij degradatie van hemoglobine waardoor een voor de parasiet toxisch complex ontstaat. De verhoogde resistentie van deze mutant tegen chloroquine is dan ook consistent met de door ons geobserveerde reductie/afwezigheid van hemoglobine digestie. Deze bevindingen hebben belangrijke implicaties voor de ontwikkeling van een resistentie tegen malariamedicijnen, vooral voor malariaparasieten die zich in reticulocyten kunnen ontwikkelen waarbij hemoglobine digestie niet langer essentieel is.

Van de 41 geselecteerde genen hebben we 22 single knock-out mutanten gemaakt en 2 dubbel knock-out mutanten. De hierboven beschreven mutant is deficiënt voor zowel plasmepsin-4 als berghepain-2 ($\Delta pm4\Delta bp2$) en de tweede dubbel knock-out mutant is deficiënt voor plasmepsin-4 en SMAC (schizont membrane-associated cytoadherence protein, $\Delta pm4\Delta smac$). De groei- en virulente eigenschappen van de 24 mutanten is beschreven in **Hoofdstuk 6**. Negen mutanten lieten een sterk gereduceerde *in vivo* groei zien en 7 van deze 9 mutanten hebben een verminderde virulentie en induceren geen experimentele cerebrale malaria (ECM) in ECM gevoelige (C57BL/6) muizen. Alle 4 mutanten die significant minder hemozoin produceren induceren geen ECM. De Δlap , Δapp en $\Delta pm4\Delta bp2$ mutanten brengen infecties teweeg die zichzelf niet kunnen handhaven in C57BL/6 muizen en ECM-resistente BALB/c muizen.

Een belangrijke uitkomst van mijn onderzoek is dat deze studies laten zien dat het mogelijk is mutanten te genereren met een sterk gereduceerde groei van de bloedstadia en met een verminderde virulentie en dat het door het uitschakelen van meerdere genen mogelijk is mutanten te maken die niet-handhaafbare infecties teweegbrengen in muizen, zonder vorming van hyperparasitemie. Deze mutanten laten dus een geatenuerd phenotype zien, zowel wat betreft groei als virulentie eigenschappen.

Desondanks, zelfs bij infecties met parasieten met sterk gereduceerde groei eigenschappen, zijn zowel C57BL/6 and BALB/c muizen niet in staat om snel een effectieve immunoreactie op te wekken, krachtig genoeg om een acute infectie met lage

parasitemie te controleren. Hierbij moet opgemerkt worden dat in al ons experimenten de muizen werden gevaccineerd met relatief hoge aantallen parasieten ($10^5 - 10^6$). Het is mogelijk dat vaccinatie met minder parasieten de muizen in staat zou stellen de infecties te controleren nog voor de totstandkoming van een hoge parasitemie waardoor infecties zouden kunnen ontstaan met zeer lage parasitemie of 'subpatent' infecties. Deze studies en de studies naar *P. falciparum* infecties bij de mens waarbij beschermende cellulaire immuunreacties worden geïnduceerd met kleine hoeveelheden geïnfecteerde rode bloedcellen (iRBC) zouden kunnen suggereren dat voor de totstandkoming van een beschermende immuniteit, afhankelijk van de gewenste immuunreactie (humoraal of cellulair), verschillende parasieten hoeveelheden nodig zijn. Het is duidelijk dat verder onderzoek nodig is om de factoren van zowel de parasiet als de gastheer die een rol zouden kunnen spelen bij de totstandkoming van een beschermende afweerreactie tegen bloedstadia in kaart te brengen. De toepassing van verzwakte bloedstadium-parasieten kan een bijzonder goed hulpmiddel zijn om meer inzicht te krijgen in geïnduceerde afweerreacties tegen Plasmodium en zou kunnen bijdragen aan de ontwikkeling van het malariavaccin met de hoogste effectiviteit en de breedste werking.

List of Publications

1. [Lin JW](#), Spaccapelo R, Sajid M, Annoura T, Franke-Fayard BMD, Chevalley-Maurel S, Ramesar J, Aime E, Schwarzer E, Arese P, Deroost K, Van den Steen PE, O'Toole T, Prins F, Mommaas-Kienhuis AM, Koster AJ, Tanke HJ, Ravelli RBG, Janse CJ, Khan SM (2013) Malaria parasites lacking critical proteases involved in hemoglobin degradation are viable and are less sensitive to chloroquine. (*submitted*)
2. Annoura T, van Schaijk BCL, Ploemen IHJ, Sajid M, [Lin JW](#), Vos MW, Dinmohamed AG, van Gemert G-J, Chevalley-Maurel S, Kielbasa S, Scheltinga F, Franke-Fayard BMD, Klop O, Hermsen CC, Gego A, Franetich J-F, Mazier D, Hoffman SL, Janse CJ, Sauerwein RW, Khan SM (2013) New members of the *Plasmodium* 6-Cys family have distinct and critical roles in liver stage development. (*submitted*)
3. [Lin JW](#), Meireles P, Prudêncio M, Engelmann S, Annoura T, Sajid M, Chevalley-Maurel S, Ramesar J, Nahar C, Avramut CMC, Koster AJ, Matuschewski K, Waters AP, Janse CJ, Mair GR, Khan SM (2013) Loss-of-function analyses defines vital and redundant functions of the *Plasmodium* rhomboid protease family. *Molecular Microbiology*, 88(2): 318–38.
4. Deroost K, Tyberghein A, Lays N, Noppen S, Schwarzer E, Vanstreels E, Komuta M, Prato M, [Lin JW](#), Pamplona A, Janse CJ, Arese P, Roskams T, Daelemans D, Opendakker G, Van den Steen PE (2013) Hemozoin induces lung inflammation and correlates with malaria-associated acute respiratory distress syndrome. *Am J Respir Cell Mol Biol*, 48(5):589–600.
5. [Lin JW](#), Sajid M, Ramesar J, Khan SM, Janse CJ, Franke-Fayard B (2013) Screening inhibitors of *P. berghei* blood stages using bioluminescent reporter parasites. *Methods Mol Biol*, 923: 507–22.
6. [Lin JW](#), Annoura T, Sajid M, Chevalley-Maurel S, Ramesar J, Klop O, Franke-Fayard B, Janse CJ, Khan SM (2011) A novel 'gene insertion/marker out' (GIMO) method for transgene expression and gene complementation in rodent malaria parasites. *PLoS One*, 6(12): e29289.
7. Balu B, Maher SP, Pance A, Chauhan C, Naumov AV, Andrews RM, Ellis PD, Khan SM, [Lin JW](#), Janse CJ, Rayner JC, Adams JH (2011) CCR4-associated factor 1 coordinates the expression of *Plasmodium falciparum* egress and invasion proteins. *Eukaryot Cell*, 10(9):1257–63.

8. Barker RH Jr, Urgaonkar S, Mazitschek R, Celatka C, Skerlj R, Cortese JF, Tyndall E, Liu H, Cromwell M, Sidhu AB, Guerrero-Bravo JE, Crespo-Llado KN, Serrano AE, Lin JW, Janse CJ, Khan SM, Duraisingh M, Coleman BI, Angulo-Barturen I, Jiménez-Díaz MB, Magán N, Gomez V, Ferrer S, Martínez MS, Wittlin S, Papastogiannidis P, O'Shea T, Klinger JD, Bree M, Lee E, Levine M, Wiegand RC, Munoz B, Wirth DF, Clardy J, Bathurst I, Sybertz E (2011) Aminoindoles, a novel scaffold with potent activity against *Plasmodium falciparum*. *Antimicrob Agents Chemother*, 55(6):2612–22.
9. Booker ML, Bastos CM, Kramer ML, Barker RH Jr, Skerlj R, Sidhu AB, Deng X, Celatka C, Cortese JF, Guerrero Bravo JE, Crespo Llado KN, Serrano AE, Angulo-Barturen I, Jiménez-Díaz MB, Viera S, Garuti H, Wittlin S, Papastogiannidis P, Lin JW, Janse CJ, Khan SM, Duraisingh M, Coleman B, Goldsmith EJ, Phillips MA, Munoz B, Wirth DF, Klinger JD, Wiegand R, Sybertz E (2010) Novel inhibitors of *Plasmodium falciparum* dihydroorotate dehydrogenase with anti-malarial activity in the mouse model. *J Biol Chem*, 285(43): 33054–64.

Acknowledgements

I would like to express my sincere gratitude to all the people who have helped me and made this thesis possible.

First, I want to thank my supervisors **Dr. Chris Janse** and **Dr. Shahid Khan**, who gave me the opportunity to work in Leiden Malaria Research Group. Thank you for all your kind help, your patient guidance and unyielding support. You are more than supervisors to me, you not only showed to me how to plan and carry out a research project, how to coordinate and collaborate with other groups, how to structure and write a paper, more importantly you taught me how to become a responsible scientific researcher. Thanks for always being patient in our discussions, for hearing me out and giving me chances to try out my ideas and for always being there when I needed guidance... Chris, thank you for helping me realize the value of maintaining scientific curiosity and relishing the joy of learning and discovery even in difficult times. Shahid, thanks for also being a friend to me, for being so supportive and for your countless kind help...

To everyone who worked in **Leiden Malaria Research Group**: Blandine, the master of imaging and microscopy; Jai, the master of PFG and Northern and animal work; Hans, the master of molecular cloning; Takeshi and Severine, the masters of mosquito and liver stage work; Saj, the master of protein work; Onny, the master of FACS... thank you so much for making my work much easier and enjoyable! Takeshi, thanks for your teaching and guidance and your valuable time, thanks for all the tips in molecular biology! I learned a lot from you, not only on the technical part, but also your way of thinking and your careful plan and execution of experiments. I really enjoyed our discussions, our 'Chinese-Japanese cultural exchange'. Saj, thanks for showing me around during my first day in Leiden, for making the lab such a fun place to work in, for all your kind guidance on protein work, for being a big brother to me! Blandine, thanks for all your kind guidance, help and encouragement, and for all your assistance with imaging experiments. Jai, thanks for all your invaluable help and technical support, my projects cannot be completed without your help! Hans, thanks for your countless kind help, for being the go-to person in the group and for always being so kind to me. Sev, thanks for always being there to help, to support and for being a good friend to me. Eliane, thanks for helping me fit in the new environment when I first arrived, for reminding me to enjoy life other than diving headlong into never-ending experiments. Aga and Ahmed, thanks for all our discussions. It was so fun to have fellow PhD students around. To Anneke, Jannik, Kevin and to the all students who did their internship with me: Joana, Jasper (The JJJ team!), Pascale and Tracy, thank you all!

I am very grateful for all the support I've got in LUMC: from FACS facility (Guido) and the Electron Microscopy Section (Raimond, Cristina and Prof. Abraham Koster), Department of Pathology (Frans) and Department of Infectious Diseases (Susan, Annemieke, Kees and Prof. Tom Ottenhoff).

I also really appreciate all the help I've got from all the collaborators. Thanks to the labs of Dr. Roberta Spaccapelo, Dr. Gunnar Mair, Dr. Miguel Prudêncio, Dr. Evelin Schwarzer, Dr. Photini Sinnis, Prof. John Adams, Prof. Kai Matuschewski, Prof. Gordon Langsley and Dr. Tom O'Toole. A special 'thank you' to Katrien, thanks for hosting me in Leuven and for being a friend.

I'd like to acknowledge the support from China Scholarship Council-Leiden University joint scholarship program and thank Prof. Cangsang Pan for his kind guidance during my Master training and for continuing to encourage and inspire me during my PhD.

I am very grateful to my friends in Leiden. To Xiaolei and Bo, thank you for helping me settle down in DUWO and for all the fun talks. Many thanks again to Xiaolei, and Hua, for always being there to help and for being good friends to me. To Xiaole, Sha, Bing, Qifang and Yuntao, thanks for being so nice to me. You made my second home from home a lot warmer and sweeter!

My friends in China, thank you so much for your friendship! Xiaoyu, Aya, Xuxu, Dawan, Cua and Jing, thanks for going out with me when I was back home and for the kind regards and encouragement you sent me on QQ. And Sijing, I could never thank you enough. You are a sister to me!

Lu, thanks for being in my life, for your love and understanding, for always being there to support me, comfort me and encourage me. Thank you!

In the end, I want to express my gratitude to my relatives at home, thanks so much for helping and looking after my parents. To my parents, my dearest mama and papa, thank you for unconditional love and support and for cultivating my creativity and scientific curiosity. Thanks for the understanding and encouragement you have been giving all these years. I am eternally grateful to you.

最后，感谢我的亲戚们对我父母的关心和帮助，谢谢！我敬爱的父母，我最亲爱的爸爸妈妈，深深的感谢你们！感谢你们为我付出的一切！没有你们无私的爱与支持，我不可能有敢于追逐梦想的勇气。谢谢你们这些年来给的理解与鼓励，它们是我努力的动力。我永远感激你们，爱你们。

Curriculum Vitae

Jingwen Lin was born on 19th of October, 1982 in Xiamen, a coastal city in southeast China. She received her middle school and high school education in Xiamen No. 1 Middle School. She won the first prize in China High School Biology Olympia in Fujian Province in 2000 and gained the exemption from National University Entrance Examination. She entered Xiamen University in 2001 and majored in Biology.

She graduated from the School of Life Sciences in 2005, with the 'Best Bachelor's Thesis' award and 'Excellent student leadership' award. Based on her academic record during her undergraduate degree, she was granted an exemption of National Postgraduate Entrance Examination. She continued her Master's degree in Zoology (Parasitology) from 2005 to 2008 with a scholarship from Ministry of Education of China. Her master thesis was on early diagnosis and rapid detection of *Bursaphelenchus xylophilus* and differential proteome analysis of *B. xylophilus* and *B. mucronatus*, under the guidance of Prof. Cangsang Pan and Prof. Liang Chen.

In 2008, she was enrolled as a PhD student of Medicine in Leiden Malaria Research Group, Department of Parasitology, Leiden University Medical Center (LUMC, The Netherlands) with support from China Scholarship Council-Leiden University joint program. Here she performed studies on malaria using a rodent model of malaria, *Plasmodium berghei*. Under the supervision of Dr. Chris Janse and Dr. Shahid Khan, she carried out her PhD project principally focusing on screening and characterization of genetically attenuated blood-stage malaria parasites that could serve as protective immunogens, and also on improving transfection methods in rodent malaria parasites including rapid gene-insertion mutagenesis. The results of this research have been presented in this thesis. Currently she is engaged in post-doctoral research on immunological responses to virulent and non-virulent malaria infection in mouse model, in the group of Dr. Jean Langhorne, National Institute for Medical Research, London, United Kingdom.

